POPULATION GENETICS, INTRASPECIFIC GROUPS, AND HISTOPATHOLOGY OF *RHIZOCTONIA SOLANI* AG 2-2 ON SUGAR BEET

By

Douglas H. Minier

A DISSERTATION

Submitted to
Michigan State University
in partial fulfillment of the requirements
for the degree of

Plant Pathology – Doctor of Philosophy

ABSTRACT

Sugar beet is grown in temperate regions around the world for the sucrose that accumulates in its root tissues and accounts for about 12% of global sugar production. In the United States, sugar beet accounts for roughly half of domestic sugar production with an estimated value of around \$1.9 billion annually. However, Rhizoctonia root and crown rot is a persistent problem in growing regions around the world and is one of the most important soil-borne diseases of sugar beets. Losses to Rhizoctonia root and crown rot in the U.S. are estimated to exceed \$38 million annually affecting harvestability, processing quality, and storability. The causal agent of Rhizoctonia root and crown rot is *Rhizoctonia solani* AG 2-2 (Kühn), a soil-borne fungus in the Basidiomycota. Strains of R. solani AG 2-2 that affect sugar beet have traditionally been separated into intraspecific groups (ISGs), known as AG 2-2IIIB and AG 2-2IV, that commonly are classified by their ability to grow at 35°C. It has been evident for some time now that, based on ITS sequences, these subgroups are polyphyletic. In the current study, a multigene phylogenetic analysis was used to clarify the relationship between the subgroups and the results indicated that the subgroups 2-2IIIB and 2-2IV are indeed artificial. Therefore, the subgroups of AG 2-2 were redefined to represent a more natural classification. These new subgroups, referred to as AG 2-2BR and AG 2-2PR in the current work, each consisted of two genetic clusters that all have unique genetic characteristics.

To examine the characteristics of these newly identified genetic clusters and to address some open questions regarding the population biology of *R. solani* AG 2-2, a set of microsatellite markers was developed and utilized to genotype 164 isolates from eight growing regions around the world. Sexual reproduction in AG 2-2 has been controversial, but evidence provided by the microsatellite analysis supports sexual reproduction occurring in natural populations, although, it

is likely restricted to members of one genetic cluster within AG 2-2BR. In addition, evidence of hybridization between the subgroups 2-2BR and 2-2PR is presented and it appears this hybridization can occur in natural populations. These life-cycle processes have important implications in the generation of genetic diversity in populations. Population studies using the newly developed set of microsatellite markers also revealed evidence of long-distance dispersal that appears to occur across continents and across oceans. These observations highlight the importance of sanitation in managing Rhizoctonia root and crown rot to limit or prevent the movement of inoculum on equipment, crop residues, or personal apparel.

The current research project also examines the infection process for Rhizoctonia root and crown rot of sugar beet. Observations provide evidence for the involvement of cell wall degrading enzymes, including lignin degrading enzymes, pectin lyase, and polygalacturonase/polygalacturonase-inhibiting proteins, in the invasion and colonization of sugar beet root tissue. The involvement of these enzymes has been previously reported in sugar beet, but they have not received a lot of attention since their original reporting. It is anticipated that this work may renew interest in the enzymes involved in the invasion of sugar beet roots and the development of Rhizoctonia root and crown rot and provide additional targets for resistance breeding.

Additionally, this dissertation provides a novel perspective on the generation of genetic diversity in *R. solani* AG 2-2 which is expected to inspire innovative hypotheses regarding strategies of resistance breeding in sugar beet.

To my Mom

ACKNOWLEDGMENTS

I would like to take this opportunity to thank the individuals who have helped me achieve this major milestone in my career. First, I would like to thank my major advisor, Dr. Linda Hanson, for her patience and mentorship. This has been a challenging journey for me, and I have experienced many personal difficulties during my graduate studies. Dr. Hanson was very understanding and allowed me the time I needed to work through all these issues. I believe that under Dr. Hanson mentoring, I have become a well-rounded pathologist and have really developed the ability to think about problems in much more than a superficial way. I would also like to thank my other committee members, Dr. Ray Hammerschmidt, Dr. Greg Bonito, and Dr. Jaime Willbur, for their support, advice, and willingness to help me through this process. There have been numerous individuals that I have met during my graduate studies that have encouraged and supported me, including Tom Goodwill, Qianwei Jiang, Daniel Bublitz, and Celeste Dmytryszyn. I would like to extend a special thanks to Dr. Camen Medina-Mora who was the most supportive and encouraging person during this process. I do not know how I could have made it through without you.

TABLE OF CONTENTS

CHAPTER 1: REVIEW OF LITERATURE	
REFERENCES	41
CHAPTER 2: DEVELOPMENT OF MICROSATELLITE MARKERS AND THE	
PHYLOGENETIC ANALYSIS OF RHIZOCTONIA SOLANI AG 2-2	60
REFERENCES	108
CHAPTER 3: POPULATION STRUCTURE OF <i>RHIZOCTONIA SOLANI</i> AG 2-2	
REVEALS CRYPTIC SOURCES OF GENETIC DIVERSITY	116
REFERENCES	168
CHAPTER 4: HISTOPATHOLOGY OF RHIZOCTONIA ROOT AND CROWN ROT	
OF SUGAR BEET	174
REFERENCES	
CHAPTER 5: CONCLUSIONS	221
REFERENCES	229

CHAPTER 1:

REVIEW OF LITERATURE

Introduction to sugar beets

Sugar beet (*Beta vulgaris* subsp. *vulgaris* L.) is grown in temperate regions throughout the world for the sucrose that accumulates in its root. Worldwide, about 4.4 million hectares of sugar beet are planted annually, yielding around 270 million tons of white sugar (FAO 2022). Sucrose from sugar beets accounts for about 12% of global sugar production, with the remainder coming primarily from sugar cane. The Russian Federation led global sugar beet production in 2021 with 41 million metric tons grown on 994,000 hectares followed by France with 34 million metric tons on 402,000 hectares (FAO 2022). The United States was the third largest producer of sugar beets in 2021 with 33 million metric tons on 448,000 hectares. Total value in 2021 for world production of sugar beet was approximately \$12.5 billion (FAO 2022) and about \$1.9 billion in the United States (US Department of Agriculture; National Agricultural Statistics Services).

Cultivated beets were likely domesticated from the wild relative *Beta vulgaris* subsp.

maritima that is native to the Mediterranean basin and western Europe (Biancardi & Lewellen 2012). Cultivar groups related to sugar beet such as table beets, chards, and fodder beets are included in *Beta vulgaris* subsp. *vulgaris*. Each of these cultivar lineages has been adapted to specific end uses and exhibit distinctive phenotypic differences (Winner 1993). Table beets have been selected for an expanded hypocotyl and crown tissue and the accumulation of betanin, the pigment that gives many table beets their red color (Lange et al. 1999). Chards were developed for their edible leaves. While the leaves of all beet types are edible, chards have larger, nutritious leaves that can be green or reddish (Ninfali & Angelino 2013). Fodder beet was developed primarily as feed for cattle and other livestock (Winner 1993). It is the most similar cultivar group to sugar beet with an expanded root and crown and higher levels of sucrose accumulation

than table beets or chards. It is likely the ancestral group from which sugar beet was developed (Biancardi & Tamada 2016; Fasahat et al. 2018).

Sugar beets are the most economically important cultivar group of *B. vulgaris* subsp. *vulgaris* and have been adapted for a greatly expanded root and crown with high levels of sucrose accumulation (Winner 1993). Unlike sugar cane, sugar beets are grown primarily in temperate regions, where planting usually occurs as early in the spring as feasible to maximize the growing season and biomass accumulation (Scott & Jaggard 1993). Sucrose yield has steadily increased since domestication through selective breeding programs and improved agronomic practices (Fasahat et al. 2018; Hoffmann 2010; McGrath & Panella 2018). Dry matter makes up about 23-24% of the sugar beet root, the remainder being water, and sucrose accounts for about 18% of the total dry mass (Hoffmann et al. 2005). Thus, a typical ton of sugar beets will yield about 180 kg of sugar, 150 kg of which will be recovered as marketable sugar, the rest being lost to molasses or during storage (Campbell 2002).

The sugar beet crop is susceptible to a number of diseases that can reduce yield and constrain production. Major soil-borne diseases include Fusarium yellows (*Fusarium oxysporum* f.sp. *betae*; Hanson & Jacobsen 2009; Harveson 2008a), Aphanomyces root rot (*Aphanomyces cochlioides*; Poindexter 2014; Windels & Harveson 2009), Rhizomania (Beet necrotic yellow vein virus (vector *Polymyxa betae*); Biancardi & Tamada 2016; Rush 2009) and Rhizoctonia root and crown rot (*Rhizoctonia solani* AG 2-2; Khan & Bolton 2021; Schneider & Whitney 1986). Important foliar diseases include Cercospora leaf spot (*Cercospora beticola*; Harveson 2013; Jacobsen & Franc 2009a), Phoma leaf spot (*Phoma betae*; Jacobsen & Franc 2009b; Koenick et al. 2019), Alternaria leaf spot (*Alternaria alternata*; Cortes et al. 2022; Franc 2009), beet curly top (Beet curly top virus (vector *Circulifer tenellus*); Harveson 2015; Wintermantel 2009), and

powdery mildew (*Erysiphe polygoni*; Francis 2002; Hanson 2009). There are also several arthropods and nematodes that can cause substantial economic damage to sugar beet crops. These include the sugar beet root aphid (*Pemphigus betae*; Hein et al. 2009b; Pretorius et al. 2016), the root maggot (*Tetanops myopaeformis*; Hein et al. 2009a; Wenninger et al. 2019), cyst nematode (*Heterodera schachtii*; Gary 2009a; Khan & Arabiat 2021) and the root-knot nematode (*Meloidogyne* spp.; Gary 2009b; Westerdahl & Becker 2016).

In addition to losses that occur in the field, severe losses can occur during storage, prior to roots being processed in the sugar factories, that can reduce recoverable sucrose. In many regions, harvested sugar beets are placed in large storage piles to await processing (Bugbee 1993). Exposed to ambient weather conditions, these piles can incur substantial annual losses (Stausbaugh 2018; Van Driessche 2012), with the majority of loss occurring from respiration (Campbell & Klotz 2006). However, there are a number of fungi and bacteria that are responsible for storage rots including *Phoma betae* (Bugbee & Cole 1981), *Botrytis cinerea* (Isaksson 1942), *Fusarium* spp. (Christ et al. 2011), *Pennicillium* spp. (Strausbaugh & Dugan 2017), and *Leuconostoc* spp. (Strausbaugh 2016). Additionally, primary diseases such as Rhizoctonia root and crown rot may predispose the sugar beet roots to storage rots and increase their severity (Kusstatscher et al. 2019; Strausbaugh et al. 2011b, 2013).

Rhizoctonia root and crown rot

Rhizoctonia root and crown rot (RRCR) is one of the most serious and prevalent soil-borne diseases in most growing regions around the world (Buhre et al. 2009; Harveson 2008b; Khan & Bolton 2021; Strausbaugh et al. 2011a). The disease has economic impact on an estimated 25% of the sugar beet production area in the United States with yield losses amounting to about 2%

annually (Harveson 2008b; Kiewnick et al. 2001). The losses in individual fields can vary greatly, from negligible to over 50% depending on field history and environmental conditions (Harveson 2008b; Kiewnick et al. 2001).

The causal agent of Rhizoctonia root and crown rot is *Rhizoctonia solani* Kühn anastomosis group (AG) 2-2, a fungal pathogen in the family Ceratobasidiaceae (phylum: Basidiomycota, order: Cantharellales). *Rhizoctonia solani* is a large species complex that has proved challenging to classify and accurately define relationships within the group (Cubeta & Vilgalys 1997). Current classification within the genus is based on the anastomosis group (AG) concept which groups individuals based on the ability of their hyphae to fuse, or anastomose, with other members of the same AG (Parmeter et al. 1969; Sneh et al. 1991). To date, there have been at least 13 AG identified, each representing an independent evolutionary lineage within *R. solani* (Salazar et al. 2000; Sharon et al. 2008; Sneh et al. 1991). Although anastomosis groups can sometimes be challenging to determine and are occasionally imprecise due to the ability of some AG to fuse with other AG at low levels (Sneh et al. 1991), the anastomosis group currently represents our best understanding of relationships with the *R. solani* complex (Carling et al. 2002; Sharon et al. 2008; Sneh et al. 1991).

Several AG have been further subdivided into intraspecific groups (ISG), based on characteristics such as DNA hybridization, sclerotia size, zymography patterns, and temperature tolerance (Sharon et al. 2008; Sneh et al. 1991; Cubeta & Vilgalys 1994). *Rhizoctonia solani* AG 2-2 is currently separated into at least three subgroups, AG 2-2IIIB, AG 2-2IV, and AG 2-2LP. Originally, the subgroups were separated by host range, with AG 2-2IIIB affecting mat rush (*Juncus effusus*), AG 2-2IV affecting sugar beet (Ogoshi 1987), and AG 2-2LP affecting *Zoysia* spp. (Hyakumachi et al. 1998). However, AG 2-2IIIB and AG 2-2IV are now

known to both affect sugar beet and are no longer separated by host. Instead, the two subgroups are currently distinguished by the ability to grow at 35°C, where AG 2-2IIIB grows at 35°C while AG 2-2IV does not (Sneh et al. 1991).

In addition to a lack of distinction in host range, the monophylly of the subgroups AG 2-2IIIB and AG 2-2IV is questionable. Carling et al. (2002) showed that subgroup AG 2-2IV was polyphyletic with at least two clusters of AG 2-2IV isolates surrounding a cluster of AG 2-2IIIB isolates. Strausbaugh et al. (2011a) reported similar results with isolates of AG 2-2IIIB being paraphyletic. Because of the irregularities, Martin et al. (2014) analyzed the relationship of 64 AG 2-2 isolates using a multigene phylogeny and confirmed that the subgroups AG 2-2IIIB and AG 2-2IV were not supported. Instead, Martin et al. (2014) suggested the presence of at least three genetic groups that contained a mix of AG 2-2IIIB and AG 2-2IV isolates. Reported differences in virulence between the subgroups (Carling et al. 2002; Engelkes & Windels 1996; Strausbaugh et al. 2011a) has maintained interest in retaining them, despite their clear lack of phylogenetic support. Clarification of the relationships and subgroups within AG 2-2 is needed to better predict the functional characteristics of a given population and the potential effects on agronomical practices.

Anatomy and development of the sugar beet root

The anatomy of the sugar beet was described by Artschwager (1926) and later reviewed by Elliot & Weston (1993). The body of the sugar beet root consists of three regions with distinctive morphology. These regions are referred to as the crown, the neck, and the root. The crown forms a dome shape from which a tuft of leaves develops. The neck forms a smooth region between the crown and the root and is ontologically derived from the hypocotyl. This region is highly

expanded and forms the broadest part of the beet, although it may be difficult to distinguish from the crown and root in mature beets. The root region forms the bulk of the beet tissues and is slender and tapering with somewhat flattened grooves on two sides. These depressions form a shallow spiral that extends downward to a slender taproot and contain irregularly arranged lateral roots. The surface of the mature beet is covered by a thin corky layer rather than an epidermis that covers most herbaceous roots (Scheres et al. 2002).

Sugar beet is a biennial plant with seed borne on stalks that develop from the previous year's growth after sufficient vernalization (Cooke & Scott 1993). Clusters of two to seven flowers form at each node of the inflorescence and the perianth of adjoining flowers fuse to produce a mass of cork 3-5 mm in diameter that contains multiple germ. Planting these 'multigerm' clusters results in the germination of multiple seedlings from each 'seed' that will require hand-thinning to limit overcrowding (Smith & Fehr 1987). Breeding efforts have produced germline that form only a single flower at an inflorescence node, producing a 'monogerm' seed that can be directly planted, minimizing thinning (Savitsky 1950). Modern commercial varieties of sugar beet are primarily monogerm (Biancardi et al. 2010).

Seedlings emerge by epigeal germination with two cotyledons that are long and thin (Elliot & Weston 1993). Very young seedlings, less than 10 days after germination, consist of a tap root, a hypocotyl and a pair of cotyledons and are about 2 to 3 mm in diameter. In cross section, the root consists of primary vascular tissue at the core surrounded by an endodermis. Inside of the endodermis is a layer of pericycle and outside of the endodermis are a couple rows of parenchyma cells that form the primary cortex. The cortex is surrounded by a row of cutinized epidermal cells that are somewhat elongated (Artschwager 1926).

About 10 days after germination, vascular tissue in the central stele differentiates and the primary xylem forms in a plate that is oriented in line with what will eventually become the root grooves (Artschwager 1926). Primary phloem forms adjacent to the pericycle. Normal primary cambium forms between the primary xylem and the primary phloem and produces xylem to the inside and phloem to the outside. Primary growth concludes with the appearance of the second pair of leaflets, which takes between 10 and 12 days after germination (Artschwager 1926).

After emergence of the second leaflets, the parenchyma cells between the primary xylem and primary phloem begin to elongate axially and become meristematic to form the primary cambium and the development of xylem and phloem proceeds in the normal manner with xylem developing to the inside of the primary cambium and phloem developing to the outside of the primary cambium. This primary cambium development gives rise to the innermost vascular ring (Artschwager 1926).

When the primary cambium initials first divide, the outer cells become the initials of a new meristematic tissue, the secondary cambium. The inner cambium cells continue to divide and produce xylem and phloem normally. This process is repeated until all supernumerary cambia are formed. At each division, the inner-most cells produce xylem and phloem while the outer cells remain meristematic and produce a new cambium annular ring. Mature beet roots typically have between 7 and 11 annular rings (Artschwager 1952). Each secondary cambium is a direct descendant of the next inner ring, resulting in the inner rings maturing earlier than the outer rings. The outmost rings never fully mature and the tissue remains in the process of differentiation where occasionally cells will mature into small groups of sieve tubes and companion cells (Artschwager 1926).

Each annular ring matures a wide band of parenchyma cells which forces the vascular bands apart. Since the supernumerary cambia form in rapid succession, young plants will essentially have all cambia formed when they are still less than 12 mm in diameter, about 9 to 11 weeks old, at the 6 to 8 leaf growth stage. At this stage, new supernumerary cambiums stop developing and tissue expansion occurs by cell division and enlargement that occurs in all annular rings simultaneously (Artschwager 1926).

Because the development of supernumerary vascular rings occurs inside of the endodermis, tissue expansion forces the endodermis, primary cortex, and epidermis outward where they are eventually sloughed off. The pericycle divides tangentially into a band of meristematic tissue that establishes the phellogen or cork cambium. A thin covering, 5 to 8 cells wide, develops from the cork cambium consisting of phelloderm inside of the phellogen and cork cells on the outside. The cells of the periderm are thin and suberized and act as a protective layer since the epidermis is lost when the seedling is 6 to 8 weeks old (Artschwager 1926).

The transition between seedling beets and mature beets has been reported to occur about the same time that supernumerary vascular rings are formed and the periderm matures. The pattern of gene expression makes a dramatic change during this period of growth as well (Trebbi & McGrath 2009). This transition from seedling to mature beet supports the observation of limited reports of AG 4 and AG 5 on adult beets while AG 4 and AG 5 historically predominate on seedlings (Windels & Nabben 1989). While isolates of AG 4 were the most aggressive on seedlings, when inoculated on 8 to 9-week-old plants these AG 4 isolates caused only superficial lesions. In contrast, isolates of AG 2-2 were most aggressive on older plants, although they could still cause damage to seedlings, just not quite as severe as isolates of AG 4 (Windels & Nabben 1989). Gaskill (1968) and Liu et al (2019) have reported that no appreciable resistance to

Rhizoctonia root and crown rot developed until the 6 to 8 leaf growth stage, which occurs about 4 weeks after emergence. These observations are consistent with patterns of gene expression that change dramatically during this period and represent a transition in functional development from the seedling to the adult stage (Trebbi & McGrath 2009).

Crop rotation

Crop rotations can be effective at reducing disease severity of many plant diseases (Sumner et al. 1981; Wilson 2013). Recommendations for management of Rhizoctonia root and crown include a minimum of three years between sugar beet crops to prevent the build-up of inoculum (Harveson 2008b; Windels et al. 2009). Ideally, rotations should include non-host crops, particularly immediately preceding a sugar beet crop (Ruppel 1985; Windels et al. 2009). Unfortunately, many of the crops commonly grown in rotation with sugar beet are susceptible to the same strains that cause Rhizoctonia root and crown rot (Engelkes & Windels 1996; Herr 1987; Ruppel 1985; Sneh et al. 1991).

Engelkes & Windels (1996) showed that all strains of *R. solani* AG 2-2IIIB and AG 2-2IV tested caused disease on dry beans. Isolates of AG 2-2IIB from Ohio that were virulent on dry bean roots failed to cause foliar symptoms on dry beans or soybeans (Muyolo et al. 1993). Godoy-Lutz et al. (2008) identified isolates of AG 2-2 that caused foliar web blight on common beans, but they found these isolates clustered together in a genetic clade independent from AG 2-2IIIB or AG 2-2IV and identified them as subgroup AG 2-2WB. Further reports of isolates related to the AG 2-2WB clade are unknown. Minier (2019) found significant differences in virulence on dry beans and sugar beet seedlings between the clades of AG 2-2 identified by Martin et al. (2014) that were unrelated to the subgroups AG 2-2IIIB and AG 2-2IV. This raises

the possibility that strains that are more virulent on dry beans could increase in prevalence when dry beans are included in rotation. Recommendations have been to avoid close rotation between sugar beet and dry beans (Engelkes & Windels 1996).

Soybean is another common rotation crop grown in many regions that is also susceptible to *R. solani* AG 2-2 (Windels & Brantner 2005). To the best of my knowledge, only *R. solani* AG 2-2IIIB strains have been reported from soybean (Ajayi-Oyetunde et al. 2019; Dorrance et al. 2003; Fenille et al. 2002; Muyolo et al. 1993), although some reports do not indicate subgroup of the AG 2-2 isolates examined. One of the only studies to examine population structure of *R. solani* AG 2-2, especially in regard to the potential of sexual reproduction, was conducted using isolates recovered from soybean (Ajayi-Oyetunde et al. 2019). The researchers concluded a mixed reproduction strategy for the population from Ontario and primarily clonal reproduction in Ohio and Illinois. While the sexual stage is rarely reported from *R. solani* AG 2-2, results of the population genetics work by Ajayi-Oyetunde et al. (2019) indicate the potential of sexual reproduction, at least in limited situations or regions.

Corn is often grown in rotation with sugar beet but has a controversial history in regard to the effect it has on a subsequent beet crop. Coons and Kotila (1935) showed that corn decreased disease severity in a following sugar beet crop as did Maxson (1938), who recommended corn for rotation with sugar beet. Ruppel (1985) determined that corn was a host but states personal observation and the experiences of growers throughout the Plains region indicated that disease severity was reduced following corn. In the early 1980's, *R. solani* AG 2-2 was reported causing a brace root rot of corn in the southern United States (Sumner & Bell 1982). By the early 2000's, *R. solani* AG 2-2IIIB was reported causing disease on corn in northern growing areas such as Minnesota (Windels & Brantner 2005) and Germany (Buddemeyer et al. 2004; Ithurrart et al.

2004). Close rotations with corn were then shown to increase disease severity in a subsequent sugar beet crop (Windels & Brantner 2008). Similar results were reported for table beet in New York (Ohkura et al. 2009). Whether the warming climate allowed the disease to develop in more northern areas or rotations with corn selected for the more virulent *R. solani* AG 2-2 strains is uncertain.

Testing alfalfa and wheat as rotational crops has also resulted in contradictory results. Maxson (1938) determined small grains, such as wheat, were non-hosts and effective at reducing disease in a following sugar beet crop. Götze et al. (2017) determined that including alfalfa in rotation enabled shorter rotation intervals without negative yield affects. Alfalfa was also considered to be a non-host by Ruppel (1985) and Schuster and Harris (1960), but Coons and Kotila (1935) reported an increase in damping-off of sugar beet associated with *Rhizoctonia solani* when following alfalfa. Personal observations reported by Ruppel (1985) also suggest that alfalfa may increase disease in a following sugar beet crop. Field studies by Rush and Winter (1990) supported these observations that disease could increase following alfalfa. Some of the inconsistency between susceptibility and affect in field studies were attributed to residual soil NO₃-N and the colonization of crop residues (Ruppel 1985; Rush & Winter 1990).

Additional crops have been reported as being susceptible to *R. solani* AG 2-2, including clover (Hwang et al. 1996), canola seedlings (Verma 1996), radish, carrot (Grisham & Anderson 1983), sunflower (Rush & Winter 1990), tobacco (Gonzalez et al. 2011) and other brassicas (Cappelli et al. 1999). Although reported much less frequently than the primary potato type *R. solani* AG 3, AG 2-2 was reported to cause stem canker on potato (Muzhinji et al. 2015; Yanar et al. 2005). While not a crop commonly grown in rotation with sugar beet, *R. solani* AG 2-2IIIB

causes brown patch of creeping bentgrass (*Agrostis pulustris*; Blazier & Conway 2004) and other cool-season grasses (Burpee & Martin 1996).

When determining what crops to include in rotation, more than just susceptibility of the crop must be considered. Sugar beet cultivar had by far the largest effect on disease severity in a study by Buhre et al. (2009) followed by the interaction between environment and cultivar.

Rhizoctonia-resistant cultivars are commercially available but may have lower yields compared to susceptible varieties, often making their use disagreeable to growers (Khan et al. 2017; Panella & Hanson 2006; Panella & Ruppel 1996).

Many environmental factors are involved in disease development including nitrogen levels and distribution, organic residues (Rush & Winter 1990), temperature, and moisture effects (Bolton et al. 2010). Essentially, environmental conditions that favor the pathogen over the plant lead to higher levels of disease (Baker & Martinson 1970; Leach 1947). Planting timing could be a factor in disease development as well, with planting into soils that favor the plant over the pathogen recommended (Leach 1947; Ruppel 1985).

Ruppel (1985) proposed that the colonization of plant residues could account for the increase in disease severity when following what appeared to be a non-host, such as alfalfa. However, increased populations of *R. solani* surviving in residues does not always result in increased disease severity in the following crop (Herr 1987). Even without direct influence of pathogen survival, crop residues can influence soil nitrogen levels and soil moisture that could affect pathogen populations (Rush & Winter 1990). The effects of crop rotation are likely to be somewhat specific to the conditions within local areas depending on the composition of the pathogen population, soil type, climate, and sugar beet cultivar. This is consistent with varied

reports of the effect of crop rotation on disease, such as those reported by Rush and Winter (1990) versus those reported by Ruppel (1985).

Despite the issues described above, crop rotation remains an important aspect for managing disease, particularly for those diseases whose inoculum levels can build up in the soil. Effective crop rotation has been shown to increase sugar yield (Buhre et al. 2009) and overall, promotes more stable yields than monoculture (Götze et al. 2017). Despite being susceptible to *R. solani* AG 2-2, intercropping sugar beet with *Raphanus sativus* (radish) or *Brassica rapa* (field mustard/turnip) had a positive effect on white sugar yield compared to fallow (Kluth et al. 2010). This could be due to other factors such as the effect on other pathogens like the sugar beet cyst nematode (Smith et al. 2004) or the local soil structure (Allmaras et al. 1988).

Thus, selecting appropriate crops for rotation schemes should be carefully considered by employing experiments that examine the effects of specific rotational crops, not just on the subsequent crops, but also on the pathogen populations. The most critical aspects of crop rotation choices seem to be the crop immediately preceding the sugar beet crop and the amount of time between sugar beet crops with longer time out of sugar beet reducing disease severity and improving yield (Götze et al. 2017; Kluth et al. 2010; Schuster & Harris 1960).

Basidiospore production / heterokaryon formation

The sexual stage of *R. solani* is *Thanatephorus cucumeris* (A.B. Frank) Donk, although it has rarely been observed in AG 2-2 (Ajayi-Oyetunde et al. 2019; Qu et al. 2013). The sexual stage, if formed, may develop in the form of a greyish white to pale brown hymenial layer on aboveground plant parts or at the soil surface (Naito 1996). Basidiospores are small (< 9 µm), ovate,

single-celled and borne on thin sterigmata (Talbot 1970). The number of basidiospores per basidium is variable but typically averages four.

Other anastomosis groups of *R. solani* such as AG 3, AG 4, and AG 1, readily form a sexual stage (Adams & Butler 1983; Anderson 1982) but the sexual stage for AG 2-2 is rarely observed. It is uncertain as to why this is given that isolates of AG 2-2 have been observed producing hymenium in the lab (Kiyoshi et al. 2014). Curiously, only isolates identified as AG 2-2IV have been reported producing a sexual stage and the sexual stage has not been reported in AG 2-2IIIB. Most, if not all, reports of the sexual stage in AG 2-2IV have come out of Japan (Kiyoshi et al. 2014; Toda & Hyakumachi 2006). In addition, AG 2-2IV has been associated with foliar blight of sugar beet, presumably initiated by basidiospores (Naito 1990). Since basidiospores can be dispersed aerially, connecting foliar blight to isolates that can form the sexual stage would be a reasonable conclusion (Kiyoshi et al. 2014; Naito 1996).

Rhizoctonia solani AG 2-2 is heterokaryotic and multinucleate with between 4 and 13 nuclei per cell (Sneh et al. 1991). Single-basidiospore isolates derived from multinucleate individuals can all be in the same somatic compatibility group (homogeneous) or in multiple somatic compatibility groups (heterogeneous; Kiyoshi et al. 2014). Consequently, homogeneous isolates generate progeny with the same genotypes while heterogeneous isolates generate progeny with different genotypes.

Somatic compatibility is considered a separate genetic phenomenon from mating compatibility (Julián et al. 1996). Somatic compatibility describes the ability of hyphae to distinguish self from non-self (Worral 1997). In *R. solani*, different anastomosis groups are, for the most part, somatically incompatible, although a few AG can form bridging reactions that exhibit low levels of somatic compatibility (Sneh et al. 1991). Within AG 2-2, isolates can have

differing levels of compatibility and the terminology used to describe these interactions between hyphae was outlined by Parmeter et al. (1969) and Carling (1996). When isolates are somatically compatible, or very closely related, their hyphae can fuse completely, sharing membranes and cytoplasm. Isolates that are in closely related but different somatic compatibility groups do not fuse completely. Cell walls may fuse but membrane fusion is absent, or uncertain, and cytoplasm is not shared between hyphae. Adjacent cells typically die within a couple hours of fusion. Very different somatic groups, such as those of different anastomosis groups, do not fuse at all.

Because anastomosis represents a continuum, Carling et al. (2002) and Todo and Hyakumachi (2006) introduced additional categories for anastomosis reactions that were intermediate or distinct from categories defined by Carling (1996) and Parmeter et al. (1969).

It is unclear whether genetic material is exchanged between isolates that are somatically incompatible but can still fuse to some extent. In *R. solani*, Todo and Hyakumachi (2006) observed heterokaryon formation between incompatible isolates and hypothesized nuclei could migrate more rapidly than cell death occurs. Studies concerning heterokaryon formation in AG 2-2 have only involved subgroup AG 2-2IV (Kiyoshi et al. 2014; Toda & Hyakumachi 2006) and reports of AG 2-2IIIB forming heterokaryons are unknown.

Since basidiospore production has only been reported for AG 2-2IV, it is unclear whether AG 2-2IIIB isolates have a functioning sexual mating system. Both heterothallic and homothallic mating systems have been observed in AG 2-2IV (Todo & Hyakumachi 2006), but it is unknown whether this also applies to AG 2-2IIIB. Given the extent of diversity present within AG 2-2IIIB populations (Ajayi-Oyetunde et al. 2019; Liu & Sinclair 1992; Strausbaugh et al. 2011a), a mechanism for the generation of genetic diversity must exist within AG 2-2IIIB even if the sexual stage is nonfunctional. Isolates within AG 2-2IIIB anastomose freely and so could

presumably exchange nuclei. However, to the best of my knowledge empirical demonstration of this phenomenon is very limited or nonexistent.

Infection process of Rhizoctonia solani

The infection process for *Rhizoctonia solani* follows a generalized progression that includes recognition of a potential host, attachment to the host surface, development of an infection structure, penetration of the outer cell layers, colonization of host tissue and modulating host response (Ferreira et al. 2006). Much of the work investigating the infection process of *R. solani*, as a whole, focuses on infections that affect above-ground parts of the plant. In addition, most of the work has examined the infection process of AG 1 and AG 4 (Weinhold & Sinclair 1996), with limited work considering AG 2-2 on roots. Never-the-less, some generalizations of the infection process can be made.

Rhizoctonia solani survives in the soil primarily as sclerotia, which are highly melanized masses of barrel-shaped hyphae called monilioid cells (Sumner 1996). When moisture and temperature conditions are suitable, the sclerotia can germinate and mycelial threads grow towards the plant roots, presumably as a result of an attraction to exudates produced by the plant (Badri & Vivanco 2009; Bongard 2012; Lombardi et al. 2018; Narula et al. 2009). Root exudates such as amino acids, carbohydrates, phenols, and organic acids have been shown to stimulate growth, influence inoculum density, and promote disease formation (Keijer 1996; Reddy 1980). Whether this enhanced growth and attraction is due to an increase in available nutrients, such as carbohydrates, or a direct response to a chemical signal is still not completely resolved and the specifics may depend on the precise pathosystem under consideration.

Once the hyphae come in contact with the root surface of a suitable host, they begin to grow over the plant surface (Keijer 1996). Initially, the hyphae do not attach to the surface, but form rounded, "runner" hyphae that spread out over the surface (Keijer 1996). These rounded hyphae eventually become flattened and adhere to the epidermal cells. A mucilaginous sheath has been observed surrounding the appressed hyphae that is apparently responsible for attachment (Flentje 1956; Keijer 1996; Matsuura 1986). Since attachment appears to be a prerequisite for infection (Keijer 1996), identifying the factors that regulate attachment could be beneficial to further understanding of the infection process.

Once the hyphae are firmly attached, a process known as directed growth begins, where the growth of the hyphae follows the anticlinal epidermal cell walls (Armentrout & Downer 1987; Keijer 1996). Surface topology is thought to play a role in directed growth as artificial surfaces have been created that mimic directed growth of the hyphae (Armentrout et al. 1987; Kou & Naqvi 2016; Łaźniewska et al. 2012). Additionally, the contact between epidermal cells could result in the leakage of stimulatory compounds that direct hyphal growth (Marshall & Rush 1980). The hyphae then begin to form T-shaped branches of swollen hyphal tips that might be considered appressoria (Chethana et al. 2021). This branching process can continue, forming more complex aggregates that may originate from several parental hyphae (Hofman & Jongebloed 1988; Keijer 1996). These aggregates can develop into larger structures known as infection cushions that form more-or-less dome-shaped structures of densely packed hyphae (Armentrout & Downer 1987; Marshall & Rush 1980).

The process of infection cushion development has been studied in several pathosystems and some generalizations can be made from these studies. In cotton seedlings, infection cushions were well-formed 21 hours after inoculation (Armentrout & Downer 1987). Prior to cushion

formation, hyphae were observed shifting from relatively unbranched hyphae growing on the surface to hyphae with restricted branching in limited areas and then to more dense branching with accumulations of hyphae. This shift in growth patterns occurred in about 9 to 10 hours (Armentrout & Downer 1987). Mucilage-like material accumulated among the hyphae and appeared to function to adhere the hyphae to the plant surface. Formation of the cushions followed a predictable pattern, with repeated branching and t-shaped foot cells resulting in a cushion composed of axial hyphae with lateral connections. Once the cushion consisted of a sufficient size and density of hyphae, bulbous cells on the underside of the cushion formed penetration tips and penetrated the plant surface in large numbers (Armentrout & Downer 1987). The defining characteristic of infection cushions on cotton seedlings was described as a welldefined pattern of interwoven hyphae rather than an amorphous hyphal aggregation. However, although Armentrout and Downer (1987) describe infection cushions as the "typical" infection structure for members of the R. solani species complex, they warn against attempts to draw generalizations with regard to cushion formation on other crops citing observed variations in cushion formation reported by other authors.

Observations have implicated surface patterns as an inducer of infection cushion formation with hyphae following anticlinal epidermal walls and t-shaped branches developing that follow cell junctions (Armentrout & Downer 1987; Keijer 1996; Yang et al. 1992). However, this does not appear to always be the case. Marshall and Rush (1980) reported that fungal development on polystyrene replicas of rice sheaths did not follow junctions of the epidermal cells. While susceptible varieties had little or no cuticular wax deposits, resistant cultivars had an abundance of wax deposits on the outer sheath surface and infection cushion formation was limited or nonexistent. When the wax deposits were removed using chloroform, lobate appressoria and

infection cushions were formed, similar to those on susceptible cultivars. The implication then would be that infection cushion formation may be stimulated by exudates resulting from cell leakage and that cuticular waxes either reduce leakage, affect surface topology, or have some other inhibitory effect on infection cushion formation.

Infection cushions are not always necessary for infection. Hyphae have been observed entering through stomatal openings on leaves of rice (Manian & Manibhushanrao 1982), soybean (Zheng & Wang 2011) and potato (Zhang et al. 2016). Hyphae have also been observed directly penetrating the epidermis without an infection cushion developing or through natural openings (Manian & Manibhushanrao 1982; Zhang et al. 2016; Zheng & Wang 2011). These directpenetrating hyphae have been described as appressoria with various associated shapes or morphologies attributed to their formation (Zhang et al. 2016). In Rhizoctonia species, appressoria tend to be lobate, flattened and strongly adhered to the plant surface (Dodman & Flentje 1970; Flentje 1957). In many fungi, appressoria are highly melanized, which reduces porosity and allows internal hydrostatic pressure to increase to levels that allow enough force to be generated to penetrate the plant cuticle and outer epidermal cells (Howard & Ferrari 1989). Glycerol provides an osmotic gradient, drawing water into the cell (de Jong et al. 1997). As melanin is impermeable to glycerol, internal pressure increases to levels as high as 8.0 MPa (Bechinger et al. 1999; Money 1995; Wang et al. 2005). A thin infection peg emerges from the appressorium and is pushed by pressure generated in the appressorium through the cuticle and into the underlying epidermal cells.

The role of enzymes in penetration remains somewhat controversial. Infection pegs have been shown to penetrate paraffin wax, collodion membranes and even gold leaf, which are substances not likely to be degraded by enzymatic action and require mechanical force to

penetrate (Brown & Harvey 1927; Talbot 2019). It is therefore often presumed that the presence of cell wall degrading enzymes is not a requirement for penetration. However, studies have shown that impaired penetration occurred in isolates of *Pyricularia oryzae* (syn: Magnaporthe oryzae) as a result of the knock down of xylanase or cellulase genes (Nguyen et al. 2011; Vu et al. 2012). Inhibition of cutinase also prevented infection of *Pisum sativum* by *Fusarium solani* f. sp. pisi (Köller et al. 1982) and of Carica papaya by Colletotrichum gloeosporioides (Dickman et al. 1982). However, this was not the case of infection of cucumber by Gloeosporium orbiculare (syn: Colletotrichum lagenarium) where inhibition of cutinase did not reduce penetration (Bonnen & Hammerschmidt 1989). Infection of barley by *Blumeria graminis* f. sp. hordei (syn: Erysiphe graminis f. sp. hordei) begins with enzymatic digestion of the epidermal wall prior to mechanical penetration (Edwards & Allen 1970; Pryce-Jones et al. 1999). These studies suggest that the role that enzymatic versus mechanical factors play in plant penetration varies based on the fungus and host involved. Fungi that produce highly melanized appressoria may rely more on mechanical force while enzymes may play a larger role in those that produce less melanized appressoria (Talbot 2019).

While infection cushions may not be required for infection by *R. solani*, several researchers have noted differences in the formation of infection cushions on resistant and susceptible varieties (Bashyal et al. 2018; Bassi et al. 1979; Pannecoucque & Höfte 2009; Yang et al. 1992; Zhang et al 2016). The correlation between infection cushion formation and disease severity is well established. However, the factors that contribute to variability in infection cushion formation are not as clear-cut. In potato, reduced infection cushion formation on a resistant variety was attributed to physical factors such as a thicker cuticle (Zhang et al. 2016). The thicker cuticle may result in less leakage of infection cushion-stimulating compounds. One

function of the periderm is to reduce dehydration (Campilho et al. 2020), which supports the hypothesis of reduced leakage of stimulating compounds. However, the presence of a thickened cuticle was inconsistent in a study that noted differences in infection cushion formation between resistant and susceptible tomato fruit (Bassi et al. 1979). Epidermal and subepidermal cells were smaller and more densely packed in the resistant variety indicating that the structure of the epidermis may play a role in resistance. Alternatively, it could be viewed that infection cushion formation was stimulated in the susceptible variety, which may be due to exudates, a thin cuticular layer, or surface cues that are unique to the susceptible varieties.

Reduced disease severity in cauliflower has also been associated with reduced infection cushion formation (Pannecoucque & Höfte 2009). In addition, reduced disease severity was associated with a reduction in pectin degradation. The ability of *R. solani* AG 2-2 isolates to produce pectin degrading enzymes is well established (Barker & Walker 1962; Bateman 1963; Sherwood 1966) but in cauliflower, pectin degradation was not observed for the AG 2-2 isolate tested (Pannecoucque & Höfte 2009). The reason for this may be due to incompatible specificity of the cell wall degradation enzymes involved or production in insufficient quantities.

Alterations to pectic structure of the cell wall, methylation patterns, or inhibitor proteins produced by the plant could reduce the effectiveness of a specific enzyme to degrade the pectin matrix (Bellicampi et al. 2104; D'Ovidio et al. 2004; Daher & Braybrook 2015).

Several cues have been identified that induce infection structures including topographic signals, surface hardness, hydrophobicity, surface waxes and cutin, ethylene, and secreted enzymes (Kou & Naqvi 2016). While these induction clues have been demonstrated in several systems (Armentrout et al. 1987; Badri & Vivanco 2009; Bellincampi et al. 2014; Kou & Naqvi 2016; Yang et al. 1992), the specific mechanisms depend on the particular system involved and

the precise role of each signal is complicated and not universal. The lack of pectin degradation in cauliflower could be due to a lack of appropriate signals which induce cell wall degrading enzyme production. This lack of signal initiation could also relate to infection cushion formation (Pannecoucque & Höfte 2009).

Cell wall components and structure

Plant cell walls not only provide rigidity and structure to the cell but also serve as a primary line of defense against plant pathogens (Albersheim et al. 2011; Bellincampi et al. 2014). Composed primarily of polysaccharides, the cell wall consists of a network of microfibrils that allow for diverse shapes and properties that fulfill various roles in different organs and at different stages of development. Because of this need for diverse structures, the cell wall must be dynamic and adaptable. During growth, development, and movement, it may be necessary to reshape and remodel the cell wall to fit the changing needs of the plant (Daher & Braybrook 2015; Wu et al. 2018). Enzymes play a primary role in this process by altering cell wall elasticity, porosity, and integrity (Ene et al. 2015; Tenhaken 2015).

Many of the same types of enzymes that plants use to modify the cell wall are also utilized by plant pathogens to compromise the integrity of the cell wall and gain access to plant tissues. These enzymes include polygalacturonases, pectin lyases, pectin methylesterases, cellulases, and hemicellulases (Bellincampi et al. 2014). Plants employ sophisticated regulatory controls over cell wall modifications to manage the effects of cell wall degrading enzymes (Ene et al. 2015; Wolf & Greiner 2012) and in order for a plant pathogen to successfully invade, it must either a) degrade tissue at a faster rate than the plant can respond (ie. necrotrophs) or b) interfere with the signaling networks that regulate cell wall modifications (ie. biotrophs). In addition, plants have

evolved a sophisticated defense system that monitors cell wall integrity through the detection of microbial/pathogen-associated molecular patterns (MAMPS/PAMPs) and damage-associated molecular patterns (DAMPs; Bellincampi et al. 2014; Ferrari et al. 2013; Hou et al. 2019). Thus, the cell wall serves as a key battleground between pathogen and host, with a constant struggle between detection, cell wall integrity, response intensity, and the timing of interactions.

One of the primary constituents of plant cell walls is cellulose which provides the major load-bearing component of the cell wall (Albersheim et al. 2011). Cellulose is a polysaccharide consisting of hundreds or thousands of β -1,4-linked D-glucose units. The β -1,4 linkages of the glucosyl chain require that alternate residues be oriented 180° relative to one another, thus the cellulose backbone consists of disaccharide repeating units and the resulting polymer is both simple and stable in terms of its organization (Albersheim et al. 2011). Much of the stability and stiffness of cellulose comes from the ability of the β -1,4-linked glucan chains to form intra- and intermolecular hydrogen bonds, resulting in between 30 and 50 chains oriented in the same direction forming a cellulose microfibril (Klemm et al. 2005). These microfibrils are arranged in loose parallel sheets that are interconnected by hemicellulose.

Hemicellulose consists of a backbone similar to cellulose, but with xyloglucan being the principal component with β -1,4-linked glucosyl chains with the hydroxyl group at C-6 substituted with α -D-xylosyl residues at approximately 75% of the glycosyl resides (Albersheim et al. 2011). Some of these xylosyl residues have additional saccharide residues attached at C-2, such as β -D-galactosyl or α -L-fucosyl, which results in a highly branched polymer that adheres strongly to cellulose microfibrils through hydrogen bonding. These hemicellulose networks form a framework of cellulose microfibrils around which other wall polysaccharides are organized (Albersheim et al. 2011; Rao et al. 2023).

Pectic polysaccharide polymers comprise the largest share of non-cellulosic polysaccharides in the cell wall, and in some cases, pectin is the most prevalent component of the cell wall making up approximately 35% of the composition (Voragen et al. 2009). Pectin is primarily composed of α -1,4-linked galacturonic acid residues with various structural and chemical modifications such as neutral sugar side chains and varying levels of methyl esterification (Mohnen 2008). These pectin polymers connect and anchor the hemicellulose-cellulose network and form a water-retentive matrix that provides the cell wall with resistance to compressive and shearing forces (Albersheim et al. 2011).

Several types of pectin polymers have been described based on the composition of the backbone and the side chain unit substitutions, the simplest and most common being homogalacturonan (Voragen et al. 2009). Consisting exclusively of β-1,4-linked galacturonic acid residues, homogalacturonan is the gel-forming polysaccharide of the cell wall (Voragen et al. 2009). The degree of methyl esterification varies depending on plant species and tissue type with up to 70% of carboxyl groups methyl esterified. Not only the degree, but the pattern of methylation is important as well (Willats et al. 2001). Regions of unesterified galacturonic acid residues form calcium cross-links between adjacent chains. These regions of low or unesterified homogalacturonan are found in the middle lamella and cell junctions and are responsible for cell-to-cell adhesion (Daher & Braybrook 2015). Treatment with calcium chelators such as ethylenediaminetetraacetic acid (EDTA) and 1,2-Diaminocyclohexanetetraacetic (CDTA) results in cell separation in some plants (Dahar & Braybrook 2015; McCartney & Knox 2001; Tibbits et al. 1998) highlighting the role methylation plays in cell adhesion.

Rhamnogalacturonan I (RG-I) is a pectic polysaccharide closely related to homogalacturonan that consists of repeated disaccharide units of α -D-galacturonic acid and α -L-rhamnose (Willats

et al. 2001). Many rhamnose units have side branches made up of neutral sugars such as D-galactose, L-arabinose and D-xylose, the types and proportions varying with different sources. The precise organization of the side chains is highly variable with roughly 40 structurally different side chains known (Ridley et al. 2001; Voragen et al. 2009). Arabinosyl and galactosyl residues are the most common components of the side chains, but fucosyl, glucosyluronic acid and 4-O-methyl glucosyluronic acid residues can also be present. Side chains are attached to the C-4 or the rhamnosyl residues of the rhamnogalacturonan backbone. The nature of the relationship between homogalacturonan and rhamnogalacturonan-I is uncertain, but it is thought that RG-I and HGA are covalently attached through glycosidic linkages, connecting HG and RG-I into larger units (Kaczmarska et al. 2022; Willats et al. 2001). Thus RG-I may serve as a scaffold to which other pectic polysaccharides attach to form the pectic matrix and which determines key characteristics such as cell wall strength, elasticity, and flexibility (Yapo 2011). The diversity of structure of RG-I is indicative of diverse functional specialization (Mohnen 2008).

Rhamnogalacturonan II (RG-II) is the third type of pectic polysaccharide present in plant cell walls and is considered to be the most complex polysaccharide known (Willats et al. 2001). While consisting of only about 30 residues, there have been at least 11 different monosaccharides identified as components of RG-II, organized into a backbone of seven to nine α-1,4-linked D-galacturonic acid residues bearing four oligosaccharide side chains (Pérez et al. 2003). The structure of RG-II is highly conserved across disparate plant types despite such a large number of different sugars linked with more than 20 different glycosidic linkages (Albersheim et al. 2011; Bar-Peled et al. 2012), which likely indicates a conserved function or role in plant cell wall structure.

The complexity and conservation of RG-II appears to be related to the capacity to form dimers through borate cross-linking, but whether there is some other function that constrains variation is unknown (Bar-Peled et al. 2012). Borate cross-linking is associated with several physical properties of the cell wall including pore size and wall strength. Deficiencies in borate result in reduced plant growth, thickened, brittle cell walls, and the inability to form borate cross-links has been shown to be deleterious to plant growth and development (Ahn et al. 2006; Fleischer et al. 1999; Voxeur et al. 2011).

Evidence indicates that HG, RG-I and RG-II are covalently linked in a pectin network, although it is not yet established that this is always the case (Pérez et al. 2003). While the precise arrangement of the different types of pectin is uncertain, there are a couple generalities that have been identified. Based on studies with antibodies, RG-II is widely present in primary cell walls but appears to be absent from the middle lamella (Matoh et al. 1998), while nonesterified HG is found mostly in the middle lamella and esterified HG is found in the primary cell wall (Albersheim et al. 2011).

Composition of sugar beet cell walls

Sugar beet cell walls are rather unique when compared to most other crops having very low levels of xyloglucans and high levels of pectin (McGrath & Townsend 2015). Sugar beet pectin has an abundance of neutral sugar side chains, particularly arabinose (Marry et al. 2000). These neutral sugars directly link the pectin network with the cellulosic material which directly influences cell wall properties (Zykwinska et al. 2005). Sugar beet homogalacturonan is highly acetylated (Dea & Madden 1986) making it particularly resistant to degradation by enzymes (Volpi et al. 2011; Yadav et al. 2009). Consequently, cell wall modification that reduces

acetylation levels may be necessary prior to degradation by pectin degrading enzymes (Karr & Albersheim 1970; Wu et al. 2018).

Calcium cross-linking is important to cell-cell adhesion in most higher plants (Daher & Braybrook 2015), but in addition to calcium cross-linking, sugar beet cell walls rely on ester bonds to maintain cell wall integrity (Marry et al. 2006). Substantial levels of ferulic acid are cross-linked to pectic arabinosyl and galactosyl residues and the combination of these linkages influences such properties as intercellular adhesion, extensibility, enzymatic digestion, texture, and lignification (Guillon & Thibault 1989; Waldron et al. 1999). Ferulic cross-links also occur in grasses (Anders et al. 2012), but in contrast to grasses, sugar beet cell walls contain relatively low levels of lignin (Dinand et al. 1999; McGrath & Townsend 2015). Phenolic cross-links, such as occur with ferulic acid, hinder degradation by reducing access to hydrolytic enzymes (Hartley et al. 1992).

Cell wall degrading enzymes

Because the plant cell wall is an important barrier to pathogen penetration, pathogens have evolved several strategies to overcome this obstacle. Some fungi, such as the Pucciniales (rust fungi), use appressoria to directly penetrate the cell wall using mechanical pressure (Talbot 2019; Wang et al. 2005). Other plant pathogenic fungi penetrate through stomata or other natural openings, such as wounds (Latunde-Dada et al. 1999; Misaghi 1982). However, the majority of fungi rely on cell wall degrading enzymes to not only penetrate cells and colonize tissues, but also to break down cell wall polymers into usable nutrients (Annis & Goodwin 1997). The cell wall is complex and heterogeneous in its construction and the arsenal of cell wall degrading enzymes produced by plant pathogens mirrors this diversity (Kubicek et al. 2014). Major classes

of cell wall-degrading enzymes produced by pathogenic fungi include pectinases, cellulases, hemicellulases, cutinases, and polysaccharide lyases (Kubicek et al. 2014).

Glycoside hydrolase (GH) is the general term for enzymes that cleave glycosidic bonds in oligo- or polysaccharides using hydrolysis (EC 3.2.1.-). Glycoside hydrolases are an extensive group of enzymes grouped into roughly 173 families based on amino acid sequence and folding similarity (Carbohydrate Active Enzyme database, http://www.cazy.org; Drula et al. 2022). While members of this large family differ in many aspects, most have a common hydrolytic mechanism. Hydrolysis of the glycosidic bond is catalyzed by two amino acid residues, one that acts as a proton donor and the other as a nucleophile. Depending on the position of the nucleophile, the reaction will result in either a retention or an inversion of the anomeric carbon (ie. inversion would result in β -GalA $\Rightarrow \alpha$ -GalA). The catalytic residues in retaining enzymes are \sim 5.5Å as opposed to \sim 10Å for inverting enzymes (Davies & Henrissat 1995; McCarter & Withers 1994).

Cellulases are characterized by the ability to hydrolyze the β -1,4-glycosidic bonds in cellulose. Three main types of glycosidic enzymes are known: endoglucanases (EC 3.2.1.4), exoglucanases, including glucohydrolases (EC 3.2.1.74) and cellobiohydrolases (EC 3.2.1.91), and β -glucosidases (EC 3.2.1.21; Teeri 1997). Endoglucanases randomly cut within the disordered, non-crystalline regions of the cellulose chains, resulting in oligosaccharides of various lengths. Exoglucanases act progressively on the free ends to release monosaccharide units. Glucohydrolases cleave 1 or 2 units from the reducing end producing glucose or cellodextrins (disaccharide of glucose) and cellobiohydrolases cleave from the non-reducing end producing cellobiose. β -glucosidases hydrolyze cellodextrins and cellobiose into glucose.

Collectively, this combination of enzymes can reduce the cellulosic network of the cell wall completely to glucose and thus a readily available source of energy (Mota et al. 2018).

Because hemicellulose cross-links the cellulose microfibrils, much of the cellulose network is inaccessible to cellulases. Thus, enzymes are needed that can degrade the hemicellulose network. Hemicellulose is a branched polymer made up of a number of different saccharide bonds, particularly a xylanglucan backbone (Scheller & Ulvskov 2010). Major types of enzymes with activity against hemicellulose include xylanases (EC 3.2.1.8), xyloglucanases (EC 3.2.1.151), α-galactosidases (EC 3.2.1.22), α-arabinosidases (EC 3.2.1.55) and β-galactosidases (EC 3.2.1.23). Several additional enzymes are involved in the disassembly of hemicellulose that can affect the various sugars and bonds involved (Shallom & Shoham 2003).

Pectic polymers fill in the voids between the cellulose-hemicellulose network, reducing access to the cellulosic chains. In order to access the cellulose, the network of pectin molecules needs to be disassembled. The major enzymes involved in degredation of pectin include: endopolygalacturonase (EC 3.2.1.15), exopolygalacturonase (EC 3.2.1.67), and rhamnogalacturonase (EC 3.2.1.171), all three types are accommodated in glycoside hydrolase (GH) family 28 (Kubicek et al. 2014). Endopolygalactuonases (Endo-PG) hydrolyze the α-1,4-D-galactosiduronic bonds of the homogalacturonan backbone randomly yielding oligogalacturonides of various lengths. Endo-PGs typically have a preference for unesterified substrates, but different forms of the enzyme have varying tolerance for esterification. Exopolygalacturonases (Exo-PG) cleave a single galacturonic residue from the non-reducing end of the homogalacturonan polymer and are unable to degrade esterified substrates (Albersheim et al. 2011; Kubicek et al. 2014). Rhamnogalacturonan hydrolyzes the bond between α-D-galacturonic acid and α-L-rhamnose in rhamnogalacturonan I. Additional enzymes are

involved in degradation of side chains of RG-I as well as for RG-II such as α -L-rhammosidase (EC 3.2.1.40), β -L-rhammosidase (EC 3.2.1.43), and α -L-fucosidase (EC 3.2.1.51). Because there are more than 20 distinct glycosidic linkages between RG-I and RG-II, each bond requires a different enzyme to catalyze the various linkages (Cook et al. 1999; Voragen et al. 2009).

Another family of enzymes that play a prominent role in cell wall deconstruction are pectinolytic lyases. These enzymes break the α -1,4-D-galacturonan bonds by means of β -elimination rather than hydrolysis (Zheng et al. 2021). This cleavage mechanism typically relies on an arginine or lysine residue that functions as a Brønsted base with a water molecule acting as a Brønsted acid. Transition metal ions or Ca²⁺ ions can assist in catalyzing the reaction by assisting in binding the substrate and affecting the charge of target protons. The pectinolytic lyases are differentiated by their affinity for methylated or demethylated pectin with pectin lyases (EC 4.2.2.10) favoring methylated pectin and pectate lyases (EC 4.2.2.2) favoring demethylated pectate (Zheng et al. 2021).

Pectin is synthesized in the Golgi apparatus and deposited in the cell wall in its methylesterified form with 70-80% of the GalA residues methylesterified (Mohnen 2008). During cell wall construction, plant pectin methylesterases (EC 3.1.1.11) facilitate the removal of the methyl group from the esterified carboxyl at C-6 by transfer of the methyl group to a water molecule producing de-esterified pectate and methanol (Daher & Braybrook 2015; Mohnen 2008; Kohll et al. 2015). The de-esterified HG can then be readily cross-linked with Ca²⁺ ions, which occurs primarily in the middle lamella and contributes to cell-to-cell adhesion (Daher & Braybrook 2015). When the cell wall needs modification, methylesterases regulate access of the pectic substrate to various enzymes allowing the regulation of construction and deconstruction of

the cell wall (Daher & Braybrook 2015; Wu et al. 2018). This process has implications in abscission, fruit ripening and softening, cell growth and dehiscence.

Evolution of gene families

A gene family is a set of functionally related genes that are thought to have been formed by the duplication and diversification of a single original gene (Ohta 2000). Gene families range greatly in dimension and heterogeneity from families with a small number of closely related gene copies to families with thousands of copies of transposable genetic components that have no identified function. Family members can be located in a cluster on one chromosome or scattered throughout the entire genome (Ohta 2000; Panchy et al. 2016). The concept of gene families applies not only to genes within a single genome (paralogs), but also to related genes between genomes (orthologs) that have arisen by duplication from an ancestral gene. The result is a set of related genes that can function at different stages of development, in various tissues, or on diverse substrates, thus potentially providing an adaptive advantage (Lažetić & Troemel 2021).

Gene families can be organized into several types (Ohta 2000). Tandemly arrayed gene families are typically associated with large gene families that require substantial quantities of gene products, such as ribosomal RNA. Pseudo gene families have members that resemble functional genes but contain errors or only partial copies exist such that a functional product is not produced (Zhang & Gerstein 2003). Gene families originating from "selfish" genetic elements can propagate within the genome despite their being neutral or even detrimental to the organism (Doolittle & Sapienza 1980). Often these elements have the capacity to be self-replicating and exist primarily because of this capacity to duplicate (Muñoz-López & Garcia-Pérez 2010). Diverse multigene families contain large numbers of genes with diverse functions

(Ohta 1991). Gene families are an important feature of organismal genomes that provide genetic diversity and present opportunities for the evolution of new genes and functions.

Duplication events that result in the formation and expansion of gene families can occur at four structural levels: 1) exon duplication and shuffling, 2) entire gene duplication, 3) multigene duplication, and 4) whole genome duplication (Panchy et al. 2016). These genomic events result in structural variations that have been associated with fitness benefits such as fungicide resistance (Jones et al. 2014). For example, in *Erysiphe necator*, structural variation resulting in copy number variations, increased the prevalence of a fungicide tolerant allele (Jones et al. 2014). The struggle between host and pathogen is a strong driver of diversification and expansion of gene families, especially in situations where there is direct contact between host and pathogen proteins (Lažetić & Troemel 2021). Expansion of gene families in pathogens have been associated with cell wall degradation gene families, which, based on the host/pathogen struggle concept, implicates cell wall degradation as a substantial factor in virulence and possibly for pathogenicity (Morales-Cruz et al. 2015).

Prior to 1970, the accepted model for the evolution of gene families was based on the sequence patterns observed in hemoglobin α , β , γ , and δ chains and myoglobin (Ingram 1961). In this model, divergence of family members is gradual with each gene copy evolving independently after the duplication. Thus, orthologous genes are more closely related than paralogous genes. This model is known as divergent evolution and has been considered to be the predominant mode of evolution for gene families, especially when member genes are separated in the genome (Ohta 2000). However, during the 1970's, it was determined that not all gene families evolved in the same manner as the globin protein families. Notably, sequence patterns of the ribosomal RNAs (rRNA) in *Xenopus* could not be explained using the divergent evolution

model (Nei & Rooney 2005). Ribosomal RNA is encoded by a large number of tandemly repeated genes separated by intergenic regions. Brown et al. (1972) showed that, in *Xenopus*, nucleotide sequences of these intergenic regions were more similar within a species than they were between species. This observation becomes even more difficult to explain using the divergent evolution model when it is noted that the coding regions for the 18S and 28S ribosomal subunits are highly conserved and are very similar even among distantly related species.

In order to explain the observed patterns in rRNA genes, Brown et al. (1972) proposed the model of concerted evolution. According to this model, member genes evolve together, in a concerted manner rather than independently and mutations that occur in individual repeat units spread through all member genes within a species (Liao 2003). This process has the effect of homogenizing member genes, and the result is that paralogous genes are more similar than orthologous genes. Two key mechanisms that appear to be responsible for the molecular pattern attributed to concerted evolution are repeated unequal crossing over and gene conversion. Unequal crossing over occurs when homologous sequences are not paired precisely and results in the deletion of a sequence in one strand and replacement with a duplication from its sister chromatid. Repeated occurrence of unequal crossing over has the tendency to homogenize the gene family (Panchy et al. 2016). Gene conversion involves the unidirectional transfer of genetic material during homologous recombination and can occur between sister chromatids or between homologous sequences on either the same or different chromosome (Chen et al. 2007). The exchange is initiated by double strand breaks and subsequent mismatch repairs that occur during DNA replication. With the intact strand used as a template to repair the broken strand, an allele at one locus is changed by copying a sequence form a different locus, thus resulting in multiple copies of the same allele.

A third model of gene family evolution is known as the birth-and-death model of evolution which was first proposed to explain the pattern of evolution of the major histocompatibility complex (MHC) gene family of mammals (Hughes & Nei 1989; Nei et al. 1997). This model also recognizes the creation of new genes through duplication, but proposes some duplicates are maintained in the genome for long periods of time but others are lost due to deletions or deleterious mutations (Demuth & Hahn 2009; Elrin- López et al. 2012). Multigene families such as MHC and immunoglobin (Ig), known for having large copy numbers, were found to be inconsistent with concerted evolution since member genes from the same species were not necessarily more closely related to each other rather than to member genes of other species (Nei et al. 1997).

Purifying selection has also been proposed as an alternative to the concerted model as an explanation for highly conserved gene families (Nei & Rooney 2005). Gene families responsible for essential cell processes, such as ribosomal RNA, tend to expand and contract under purifying selection that produces many members with redundant functions. While in some gene families, duplication allows for diversification, purifying selection removes gene copies that function at less than optimal capacity. In the case of rRNA, cells can require a large number of ribosomes to efficiently translate the proteins necessary to carry out cellular functions. Multiple copies of rRNA genes help to produce the necessary amount of ribosomal materials, however, divergence in rRNA sequence can reduce or impair translation efficiency. Additional evidence of purifying selection comes from the example of histone genes where researchers determined that the number of differences in synonymous sites was greater than differences in nonsynonymous sites for member genes (Rooney et al. 2002). The reasoning for this being that under purifying

selection, synonymous substitutions are expected to accumulate continuously while nonsynonymous substitutions should not.

Baroncelli et al. (2016) examined genomic content of 10 *Colletotrichum* species, as well as six additional members of the Sordariomycetes, in order to better understand the molecular determinants of host range. They found that gene content was closely associated with host range, particularly for carbohydrate active enzymes (CAZymes) and peptidases, which appear to be an important controlling factor regarding host range. Interestingly, it was not only expansion of these gene families that influenced host range, but also gene family contraction or loss seemed to play a major role in host range. Thus, the authors concluded that the factors that influenced host range in *Colletotrichum* have evolved according to the birth-and-death model of gene family evolution. Indeed, many gene families involved in production of secondary metabolites are thought to evolve by the birth-and-death model (Morales-Cruz et al. 2015).

Further evidence of the role of expansion and contraction in the evolution of gene families, particularly those associated with secondary metabolism, comes from Morales-Cruz et al. (2015). In a study of 10 fungal genomes, 114 gene families were found with higher-than-expected rates of gains/losses. Gene families identified as overrepresented included pathogen-host interaction genes, secreted carbohydrate-active genes (CAZymes), and P450 enzymes (Morales-Cruz et al. 2015). These functional groups are often associated with fungal virulence (Morales-Cruz et al. 2015) and the expectation is that expansion of these gene families could provide an adaptive advantage. Notably, species that were associated with similar symptoms on their respective host had similar repertoires within these expanded gene families even though there may not be a correlation with phylogenetic relationship.

Expansion and contraction of gene families can be expected to reflect the strength and type of selection forces. Gene families that interact with substrates that are highly diverse or can evolve rapidly would be expected to maintain a diverse repertoire of member genes under positive selection. These types of families typically involve proteins with direct interactions between host and pathogen and these interactions can create some of the strongest drivers for diversification and expansion (Lažetić & Troemel 2020).

Polygalacturonase gene families provide an example of the type of genes that would be expected to be maintained under positive selection due to direct interactions between host and pathogens. The genome repertoire of polygalacturonase genes has been associated with host range (King et al. 2011) and ecological strategy (Sprockett et al. 2011). Pathogens with a large host range face increased challenges related to virulence, cell wall degradation, and plant defense responses compared to pathogens with a narrower host range (King et al. 2011; Park et al. 2008; Sprockett et al. 2011). The diversity of polygalacturonase genes is expected to reflect the variety of pectic substrates present across the various host species susceptible to the pathogen (Cook et al. 1999; King et al. 2011; Park et al. 2008). Likewise, necrotrophic fungi have an expanded repertoire of polygalacturonase genes compared to biotrophs and saprophytes, possibly related to interactions with polygalacturonase-inhibiting proteins (PGIP) and directed by diversifying selection (Sprockett et al. 2011).

Rhizoctonia solani AG 2-2 is an aggressive necrotroph with a fairly broad host range, affecting at least 20 crop species (Sneh et al. 1991). As predicted based on host range and ecological strategy, the draft genome of *R. solani* AG 2-2 reported by Wibberg et al. (2016) encodes large numbers of secreted proteins and in particular, glycoside hydrolases, the gene family that includes polygalacturonase. The contribution of polygalacturonase (PG) to disease

development for *R. solani* has been well established (Barker & Walker 1962; Bateman 1963; Sherwood 1966). Multiple forms of PG, having varied activity, have been characterized from *R. solani* strains with the number of isoenzymes per isolate significantly correlated to host range (Scala et al. 1980). Minier & Hanson (2020) analyzed the genomes of nine *R. solani* AG 2-2 isolates and identified 151 putative polygalacturonase genes (average of 16.8 genes per isolate) with the most aggressive isolates having the greatest number of PG genes. Future work examining the distribution and variability of polygalacturonase genes in *R. solani* AG 2-2 could provide targets for novel polygalacturonase-inhibitor proteins that may help breeders develop better disease resistant varieties (Li & Smigocki 2018).

Conclusions

Interactions between pathogens and their host are complex and function at multiple levels.

Not only is it difficult to identify the range of interactions within a single host-pathogen system, but these interactions can vary greatly even between different hosts of the same pathogen

(Albersheim et al. 2011; Bellincampi et al. 2014; Dodman & Flentje 1970; Weinhold & Sinclair 1996). Thus, generalization of host-pathogen interactions, especially of specific details, can be unreliable.

Much work has been done examining the effects of *Rhizoctonia solani* AG 2-2 on sugar beet and other hosts grown in rotation. However, many of these studies relied on a small number of isolates from which to draw conclusions and, in my opinion, were overly dependent on generalizations. For example, much of the work on the infection process of *R. solani* has been done using *R. solani* AG 1 or AG 4 on rice and other foliar blight systems (Keijer 1996; Marshall & Rush 1980; Weinhold & Sinclair 1996; Zheng & Wang 2011). Much less work has been done

examining the infection process of roots by AG 2-2, or other AG, compelling a reliance on the assumption that foliar and root pathogens behave similarly.

In addition, the subgroups of *R. solani* AG 2-2 that form the basis of behavioral distinction have come into question as to the reliability of their relationships. The ascription of behavioral characteristics to a group that may not reflect natural relationships is likely to present inconsistencies. Evolutionary relationships form the backbone for the study of any biological organism and are an essential tool for examining behavior, function, and inherited traits (Smith et al. 2020). This is especially true in predator/prey systems where the struggle to survive drives an arms race, with the predator developing new strategies to overcome prey defenses and the prey adopting new defenses to prevent the predator from robbing it of resources.

With these principals in mind, this dissertation project had three key objectives:

- 1) Generate a more natural classification scheme within *R. solani* AG 2-2 that does not rely on criteria that defined previous subgroups, namely growth at 35°C. A classification scheme that was based on evolutionary relationships was expected to provide novel insights into the population biology, behavior, and life history strategy of this complex group.
- 2) Provide an overview of the population structure and distribution of *R. solani* AG 2-2 at multiple scales, including global, regional, and local levels. In order to accomplish this objective, we developed and utilized a set of microsatellite markers to genotype individuals from sugar beet growing regions around the world. These populations included isolates recovered from several crops in addition to sugar beet, such as soybean and dry bean, with the goal of providing growers and fellow researchers insight into the potential effects of including these crops in rotation.

3) Present an updated histopathological examination of the infection process of *R. solani* AG 2-2 using modern microscopy techniques. A comprehensive histopathological examination of sugar beet has not been performed since Rupple (1972). Open questions regarding the symptomology of Rhizoctonia root and crown rot still remain and this histopathological assessment was conducted with a focus on determining physiological factors that influence the development of the characteristic symptoms of Rhizoctonia root and crown rot. The project was also expected to provide insights into the mechanisms of both the infection process and the host defense response during plant-pathogen interaction.

REFERENCES

- Adams, G.C., jr. and Butler, E.E. 1983. Environmental factors influencing the formation of basidia and basidiospores in *Thanatephorus cucumeris*. Phytopathology, 73:152-155.
- Ajayi-Oyetunde, O.O., Everhart, S.E., Brown, P.J., Tenuta, A.U., Dorrance, A.E. and Bradley, C.A. 2019. Genetic structure of *Rhizoctonia solani* AG-2-2IIIB from soybean in Illinois, Ohio, and Ontario. Phytopathology, 109:2132-2141.
- Ahn, J.W., Verma, R., Kim, M., Lee, J.Y., Kim, Y.K., Bang, J.W., Reiter, W.D. and Pai, H.S. 2006. Depletion of UDP-D-apiose/UDP-D-xylose synthases result in rhamnogalacturonan-II deficiency, cell wall thickening, and cell death in higher plants. J Biol Chem, 281:13708-13718.
- Albersheim, P., Darvill, A., Roberts, K., Sederoff, R., and Staehelin, A. 2011. Plant Cell Walls: From Chemistry to Biology. Garland Science, Taylor & Fransis Group, LLC., New York, NY
- Allmaras, R.R., Kraft, J.M and Miller, D.E. 1988. Effects of soil compaction and incorporated crop residue on root health. Ann Rev Phytopathol, 26:219-243.
- Anders, N., Wilkinson, M.D., Lovegrove, A., Freeman, J., Tryfona, T., Pellny, T.K., Weimar, T., Mortimer, J.C., Stott, K., Baker, J.M., Defoin-Platel, M., Shewry, P.R., Dupree, P. and Mitchell, R.A.C. 2012. Glycosyl transferases in family 61 mediate arabinofuranosyl transfer onto xylan in grasses. P Natl Acad Sci USA, 109:989-993.
- Anderson, N.A. 1982. The genetics and pathology of *Rhizoctonia solani*. Ann Rev Phytopathol, 20:329-347.
- Annis, S.L. and Goodwin, P.H. 1997. Recent advances in the molecular genetics of plant cell wall-degrading enzymes produced by plant pathogenic fungi. Eur J Plant Pathol, 103:1-14.
- Armentrout, V.N. and Downer, A.J. 1987. Infection cushion development by *Rhizoctonia solani* on cotton. Phytopathology, 77:619-623.
- Armentrout, V.N., Downer, A.J., Grasmick, D.L. and Weinhold, A.R. 1987. Factors affecting infection cushion development by *Rhizoctonia solani* on cotton. Phytopathology, 77:623-630.
- Artschwager, E. 1926. Anatomy of the vegetative organs of the sugar beet. J Agric Res, 33:143-176
- Artschwager, E. 1952. Sugar beet types based on internal morphology. P Am Soc Sugar Beet Technol, 7:434-440.
- Badri, D.V. and Vivanco, J.M. 2009. Regulation and function of root exudates. Plant Cell Environ, 32:666-681.

- Baker, R. and Martinson, C.A. 1970. Epidemiology of diseases caused by *Rhizoctonia solani*. Pgs. 172-188 in: *Rhizoctonia solani*: Biology and Pathology. Parmeter, J.R. Jr. (ed.) University of California Press, Berkeley, CA.
- Bar-Peled, M., Urbanowicz, B.R. and O'Neill, M.A. 2012. The synthesis and origin of the pectic polysaccharide rhamnogalacturonan II insights from nucleotide sugar formation and diversity. Front Plant Sci, 3:92. doi:10.3389/fpls.2012.00092
- Barker, K.R. and Walker, J.C. 1962. Relationship of pectolytic and cellulytic enzyme production by strains of *Pellicularia filamentosa* to their pathogenicity. Phytopathology, 52:1119-1125.
- Baroncelli, R., Amby, D.B., Zapparata, A., Sarrocco, S., Vannacci, G., Le Floch, G., Harrison, R.J., Holub, E., Sukno, S.A., Sreenivasaprasad, S. and Thon, M.R. 2016. Gene family expansions and contractions are associated with host range in plant pathogens of the genus *Colletotrichum*. BMC Genomics, 17:555. doi:10.1186/s12864-016-2917-6
- Bashyal, B.M., Kharayat, B.S., Kumar, J., Dubey, S.C. and Aggarwal, R. 2018. Histopathological studies of *Rhizoctonia solani* infection process in different cultivars of mungbean (*Vigna radiata* (L.) Wilczek). Natl Acad Sci Lett, 41:269-273.
- Bassi, A. Jr., Moore, E.L. and Batson, W.E., Jr. 1979. Histopathology of resistant and susceptible tomato fruit infected with *Rhizoctonia solani*. Phytopathology, 69:556-559.
- Bateman, D.F. 1963. The macerating enzyme of *Rhizoctonia solani*. Phytopathology, 53:1178-1186.
- Bechinger, C., Giebel, K., Schnell, M., Leiderer, P., Deising, H.B. and Bastmeyer, M. 1999. Optical measurements of invasive forces exerted by appressoria of a plant pathogenic fungus. Science, 285:1896-1899.
- Bellincampi, D., Cervone, F. and Lionetti, V. 2014. Plant cell wall dynamics and wall-related susceptibility in plant-pathogen interactions. Front Plant Sci, 5:228. doi:10.3389/fpls.2014.00228
- Biancardi, E. and Lewellen, R.T. 2012. History and current importance. Pgs. 1-48 in: *Beta maritima*: The Origin of Beets. Biancardi, E., Panella, L.W. and McGrath, J.M. (eds.) Springer International Publishing, Cham, Switzerland.
- Biancardi, E., McGrath, J.M., Panella, L.W., Lewellen, R.T. and Stevanato, P. 2010. Sugar beet. Pgs. 173-219 in: Root and Tuber Crops. Handbook of Plant Breeding, vol 7. Bradshaw, J.E. (ed.) Springer, New York, NY.
- Biancardi, E. and Tamada, T (eds.) 2016. *Rhizomania*. Springer International Publishing, Cham, Switzerland.
- Blazier, S.R. and Conway, K.E. 2004. Characterization of *Rhizoctonia solani* isolates associated with patch diseases on turfgrass. Proc Okla Acad Sci, 84:41-51.

- Bolton, M.D., Panella, L. Campbell, L. and Khan, M.F.R. 2010. Temperature, moisture, and fungicide effects in managing Rhizoctonia root and crown rot of sugar beet. Phytopathology, 100:689-697.
- Bongard, C. 2012. A review of the influence of root-associating fungi and root exudates on the success of invasive plants. NeoBiota, 14:21-45.
- Bonnen, A.M. and Hammerschmidt, R. 1989. Role of cutinolytic enzymes in infection of cucumber by *Colletotrichum lagenarium*. Physiol Mol Plant Pathol, 35:475-481.
- Brown, D.D., Wensink, P.C., Jordan, E. 1972. A comparison of the ribosomal DNA's of *Xenopus laevis* and *Xenopus mulleri*: the evolution of tandem genes. J Mol Biol, 63:57–73.
- Brown, W. and Harvey, C.C. 1927. Studies in the physiology of parasitism. X. On the entrance of parasitic fungi into the host plant. Ann Bot-London, 41:643-662.
- Buddemeyer, J, Pfähler, B., Petersen, J. and Märländer, B. 2004. Genetic variation in susceptibility of maize to *Rhizoctonia solani* (AG 2-2IIIB) symptoms and damage under field conditions in Germany. J Plant Dis Protect, 111:521-533.
- Bugbee, W.M. 1993. Storage. Pgs. 551-570 in: The Sugar Beet Crop: Science into Practice. Cooke, D.A. and Scott, R.K. (eds.) Chapman and Hall, London, UK.
- Bugbee, W.M. and Cole, D.F. 1981. The effect of seed infected with *Phoma betae* on root and sucrose yield of stored sugar beet. Phytopathology, 71:357-359.
- Buhre, C., Kluth, C., Bürcky, K., Märländeer, B. and Varrelmann, M. 2009. Integrated control of root and crown rot in sugar beet: combined effects of cultivar, crop rotation, and soil tillage. Plant Dis, 93:155-161.
- Burpee, L.L and Martin, S.B. 1996. Biology of turfgrass diseases incited by *Rhizoctonia* species. Pgs. 359-368 in: *Rhizoctonia* species: taxonomy, molecular biology, ecology, pathology and disease control. Sneh, B., Jabaji-Hare, S., Neate, S. and Dijst, G. (eds.) Kluwer Academic Publishers, Dordrecht, The Netherlands.
- Campbell, L.G. 2002. Sugar beet quality improvement. J Crop Prod, 5:395-413.
- Campbell, L.G. and Klotz, K.L. 2006. Storage. Pgs. 387-408 in: Sugar Beet. Draycott, A.P. (ed.) Blackwell Publishing Ltd. Oxford, UK.
- Campilho, A., Nieminen, K. and Ragni, L. 2020. The development of the periderm: the final frontier between a plant and its environment. Curr Opin Plant Biol, 53:10-14.
- Cappelli, C., Corazza, L., Luongo, L. and Stravato, V.M. 1999. Interactions between crucifers and *Rhizoctonia solani* AG 2-1, AG 2-2IIIB, AG 2-2IV, AG 4. Phytopathol Mediter, 38:37-39.

- Carling, D.E. 1996. Grouping in *Rhizoctonia solani* by hyphal anastomosis reaction. Pgs. 37-47 in: *Rhizoctonia* species: taxonomy, molecular biology, ecology, pathology and disease control. Sneh, B, Jabaji-Hare, S., Neate, S. and Dijst, G. (eds.) Kluwer Academic Publishers, Dordrecht, The Netherlands.
- Carling, D. E., Kuninaga, S. and Brainard, K. A. 2002. Hyphal anastomosis reactions, rDNA internal transcribed spacer sequences, and virulence level among subsets of *Rhizoctonia solani* anastomosis group-2 (AG-2) and AG-BI. Phytopathology, 92:43-50.
- Chen, J.-M., Cooper, D.N., Chuzhanova, N., Férec, C. and Patrinos, G.P. 2007. Gene conversion: mechanisms, evolution and human disease. Nat Rev Gen, 8:762-775.
- Chethana, K.W.T., Jayawardena, R.S., Chen, Y-J., Konta, S., Tibpromma, S., Abeywickrama, P.D., Gomdola, D., Balasuriya, A., Xu, J., Lumyong, S. and Hyde, K.D. 2021. Diversity and function of appressoria. Pathogens, 10:746. doi:10.3390/pathogens10060746
- Christ, D.S., Märländer, B. and Varrelmann, M. 2011. Characterization and mycotoxigenic potential of *Fusarium* species in freshly harvested and stored sugar beet in Europe. Phytopathology, 101:1330-1337.
- Cortes, S.C., Hanson, L., Miles, L., Willbur, J. and Naegele, R. 2022. Diagnostic guide for Alternaria leaf spot on sugar beet, red beet, and chard. Plant Health Prog, 23:497-506.
- Cook, B.J., Clay, R.P., Bergmann, C.W., Albersheim, P. and Darvill, A.G. 1999. Fungal polygalacturonases exhibit different substrate degradation patterns and differ in their susceptibilities to polygalacturonase-inhibiting proteins. Mol Plant Microbe In, 12:703-711.
- Cooke, D.A. and Scott, R.K. (eds.) 1993. The Sugar Beet Crop: Science into Practice. Chapman & Hall, London, UK.
- Coons, G.H. and Kotila, J.E. 1935. Influence of preceding crops on damping off of sugar beets. Phytopathology, 25:13. (Abstr.)
- Cubeta. M.A. and Vilgalys, R. 1997. Population biology of the *Rhizoctonia solani* complex. Phytopathology, 87:480-484.
- D'Ovidio, R., Mattei, B., Roberti, S. and Bellincampi, D. 2004. Polygalacturonases, polygalacturonase-inhibiting proteins and pectic oligomers in plant-pathogen interactions. Biochim Biophys Acta, 1696:237-244.
- Daher, F.B. and Braybrook, S.A. 2015. How to let go: pectin and plant cell adhesion. Front Plant Sci, 6:523. doi:10.3389/fpls.2015.00523
- Davies, G. and Henrissat, B. 1995. Structures and mechanisms of glycosyl hydrolases. Structure, 3:853-859.
- de Jong, J.C., McCormack, B.J., Smirnoff, N. and Talbot, N. 1997. Glycerol generates turgor in rice blast. Nature, 389: 244-245.

- Dea, I.C.M. and Madden, J.K. 1986. Acetylated pectic polysaccharides of sugar beet. Food Hydrocolloid, 1:71-88.
- Demuth, J.P. and Hahn, M.W. 2009. The life and death of gene families. BioEssays, 31:29-39.
- Dickman, M.B., Patil, S.S. and Kolattukudy, P.E. 1982. Purification, characterization and role in infection of an extracellular cutinolytic enzyme from *Colletotrichum gloeosporioides* Penz. on *Carica papaya* L. Physiol Plant Path, 20:333-347.
- Dinand, E., Chanzy, H. and Vignon, M.R. 1999. Suspension of cellulose microfibrils from sugar beet pulp. Food Hydrocolloid, 13:275-283.
- Dodman, R.L. and Flentje, N.T. 1970. The mechanism and physiology of plant penetration by *Rhizoctonia solani*. Pgs 149-160 in: *Rhizoctonia solani*: Biology and Pathology. Parmeter, J.R. Jr. (ed.) University of California Press, Berkeley, CA.
- Doolittle, W.F. and Sapienza, C. 1980. Selfish genes, the phenotype paradigm and genome evolution. Nature, 284:601-603.
- Dorrance, A.E., Kleinhenz, M.D., McClure, S.A. and Tuttle, N.T. 2003. Temperature, moisture, and seed treatment effects on *Rhizoctonia solani* root rot of soybean. Plant Dis, 87:533-538.
- Drula, E., Garron, M., Dogan, S., Lombard, V., Henrissat, B. and Terrapon, N. 2022. The carbohydrate-active enzyme database: functions and literature. Nucleic Acids Res, 50:D571-D577.
- Edwards, H.H. and Allen, P.J. 1970. A fine-structure study of the primary infection process during infection of barley by *Erysiphe graminis* f. sp. *hordei*. Phytopathology, 60:1504-1509.
- Elliot, M.C. and Weston, G.D. 1993. Biology and physiology of the sugar beet plant. Pgs. 37-66 in: The Sugar Beet Crop: Science into Practice. Cooke, D.A. and Scott, R.K. (eds.) Chapman & Hall, London, UK.
- Elrin-López, J.M., Rebordinos, L., Rooney, A.P. and Rozas, J. 2012. The birth-and-death evolution of multigene families revisited. Repetitive DNA, 7:170-196.
- Ene, I.V., Walker, L.A., Schiavone, M., Lee, K.K., Martin-Yken, H., Dague, E., Gow, N.A.R, Munro, C.A. and Brown, A.J.P. 2015. Cell wall remodeling enzymes modulate fungal cell wall elasticity and osmotic stress resistance. mBio, 6:e00986-15. doi:10.1128/mBio.00986_15
- Engelkes, C.A. and Windels, C.E. 1996. Susceptibility of sugar beet and beans to *Rhizoctonia solani* AG-2-2IIB and AG-2-2IV. Plant Dis, 80:1413-1417.
- FAO. 2022. FAOSTAT: Production: in: FAO. Rome. Cited June 2023. https://www.fao.org/faostat/

- Fasahat, P., Aghaeezadeh, M., Jabbari, L., Hemayati, S.S. and Townson, P. 2018. Sucrose accumulation in sugar beet: from fodder beet selection to genomic selection. Sugar Tech, 20:635-644.
- Fenille, R.C., de Souza, N.L. and Kuramae, E.E. 2002. Characterization of *Rhizoctonia solani* associated with soybean in Brazil. Eur J Plant Pathol, 108:783-792.
- Ferrari, S., Savatin, D.V., Sicilia, F., Gramegna, G. Cervone, F. and De Lorenzo, G. 2013. Oligogalacturonides: plant damage-associated molecular patterns and regulators of growth and development. Front Plant Sci, 4:49. doi:10.3389/fpls.2013.00049
- Ferreira, R.B., Monteiro, S., Freitas, R., Santos, C.N., Chen, Z., Batista, L.M., Duarte, J., Borges, A. and Teixeira, A.R. 2006. Fungal pathogens: the battle for plant infection. Crit Rev Plant Sci, 25:505-524.
- Fleisher, A., O'Neill, M.A. and Ehwald, R. 1999. The pore size of non-graminaceous plant cell walls is rapidly decreased by borate ester cross-linking of the pectic polysaccharide rhamnogalacturonan II. Plant Physiol, 121:829-839.
- Flentje, N.T. 1956. Studies on *Pellicularia filamentosa* (Pat.) Rogers. I. Formation of the prefect state. Trans Brit Mycol Soc, 39:343-356.
- Flentje, N.T. 1957. Studies on *Pellicularia filamentosa* (Pat.) Rogers. III. Host penetration and resistance, and strain specialization. Trans Brit Mycol Soc, 40:322-336.
- Franc, G.D. 2009. Alternaria leaf spot. Pgs. 12-13 in: Compendium of Beet Diseases and Pests 2nd ed.). Harveson, R.M., Hanson, L.E. and Hein, G.L. (eds.). APS Press, St. Paul, MN.
- Francis, S. 2002. Sugar-beet powdery mildew (Erysiphe betae). Mol Plant Pathol, 3:119-124.
- Gaskill, J.O. 1968. Breeding for *Rhizoctonia* resistance in sugarbeet. J Am Sugar Beet Technol, 15:107-119.
- Godoy-Lutz, G., Kuninaga, S., Steadman, J.R. and Powers, K. 2008. Phylogenetics analysis of *Rhizoctonia solani* subgroups associated with web blight symptoms on common bean based in ITS-5.8S rDNA. J Gen Plant Pathol, 74:32-40.
- Gonzalez, M., Pujol, M., Metraux, J., Gonzalez-Garcia, V., Bolton, M.D. and Borrás-Hidalgo, O. 2011. Tobacco leaf spot and root rot caused by *Rhizoctonia solani* Kühn. Mol Plant Pathol, 12:209-216.
- Götze, P., Rücknagel, M., Wensch-Dorendorf, M., Märländer, B. and Christen, O. 2017. Crop rotation effects on yield, technological quality and yield stability of sugar beet after 45 trial years. Eur J Agron, 82:50-59.
- Gray, F.A. 2009a. Sugar beet cyst nematode. Pgs. 64-67 in: Compendium of Beet Diseases and Pests (2nd ed). Harveson, R.M., Hanson, L.E. and Hein, G.L. (eds.). APS Press, St. Paul, MN.

- Gray, F.A. 2009b. Root-knot nematode. Pgs. 67-68 in: Compendium of Beet Diseases and Pests (2nd ed.). Harveson, R.M., Hanson, L.E. and Hein, G.L. (eds.). APS Press, St. Paul, MN.
- Grisham, M.P. and Anderson, N.A. 1983. Pathogenicity and host specificity of *Rhizoctonia solani* isolated from carrot. Phytopathology, 73:1564-1569.
- Guillon, F. and Thibault, J.-F. 1989. Methylation analysis and mild acid hydrolysis of the 'hairy' fragments of sugar beet pectins. Carbohyd Res, 190:85-96.
- Hanson, L.E. 2009. Powdery mildew. Pgs. 15-17 in: Compendium of Beet Diseases and Pests (2nd ed.). Harveson, R.M., Hanson, L.E. and Hein, G.L. (eds.). APS Press, St. Paul, MN.
- Hanson, L.E. and Jacobsen, B.J. 2009. Fusarium yellows. Pgs. 28-29 in: Compendium of Beet Diseases and Pests (2nd ed.). Harveson, R.M., Hanson, L.E. and Hein, G.L. (eds.). APS Press, St. Paul, MN.
- . Hartley, R.D., Morrison, W.H., Borneman, W.S., Rigsby, L.L., O'Neill, M., Hanna, W.W., Akin, D.E. 1992. Phenolic constituents of cell wall types of normal and brown midrib mutants of pearl millet (*Pennisetum glaucum* (L) R Br) in relation to wall degradability. J Sci Food Agric, 59:211–216.
- Harveson, R.M. 2008a. Fusarium yellows and Fusarium root rot. University of Nebraska-Lincoln Extension, G1843. https://extensionpublications.unl.edu/assets/pdf/g1843.pdf
- Harveson, R.M. 2008b. Rhizoctonia root and crown rot of sugar beet. University of Nebraska-Lincoln Extension, G1841. https://extensionpublications.unl.edu/assets/pdf/g1841.pdf
- Harveson, R.M. 2013. Cercospora leaf spot of sugar beet. University of Nebraska-Lincoln Extension, G1753. https://extensionpublications.unl.edu/assets/pdf/g1753.pdf
- Harveson, R.M. 2015. Beet curly top: America's first serious disease of sugar beets. APS Features, doi:10.1094/APSFeature-2015-02.
- Hein, G.L., Boetel, M.A. and Godfrey, L.D. 2009a. Sugarbeet root maggot. Pgs. 95-97 in: Compendium of Beet Diseases and Pests (2nd ed.). Harveson, R.M., Hanson, L.E. and Hein, G.L. (eds.). APS Press, St. Paul, MN.
- Hein, G.L., Boetel, M.A. and Godfrey, L.D. 2009b. Sugarbeet root aphid. Pgs. 100-102 in: Compendium of Beet Diseases and Pests (2nd ed.). Harveson, R.M., Hanson, L.E. and Hein, G.L. (eds.). APS Press, St. Paul, MN.
- Herr, L.J. 1987. Populations of *Rhizoctonia solani* in soil under crops in rotation with sugar beet. Ann Appl Biol, 110:17-24.
- Hofman, T.W. and Jongebloed, P.H.J. 1988. Infection process of *Rhizoctonia solani* on *Solanum tuberosum* and effects of granular nematicides. Neth J Plant Pathol, 94:243-252.
- Hoffmann, C.M. 2010. Root quality of sugarbeet. Sugar Tech, 12:276-287.

- Hoffmann, C.M., Kenter, C. and Bloch, D. 2005. Marc concentration of sugar beet (*Beta vulgaris* L.) in relation to sucrose storage. J Sci Food Agr, 85:459-465.
- Howard, R.J. and Ferrari, M.A. 1989. Role of melanin in appressorium function. Exp Mycol, 13:403-418.
- Hou, S., Liu, Z., Shen, H. and Wu, D. 2019. Damage-associated molecular pattern-triggered immunity in plants. Front Plant Sci, 10:546. doi:10.3389/fpls.2019.00646
- Hughes, A.L. and Nei, M. 1989. Evolution of the major histocompatibility complex: independent origin of nonclassical class I genes in different groups of mammals. Mol Biol Evol, 6:559-579.
- Hyakumachi, M., Mushika, T., Ogiso, Y., Tdoa, T., Kageyama, K. and Tsuge, T. 1998. Characterization of a new cultural type (LP) of *Rhizoctonia solani* AG2-2 isolated from warm-season turfgrasses, and its genetic differentiation from other cultural types. Plant Pathol, 47:1-9.
- Hwang, S., Howard, R.J. and Chang, K. 1996. Forage and oilseed legume disease incited by *Rhizoctonia* species. Pgs. 289-301 in: *Rhizoctonia* species: taxonomy, molecular biology, ecology, pathology and disease control. Sneh, B, Jabaji-Hare, S., Neate, S. and Dijst, G. (eds.) Kluwer Academic Publishers, Dordrecht, The Netherlands.
- Ingram, V.M. 1961. Gene evolution and the haemoglobins. Nature, 189:704-708.
- Isaksson, A. 1942. A *Botrytis* form causing storage rot in sugar beets. P Am Soc Sugar Beet Technol, 3:423-430.
- Ithurrart, M.E.F., Büttner, G. and Petersen, J. 2004. Rhizoctonia root rot in sugar beet (*Beta vulgaris* ssp. a*ltissima*) epidemiological aspects in relation to maize (*Zea mays*) as a host plant. J Plant Dis Protect, 111:302-312.
- Jacobsen, B.J. and Franc, G.D. 2009a. Cercospora leaf spot. Pgs. 7-10 in: Compendium of Beet Diseases and Pests (2nd ed.). Harveson, R.M., Hanson, L.E. and Hein, G.L. (eds.). APS Press, St. Paul, MN.
- Jacobsen, B.J. and Franc, G.D. 2009b. Phoma leaf spot. Pgs. 11-12 in: Compendium of Beet Diseases and Pests (2nd ed.). Harveson, R.M., Hanson, L.E. and Hein, G.L. (eds.). APS Press, St. Paul, MN.
- Jones, L., Riaz, S., Morales-Cruz, A., Amrine, K.C.H., McGuire, B., Gubler, W.D., Walker, M.A. and Cantu, D. 2014. Adaptive genomic structural variation in the grape powdery mildew pathogen, *Erysiphe necator*. BMC Genomics, 15:1081. doi:10.1186/1471-2164-15-1081

- Julián, M.C., Debets, F. and Keijer, J. 1996. Independence of sexual and vegetative incompatibility mechanisms of *Thanatephorus cucumeris* (*Rhizoctonia solani*) anastomosis group 1. Phytopathology, 86:566-574.Kaczmarska, A., Pieczywek, P.M., Cybulska, J. and Zdunek, A. 2022. Structure and functionality of rhamnogalacturonan I in the cell wall and in solution: a review. Carbohyd Polym, 278:118909. doi:10.1016/j.carbpol.2021.118909
- Karr, A.L. jr. and Albersheim, P. 1970. Polysaccharide-degrading enzymes are unable to attack plant cell walls without prior action by a "wall-modifying enzyme". Plant Physiol, 46:69-80.
- Keijer, J. 1996. The initial steps of the infection process in *Rhizoctonia solani*. Pgs. 149-162 in: *Rhizoctonia* species: taxonomy, molecular biology, ecology, pathology and disease control. Sneh, B, Jabaji-Hare, S., Neate, S. and Dijst, G. (eds.) Kluwer Academic Publishers, Dordrecht, The Netherlands.
- Khan, M.F.R. and Arabiat, S. 2021. Sugarbeet cyst nematode. North Dakota State University Extension, PP1788. https://www.ndsu.edu/agriculture/ag-hub/publications/sugarbeet-cyst-nematode
- Khan, M.F.R. and Bolton, M.D. 2021. Management of Rhizoctonia root and crown rot of sugarbeet. North Dakota State University Extension, PP1495. https://www.ndsu.edu/agriculture/ag-hub/publications/management-rhizoctonia-root-and-crown-rot-sugarbeet
- Khan, A.F., Liu, Y. and Khan, M.F.R. 2017. Efficacy and safety of generic azoxystrobin at controlling *Rhizoctonia solani* in sugar beet. Crop Protect, 93:77-81.
- Kiewnick, S., Jacobsen, B.J., Braun-Kiewnick, A., Eckhoff, J.L.A. and Bergman, J.W. 2001. Integrated control of Rhizoctonia crown and root rot of sugar beet with fungicides and antagonistic bacteria. Plant Dis, 85:718-722.
- King, B.C., Waxman, K.D., Nenni, N.V., Walker, L.P., Bergstrom, G.C. and Gibson, D.M. 2011. Arsenal of plant cell wall degrading enzymes reflects host preference among plant pathogenic fungi. Biotechnol Biofuels, 4:4. doi:10.1186/1754-6834-4-4
- Kiyoshi, T., Naito, S., Akino, S., Ochi, S. and Kondo, N. 2014. Progeny derived from *Thanatephorus cucumeris* (*Rhizoctonia solani*) AG-2-2 IV isolates on sugar beet foliage show more clonal diversity in somatic compatibility grouping than those from roots and petioles. J Gen Plant Pathol, 80:136-146.
- Klemm, D., Heublein, B., Fink, H.-P. and Bohn, A. 2005. Cellulose: fascinating biopolymer and sustainable raw material. Angew Chem Int Ed, 44:3358-3393.
- Kluth, C., Buhre, C. and Varrelmann, M. 2010. Susceptibility of intercrops to infection with *Rhizoctonia solani* AG 2-2 IIIB and influence on subsequently cultivated sugar beet. Plant Pathol, 59:683-692.
- Koenick, L.B., Kikkert, J.R. and Pethybridge, S.J. 2019. Phoma leaf spot susceptibility and horticultural characteristics of table beet cultivars in New York. Plant Health Prog, 20:95-103.

- Köller, W., Allan, C.R. and Kolattukudy, P.E. 1982. Protection of *Pisum sativum* from *Fusaruim solani* f. sp. *pisi* by inhibition of cutinase with organophosphorus pesticides. Phytopathology, 72:1425-1430.
- Kou, Y. and Naqvi, N.I. 2016. Surface sensing and signaling networks in plant pathogenic fungi. Semin Cell Dev Biol, 57:84-92.
- Kohll, P., Kalla, M. and Gupta, R. 2015. Pectin methylesterases: a review. J Bioprocess Biotech, 5:5. doi:10.4172/2155-9821-1000227
- Kohorn, B.D., Kohorn, S.L., Saba, N.J. and Martinez, V.M. 2014. Requirement for pectin methyl esterase and preference for fragmented over native pectins for wall-associated kinase-activated, EDS1/PAD4-dependent stress response in *Arabidopsis*. J Biol Chem, 289:18978-18986.
- Kubicek, C.P., Starr, T.L. and Glass, N.L. 2014. Plant cell wall-degrading enzymes and their secretion in plant-pathogenic fungi. Annu Rev Phytopathol, 52:427-451.
- Kusstatscher, P., Cernava, T., Harms, K., Maier, J., Eigner, H., Berg, G. and Zachow, C. 2019. Disease incidence in sugar beet fields is correlated with microbial diversity and distinct biological markers. Phytobiomes J, 3:22-30.
- Lange, W., Brandenburg, W.A. and De Bock, T.S.M. 1999. Taxonomy and cultonomy of beet (*Beta vulgaris* L.). Bot J Linn Soc, 130:81-96.
- Latunde-Dada, A.O., O'Connell, R.J., Nash, C. and Lucas, J.A. 1999. Stomatal penetration of cowpea (*Vigna unguiculata*) leaves by a *Colletotrichum* species causing latent anthracnose. Plant Pathol, 48:777-785.
- Lažetić, V. and Troemel, E.R. 2021. Conservation lost: host-pathogen battles drive diversification and expansion of gene families. FEBS J, 288:5289-5299.
- Łaźniewska, J., Macioszek, V.K. and Kononowicz, A.K. 2012. Plant-fungus interface: the role of surface structures in plant resistance and susceptibility to pathogenic fungi. Physiol Mol Plant Pathol, 78:24-30.
- Leach, L.D. 1947. Growth rate of host and pathogen as factors determining the severity of preemergence damping-off. J Agric Res, 75:161-179.
- Li, H and Smigocki, A.C. 2018. Sugar beet polygalacturonase-inhibiting proteins with 11 LRRs confer *Rhizoctonia, Fusarium* and *Botrytis* resistance in *Nicotiana* plants. Physiol Mol Plant P, 102:200-208.
- Liao, D. 2003. Concerted evolution. Nat Enc Hum Genome, 1:938-942.
- Liu, Y., Qi, A. and Khan, M.F.R. 2019. Age-dependent resistance to *Rhizoctonia solani* in sugar beet. Plant Dis, 103:2322-2329.

- Liu, Z.L. and Sinclair, J.B. 1992. Genetic diversity of *Rhizoctonia solani* anastomosis group 2. Phytopathology, 82:778-787.
- Lombardi, N., Vitale, S., Turrà, D., Reverberi, M., Fanelli, C., Vinale, F., Marra, R., Ruocco, M., Pascale, A., d'EErrico, G., Woo, S.L. and Lorito, M. 2018. Root exudates of stressed plants stimulate and attract *Trichoderma* soil fungi. Mol Plant Microbe In, 31:982-994.
- Manian, S. and Manibhushanrao, K. 1982. Histopathological studies in rice sheath blight disease incited by *Rhizoctonia solani*. J Plant Dis Protect, 89:523-531.
- Marry, M., McCann, M.C., Kolpak, F., White, A.R., Stacey, N.J. and Roberts, K. 2000. Extraction of pectic polysaccharides from sugar-beet cell walls. J Sci Food Agr, 80:17-28.
- Marry, M., Roberts, K., Jopson, S.J., Huxham, I.M., Jarvis, M.C., Corsar, J., Robertson, E. and McCann, M.C. 2006. Cell-cell adhesion in fresh sugar-beet root parenchyma requires both pectin esters and calcium cross-links. Physiol Plantarum, 126:243-256.
- Marshall, D.S. and Rush, M.C. 1980. Infection cushion formation on rice sheaths by *Rhizoctonia solani*. Phytopathology, 70:947-950.
- Martin, F., Windels, C., Hanson, L. and Brantner, J. 2014. Analysis of population structure and pathogenicity of *Rhizoctonia solani* AG2-2 (ISG IIIB and IV) isolates from Michigan, Minnesota and North Dakota. Sugarbeet Res Rep. Beet Sugar Development Foundation, Denver, CO.
- Matsuura, K. 1986. Scanning electron microscopy of the infection process of *Rhizoctonia solani* in leaf sheaths of rice plants. Phytopathology, 76:811-814.
- Matoh, T., Takasaki, M., Takabe, K., Kobayashi, M. 1998. Immunochemistry of rhamnogalacturonan II in cell walls of higher plants. Plant Cell Physiol, 39:483-491.
- Maxson, A.C. 1938. Root-rots of the sugar beet. P Am Soc Sugar Beet Technol, 1938:60-66.
- McCartney, L. and Knox, J.P. 2001. Regulation of pectic polysaccharide domains in relation to cell development and cell properties in the pea testa. J Exp Bot, 53:707-713.
- McCarter, J.D. and Withers, S.G. 1994. Mechanisms of enzymatic glycoside hydrolysis. Curr Opin Struct Biol, 4:885-892.
- McGrath, J.M. and Townsend, B.J. 2015. Sugar beet, energy beet, and industrial beet. Pgs. 81-100 in: Industrial Crops Breeding for BioEnergy and Bioproducts. Cruz, V.V. and Dierig, D.A. (eds.). Springer, New York, NY.
- McGrath, J.M. and Panella, L. 2018. Sugar beet breeding. Pgs. 167-218 in: Plant Breeding Reviews. Goldman, I. (ed.). John Wiley & Sons, Hoboken, NJ.
- Minier, D.H. 2019. Diversity of the fungal pathogen *Rhizoctonia solani* AG 2-2. (Master's thesis). Michigan State University, East Lansing, MI. ProQuest, Ann Arbor, MI.

- Minier, D.H. and Hanson, L.E. 2020. Diversity of polygalacturonase genes in *Rhizoctonia solani* AG 2-2. (Abstr.) Phytopathology, 110:S2.1. doi:10.1094/PHYTO-110-12-S2.1
- Misaghi, I.J. 1982. Attraction to and penetration of plants by pathogens. Pgs. 5-14 in: Physiology and Biochemistry of Plant-Pathogen Interactions. Springer, Boston, MA.
- Mohnen, D. 2008. Pectin structure and biosynthesis. Curr Opin Plant Biol, 11:266-277.
- Money, N.P. 1995. Turgor pressure and the mechanics of fungal penetration. Can J Botany, 73:96-102.
- Muñoz-López, M. and Garcia-Pérez, J.L. 2010. DNA transposons: nature and applications in genomics. Curr Genomics, 11:115-128.
- Morales-Cruz, A., Amrine, K.C.H., Blanco-Ulate, B., Lawrence, D.P., Travadon, R., Rolshausen, P.E., Baumgartner, K. and Cantu, D. 2015. Distinctive expansion of gene families associated with plant cell wall degradation, secondary metabolism, and nutrient uptake in the genomes of grapevine trunk pathogens. BMC Genomics, 16:469. doi:10.1186/s12864-015-1624-z
- Mota, T.R., de Oliveira, D.M., Marchiosi, R., Ferrarese-Filho, O. and dos Santos, W.D. 2018. Plant cell wall composition and enzymatic deconstruction. AIMS Bioengineering, 5:63-77.
- Muyolo, N.G., Lipps, P.E. and Schmitthenner, A.F. 1993. Anastomosis grouping and variation in virulence among isolates of *Rhizoctonia solani* associated with dry bean and soybean in Ohio and Zaire. Phytopathology, 83:438-444.
- Muzhinji, N., Truter, M., Woodhall, J.W. and van der Waals, J.E. 2015. Anastomosis groups and pathogenicity of *Rhizoctonia solani* and binucleate *Rhizoctonia* from potato in South Africa. Plant Dis, 99:1790-1802.
- Naito, S. 1990. Ecological role of basidiospore of *Thanatephorus cucumeris* (Frank) Donk in the incidence of foliage blight of sugar beets in Japan. Japan Agr Res Q, 23:268-275.
- Naito, S. 1996. Basidiospore dispersal and survival. Pgs. 197-205 in: *Rhizoctonia* species: taxonomy, molecular biology, ecology, pathology and disease control. Sneh, B, Jabaji-Hare, S., Neate, S. and Dijst, G. (eds.) Kluwer Academic Publishers, Dordrecht, The Netherlands.
- Narula, N., Kothe, E. and Behl, R.K. 2009. Role of root exudates in plant-microbe interactions. J Appl Bot Food Qual, 82:122-130.
- Nei, M., Gu, X. and Sitnikova, T. 1997. Evolution by the birth-and-death process in multigene families of the vertebrate immune system. P Natl Acad Sci USA, 94:7799-7806.
- Nei, M. and Rooney, A.P. 2005. Concerted and birth-and-death evolution of multigene families. Annu Rev Genet, 39:121-152.

- Ninfali, P. and Angelino, D. 2013, Nutritional and functional potential of *Beta vulgaris cicla* and *rubra*. Fitoterapia, 89:188-199.
- Nguyen, Q.B., Itoh, K., Vu, B.V., Tosa, Y. and Nakayashiki, H. 2011. Simultaneous silencing of endo-β-1,4 xylanase genes reveals their roles in the virulence of *Magnaporthe oryzae*. Mol Microbiol, 81:1008-1019.
- Ogoshi, A. 1987. Ecology and pathology of anastomosis and intraspecific groups of *Rhizoctonia solani* Kühn. Annul Rev Phytopathol, 25:124-143.
- Ohkura, M., Abawi, G.S., Smart, C.D. and Hodge, K.T. 2009. Diversity and aggressiveness of *Rhizoctonia solani* and *Rhizoctonia*-like fungi on vegetables in New York. Plant Dis, 93:615-624.
- Ohta, T. 1991. Multigene families and the evolution of complexity. J Mol Evol, 33:34-41.
- Ohta, T. 2000. Evolution of gene families. Gene, 259:45-52.
- Panchy, N., Lehti-Shiu, M. and Shiu, S.-H. 2016. Evolution of gene duplication in plants. Plant Physiol, 171:2294-2316.
- Panella, L.W. and Hanson, L.E. 2006. Registration of FC720, FC722, and FC722CMS monogerm sugarbeet germplasm resistant to Rhizoctonia root rot and moderately resistant to Cercospora leaf spot. Crop Sci, 46:1009-1010.
- Panella, L.W. and Ruppel, E.G. 1996. Registration of FC725, FC726, and FC728 sugarbeet germplasms resistant to Rhizoctonia root rot and moderately resistant to Cercospora leaf spot. Crop Sci, 36:819-820.
- Pannecoucque, J. and Höfte, M. 2009. Interactions between cauliflower and *Rhizoctonia* anastomosis groups with different levels of aggressiveness. BMC Plant Biol, 9:95. doi:10.1186/1471-2229-9-95
- Park, K.-C., Kwon, S.-J., Kim, P.-H., Bureau, T. and Kim, N.-S. 2008. Gene structure dynamics and divergence of the polygalacturonase gene family of plants and fungus. Genome, 51:30-40.
- Parmeter, J.R. jr., Sherwood, R.T. and Platt, W.D. 1969. Anastomosis grouping among isolates of *Thanatephorus cucumeris*. Phytopathology, 59:1270-1278.
- Pérez, S., Rodríguez-Carvajal, M.A. and Doco, T. 2003. A complex plant cell wall polysaccharide: rhamnogalacturonan II. A structure in quest of a function. Biochimie 85:109-121.
- Pretorius, R.J., Hein, G.L. and Bradshaw, J.D. 2016. Ecology and management of *Pemphigus betae* (Hemiptera: Aphidiae) in sugar beet. J Intergr Pest Manage, 7:10. doi:10.1093/jipm/pmw008

- Pryce-Jones, E., Carver, T. and Gurr, S.J. 1999. The roles of cellulase enzymes and mechanical force in host penetration by *Erysiphe graminis* f. sp. *hordei*. Physiol Mol Plant P, 55:175-182.
- Poindexter, S. 2014. Aphanomyces root rot in sugarbeets can affect sugarbeet quality. Michigan State University Extension, January 23. https://www.canr.msu.edu/news/aphanomyces_root_rot_in_sugarbeets_can_affect_sugarbeet_quality
- Qu, P., Saldajeno, M.G.B. and Hyakumachi, M. 2013. Mechanism of the generation of new somatic compatibility groups within *Thanatephorus cucumeris* (*Rhizoctonia solani*). Microbes Environ, 28:325-335.
- Rao, J., Lv, Z., Chen, G. and Peng, F. 2023. Hemicellulose: structure, chemical modification, and application. Prog Polym Sci, 140:101675. doi:10.1016/j.progpolymsci.2023.1016
- Reddy, M.N. 1980. Studies on groundnut hypocotyl exudates and the behaviour of *Rhizoctonia solani* in influencing the disease. Plant Soil, 55:445-454.
- Ridley, B.L., O'Neill, M.A. and Mohnen, D. 2001. Pectins: structure, biosynthesis, and oligogalacturonide-related signaling. Phytochemistry, 57:929-967.
- Rooney, A.P., Piontkivska, H. and Nei, M. 2002. Molecular evolution of the nontandemly repeated genes of histone 3 multigene family. Mol Biol Evol, 19:68-75.
- Rupple, E.G. 1972. Histopathology of resistant and susceptible sugar beet roots inoculated with *Rhizoctonia solani*. Phytopathology, 63:123-126.
- Ruppel, E.G. 1985. Susceptibility of rotation crops to a root rot isolate of *Rhizoctonia solani* from sugar beet and survival of the pathogen in crop residues. Plant Dis, 69:871-873.
- Rush, C.M. 2009. Viruses transmitted by *Polymyxa betae*. Pgs. 41-46 in: Compendium of Beet Diseases and Pests (2nd ed.). Harveson, R.M., Hanson, L.E. and Hein, G.L. (eds.). APS Press, St. Paul, MN.
- Rush, C.M. and Winter, S.R. 1990. Influence of previous crops on Rhizoctonia root and crown rot of sugar beet. Plant Dis, 74:421-425.
- Salazar, O., Julian, M.C. and Rubio, V. 2000. Primers based on specific rDNA-ITS sequences for PCR detection of *Rhizoctonia solani*, *R. solani* AG2 subgroups and ecological types, and binucleate *Rhizoctonia*. Mycol Res, 104:281-285.
- Savitsky, V.F. 1950. Monogerm sugar beets in the United States. P Am Soc Sugar Beet Technol, 6:156-159.
- Scala, A., Camardella, L., Scala, F. and Cervone, F. 1980. Multiple forms of polygalacturonase in two strains of *Rhizoctonia solani*. J Gen Microbiol, 116:207-211.
- Scheller, H.V. and Ulvskov, P. 2010. Hemicellulose. Annu Rev Plant Biol, 61:263-289.

- Scheres, B., Benfey, P. and Dolan, L. 2002. Root Development. The Arabidopsis Book, 1:e0101. doi:10.1199/tab.0101.
- Schneider, C.L. and Whitney, E.D. 1986. Rhizoctonia root and crown rot. Pg. 21 in: Compendium of Beet Diseases and Insects. Whitney, E.D. and Duffus, J.E. (eds.). APS Press, St. Paul, MN.
- Schuster, M.L. and Harris, L. 1960. Incidence of Rhizoctonia crown and root rot of sugar beets in irrigated crop rotation. J Am Soc Sugar Beet Technol, 11:128-136.
- Scott, R.K. and Jaggard, K.W. 1993. Crop physiology and agronomy. Pgs. 179-237 in: The Sugar Beet Crop: Science into Practice. Cooke, D.A. and Scott, R.K. (eds.) Chapman & Hall, London, UK.
- Shallom, D. and Shoham, Y. 2003. Microbial hemicellulases. Curr Opin Microbiol, 6:219-228.
- Sharon, M., Kuninaga, S., Hyakumachi, M., Naito, S. and Sneh, B. 2008. Classification of *Rhizoctonia* spp. using rDNA-ITS sequence analysis supports the genetic basis of the classical anastomosis grouping. Mycoscience, 49:93-114.
- Sherwood, R.T. 1966. Pectin lyase and polygalacturonase production by *Rhizoctonia solani* and other fungi. Phytopathology, 56:279-286.
- Smith, G.A. and Fehr, W.R. 1987. Principals of cultivar development. Crop Species: Sugar Beet, 2:577-625.
- Smith, H.J., Gray, F.A. and Koch, D.W. 2004. Reproduction of *Heterodera schachtii* Schmidt on resistant mustard, radish, and sugar beet cultivars. J Nematol, 36:123-130.
- Smith, S.D., Pennell, M.W., Dunn, C.W. and Edwards, S.V. 2020. Phylogenetics is the new genetics (for most of biodiversity). Trends Ecol Evol, 35: 415-425.
- Sneh, B., Burpee, L. and Ogoshi, A. 1991. Identification of *Rhizoctonia* Species. APS Press, St. Paul, MN.
- Sprockett, D.D., Piontkivska, H. and Blackwood, C.B. 2011. Evolutionary analysis of glycosyl hydrolase family 28 (GH28) suggests lineage-specific expansions in necrotrophic fungal pathogens. Gene, 479:29-36.
- Strausbaugh, C.A. 2016. *Leuconostoc* spp. associated with root rot in sugar beet and their interaction with *Rhizoctonia solani*. Phytopathology, 106:432-441.
- Strausbaugh, C.A. 2018. Incidence, distribution, and pathogenicity of fungi causing root rot in Idaho long-term sugar beet storage piles. Plant Dis, 102:2296-2307.
- Strausbaugh, C.A. and Dugan, F. 2017. A novel *Penicilium* sp. causes root rot in stored sugar beet root in Idaho. Plant Dis, 101:1781-1787.

- Strausbaugh, C.A., Eujayl, I. and Foote, P. 2013. Selection for resistance to the Rhizoctonia-bacterial root rot complex in sugar beet. Plant Dis, 97:93-100.
- Strausbaugh, C.A., Eujayl, I.A., Panella, L.A. and Hanson, L.E. 2011a. Virulence, distribution and diversity of *Rhizoctonia solani* from sugar beet in Idaho and Oregon. Can J Plant Pathol, 33:210-226.
- Strausbaugh, C.A., Rearick, E., Eujayl, I. and Foote, P. 2011b. Influence of root rot on storage. J bSugar Beet Res, 48:155-180.
- Sumner, D.R. 1996. Sclerotia formation by *Rhizoctonia* species and their survival. Pgs. 207-215 in: *Rhizoctonia* species: taxonomy, molecular biology, ecology, pathology and disease control. Sneh, B, Jabaji-Hare, S., Neate, S. and Dijst, G. (eds.) Kluwer Academic Publishers, Dordrecht, The Netherlands.
- Sumner, D.R. and Bell, D.K. 1982. Root diseases induced in corn by *Rhizoctonia solani* and *Rhizoctonia zeae*. Phytopathology, 72:86-91.
- Sumner, D.R., Doupnik, B., Jr., and Boosalis, M.G. 1981. Effects of reduced tillage and multiple cropping on plant diseases. Annu Rev Phytopathol, 19:167-187.
- Talbot, N.J. 2019. Appressoria. Curr Biol, 29:R144-R146.
- Talbot, P.H.B. 1970. Taxonomy and nomenclature of the perfect state. Pgs. 20-31 in: *Rhizoctonia solani*, biology and pathology. Parmeter, J.R. (ed.) University of California Press, Berkely, CA.
- Tenhaken, R. 2015. Cell wall remodeling under abiotic stress. Front Plant Sci, 5:771. doi:10.3389/fpls.2014.00771
- Teeri, T.T. 1997. Crystalline cellulose degradation: new insight into the function of cellobiohydrolases. Trends Biotechnol, 15:160-167.
- Tibbits, C.W., MacDougall, A.J. and Ring, S.G. 1998. Calcium binding and swelling behavior of a highly methoxyl pectin gel. Carbohyd Res, 310:101-107.
- Toda, T and Hyakumachi, M. 2006. Heterokaryon formation in *Thanatephorus cucumeris* anastomosis group 2-2 IV. Mycologia, 98:726-736.
- Trebbi, D. and McGrath, J.M. 2009. Functional differentiation of the sugar beet root system as indicator of developmental phase change. Physiol Plantarum, 135:84-97.
- Van Driessche, R. 2012. Michigan sugar company "Ten years of progress". Sugar Prod Mag, March 2012:12.
- Van Vu, B., Itoh, K., Nguyen, Q.B., Tosa, Y. and Nakayashiki, H. 2012. Cellulases belonging to glycoside hydrolase families 6 and 7 contribute to the virulence of *Magnaporthe oryzae*. Mol Plant Microbe In, 25:1135-1141.

- Verma, P.R. 1996. Oilseed rape and canola diseases incited by *Rhizoctonia* species. Pgs. 249-258 in: *Rhizoctonia* species: taxonomy, molecular biology, ecology, pathology and disease control. Sneh, B, Jabaji-Hare, S., Neate, S. and Dijst, G. (eds.) Kluwer Academic Publishers, Dordrecht, The Netherlands.
- Volpi, C., Janni, M., Lionetti, V., Bellincampi, D., Favaron, F. and D'Ovidio, R. 2011. The ectopic expression of a pectin methyl esterase inhibitor increases pectin methyl esterification and limits fungal diseases in wheat. Mol Plant Microbe In, 24:1012-1019.
- Voragen, A.G.J., Coenen, G., Verhoef, R.P. and Schols, H.A. 2009. Pectin, a versatile polysaccharide present in plant cells. Struct Chem, 20:263-275.
- Voxeur, A., Gilbert, L., Rihouey, C., Driouich, A., Rothan, C., Baldet, P. and Lerouge, P. 2011. Silencing of the GDP-D-mannose 3,5-epimerase affects the structure and cross-linking of the pectic polysaccharide rhamnogalacturonan II and plant growth in tomato. J Biol Chem, 286:8014-8023.
- Waldron, K.W., Ng, A., Parker, M.L. and Parr, A.J. 1999. Ferulic acid dehydrodimers in the cell walls of *Beta vulgaris* and their possible role in texture. J Sci Food Agr, 74:221-228.
- Wang, Z.-Y., Jenkinson, J.M., Holcombe, L.J., Soanes, D.M., Veneault-Fourrey, C., Bhambra, G.K. and Talbot, N.J. 2005. The molecular biology of appressorium turgor pressure generation by the rice blast fungus *Magnaporthe grisea*. Biochem Soc Trans, 33:384-388.
- Weinhold, A.R. and Sinclair, J.B. 1996. *Rhizoctonia solani*: penetration, colonization, and host response. Pgs. 163-174 in: *Rhizoctonia* species: taxonomy, molecular biology, ecology, pathology and disease control. Sneh, B, Jabaji-Hare, S., Neate, S. and Dijst, G. (eds.) Kluwer Academic Publishers, Dordrecht, The Netherlands.
- Wenninger, E.J., Daley, T.B., Neher, O.T. and Bechinski, E.J. 2019. Sugar beet root maggot: Identification, biology, and management. University of Idaho Extension, Bulletin 942. https://www.uidaho.edu/-/media/UIdaho-Responsive/Files/Extension/publications/bul/bul942.pdf
- Westerdahl, B.B. and Becker, J.O. 2016. Nematodes. UC IPM Pest Management Guidelines: Sugarbeet, UC ANR Publication 3469. https://ipm.ucanr.edu/agriculture/sugarbeet/nematodes/
- Wibberg, D., Andersson, L., Tzelepis, G., Rupp, O., Blom, J., Jelonek, L., Pülher, A., Fogelqvist, J., Varrelmann, M., Schlüter, A. and Dixelius, C. 2016. Genome analysis of the sugar beet pathogen *Rhizoctonia solani* AG2-2IIIB revealed high numbers in secreted proteins and cell wall degrading enzymes. BMC Genomics, 17:245. doi:10.1186/s12864-016-2561-1
- Willats, W.G.T., McCartney, L., Mackie, W. and Knox, J.P. 2001. Pectin: cell biology and prospects for functional analysis. Plant Mol Biol, 47:9-27.
- Wilson, R.G. 2013. Crop Rotation. Pgs. 25-26 in: Sugarbeet Production Guide. Wilson, R., Miller, S. and Smith, J. (eds.) University of Nebraska-Lincoln Extension. EC156.

- Windels, C.E. and Brantner, J.R. 2005. Crop rotation effects on *Rhizoctonia solani* AG 2-2. Sugarbeet Res Ext Rep, 36:288-290.
- Windels, C.E. and Brantner, J.R. 2008. *Rhizoctonia* on sugarbeet following rotational crops. Sugarbeet Res Ext Rep, 38:272-280.
- Windels, C.E. and Harveson, R.M. 2009. Aphanomyces root rot. Pgs. 24-27 in: Compendium of Beet Diseases and Pests (2nd ed.). Harveson, R.M., Hanson, L.E. and Hein, G.L. (eds.). APS Press, St. Paul, MN.
- Windels, C.E., Jacobsen, B.J. and Harveson, R.M. 2009. Rhizoctonia root and crown rot. Pgs. 33-36 in: Compendium of Beet Diseases and Pests (2nd ed.). Harveson, R.M., Hanson, L.E. and Hein, G.L. (eds.). APS Press, St. Paul, MN.
- Windels, C.E. and Nabben, D.J. 1989. Characterization and pathogenicity of anastomosis groups of *Rhizoctonia solani* isolated from *Beta vulgaris*. Phytopathology, 79:83-88.
- Winner, C. 1993. History of the crop. Pgs. 1-35 in: The Sugar Beet Crop: Science into Practice. Cooke, D.A. and Scott, R.K. (eds.) Chapman & Hall, London, UK.
- Wintermantel, W.M. 2009. Curly top. Pgs. 51-53 in: Compendium of Beet Diseases and Pests (2nd ed.). Harveson, R.M., Hanson, L.E. and Hein, G.L. (eds.). APS Press, St. Paul, MN.
- Wolf, S. and Greiner, S. 2012. Growth control by cell wall pectins. Protoplasma, 249:S169-S175.
- Worral, J.J. 1997. Somatic incompatibility in basidiomycetes. Mycologia, 89:24-36.
- Wu, H.-C., Bulgakov, V.P. and Tsung-Luo, J. 2018. Pectin methylesterases: cell wall remodeling proteins are required for plant responses to heat stress. Front Plant Sci, 9:1612. doi:10.3389/fpls.2018.01612
- Yadav, S., Yadav, P.K., Yadav, D. and Yadav, K.D.S. 2009. Pectin lyase: a review. Process Biochem, 44:1-10.
- Yanar, Y., Yilmaz, G., Cesmeli, I. and Coskun, S. 2005. Characterization of *Rhizoctonia solani* isolates from potatoes in Turkey and screening potato cultivars for resistance to AG-3 isolates. Phytoparasitica, 33:370-376.
- Yang, J., Verma, P.R. and Tewari, J.P. 1992. Histopathology of resistant mustard and susceptible canola hypocotyls infected by *Rhizoctonia solani*. Mycol Res, 96:171-179.
- Yapo, B.M. 2011. Rhamnogalacturonan-I: a structurally puzzling and functionally versatile polysaccharide from plant cell walls and mucilages. Polym Rev, 51:391-413.
- Zhang, Z. and Gerstein, M. 2003. The human genome has 49 cytochrome *c* pseudogenes, including a relic of a primordial gene that still functions in mouse. Gene, 312:61-72.

- Zhang, X.Y., Huo, H.L., Xi, X.M., Liu, L.L., Yu, Z and Hao, J.J. 2016. Histological observation of potato in response to *Rhizoctonia solani* infection. Eur J Plant Pathol, 145:289-303.
- Zheng, L., Xu,. Y., Li, Q. and Zhu, B. 2021. Pectinolytic lyases: a comprehensive review of sources, category, property, structure, and catalytic mechanism of pectate lyases and pectin lyases. Bioresour Bioprocess, 8:79. doi:10.1186/s40643-021-00432-z
- Zheng, A. and Wang, Y. 2011. The research of infection process and biological characteristics of *Rhizoctonia solani* AG-1 IB on soybean. J Yeast Fungal Res, 2:93-98.
- Zykwinska, A.W., Ralet, M.-C. J., Garnier, C.D. and Thibault, J.-F. J. 2005. Evidence for in vitro binding of pectin side chains to cellulose. Plant Physiol, 139:397-407.

CHAPTER 2:

Introduction

Rhizoctonia root and crown rot (RRCR), caused by *Rhizoctonia solani* Kühn (teleomorph: *Thanatephorus cucumeris* Donk), is a major soil-borne disease of sugar beet (*Beta vulgaris*) that occurs in growing regions throughout the world (Windels et al. 2009). The disease is characterized by dark, shallow lesions on the root with sharply defined margins (Neher & Gallian 2011; Windels et al. 2009). As the disease progresses, the lesions expand and can eventually involve the entire root causing yield loss, reduced sucrose content, and increased susceptibility to storage rots (Strausbaugh et al. 2011b; Windels et al. 2009). In addition to variety selection, cultivation practices, and fungicide applications, rotation with non-host crops is one of the most important management strategies for controlling losses to RRCR (Kirk et al. 2008; Neher & Gallien 2011). Unfortunately, many of the crops commonly grown in rotation with sugar beet are also susceptible to many of the same strains that cause RRCR, which makes rotation choices challenging.

Rhizoctonia solani is a fungal species complex whose members can be distinguished by their ability to anastomose, or fuse, with other members of the same anastomosis group (AG; Cubeta & Vigalys 1997; Parmeter et al. 1969). Anastomosis groups within *R. solani* represent independent evolutionary lineages that are reproductively isolated but have yet to be separated into taxonomic species (Cubeta et al. 1991; Hanson & Minier 2016; McCabe et al. 1999). The major challenge in resolving *R. solani* taxonomy lies in the lack of consistent morphological characters, particularly the lack of asexual conidia and in several AG, the lack of, or at best, a very rarely observed sexual stage (*Thanatephorus cucumeris*). Since anastomosis groups are defined by the ability of members to anastomose with one another and not with members of other AG, the most reliable method of determining the AG of an individual isolate is to pair the

unknown isolate with a tester isolate of known AG and determine hyphal fusion frequency (Adams 1988; Carling 1996; Parmeter et al. 1969). However, interpreting anastomosis reactions is not always straightforward due to the challenge of reproducibility and the rather subjective nature of analyzing hyphal behavior (Cubeta & Vigalys 1997). In addition, some AG can anastomose with members of another AG at a low frequency (Sneh et al. 1991), creating additional uncertainty in the assignment of AG.

Several AGs contain well-defined cultural types, referred to as intraspecific groups (ISG), that have been separated based on a variety of characteristics such as DNA hybridization, sclerotia size and shape, pectic zymography patterns, or temperature tolerance (MacNish & Sweetingham 1993; Sharon et al. 2008; Sneh et al. 1991; Vilgalys & Cubeta 1994). Accurately determining ISG can be difficult especially with techniques such as DNA hybridization and zymography. While genetic data has been effective at separating the ISGs of some AGs, such as those of AG 4 and AG 1 (Kuninaga & Yokosawa 1985; Liu & Sinclair 1993; Sharon et al. 2008), there has been inconsistencies in other AG, such as AG 2-2, the primary causal agent of RRCR (Minier 2019; Sharon et al. 2008; Strausbaugh et al. 2011a).

Traditionally AG 2-2 has been separated into three ISGs; AG 2-2IIIB, AG 2-2IV, and AG 2-2LP. These groups were originally separated based on host range with AG 2-2IIIB affecting mat rush (*Juncus effusus*), AG 2-2IV affecting sugar beet (Ogoshi 1987), and AG 2-2LP affecting zoysia grass (*Zoysia* spp.; Hyakumachi et al. 1998). While AG 2-2LP has been relatively consistent in relation to host, AG 2-2IIIB and AG 2-2IV are both known to affect sugar beet and host preference no longer defines or distinguishes the two groups (Sneh et al. 1991). Instead, AG 2-2IIIB and AG 2-2IV are commonly separated based on growth at 35°C, where AG 2-2IIIB grows at 35°C and AG 2-2IV does not (Sneh et al. 1991). While DNA

homology has been reported to separate these groups (Sneh et al. 1991), the genetic relationship based on rRNA-ITS has been inconsistent and the monophyly of these subgroups is questionable (Carling et al. 2002; Sharon et al. 2008; Strausbaugh et al. 2011a).

Despite the inconsistencies, interest in retaining the subgroups of AG 2-2 as 'IIIB' and 'IV' has remained high, primarily due to evidence of variation in virulence and host interactions related to the subgroups (Cappelli et al. 1999; Engelkes & Windels 1996; Strausbaugh et al. 2011a). For example, corn has been shown to increase the prevalence of more aggressive strains, particularly those in AG 2-2IIIB, resulting in increased damage to sugar beet after rotation with corn (Ithurrart et al. 2004; Windels & Brantner 2004; Windels & Brantner, 2006). Since crop rotation is an important component in the management of RRCR, understanding how fungal populations are affected by crop rotation strategies is essential for making effective disease management decisions (Windels et al. 2009).

Little is known about the population biology of *R. solani* AG 2-2 primarily due to its complicated taxonomy and the limited range of reliable vegetative characteristics that can be used for identification and classification (Ajayi-Oyetunde & Bradley 2018; Vilgalys & Cubeta 1994). Consequently, the development of efficient molecular methods for evaluating *R. solani* AG 2-2 populations is a necessity. Several molecular tools have been developed for use in *R. solani* population biology, including inter-simple sequence repeats (ISSR; Zheng et al. 2013), allozymes (Liu et al. 1990; Pannecoucque et al. 2008), restriction fragment length polymorphisms (RFLP; Hyakumachi et al. 1998; O'Brien 1994), and genotyping by sequencing (GBS; Ajayi-Oyetunde et al. 2019). ISSR markers are dominant and so can lack information on heterozygosity and there is concern about reproducibility between labs, as the results can be difficult to interpret (Grover & Sharma 2016; Ng & Tan 2015). Allozyme and RFLP techniques

rely on the analysis of electrophoresis gels and the interpretation of complex banding patterns, which requires experienced personnel (Parker et al. 1998). Besides being laborious, allozymes and RFLPs may lack sufficient polymorphism to make identification of individuals practical in most systems and developing large enough libraries to address this would be cost prohibitive (Parker et al. 1998). RFLPs do not provide information about heterozygosity and allozymes may not be selectively neutral making both markers less than idea for population genetics especially when markers exist that can overcome these disadvantages.

Genotype by sequence (GBS) is one of the more modern genotyping techniques that relies on restriction enzymes to reduce genomic complexity and next-generation sequencing to identify large numbers of single nucleotide polymorphisms (SNPs). While GBS can be a powerful tool for SNP discovery and genotyping, analysis of data can require a considerable investment of time for the evaluation of large populations (Hodel et al. 2016). There is also a concern for large amounts of missing data and therefore, transferability between studies (Hodel et al. 2016). With the strengths and limitations in currently available genetic tools, our goal for the current study was to develop a marker set that was robust, reproducible, and co-dominant while remaining inexpensive and easy to analyze, even for large studies.

Microsatellites, or simple sequence repeats (SSR), are widely accepted as an effective molecular tool for examining intraspecific variation and fulfill the objectives for a suitable marker type (Ellegren 1991; Ellegren 2004; Jefferies et al. 1985; Schlötterer et al. 1991; Tautz 1989). Numerous studies have used microsatellites to investigate important factors such as mating type (Biasi et al. 2016), disease dynamics (dos Santos Pereira et al. 2017) and population structure (Vaghefi et al. 2017; Wang & Chilvers 2016). Microsatellite marker sets have been developed for *R. solani* AG 1-1A (Zala et al. 2008), AG 3 (Ferrucho et al. 2009), and AG 4

(Haratian et al. 2013) and have been used successfully to examine *R. solani* populations on potato (Ferruch et al. 2013; Muzhinji et al. 2016), soybean (Ciampi et al. 2008) and on various crops in Iran (Haratian et al. 2013). Microsatellite markers have yet to be developed for use on AG 2-2 populations and those published for use in other AGs were not effective for the AG 2-2 isolates screened (Frank Martin, personal communication).

Traditionally, the identification of candidate microsatellite loci relies on constructing genomic DNA libraries that have been enriched for SSR sequences (Edwards et al. 1996; Hodel et al. 2016; Novelli et al. 2013; Selkoe & Toonen 2006; Zane et al. 2002). In the current study, we utilized NextGen sequencing (NGS) to identify candidate microsatellite loci, screened those loci for suitability, and developed a high-throughput screening protocol using automatic fragment size detection. In addition, we developed a marker set for phylogenetic analysis in order to clarify the relationship of the subgroups within AG 2-2. Results of the current study provide much-needed tools for improving our understanding of the structure, distribution, and dynamics of *R. solani* AG 2-2 populations. A more thorough and accurate assessment of *R. solani* AG 2-2 populations may prompt the recognition and development of novel management strategies that reduce the impact of RRCR of sugar beet and rhizoctonia root rot of other crops.

Materials and Methods

Fungal material

Fungal isolates (Table 2.1) were obtained from the collection of Dr. Linda Hanson (USDA-ARS, East Lansing, MI) which had been stored on dried barley grains at -20°C (Naito et al. 1993). Infested barley grains were recovered from storage, placed on potato dextrose agar (PDA,

Sigma-Aldrich, St. Louis, MO) and allowed to grow for 5 to 7 days at room temperature.

Cultures were inspected for contamination prior to transfer or use in subsequent procedures.

DNA extraction

Isolates were grown in static culture on malt-extract broth (MEB; Sigma-Aldrich, St. Louis, MO) in a petri dish for 5 to 7 days at room temperature (20 – 22°C). The mycelial mat was harvested using forceps, placed in a sterile 50 mL centrifuge tube, and rinsed twice with phosphate buffered saline (PBS; Cold Spring Harb Protocol 2006, doi:10.1101/pdb.rec8247). Fungal tissue was lyophilized (VirTis Genesis, SP Scientific, Warminster, PA) and ground in a modified paint shaker using 6 mm ceramic beads (Zircoa, Inc., Solon, OH).

DNA extractions from *R. solani* proved challenging due to the presence of what appeared to be exopolysaccharides that clogged column-based kits and inhibited PCR. A modified protocol based on the OmniPrep for Fungi kit (G-Biosciences, St. Louis, MO) was developed for extracting genomic DNA from lyophilized, ground fungal tissue that yielded DNA suitable for use in PCR amplification and for Illumina sequencing. Approximately 20 - 25 mg of ground, lyophilized tissue was added to a 2 mL microcentrifuge tube, rinsed twice with 1 mL PBS and centrifuged at 6,500 x g for 10 min. to remove soluble contaminants. After extraction with 500 μL chloroform/isoamyl alcohol (24:1), samples were treated with 5 μl RNase-A (5 μg/μl) for 30 minutes at room temperature and extracted a second time with 500 μL chloroform/isoamyl alcohol (24:1). The aqueous phase was treated with Stripping Solution and Precipitation Solution provided with the OmniPrep for Fungi kit as described in the manufacturer's instructions.

Genomic DNA was precipitated with 500 μl of 100% isopropyl alcohol, pelletized by centrifugation at 12,000 x g for 5 min, and suspended in 450 μL Tris-EDTA (TE) buffer (Cold

Table 2.1 Rhizoctonia solani isolates used in the current study including for which aspects of the study the isolate was used.

Isolate	Original Name	AG	Proposed subgroup	Host	Origina	Collector	Seq ^c	Phylog ^d	Geno
Rs850	Rs 07-102-2 850	2-2IIIB	PR	Sugar beet	MN	C. Windels			S
Rs866	Rs 07-110-2 866	2-2IIIB	BR	Sugar beet	MN	C. Windels		X	\mathbf{S}
C-116S	C-116S	2-2IIIB	PR	Sugar beet	Japan	A. Ogoshi	X	X	X
F30	F30	2-2IIIB	PR	Sugar beet	ID	C. Strausbaugh	X	X	X
Italien	Italien	2-2IIIB	BR	Sugar beet	Europe ^b	B. Holtschulte	X	X	X
R1	R1	2-2IIIB	BR	Sugar beet	CO	E. Ruppel	X	X	X
R4	R4	2-2IIIB	BR	Sugar beet	TX	C. Rush	X	X	X
R9	R9	2-2IIIB	BR	Sugar beet	CO	E. Ruppel	X	X	X
Rs1012	Rs 08-16-1 1012	2-2IIIB	PR	Sugar beet	MN	C. Windels	X	X	X
Rs1146	Rs 08-87-1 1146	2-2IIIB	PR	Sugar beet	MN	C. Windels	X	X	X
Slovakia	Slovakia	2-2IIIB	PR	Sugar beet	Europe ^b	B. Holtschulte	X	X	X
W-22	W-22	2-2IIIB	BR	Bean root	WI	R.T. Sherwood	X	X	X
F321	F321	2-2IIIB	PR	Sugar beet	ID	C. Strausbaugh	X	X	
Rickard	Rickard	2-2IIIB	PR	Sugar beet	Europe ^b	B. Holtschulte		X	
2C1	2C1	2-2IIIB	PR	-	MT	B. Bugbee			X
F508	F508	2-2IIIB	BR	Sugar beet	ID	C. Strausbaugh			X
F517	F517	2-2IIIB	PR	Sugar beet	ID	C. Strausbaugh			X
F521	F521	2-2IIIB	BR	Sugar beet	ID	C. Strausbaugh			X
F551	F551	2-2IIIB	PR	Sugar beet	ID	C. Strausbaugh			X
Rs255	Rs 06-28-3 255	2-2IIIB	PR	Sugar beet	MN	C. Windels			X
Rs331	Rs 06-64-4 331	2-2IIIB	PR	Sugar beet	MN	C. Windels			X
Rs890	Rs 07-122-1 890	2-2IIIB	BR	Sugar beet	MN	C. Windels			X
Rs588	Rs 60-245-1 588	2-2IV	BR	Sugar beet	MN	C. Windels			\mathbf{S}
2C13	2C13	2-2IV	BR	-	MT	B. Bugbee	X	X	X
R-164S	R-164S	2-2IV	BR	Sugar beet	Japan	A. Ogoshi	X	X	X
Rs200	Rs 05-132-2 200	2-2IV	BR	Sugar beet	MN	C. Windels	X	X	X
Rs496	Rs 06-221-3 496	2-2IV	BR	Sugar beet	MN	C. Windels	X	X	X
Rs296	Rs 06-49-4 296	2-2IV	BR	Sugar beet	MN	C. Windels	X	X	
5C5	5C5	2-2IV	BR	Sugar beet	MN	B. Bugbee		X	
Rs300	Rs 06-54-3 300	2-2IV	BR	Sugar beet	MN	C. Windels		X	
Rs393	Rs 06-79-1 393	2-2IV	PR	Sugar beet	MN	C. Windels		X	X
RH188	RH188	2-2IV	BR	Sugar beet	Japan	H. Obihiro			X
RH193	RH193	2-2IV	BR	Sugar beet	Japan	H. Obihiro			X
Rs106	Rs 05-43-1 106	2-2IV	BR	Sugar beet	MN	C. Windels			X
Rs481	Rs 06-218-2 481	2-2IV	BR	Sugar beet	MN	C. Windels			X

a. Locale of isolation, abbreviations are standard for US states

b. Precise location is unknown – name of isolates from Europe does not necessarily reflect region from which they were isolated

c. Isolate genome was sequenced and assembled from Illumina paired-end reads

d. Isolate was included in the multi-gene phylogenetic analysis
e. Isolate was genotyped using 13 microsatellite markers. 'S' indicates isolate was used for initial identification of microsatellite loci

Table 2.1 Con't

Isolate	Original Name	AG	Proposed subgroup	Host	Origin ^a	Collector	Seq ^c	Phylog ^d	Geno ^e
Rs542	Rs 06-231-1 542	2-2IV	BR	Sugar beet	MN	C. Windels			X
ACC3-LP	ACC3 2-2LP	2-2LP	LP	-	-	-	X	X	X
R09-23	R09-23	2-2 (Int)	PR	Sugar beet	MI	L. Hanson	X	X	X
R09-25	R09-25	2-2 (Int)	BR	Sugar beet	MI	L. Hanson	X	X	X
24BR	24BR	2-2 (Int)	PR	Sugar beet	Canada	C. Truman			X
39AR	39AR	2-2 (Int)	PR	Sugar beet	Canada	C. Truman			X
R-5	R-5	4	-	Sugar beet	CO	E, Ruppel	X	X	
Rs14-2	Rs_14-2	5	-	Dry bean	MI	J. Jacobs	X	X	
ST6-1	ST6-1	5	-	Sugar beet	Japan	A, Ogoshi	X	X	

Spring Harb Protocol 2009, doi:10.1101/pdb.rec11601). A second DNA precipitation was performed by adding 45 µL 5M sodium acetate (pH 5.2) and 1 mL 100% ethanol and incubating at 4°C overnight. DNA was pelletized by centrifugation at 12,000 x g for 5 min. and then washed twice with 70% ethanol. The pellet was air dried and suspended in 50 µL TE buffer.

In order to minimize shearing of the DNA, samples were mixed by inversion at all steps except the initial PBS rinses where samples were mixed by vortexing to facilitate removal of soluble compounds. Transfers of sample volumes containing genomic DNA were performed using large-orifice pipette tips. While the OmniPrep for Fungi kit recommends only a single chloroform extraction, a second chloroform extraction proved beneficial as it reduced contamination as determined by spectrophotometry (Nanodrop ND-8000, Thermo Fisher Scientific, Waltham, MA). DNA quantities were assessed using a Qubit 3.0 fluorometer (Thermo Fisher Scientific).

Microsatellite marker identification and evaluation

Prospective microsatellite loci were identified *in-silico* from the genome sequences of three *R. solani* AG 2-2 isolates (Table 2.1) selected to represent each of the three genetic groups identified in the preliminary work reported by Martin et al. (2014). The genomic libraries of

isolates 'Rs850' (Martin et al. group 1), 'Rs866' (Martin et al. group 2A) and 'Rs588' (Martin et al. group 2B) were indexed and combined in a single run on an Illumina HiSeq4000 (Illumina Inc., San Diego, CA) at the Michigan State University Genomics Core (MSU-GC; East Lansing, MI). Raw sequences were assembled using CLC Genomic Workbench v.9 (Qiagen, Redwood City, CA) using default settings. Since isolate 'Rs850' was used for the initial sequence for marker selection, additional efforts were made to improve assembly quality. After the first assembly in CLC Genomics Workbench, the 'Rs850' assembly was filtered to discard contigs with less than 15X coverage. Filtered contigs were exported to SeqMan NGen v.15 (DNASTAR, Inc., Madison, WI) and Illumina reads mapped to assembled contigs in four cycles to extend to ends. Resulting contigs were imported back into CLC Genomics Workbench where a final *de novo* assembly with all contigs and Illumina reads was performed using high stringency (96% identity).

Initial marker selection was accomplished using BatchPrimer3 (You et al. 2008) to identify simple sequence repeats in isolate 'Rs850'. Search parameters were set to exclude dinucleotide repeats and limit putative fragment sizes to between 100 and 250 bp. Potential marker loci for 'Rs850' were compared to the assemblies of the other two isolates to determine suitability based on differences in the number of repeat units, indels in the flanking regions and that primer design was appropriate for all three lineages. Loci with problems based on these evaluations were discarded, and the next potential marker on the contig was evaluated until 33 putative markers were catalogued. Only one locus was selected from an assembled contig to minimize linkage.

Annealing temperature (T_a) for the thirty-three potential markers was predicted with Thermo Fisher's online Tm calculator (https://www.thermofisher.com) using Phusion polymerase parameters. Primer pairs with a predicted T_a value between 58°C and 61°C were selected and

amplification conditions were optimized using isolates 'Rs850', 'Rs866' and 'Rs588'. Four MgCl₂ concentrations (1.5, 2.0, 2.5 and 3.0 mM) were examined with no noticeable differences in amplification quality observed. Therefore, a MgCl₂ concentration of 2.5 mM was used for all subsequent reactions.

Multiplex PCR conditions and analysis

Six additional isolates were evaluated for: amplification across all lineages, band intensity, noticeable size differences between isolates, and suitability for multiplexing. Sixteen polymorphic loci that amplified for all nine isolates were selected and fluorescently labeled for automatic fragment sizing. Forward primers were labeled with either 6-FAM or HEX fluorescent dyes (Integrated DNA Technologies, Coralville, IA) for use in duplex analysis (Table 2.2). Reverse primers were assessed with and without a 5' GTTT- PIG tail (Brownstein et al. 1996) to evaluate effectiveness at reducing the incidence of stutter peaks.

Fluorescently labeled PCR products were evaluated on a total of 23 isolates using an Applied Biosystems 3130 genetic analyzer (Applied Biosystems; Foster City, CA) by the MSU-GC. GeneScan 400HD-ROX (Applied Biosystems) was used as the size standard. Loci were evaluated for: consistency of the fragment length patterns with repeat unit, the presence of stutter peaks, failure to amplify, and potential overlap in allele sizes of duplexed loci. Primer concentrations were adjusted to provide similar levels of fluorescent signal for all loci and fluorescent dyes.

Table 2.2 Microsatellite loci evaluated in the current study for use on *Rhizoctonia solani* AG 2-2. The 5' end of the forward primers were labeled with either HEX or 6-FAM fluorophores for automatic sizing. Amplicon length indicates the range of fragment lengths across all 13 loci. Primer concentrations were adjusted to the values in the 'conc. μM' column to yield similar fluorescent peak levels in multiplexed reactions.

T a	Repeat	Amplicon	D	Primer sequ	uences 5' -> 3'	conc
Locus ^a	motif	length	Dye	Forward	Reverse	(μΜ)
2547 (a)	AACA	214-222	6-FAM	AATCRCTCGAATCGGTAATT	ATCGGGAATCATACTACCGG	0.1
4660 (a)	CGA	132-159	HEX	GTRATGGTGAGAGTGAGAGAA	CTCSTCGTCTGAAGAGTCATA	0.45
5583 (b)	AGA	182-200	6-FAM	CGTCGAGGATCTCAAATATGT	TTGCTAATGGTTCCTTTACTG	0.1
5487 (b)	ACG	132-141	HEX	ATACCGAGAGTGTCTTTACSC	AAAACGACTGGGGAGGAA	0.3
759 (c)	CAG	131-170	6-FAM	CAACAGCACGCCMTYATG	CAGAGGGYAATTGTTGTTGAA	0.35
6145 (c)	CAG	146-161	HEX	ATGCAGATGGTTTTGTACG	CTAGAGATCGATGCTGTCT	0.3
8703 (d)	GTT	203-221	6-FAM	TGRGGTGGKGGATGTATTG	TCTCGGTCRAGTTACAATGG	0.2
6150 (d)	TTTC	130-166	HEX	TGATATCACCACATTCTTTSA	CRATTGACGGTCTACTGTTGY	0.25
5402	TCG	138-156	HEX	CCATACGCTCATACTTGAGAC	CGTAGACGAAAGTGGAMRTAG	0.3
7420	CGA	170-176	6-FAM	TATCARGCAAACTTRACCAAT	AGACCACTCTACGAACCTTGY	0.2
2893	GGTGTT	116-143	HEX	CAGCTGGYGTAGTAGAAGTGG	GAATCRACRCCRGCAGTAGA	0.45
1656	CAT	131-152	6-FAM	ATTCRGAACACTGGTTTGARC	CCTAACTTGAACCAGACGAY	0.3
7676	GTT	176-188	6-FAM	GAAYGGCGAGTCGTAGTG	GTGGAACAAGTAYCAAACGTC	0.3

a. Loci followed by the same letter were paired in a duplex reaction for 8 locus genotyping

Final reactions were performed in 20μl volumes with 15ng of DNA template, 1 x Phusion II HF buffer, 200μM each dNTP, 2.5mM total MgCl₂ and 1 unit of Phusion II HF polymerase (Thermo Fisher). Final primer concentrations used for each marker are shown in Table 2.2. PIGtailed reverse primers were unnecessary for reducing stuttering and unmodified reverse primers were used for all subsequent runs. Final PCR conditions consisted of 1 cycle of 98°C for 2 min. followed by 27 cycles of 98°C for 20 s, 57°C for 20 s, 72°C for 12 s and a final extension cycle of 72°C for 5 min. Samples were diluted 1:50 with sterile distilled water prior to submission to MSU-GC.

Cloning

Marker quality was assessed by cloning ten loci from seven isolates. Cloned loci were sequenced, examined for errors, and compared to data generated by automatic fragment sizing. Ten additional isolates that had potential issues at specific loci that had been noted during the examination of chromatograms, were cloned, sequenced, and assessed for errors. All loci were amplified using unlabeled primers under the conditions described above for SSR marker evaluation. PCR products were cloned using a Zero Blunt TOPO PCR cloning kit for sequencing (Thermo Fisher Scientific) following manufacturer's instructions. DNA was extracted from colonies containing the vector (pCR-4Blunt-TOPO; Invitrogen, Carlsbad, CA) and PCR product using a GeneJET plasmid miniprep kit (Thermo Fisher Scientific) following manufacturer's instructions. Vector products were sequenced by the MSU-GC using the primer set

M13Forward(-20) (5'- GTAAAACGACGCCAG) and M13Reverse
(5'-CAGGAAACAGCTATGAC). Results were analyzed using Geneious Prime 2021.2.2
(Biomatters Ltd., Auckland, New Zealand).

Microsatellite data analysis

Chromatograms from the microsatellite fragments were analyzed with Geneious Prime 2021.2.2 microsatellite plugin 1.4.4 (Biomatters, Inc., Newark, NJ). Peaks were called using the Third Order Least Squares sizing algorithm. Bin sizes were predicted using 12 isolates and additional bin sizes were added as needed as further samples were analyzed. Allele calls were examined manually for potential errors and miscalls.

Allelic and genotypic statistics were determined using MSAnalyzer v. 4.05 (Dieringer & Schlötterer 2003). Hardy-Weinberg equilibrium tests, allele frequency-based correlations (F_{IS}),

null allele frequency and population differentiation statistics (F_{ST}) were generated in Genepop v. 4.5.1 (Rousset 2008). Multi-locus genotypes and pairwise distances were determined with GenoType 1.2 (Meirmans & Van Tienderen, 2004) using the stepwise mutation model with missing data counted as one mutational step. A genotype accumulation curve (GAC) was generated in R v.4.2.1 (R Core Team 2022) using the package 'poppr' v.2.9.3 (Kamar et al. 2014; Kamar et al. 2015) to determine the minimum number of loci needed to identify 90% of the genotypes in our dataset.

The dataset was clone-corrected using 'poppr' and samples were assigned to clusters using untrained clustering ('find.clusters') where number of PCA variables ('n.pca') was set to 10 and number of clusters ('choose.n.clust') was set to 4. Cluster assignment for each isolate was added to the database and a minimum spanning network (MSN) generated using Bruvo's distances ('bruvo.msn'). An index of association plot was generated using the clone-corrected dataset to provide evidence for the predominant reproductive strategy within the population.

Polymorphism information content (PIC) was calculated according to Anderson et al. (1993), where PIC values greater than 0.500 were considered highly informative. The equation used is listed below, where p is the proportion of the jth allele at locus i.

$$PIC_i = 1 - \sum_i p_{ij}^2$$

In addition to cluster analysis performed in 'poppr', population structure was investigated using the program STRUCTURE v.2.3.4 (Pritchard et al. 2000). The admixture model was employed using sampling location as prior information about population structure. Allele frequencies were set as independent among populations and 'alpha' and 'lambda' were inferred. Analysis was run for 500,000 reps after a burn-in period of 50,000 reps. The simulation was run at five values for k (2,3,4,5,6) and the mean(ln) and Pr(X|k) of the runs were compared, with

higher values indicating a better fit for the model. Population differentiation analyses were performed in R v.4.2.1 (R Core Team 2022) using the package 'mmod' (Winter 2012). AMOVA was conducted using 'poppr' with 999 repeats and correction for clones. Discriminant analysis of principal components (DAPC) was performed using the package 'adegenet' v.2.1.8 (Jombart 2008; Jombart & Ahmed 2011) with five principal components and two discriminant analysis categories.

Illumina sequencing of representative isolates

Twenty-two *R. solani* isolates (Table 2.1) were indexed and shotgun sequenced on an Illumina HiSeq4000 (Illumina Inc., San Diego, CA) by the MSU-GC. Raw sequences were assembled using CLC Genomics Workbench v.9 using default settings. Raw reads and assembled contigs were imported into SPAdes v.3.11.0 (Nurk et al. 2013) and assembled to contigs with k-mer selection set to 'automatic', error correction 'on', and contigs considered 'untrusted'.

Assembled genomes were evaluated with QUAST v.5.0.2 (Gurevich et al. 2013) to determine number of contigs, total assembly length and N50 value. Haploid genome size, repetitive proportion of the genome, heterozygosity and sequencing coverage was estimated using Jellyfish v.2.3 (Marcais & Kingsford 2011) and GenomeScope (Vurture et al. 2017) using a k-mer setting of 21. Completeness of finished genomes were assessed using BUSCO v.5.3 (Waterhouse et al. 2017) set to genome mode with 'agaricomycetes_odb10' as the database model. The *R. solani* AG 2-2IIIB draft genome (accession no. CYGV01000000), published by Wibberg et al. (2016), was retrieved from GenBank and analyzed using the same settings to serve as a benchmark for comparison.

Phylogenetic analysis

Gene sequences for *calmodulin*, *25S-rRNA*, *rpb1*, *rpb2*, *tef1a*, and *6-tubulin* were identified from annotations associated with the draft genome of *R. solani* AG2-2IIIB accession number CYGV01000000. (NCBI; Wibberg et al., 2016). Homologous sequences were identified in the Illumina sequenced isolates using the BLAST function within Geneious Prime and primer pairs were designed using Primer3 (Table 2.3; You et al. 2008). Additional sequences were identified using the BLAST function for the remaining isolates and all sequences were trimmed using the associated primers.

Table 2.3 Primer sequences used for phylogenetic analysis of *Rhizoctonia* solani AG 2-2 isolates.

gene	primer name	sequence $(5' \rightarrow 3')$	$T_{\rm m}$
rpb2	RPB2-980modF RPB2-7modR	GARACYCCGRAAGGACAAG CCCATTGCTTGTTTRCCCATG	60
tef1	TEF 457F TEF 1142R	GATTTCATCAAGAACATGAT ACTTGACTTCAGTGGTCA	60
calmod	Cal291F Cal704R	CACCACCAAGGAACTMGGCAC TCGTAGTTGATCTGRCCATCGC	64
Btub	Btub256F Btub968R	CTACTACAACACYGTAGGAG GRAGATCAGAGTTGAGCT	60
25S	R25S368F R25S1064R	GCCTACGATTCAGAGTCCGA AGCCGTTCTTCGATRTTCGTAGC	64
rpb1	RPB1F RPB1R	CACGCCATGGCYGGTCGAGA CACCGAGCGTRACGTTCTTA	64

Primer sequences were synthesized by Integrated DNA Technologies, (Coralville, IA) and 12 additional isolates, including two that were duplicates of those sequenced *in silico*, were amplified using PCR. Reactions were performed in 50µl volumes with 20ng of DNA template, 1 x Phusion II HF buffer, 1.5 mM MgCl₂, 0.5 µM of each primer, 200 µM each dNTP, and 1 unit of Phusion II HF polymerase. Final PCR conditions consisted of 1 cycle of 98°C for 1 min. followed by 34 cycles of 98°C for 10 s, T_a for 10 s, T_a for 10 s, T_a for 15 s and a final extension cycle of

72°C for 5 min. T_a (annealing temperature) values for each primer set are listed in Table 2.3. Samples were cleaned on gel filtration columns (Sephadex G-50 superfine; GE Healthcare Life Sciences; Pittsburg, PA) and submitted to MSU-GC to be sequenced using the Sanger sequencing method according to manufacturer's specifications.

Gene sequences for individual loci were aligned in Mega11 v.11.0.13 (Tamura et al. 2021) using the muscle algorithm with default settings. The ends of aligned sequences were manually trimmed so all sequences were of the same length. Trimmed sequences for all six loci were concatenated in Geneious Prime 2021.2.2 with a spacer of 5 Ns between each gene sequence. Concatenated sequences were exported in FASTA format, and a Neighbor-joining tree (Saitou & Nei 1987) was inferred in MEGA11 v.11.0.13 using the Tamura-Nei substitution model with uniform rates among sites. A maximum-likelihood tree was generated using RAxML v.8.2.11 (Stamatakis 2014). Nucleotide data was partitioned by gene (*calmodulin*, 25S-rRNA, rpb1, rpb2, tef1a, and β-tubulin) and a tree was built using the GTR GAMMA I (general time reversable with estimated proportion of invariable sites with remaining sites gamma distributed) using the rapid bootstrapping algorithm with 1,000 replicates.

Bayesian analysis was conducted using Mr Bayes v.3.2.7a (Ronquist et al. 2012). Concatenated sequences were partitioned into six-character sets by gene (*calmodulin*, *25S-rRNA*, *rpb1*, *rpb2*, *tef1a*, and β -tubulin) and the rates, state frequency, and shape of each partition were allowed to vary independently. Rates for all partitions were set to a proportion invariant and the remaining gamma distributed ('rates=invgamma') with 6 possible states ('nst=6'). The analysis was conducted in two runs for 1,100,000 generations with a sampling frequency of 1,000 and a 25% burn-in value. Phylogenetic trees were prepared for publication using FigTree v.1.4.4 (https://github.com/rambaut/figtree).

Results

Microsatellite marker identification and evaluation

The genome assemblies of isolates 'Rs850', 'Rs688' and 'Rs588' (Table 2.4) were examined for potential microsatellite loci and 33 putative markers loci were identified (data not shown). The most abundant microsatellites were trinucleotide (18), followed by tetra- (8), hexa- (6) and penta- (1). Of the thirty-three potential marker pairs originally identified *in-silico*, six loci were eliminated because of a 5°C difference in predicted annealing temperature compared to other primer sets, which would make them unsuitable for multiplexing. Another eight loci were eliminated due to the failure to amplify in one or more isolates and six loci were eliminated because observed fragment sizes were inconsistent with repeat unit size indicating probable indels in flanking region.

Table 2.4 Results of NextGen sequencing and assembly for three isolates of *Rhizoctonia solani* AG 2-2. Data is shown for isolate 'Rs850' before (raw) and after (final) the additional assembly efforts.

Isolate	# reads (million)	# contigs	N50 (bp)	Avg. length
Rs850 (raw)	236	13,926	15.9 kb	7 kb
Rs850 (final)	-	13,792	16.6 kb	-
Rs866	246	23,128	6.1 kb	4.1 kb
Rs588	265	18,179	4.2 kb	3.1 kb

Typical stutter patterns (one or more peaks that are shorter than the main peak by an interval equal to the repeat unit) were not observed. There were, however, several instances of peaks that were 1 bp shorter than the major peak. These minor peaks generally had a peak intensity of less than 10% of the main peak and false allele calls were minimized by raising the peak threshold. PIG-tailed reverse primers showed no improvement over standard primers and were not used in the final analysis. Overall, stutter was not an issue and did not complicate analysis.

Data analysis

Thirty multi-locus genotypes (MLG) were identified among the 36 isolates evaluated using the set of 13 microsatellite loci (Table 2.5). MLG14 and MLG16 both consisted of two isolates each while MLG2 consisted of five isolates. Each of the remaining 27 MLGs contained a single isolate.

The number of alleles per locus ranged from 3 to 9 with an average of 5.62 alleles per locus. (Table 2.6). Unique genotypes per locus ranged from 3 to 12 with an average of 8.15 genotypes per locus. There was evidence that seven of the 13 loci had a deficit of heterozygotes and an estimated null frequency greater than 0.10. However, PIC values were greater than 0.500 in all but two loci.

The genotype accumulation curve indicated that 90% of the genotypes identified with 13 loci could be detected with only 8 loci (Figure 2.1). By duplexing the eight most informative markers, the genotype for a sample could be generated in only four reactions, allowing up to 24 samples to be genotyped on a single 96-well plate. Repeating the analysis using the eight loci identified 27 MLGs (Table 2.5), which was consistent with the expectation based on the genotype accumulation curve. With this reduced set of markers, the average number of alleles per locus increased from 5.62 to 6.38, observed heterozygosity increased from 0.45 to 0.50, and the average PIC value increased from 0.62 to 0.71 (Table 2.6). While the additional five loci did permit the discrimination of additional genotypes, the contribution was minimal, adding only an additional 3 MLGs (8%).

Table 2.5 Microsatellite alleles and multi-locus genotypes for 36 *Rhizoctonia solani* AG 2-2 isolates based on either 8 or 13 loci.

	13 1	oci	8 lc	oci				Locus		
Isolate	MLG^a	$N_a^{\ b}$	MLG^a	$N_a^{\ b}$	759°	1656 ^c	6145 ^c	5583 °	8703 °	6150°
C116S	5	13	5	8	131	137	146	182	212	134
R-164S	12	13	11	8	140	131	152	191	209	138
RH188	14	12	13	7	140	131	152	191	209	138
RH193	14	13	13	8	140	131	152	191	209	138
Rs542	18	14	17	9	140	146	152/158	191	209	138
Rs106	16	14	15	9	140	131	152/158	191	209	138
Rs481	16	14	15	9	140	131	152/158	191	209	138
Rs496	17	15	16	10	140	146/149	152/158	191	209	138
Rs200	15	16	14	11	140/152	149	152/158	191	209	138
Rs331	21	16	20	10	131	146/152	149	185	215/221	134
2C13	3	17	3	11	140/149	146/146	158	191	209	138
Rs588	19	17	18	12	140	144/149	152/158	191	209	138
ACC3-LP	29	16	27	11	131/140	134	152/161	-	218/218	150/166
F521	8	19	8	11	152	131	152/155	188	203/209	138/142
R1	11	19	8	11	152	131	152/155	188	203/209	138/142
Rs1012	25	19	24	12	131/140	137	149	188	206/218	130/134
R9	13	20	12	12	152	131	152/155	188	203/209	138/142
R4	26	20	12	12	152	131	152/155	188	203/209	138/142
2C1	2	21	2	13	131/137	134/140	149	185	206/218	130/138
F30	2	21	2	13	131/137	134/140	149	185	206/218	130/138
F551	2	21	2	13	131/137	134/140	149	185	206/218	130/138
R09-23	2	21	2	13	131/137	134/140	149	185	206/218	130/138
Rs1146	2	21	2	13	131/137	134/140	149	185	206/218	130/138
F508	6	21	6	14	152/158	131/134	152/158	188/200	203/209	134/142
Rs890	24	21	23	13	152/161	131/134	149/155	188	206/206	134/142
W-22	28	21	26	14	149/158	131/134	152/155	200	206/209	134/142
Italien	9	22	9	15	152/161	131/134	149/158	188/200	203/209	142/158
Rs255	20	22	19	15	131/140	134/137	146/149	185	206/218	130/142
Rs866	23	22	22	14	152/170	131/134	149/158	188/200	203/209	142
Slovakia	27	22	25	15	131/140	131/134	149/158	185/191	209/212	138
Rs393	30	22	2	14	131/137	134/140	149	185	206/218	130/138
24BR	1	23	1	16	131/140	131/134	149/158	185/191	209/212	134/138
39AR	4	23	4	16	131/140	131/134	149/158	185/191	209/215	134/138
F517	7	23	7	15	131/140	134/140	146/149	185	206/212	130/142
R09-25	10	23	10	15	152/161	131/134	149/158	188/200	203/209	134/142
Rs850	22	23	21	13	131/167	134	149/152	185/200	209/215	134

a. multi-locus genotypeb. number of allelesc. indicates locus was used in the 8-loci marker set

Table 2.5 (con't)

				Locus			
Isolate	4660 ^c	5487 ^c	2893	7676	2547	5402	7420
C116S	147	132	122	176	222	141	170
R-164S	144	135	116	179	218	144	170
RH188	-	138	116	179	218	144	170
RH193	132	138	116	179	218	144	170
Rs542	132	135	116	179	218	144	170
Rs106	132	135	116	179	218	144	170
Rs481	132	135	116	179	218	144	170
Rs496	144	135	116	179	218	144	170
Rs200	144	132/135	116	179	218	144	170
Rs331	150	132	122	179	214/218	144	170
2C13	144	135/138	116	179	218	144	170/173
Rs588	132/144	132/135	116	179	218	144	170
ACC3-LP	144	138	146	185	218	144	170
F521	144	135	116	182/188	222	141/144	170/176
R1	144	135	116	182/188	222	138/144	170/176
Rs1012	147/150	132	122	179	218/222	144/156	170
R9	144	132/135	116	182/188	222	141/144	170/176
R4	144	132/135	116	182/188	222	138/144	170/176
2C1	147/150	132	128/140	179	218/222	144/156	170
F30	147/150	132	128/140	179	218/222	144/156	170
F551	147/150	132	128/140	179	218/222	144/156	170
R09-23	147/150	132	128/140	179	218/222	144/156	170
Rs1146	147/150	132	128/140	179	218/222	144/156	170
F508	144	135	116	182	222	141/144	170/173
Rs890	144	135	116	182/185	222	141/144	170/176
W-22	144	138/141	116	182/185	222	141/144	170
Italien	144	135/138	116	182	222	141/144	170/176
Rs255	147/159	132/135	122	179	218/222	144/156	170
Rs866	144	135/138	116	182/188	222	141/144	170/173
Slovakia	144/156	135/138	116/122	179	218/222	144	170
Rs393	147/150	132/132	128/140	179	218/222	144/156	170
24BR	144/156	135/138	116/122	179	218/222	144	170
39AR	144/150	135/138	116/128	179	214/218	144	170
F517	150/159	132/135	122/128	179	218/222	144/156	170
R09-25	144	135/138	116	182/188	222	141/144	170/176
Rs850	144/150	135	116/134	179/182	218/222	144/147	170/173

Table 2.6 Summary of allele statistics for 13 microsatellite loci based on the genotypes of 36 Rhizoctonia solani AG 2-2 isolates.

Locusa	$N_{A}{}^{b} \\$	$R_{A}{}^{c} \\$	size range	$N_{G}{}^{d} \\$	H_E^e	$\mathrm{Ho^f}$	$P(H_{deficit})^g$	Null ^h	F_{IS}	PIC ⁱ
* 0759	9	1.78	131 - 170	12	0.779	0.611	0.072	0.086	0.218	0.769
* 1656	7	1.75	131 - 152	11	0.749	0.639	< 0.001	0.142	0.262	0.739
* 6145	6	1.75	146 - 161	11	0.750	0.556	0.035	0.065	0.149	0.739
* 5583	5	1.74	182 - 200	8	0.748	0.222	< 0.001	0.382	0.695	0.730
* 8703	7	1.73	203 - 221	10	0.725	0.667	0.175	0.049	0.082	0.715
* 6150	7	1.71	130 - 166	11	0.705	0.583	0.120	0.084	0.175	0.696
* 4660	6	1.68	132 - 159	9	0.662	0.361	0.004	0.209	0.458	0.671
* 5487	4	1.65	132 - 141	6	0.650	0.389	< 0.001	0.174	0.405	0.641
2893	6	1.59	116 - 146	8	0.591	0.306	< 0.001	0.194	0.487	0.583
7676	5	1.54	176 - 188	7	0.538	0.250	< 0.001	0.284	0.539	0.530
2547	3	1.53	214 - 222	4	0.534	0.389	0.054	0.531	0.274	0.526
5402	5	1.49	138 - 156	6	0.489	0.556	0.714	0.004	-0.139	0.482
7420	3	1.27	170 - 176	3	0.273	0.306	1.000	0.000	-0.119	0.270
mean (13) ^j	5.62	1.63	116 - 222	8.15	0.630	0.449	-	-	-	0.62
mean (8)	6.38	1.72	131 - 221	9.75	0.721	0.503	-	-	-	0.71

a. Loci included in multi-locus genotype using 8 loci

b. Number of alleles per locusc. Allelic richness

c. Allelic richness
d. Number of genotypes per locus
e. Expected heterozygosity
f. Observed heterozygosity
g. P-value heterozygote deficiency
h. Estimated frequency of null alleles
i. Polymorphism Information Content
i. Moon values for allele statistics calcu-

j. Mean values for allele statistics calculated for 13 loci and for the 8 most informative loci indicated by *

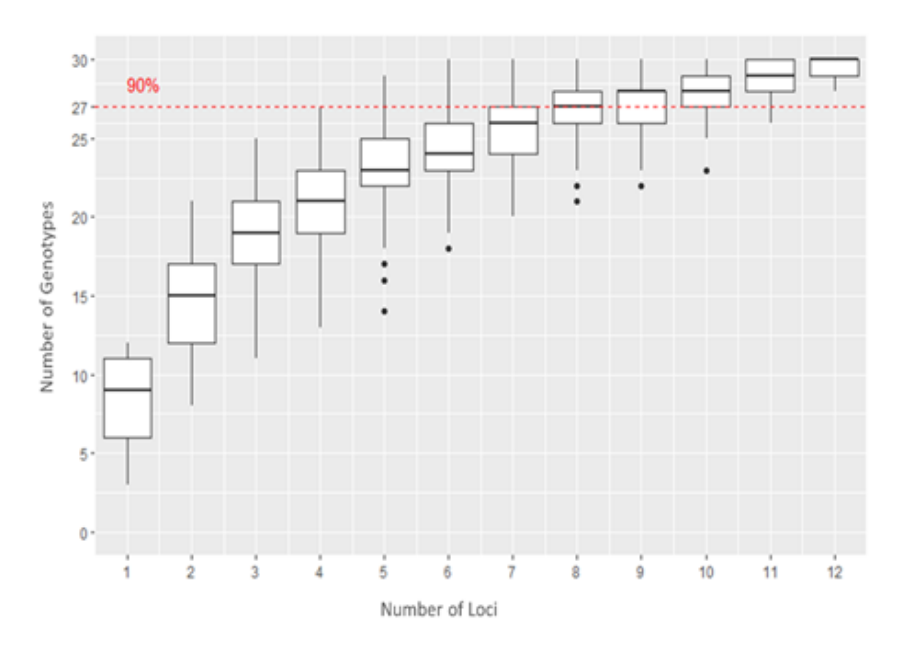


Figure 2.1 Genotype accumulation curve for 35 *Rhizoctonia* solani AG 2-2 isolates based on microsatellite loci. Red dashed line indicates 90% of the genotypes that were identified using 13 microsatellite loci.

Cluster analysis produced somewhat confusing results. When the number of clusters was determined automatically in 'poppr', between 3 and 12 clusters were identified depending on the maximum number of clusters setting. Few of these cluster assignments made sense biologically, particularly with respect to isolates 'Rs850', '24BR', and '39AR', which would cluster with isolates on different branches of the MSN despite the expectation that they would group in cluster 3. When the number of clusters exceeded five, multiple clusters were represented by a single isolate, which seemed excessively complex and uninformative. From preliminary work and the phylogenetic analysis conducted in the current study, the expectation was that there would be four clusters. By setting the number of clusters to four, cluster association was more consistent with biological expectations and the phylogenetic analysis. Interestingly, the isolates mentioned above, 'Rs850', '24BR', and '39AR', along with 'Slovakia' and 'ACC3-LP' (AG 2-2LP), clustered together on a branch leading to cluster 3 (Figure 2.2).

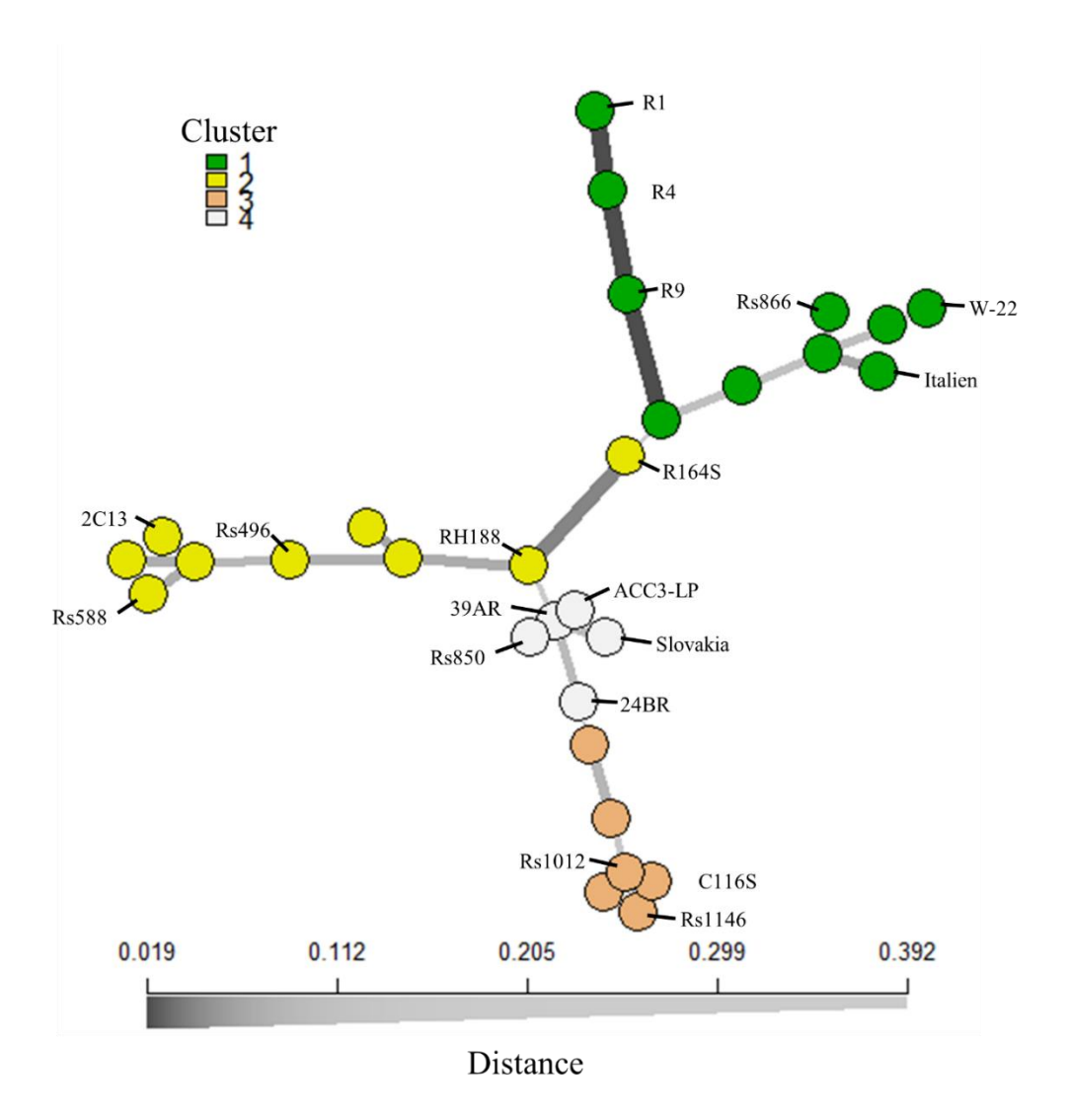


Figure 2.2 Minimum spanning network of 30 *Rhizoctonia solani* AG 2-2 isolates. Assignment of isolates to clusters was determined using cluster analysis in the R package 'poppr' (Kamvar et al. 2014). Dataset was clone corrected and each node represents a single genotype. Distance between nodes is represented by lines where thick, dark lines indicate a close relationship and thinner, lighter lines indicate a more distant relationship.

The STRUCTURE analysis had similar confusing results. Analysis with k=6 had the highest mean(ln) value, but the bar plot was unnecessarily complex (Figure 2.3A). Setting k=4, as had been done with the cluster analysis in 'poppr', produced a more straightforward, interpretable result (Figure 2.3B). The main clusters identified by STRUCTURE analysis (when k=4) matched those identified by cluster analysis in 'poppr'. Isolates 'Rs850', '24BR', '39AR', 'Slovakia', and 'ACC3-LP' did not cluster together in the STRUCTURE plot like they did in the MSN analysis (Figure 2.2), but rather showed evidence of considerable admixture (Figure 2.3B). Isolate 'C116S' also had a conspicuous level of admixture and shared a substantial amount of variation with isolate 'ACC3-LP'.

There was no evidence of population structure by geographical region of origin (p=0.592; Table 2.7), in spite of large distances between growing regions (Figure 2.4). Much of the genetic variation was shared between growing regions with the Red River Valley sharing variation with isolates from all growing regions except Canada (Figure 2.5A). AMOVA plots indicate non-significant variation between geographical populations which also supports the lack of population structure by region of isolation (Figure 2.6A; p=0.603). Despite R. solani AG 2-2 populations being primarily clonal ($\bar{r}_d=0.288$; p=0.001; Figure 2.7), our data indicates the likely occurrence of long-distance, even intercontinental, dispersal. For example, one of the isolates from Europe, 'Slovakia', had a nearly identical genotype as isolate '24BR' from Canada, varying by only 1 allele out of 26. (Table 2.5).

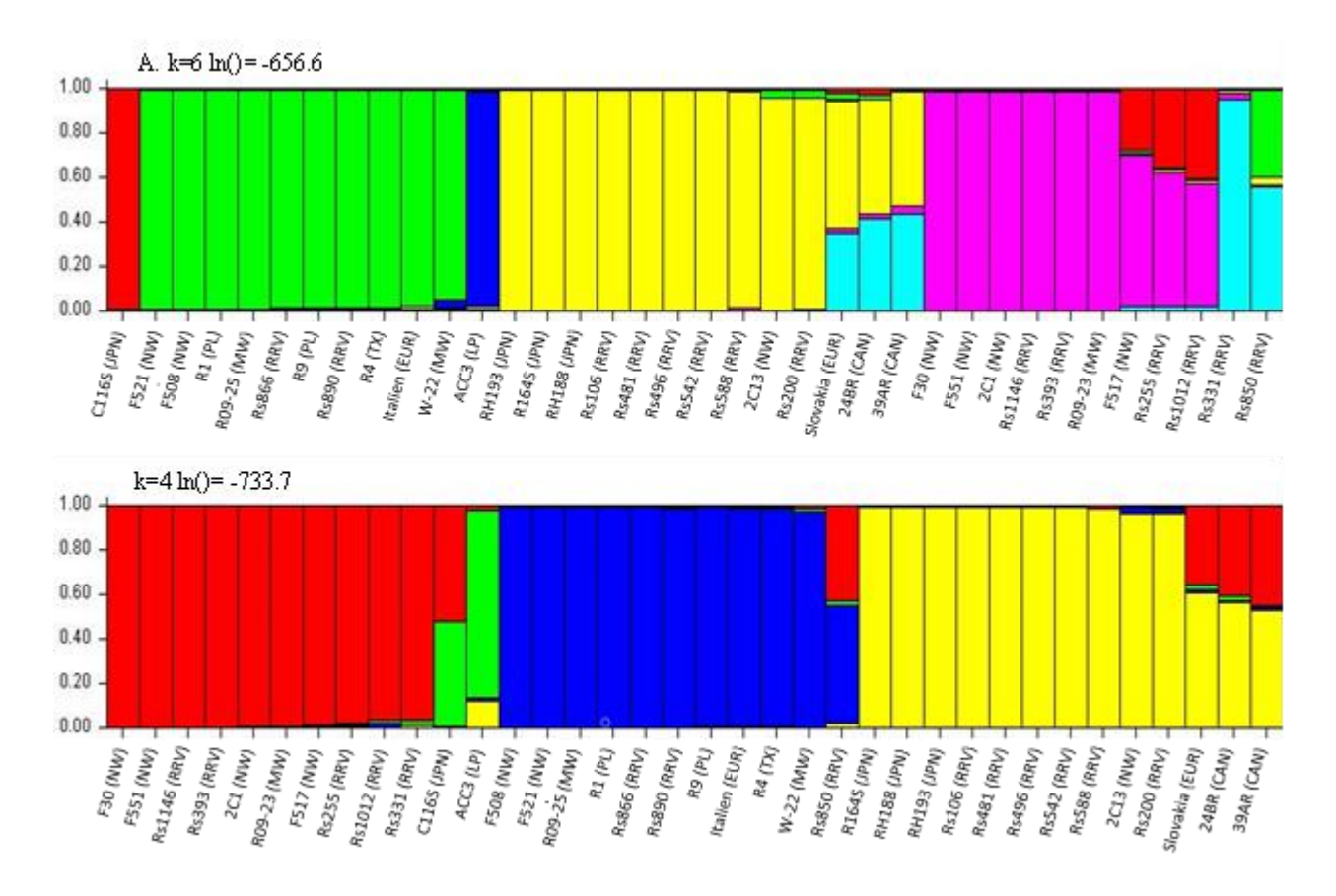


Figure 2.3 Structure plots for 36 *Rhizoctonia solani* AG 2-2 isolates inferred from 13 microsatellite loci. A) plot assuming 6 populations (k=6; mean(ln)= -656.6). B) plot assuming 4 populations (k=4; mean(ln)= -733.7). Letters in parenthesis indicate region of isolation: NW=Northwest U.S.; PL= Plains region, U.S.; MW = Midwest U.S.; RRV= Red River Valley, U.S.; TX= Texas, U.S.; EUR= Europe; JPN= Japan; CAN= Canada; LP = single isolate of AG2-2LP (location unknown). Color of clusters for k=4 plot is associated with clusters identified by minimum spanning network analysis (Figure 4.2) as such: blue = cluster 1; yellow = cluster 2; red = cluster 3; green = cluster associated with AG 2-2LP.

Table 2.7 Population differentiation statistics for *Rhizoctonia solani* AG 2-2 isolates estimated for three population substructures: geographic region of isolation, traditional ISGs (IIIB, IV, intermediate), and genetic clusters identified in the current study.

	Pop	ulation structure	;
	Geography	ISG	Cluster
H _S	0.620	0.551	0.428
H_t	0.632	0.606	0.629
G'_{ST}	0.058	0.291	0.673
D	0.037	0.184	0.468
Variation between samples within population	29.14% (<i>p</i> =0.001)	14.23% (p = 0.003)	-3.15% (<i>p</i> =0.756)
Variation between populations	-1.44% ($p = 0.592$)	20.20% ($p = 0.001$)	40.48% (<i>p</i> =0.001)

Hs – heterozygosity with population substructure

Ht – heterozygosity without population substructure

G'sT - Hendricks G'sT

D – Jost's D_{est}

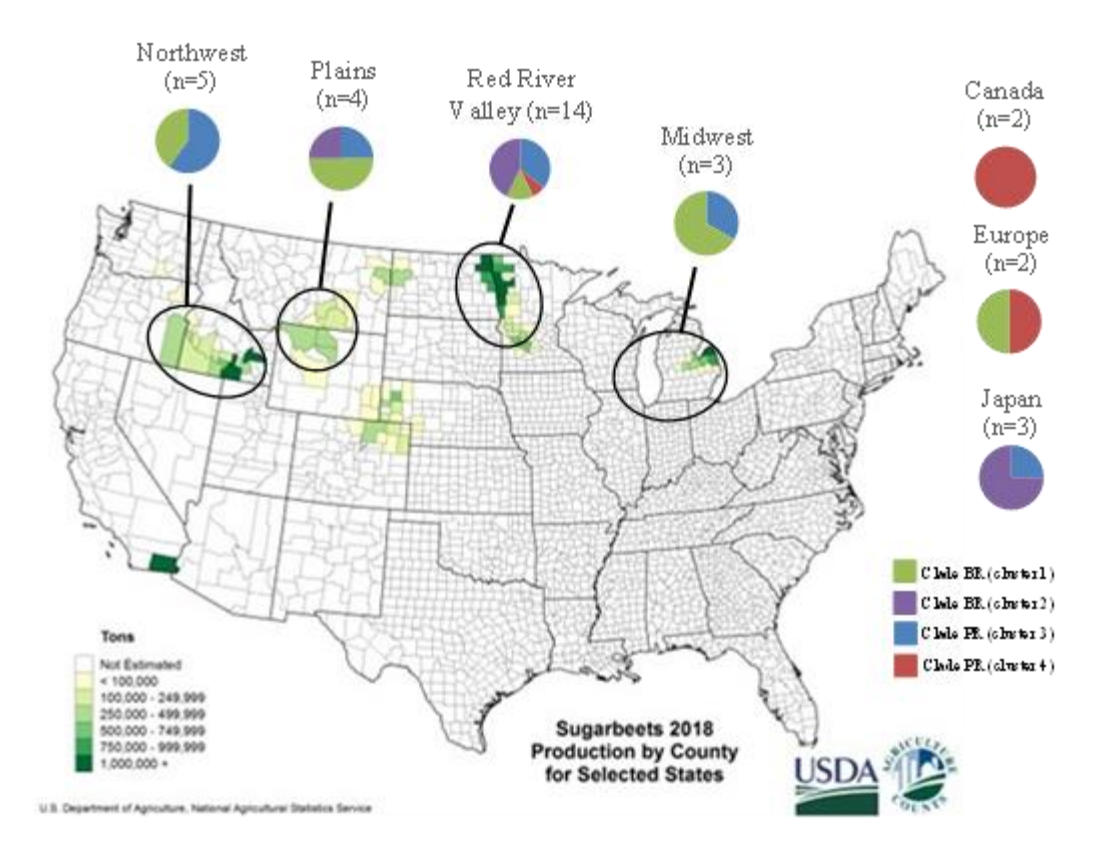


Figure 2.4 Distribution of 33 *Rhizoctonia solani* AG 2-2 isolates by growing region. Pie charts indicate proportion of isolates included from a particular region with color of the slices indicating clade/cluster. Map source: USDA-National Agricultural Statistics Services. Retrieved from: https://www.nass.usda.gov/Charts and Maps/Crops County/su-pr.php

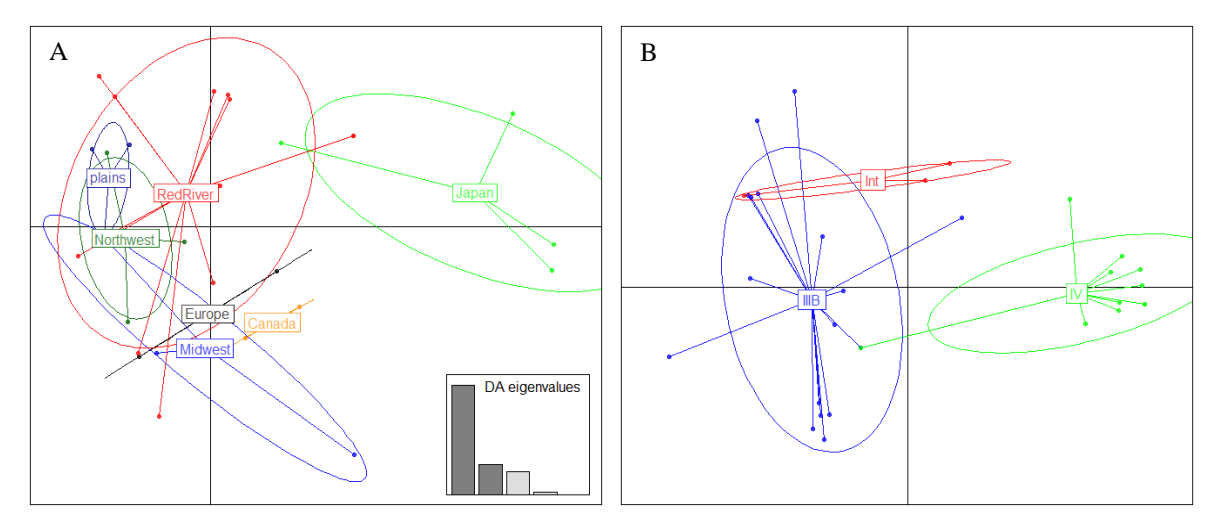


Figure 2.5 Discriminant analysis of principal components plots examining population structure for *Rhizoctonia solani* AG 2-2 isolates. Plots categorized by A) geographic region of isolation (n=28) and B) traditional subgroups 'IIIB', 'IV' and 'Intermediate' (n=29).

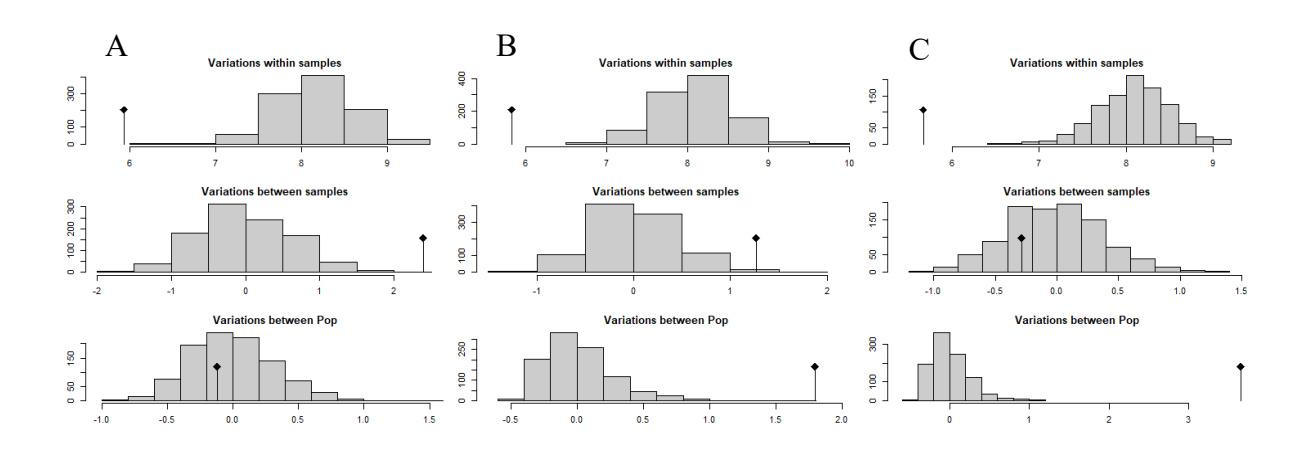


Figure 2.6 AMOVA plots to test for population structure of 36 *Rhizoctonia solani* AG 2-2 isolates. Populations were grouped by A) geographical region of isolation; B) traditional ISGs, 'IIIB', 'IV' and 'Intermediate'; and C) by the four clusters identified using cluster analysis. The bar plots represent the distribution of the expected values based on 999 permutations and the mark at the diamond represents the actual value of the data. Actual values outside the range of expected values are significant. The greater the difference between 'variations between populations' and 'variations between samples', the greater the population structure.

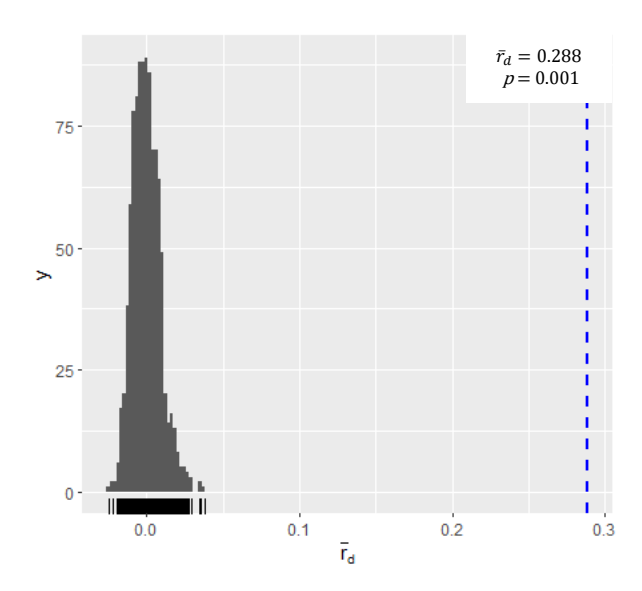


Figure 2.7 Index of association plot for clone corrected dataset of 35 *Rhizoctonia solani* AG 2-2 isolates based on 13 microsatellite loci. The bar plots represent the distribution of the expected values based on 999 permutations and the dashed line indicates actual value of the dataset.

Grouping populations by the ISGs 'type IIIB', 'type IV' and 'intermediate' provided some population structure with a significant p-value and about 20% of the variation occurring between populations (Table 2.7). Differentiation was low to moderate though, with $G'_{ST} = 0.291$ and D = 0.184 (Table 2.7). Cluster overlap occurred mainly between the 'intermediate' isolates and the 'type IIIB' isolates, with one 'type IV' isolate occurring in the 'type IIIB' cluster (Figure 2.5B). AMOVA plots indicate significant variation between populations (Figure 2.6B; p = 0.001) but variation with samples was also significant (Table 2.7; p = 0.003) indicating overlap between populations.

Population differentiation became distinct when grouped by the four clusters identified using 'poppr' (Figure 2.2). Values for G_{ST} and D increased to 0.673 and 0.468 respectively with about 40% of the total variation occurring between populations (Table 2.7). AMOVA plots confirm

that the clusters identified using 'poppr' provided the strongest evidence of population structure with significant variance between populations (Figure 2.6C; p = 0.001) and non-significant variance between samples within populations (Figure 2.6C; p = 0.715).

Cloning

A total of 210 clones were generated from 84 individual loci using the 10 primer pairs and 17 isolates indicated in Table 2.8. Analysis of the sequenced clones resulted in 117 unique sequences that were deposited to GenBank as accession numbers OR101123 to OR101084 & OR113391 to OR113484.

Based on automatic fragment sizing, a total of 122 alleles were identified across the 84 individually cloned loci with 36 loci (43%) being heterozygous (Table 2.8). Analysis of cloned sequences from those same 84 loci identified 133 unique alleles, which represents a 9% increase. The number of heterozygous loci increased to 40 (48%) based on the cloned fragments. A total of ten loci had more than one allele with the same fragment length, but with two or more single nucleotide substitutions (SNPs; Table 2.8). As many as four unique sequences were identified in some individual loci, but the majority of alleles (>90%) were represented by monomorphic sequences.

Table 2.8 Comparison of alleles for Rhizoctonia solani AG 2-2 isolates identified by automatic fragment sizing (auto) and cloning (clone). Allele fragment sizes are listed as length in base pairs. Numbers in parentheses indicate the number of unique alleles with the same fragment length but with varied nucleotide sequences.

					Lo	ocus				
	16	556	25	547	46	560	55	583	54	187
Isolate	auto	clone	auto	clone	auto	clone	auto	clone	auto	clon
Italien	131	134	222	213	144	146(2)	188	190	135	138
	134	137					200	199	138	141
								202		
R1	131	134	222	213(2)	144	146(2)	188	190	135	138
Rzc5	137	140	222	213	147	149	182	187	132	135
Rzc6	131	134	218	213	144	146	191	193	135	138
Rzc16	131	134	222	213(2)	144	146	188	192(2)	132	138(2
		140							135	
Rs850	134	137(4)	218	220(2)	144	146	185	186	135	138(
			222	223(2)	150	152	200	202		
Rs1146	134	137	218	220	147	149	185	186	132	135
	140	143	222	223(2)	150	152				
Rs393	134	137								
	140	143								
Rs200					144	146				
Rs255					147	149				
					159	161				
Rs106							191	193	135	138
Rzc146	131	134								
Rzc133							188	190		
							200	202		
Rs866										
Slovakia							185	186		
							191	193		
Rs481										
Rs542										
Total N _A	12	16	9	14	12	14	14	16	10	11
Total Ho	6	5	5	3	6	4	6	5	6	5
Total He	3	4	2	4	3	5	4	5	2	3

 $[\]begin{aligned} N_A - total \ number \ of \ alleles \\ Ho - total \ number \ of \ homozygotes \end{aligned}$

He – total number of heterozygotes

f - false allele identified as the result of improper pairing of forward primers

Table 2.8 Con't

					Lo	cus				
	7.	59	61	45	87	703	61	50	28	393
Isolate	auto	clone	auto	clone	auto	clone	auto	clone	auto	clone
Italien	152	157	149	152	203	201	142	143	116	118
	161	166	158		209		158	159		
R1	146	151	152	155	203	201	138	140	116	118
	152	157	155	158	209	207	142	144		
Rzc5	131	136	146	149	212	210	134	137	122	124
Rzc6	140	145	152	155	209	207	138	139	116	118
Rzc16	146	151	152	155	203	201	138	139	116	118
	152	157	155	158	209		142	143		
Rs850	131	136	149	152	209	207	134	137	116	118
	167	172	152	155	215			138	134	137
Rs1146	131	136	149	152	206	204	130	133	128	130
	137				218	216	138	141	140	142
					182	181(f)				
Rs393	131	136	149	152	206	204				
	137	142			218	216				
Rs200										
Rs255									122	124
Rs106										
Rzc146										
Rzc133										
Rs866	152	157								
	170	175								
Slovakia										
Rs481					209	207				
Rs542					209	207				
Total N _A	16	15	12	11	17	14	11	12	9	10
Total Ho	2	3	4	5	4	7	3	2	7	6
Total He	7	6	4	3	6	3	4	5	1	2

The observation of more than two alleles at a given locus was rare, despite *R. solani* being heterokaryotic and multinucleate with between 3 and 13 nuclei per cell (Sneh et al. 1991). One locus in which three alleles were observed during fragment analysis was locus 8703. An allele of length 182 bp was identified in about 60% of the isolates tested, although it was viewed skeptically because of its weak signal and that it was quite different in size from the other alleles. Upon analysis of cloned sequences from this locus, it was determined that the '182' allele was caused by improper binding of a pair of forward primers, one in reverse orientation, at a locus unrelated to the target microsatellite locus. Increasing stringency of the PCR reaction to the final values reported in Table 2.2 reduced this mispairing to a rare occurrence on subsequent analyses and any '182' alleles that did occur were easily removed.

Cloning revealed additional alleles with a different fragment length in three loci that were not detected by automatic fragment sizing. The reason for this is uncertain but is likely to be related to PCR conditions. In contrast, cloning failed to identify one of the alleles at five heterozygous loci. This is easily explained simply as having an inadequate number of clones to detect the second allele. Interestingly, in all five cases it was the larger allele that failed to clone.

Illumina sequencing of representative isolates

Illumina sequencing produced 103.9 Gbp of sequence data in 346,344,342 pair-end reads that passed filter with an average estimated insert size of 427 bp and an average Q-score of 35.3. Average yield per isolate ranged from 3.90 to 6.05 Gbp with an average yield of 4.72 Gbp. Data for individual isolates is shown in Table 2.9.

Genome assemblies ranged in total length from 39.8 to 78.1 Mbp with an average length of 59.1 Mbp and an average of 8713 contigs and an average N50 value of 24.6 Kb (Table 2.8).

Haploid genome sizes were estimated to be between 37.0 to 51.6 Mbp with an average of 42.8 Mbp. Heterozygosity ranged from 0.03 to 6.62%, with a mean of 2.70% and a median of 3.00%.

BUSCO scores indicate genome completeness that ranged from 65.0 - 86.1%. However, duplicated genes represented a large portion of complete scores, with BUSCO scores for duplicated genes as high as 72.5%. The proportion of BUSCO duplicates significantly correlated with heterozygosity (P< 0.001; R^2 = 0.838), providing an explanation for the high levels of duplication in assemblies.

Table 2.9 Assembly statistics for 22 *Rhizoctonia solani* isolates assembled from Illumina paired-end reads. CYGV01 was included from Wibberg et al. 2016 for reference.

Isolate	Total assembly length (Mbp)	# contigs > 750bp	N50	Coverage	% Hetero- zygosity	BUSCO score (n:2898)
C116S	39.8	2,114	64,451	35	0.03	C:83.3%[S:82.8%,D:0.5%],F:4.7%,M:12.0%
R-5	49.0	8,267	59,217	40	0.41	C:83.2%[S:82.6%,D:0.6%],F:4.3%,M:12.5%
ACC3-LP	47.7	7,131	20,937	28	0.66	C:82.4%[S:82.1%,D:0.3%],F:4.8%,M:12.8%
R-164S	45.6	5,548	24,815	36	0.79	C:78.8%[S:77.7%,D:1.1%],F:6.8%,M:14.4%
Rs496	49.1	9,664	14,489	40	1.14	C:75.7%[S:74.4%,D:1.3%],F:7.8%,M:16.5%
Rs200	55.7	12,481	11,755	41	1.26	C:76.5% [S:74.8%,D:1.7%],F:7.9%,M:15.6%
2C13	46.8	6,932	17,098	41	1.29	C:76.2%[S:75.4%,D:0.8%],F:8.1%,M:15.7%
Rs14-2	50.9	9,723	10,382	39	1.84	C:68.8% [S:64.4%,D:4.4%],F:10.7%,M:20.5%
ST6-1	51.8	10,153	9,942	41	1.93	C:66.7% [S:61.8%,D:4.9%],F:12.3%,M:21.0%
Rs1012	60.8	11,684	9,948	41	2.93	C:65.4% [S:55.2%,D:10.2%],F:11.8%,M:22.89
Rs1146	60.8	11,791	9,870	46	3.07	C:65.0% [S:54.5%,D:10.5%],F:12.7%,M:22.3
F30	60.9	11,858	9,901	42	3.11	C:65.3%[S:54.7%,D:10.6%],F:12.5%,M:22.29
F321	60.2	11,677	10,018	40	3.11	C:66.1%[S:55.3%,D:10.8%],F:12.2%,M:21.79
R09-23	60.6	11,873	9,877	34	3.16	C:64.9%[S:54.6%,D:10.3%],F:13.0%,M:22.1
W-22	78.1	13,275	15,387	40	3.66	C:71.8%[S:31.4%,D:40.4%],F:10.3%,M:17.9
Italien	71.0	7,212	20,626	51	4.35	C:72.7%[S:26.0%,D:46.7%],F:8.7%,M:18.6%
R09-25	70.6	7,974	17,846	42	4.47	C:72.6%[S:28.6%,D:44.0%],F:9.0%,M:18.4%
R1	70.4	3,895	42,795	46	4.64	C:80.3%[S:21.8%,D:58.5%],F:6.2%,M:13.5%
R4	72.5	4,080	40,411	52	5.21	C:80.6%[S:20.4%,D:60.2%],F:6.0%,M:13.4%
Slovakia	78.1	3,400	67,775	44	6.62	C:86.1%[S:13.6%,D:72.5%],F:3.5%,M:10.4%
R9	72.3	4,302	37,410	34	4.48	C:79.6%[S:20.3%,D:59.3%],F:6.6%,M:13.8%
Rs296	47.5	7,947	16,131	34	1.23	C:76.4%[S:74.9%,D:1.5%],F:8.1%,M:15.5%
CYGV01	55.9	5826	80,505	-	-	

Phylogenetic analysis

Sequences from the partial gene regions for 25S-rRNA, β -tubulin, calmodulin, RPB1, RPB2 and TEF-1 α were generated and deposited in GenBank under the accession numbers OP832036 – OP832197. The concatenated set of sequences produced a data matrix that consisted of a total of 4,341 characters with 938 that were phylogenetically informative. The phylogenetic trees generated by Bayesian analysis (Figure 2.8), neighbor-joining (Figure 2.9), and maximum-likelihood (Figure 2.10) showed remarkable similarity to one another.

While isolates of 'type IIIB' and 'type IV' did tend to cluster together in the current analysis, none of the trees examined supported the subgroups 'AG 2-2IIIB' and 'AG 2-2IV' as monophyletic. In addition to the presence of two 'type IV' isolates in clade 2, two subclades of 'type IIIB' isolates in clade 1 (cluster 1) were more closely related to a subclade of 'type IV' isolates (cluster 2) than to the 'type IIIB' isolates in clade 2. These observations are similar to those of Strausbaugh et al. (2011a) and Carling et al. (2002) that also showed 'AG 2-2IIIB' and/or 'AG 2-2IV' to be polyphyletic.

Clade 2 was well supported with isolate 'C116S' located at the basal node. 'C116S' is the original AG 2-2IIIB isolate identified by Ogoshi from mat rush (Ogoshi 1987). The reference genome from Wibberg et al. (2016), which was described as AG 2-2IIIB, is also included in clade 2. While the majority of the isolates in clade 2 were 'type IIIB', two isolates, Rs393 and R09-23, were 'type IV'. Clade 1 was split, with about half the isolates 'type IIIB' and half 'type IV', grouped into 3 subclades (Figure 2.8). All 'type IV' isolates in clade 1 grouped into a single subclade while the 'type IIIB' and 'intermediate' isolates were grouped in the other two subclades (Figure 2.8).

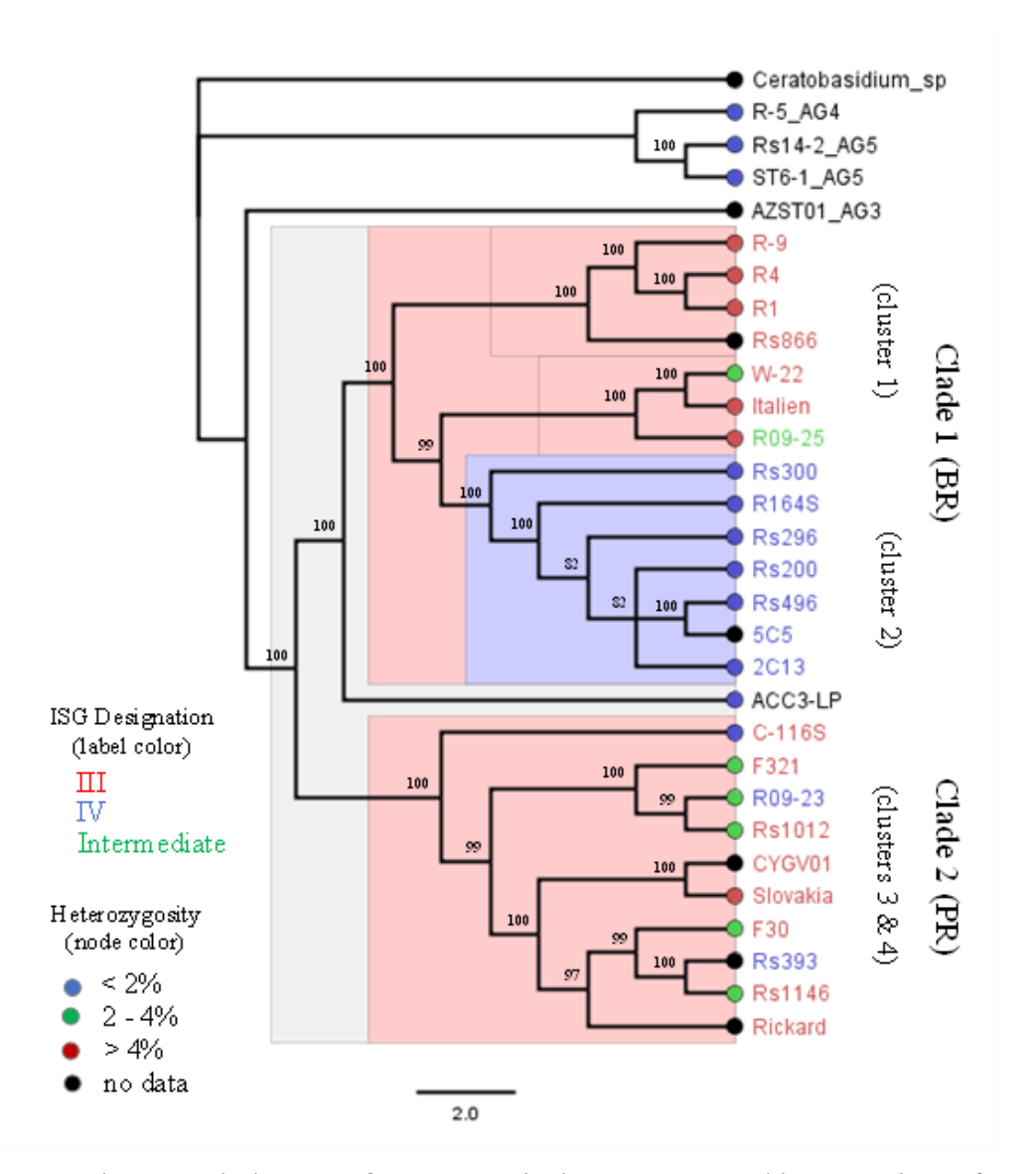


Figure 2.8 Six-gene phylogeny of 25 AG 2-2 isolates constructed by Bayesian Inference. Cluster designation identifies cluster association according to minimum spanning network analysis (Figure 4.2). Numbers at the nodes indicate posterior probabilities with values < 70% not shown. Color of the branch tip labels indicate ISG designation as determined by growth at 35°. Intermediate designation means growth tests at 35°C were inconclusive. Colored circles at the branch tips represent heterozygosity as estimated by k-mer counts of paired-end Illumina reads. *Ceratobasidium* sp. AG-I was included as the outgroup.

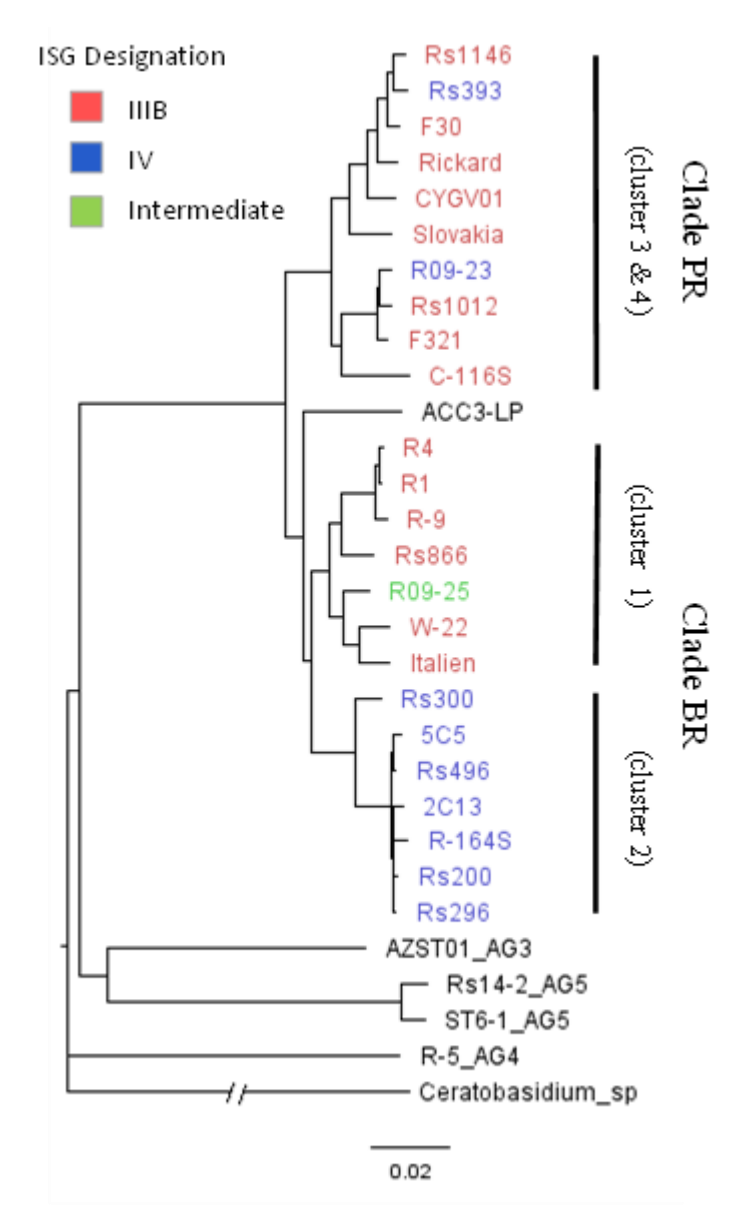


Figure 2.9 Neighbor-joining tree for 25 *Rhizoctonia solani* AG 2-2 isolates based on six gene sequences. Color of branch tip labels indicates ISG designation based on growth at 35°C with 'Intermediate' meaning growth tests were inconclusive. *Ceratobasidium* sp. AG-I was included as the outgroup.

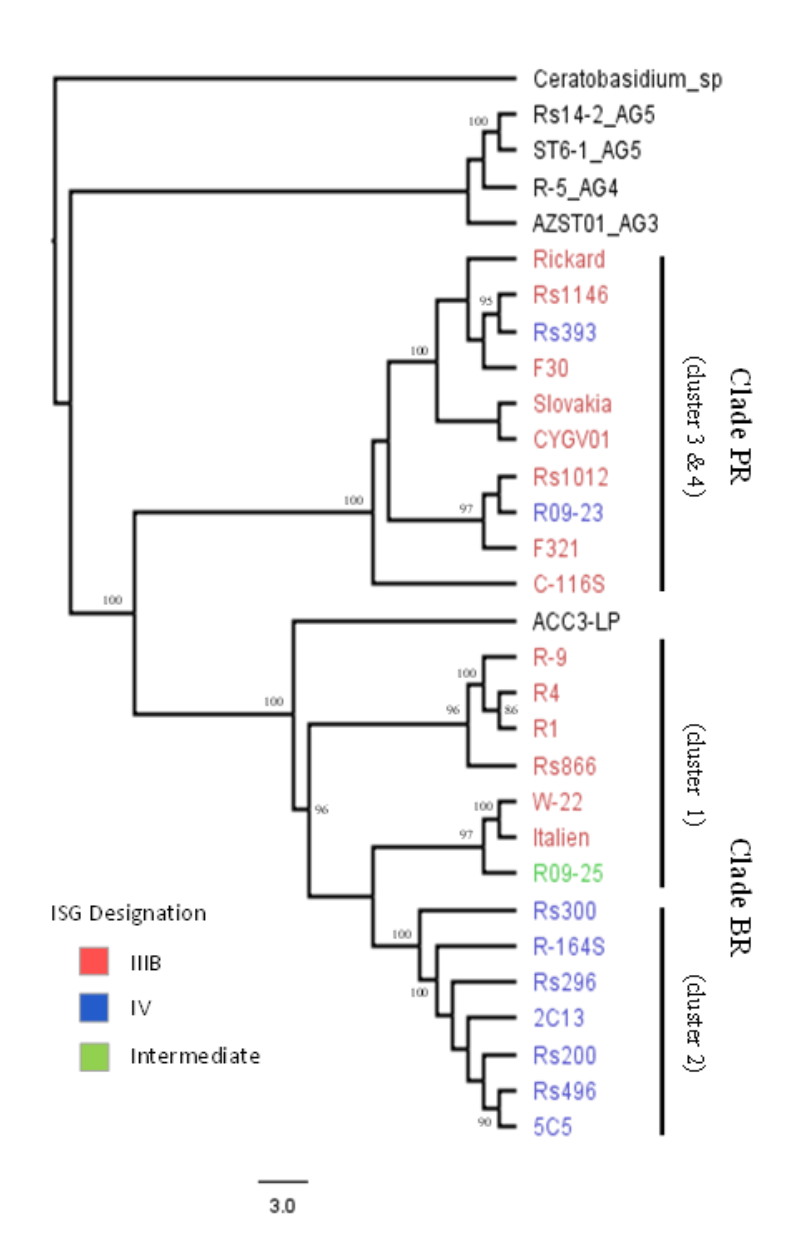


Figure 2.10 Six-gene phylogeny of 25 AG 2-2 isolates generated using Maximum-likelihood criterion. Color of branch tip labels indicates ISG designation based on growth at 35°C with 'Intermediate' meaning growth tests were inconclusive. Numbers at the nodes indicate support values based on 1000 bootstrap replicates. Ceratobasidium sp. AG-I was included as the outgroup.

Discussion

Results of the current study clearly demonstrate that the subgroups AG 2-2IIIB and AG 2-2IV are not monophyletic and instead we interpret the phylogeny as indicating there are two major genetic groups that contain a mix of isolates previously identified as belonging to the subgroups AG 2-2IIIB and AG 2-2IV. Despite several studies showing that the monophyly of AG 2-2IIIB and AG 2-2IV is questionable (Carling et al. 2002; Martin et al. 2014; Strausbaugh et al. 2011a), reports based on the subgroups AG 2-2IIIB and AG 2-2IV are still common. Much of the reason for this continued usage is due to reported differences in virulence and host range (Cappelli et al. 1999; Carling et al. 2002; Strausbaugh et al. 2011a). However, since these subgroups should be considered artificial, generalization of individual behavior based on them should be considered cautiously. Consequently, temperature tolerance should no longer be considered an acceptable criterion for the separation of subgroups within AG 2-2.

The invalidation of AG 2-2IIIB and AG 2-2IV as legitimate subgroups could help explain inconsistencies in experimental data over the years. For example, primers designed for specific amplification of AG 2-2IIIB and AG 2-2IV worked well on the set of isolates used to develop them (Carling et al. 2002; Salazar et al. 2000) but were inconsistent on an expanded set of isolates (Bolton et al. 2010; Brantner, J., Hanson, L.E. unpublished data). Similarly, designation of ISG based on temperature tolerance has resulted in inconsistent identification of individual isolates. The well characterized isolate 'R9' isolated from sugar beet in Colorado (Hecker & Ruppel 1975) has been categorized as both AG 2-2IIIB and AG 2-2IV (Carling et al. 2002; Engelkes & Windels 1996; Stojšin et al. 2007; Strausbaugh et al. 2011a). In addition, some isolates have been characterized as 'intermediate' where only very weak growth occurred at

35°C (Brantner & Windels 2007), which is another indication that temperature tolerance is an unreliable method for distinguishing subgroups.

Host range attributed to the ISGs has also been somewhat inconsistent. In addition to the original indication that 'AG 2-2IIIB' affected mat rush and 'AG 2-2IV' was the causal agent of root rot of sugar beet, not only have both groups been shown to cause root rot of sugar beet, but isolates characterized as 'AG 2-2IIIB' are generally regarded as being more aggressive on sugar beet than isolates characterized as 'AG 2-2IV' (Engelkes & Windels 1996; Strausbaugh et al. 2011a). Inconsistency in the reported susceptibility of a host can complicate choices of suitable rotational crops. For example, corn was shown to be a host for 'AG 2-2IIIB' classified populations (Sumner & Bell 1982; Sumner & Minton 1989) while 'AG 2-2IV' classified isolates caused little or no damage (Windels & Brantner 2006). However, one report showed isolates associated with 'AG 2-2IV' causing more damage on corn (Ohkura et al. 2009). An accurate assessment of the relationship between subgroup and host susceptibility is important to making suitable rotation choices. We expect the subgroup revisions proposed in the current study to improve our understanding of host susceptibility and therefore, disease management strategies related to crop rotation.

Although the evidence is clear that the subgroups 'IIIB' and 'IV' are not phylogenetically supported, interpretation of how subgroups are actually organized within AG 2-2 is not all that straightforward. It may be tempting to consider splitting ISG 'IIIB' into two subgroups (perhaps 'IIIA' and 'IIIB') and in that way retain the ISG 'IV'. However, we contend this is difficult to justify given the branching patterns shown in clade 1 (Figure 2.8), the presence of 'type IV' isolates in clade 2, and the confusion it would cause with the historical literature. Clade 1 could alternatively be interpreted as consisting of two subclades of 'type IIIB' isolates and one

subclade of 'type IV' isolates. This arrangement, however, seems unnecessarily complex, especially if clade 2 is treated in the same manner based on distances and branching patterns. In addition, both the cluster analysis and the STRUCTURE plot group 'type IIIB' isolates from clade 1 into a single cluster (Figure 2.2 & 2.8). Perhaps analyzing additional isolates could provide a better perspective on the relationship of the subclades within clade 1, but based on the current evidence, we consider clade 1 to be a single clade that consists of both 'type IIIB' and 'type IV' isolates.

Collectively, we interpret these observations as support for the clusters identified by cluster and MSN analysis. Therefore, we propose that AG 2-2 should be subdivided into three intraspecific groups (ISG) and that these groups should be given two-letter designations that are consistent with AG 2-2LP described by Hyakumachi et al. (1998). Two-letter designations would provide more consistent terminology, not just within AG 2-2, but also among different AG, most of which use two-letter designations for their ISG (Sneh et al. 1991). In addition, the designation 'IV' can cause confusion as AG 2-2IV can be mistaken for AG 4, not so much in writing, but more so when discussed verbally with growers and other stakeholders.

We propose designating clade 1 as AG 2-2BR (which includes genetic clusters 1 & 2; Figure 2.8) and clade 2 as AG 2-2PR (includes genetic clusters 3 & 4; Figure 2.8). These subgroup designations reflect host preference based on virulence testing combined with some historical perspective. AG 2-2BR (clade 1) not only contained isolates that were, on average, most aggressive on sugar beet (*Beta vulgaris*; Minier & Hanson, 2022) but also included the majority of the 'type IV' isolates, which were the original 'beet type' as described by Ogoshi (1987). Isolates from AG 2-2PR (clade 2) were, on average, more aggressive on dry beans (*Phaseolus vulgaris*) than isolates from the other groups (Minier 2019).

In the current study, the AG 2-2LP isolate clusters with other isolates associated with proposed group AG 2-2PR (clade 2) such as 'Rs850', '24BR' and 'Slovakia' (Figure 2.2), but phylogenetically, it is more closely related to isolates from group AG 2-2BR (Figure 2.8; clade 1). Several studies have shown AG 2-2LP to group with isolates of AG 2-2IV (Carling et al. 2002; Salazar et al. 2000; Sharon et al. 2008), which would be consistent with its association with AG 2-2BR, that contains most of the 'type IV' isolates. However, because of reported differences in host range (Aoyagi et al. 1998; Burpee & Martin 1996; Hyakumachi et al. 1998), we propose maintaining AG 2-2LP as a separate subgroup pending additional evidence. Another subgroup, AG 2-2WB, was proposed by Godoy-Lutz et al. (2008) but reports examining this subgroup are limited and no isolates associated with this group were included in the current study. Consequently, we cannot assess the relationship of AG 2-2WB as a subgroup until further testing can be completed.

The relationship of AG 2-2 to other AG based on rRNA-ITS sequences has also been inconsistent. An analysis of *rRNA-LSU* and *ITS* by Gonzalez et al. (2001) showed AG 2-2 was most closely related to AG 2-1 and AG 9, both from potato in the US. In contrast, the phylogeny of Sharon et al. (2008), using the same loci, showed AG 2-2 most closely related to AG 11 and AG 2-3 or AG 3, depending on tree building algorithm used. Strausbaug et al. (2011a) showed AG 5 as the closest relative to AG 2-2, although they did not include as many representative AG as did Gonzalez et al. (2001) and Sharon et al. (2008). In the current study, we included a limited number of AG in addition to AG 2-2 with a *Ceratobasidium* sp. as the outgroup. Although the primers for amplification of loci used in phylogenetic analysis developed in the current study were not evaluated on non-AG 2-2 isolates using PCR, they were developed and evaluated *insilico* on the non-AG 2-2 isolates included in the current study plus some additional

Ceratobasidium spp. that were not included in the current report. Therefore, we expect the primers reported herein should be suitable for the evaluation of relationships within *Rhizoctonia* and *Ceratobasidium*.

Rhizoctonia solani AG2-2 is multinucleate and heterokaryotic with between 3 and 13 haploid nuclei per cell (Sneh et al. 1991). Exchange of nuclei during anastomosis has been observed and can result in heterokaryons readily distinguishable from either parental type (Whitney & Parmeter 1963). Because of this, we had the expectation that isolates would have more than two alleles at some loci, as has been reported for the ITS region (Strausbaugh et al. 2011a). However, with few exceptions, we identified no more than two alleles at any individual locus, making these isolates effectively dikaryotic. One such exception occurred at locus 8703, in which three alleles were detected for 8 isolates, including one allele with a length of 182bp. Because the peaks for those instances were less than 20% the intensity of the other peaks and their expression was not consistent, we suspected that allele 182 was not a true allele. Cloning results supported our suspicions and showed the allele was the result of non-specific binding and amplification between two forward primers.

How *R. solani* AG 2-2 regulates nuclei in order to maintain this pseudo-diploid status is unknown. One possible mechanism is nuclei exclusion or retention by somatic or vegetative compatibility (Leslie 1996; Puhalla 1985). Since nuclei are presumably exchanged during anastomosis reactions, the same compatibility factors may govern both anastomosis and nuclei retention/exclusion. Classification of anastomosis reactions may give an indication as to the extent of vegetative compatibility (Carling 1996). Anastomosis reactions that are characterized as 'C3' (perfect fusion) occur between the most closely related isolates and the cells adjacent to the anastomosis site remain healthy. Thus, the exchange of genetic material can presumably

occur freely in 'C3' fusions. In contrast, 'C2' (imperfect fusion) reactions result in the death of cells adjacent to the anastomosis site, which could hinder the exchange of nuclei. While genetic exchange has been observed to occur in 'C2' reactions (Toda & Hyakumachi 2006), it is uncertain that it occurs in all or even most 'C2' reactions. Similarity between nuclei, and in particular, vegetative compatibility factors, may determine which nuclei can be exchanged during anastomosis. Consequently, heterokaryons may appear to be homozygous due to restraints in the variability of nuclei that can be exchanged during anastomosis.

Several instances of hidden allelic diversity were revealed by cloning, with some loci having up to four alleles identical in length but different in sequence (Table 2.8). Each of these alleles could potentially represent a unique nuclear type indicating a heterokaryon with four nuclear types. However, these alleles differed by only a couple SNPs and only two loci in the same isolate ('Rs850') had evidence of more than 2 alleles. Previous findings, regarding diversity in ITS sequences, showed multiple sequences present in individual isolates of *R. solani* AG 2-2 (Strausbaugh et al. 2011a) and AG 2-1 (Pannecoucque & Hofte 2009), although ITS is known to be multicopy (Vilgalys & Gonzalez 1990) and copy status of microsatellite loci in the current study is unknown. The consequence being that identification of complete genetic diversity and the actual heterokaryotic state of an individual is especially challenging to determine. Sequencing using long-read technology may help resolve karyotype, especially in regard to isolates such as 'Rs850', which show evidence of admixture (Figure 2.3).

When estimated heterozygosity is plotted on the Bayesian phylogenetic tree (Figure 2.8), levels of heterozygosity largely corresponded with phylogenetic clades. Cluster 2, that contains primarily 'type IV' isolates within clade AG 2-2BR, is the cluster with the lowest heterozygosity, with all isolates in the cluster having less than 2% heterozygosity. This is in contrast with cluster

1 within the same clade (AG 2-2BR) which consists of isolates with greater than 4% heterozygosity. Clade AG 2-2PR is made up of mostly isolates with intermediate heterozygosity (2 - 4%). Curiously, observations of these heterozygosity patterns resemble observations of aggressiveness, especially on sugar beet. Clusters with higher heterozygosity were, on average, more aggressive on sugar beet than those with lower heterozygosity (data not shown).

BUSCO scores showed high levels of duplication in some isolates (Table 2.9). Duplication levels were significantly correlated with heterozygosity as predicted by k-mer counting $(p < 0.001, R^2 = 0.838)$. The isolate 'Slovakia' had the highest level of both duplication and heterozygosity (72.5% and 6.62% respectively) and was also one of the isolates that had evidence for admixture between two clusters (Figure 2.3). This observation is consistent with the expectations of a heterokaryon consisting of nuclei from genetically distinct parental sources (Todo & Hyakumachi 2006). Curiously, two of the other isolates, 'C116S' and 'ACC3-LP', that showed evidence of admixture had some of the lowest levels of duplication (0.5% and 0.3% respectively) and heterozygosity (0.03% and 0.66% respectively). These contrasting observations may be the result of differences in heterothallic-homothallic pairings compared to heterothallic-heterothallic or homothallic-homothallic pairings (Toda & Hyakumachi 2006). Unfortunately, heterozygosity alone does not appear to be a reliable indicator of heterokaryon status.

The type of mating system present in natural populations of AG 2-2 is still an open question in *Rhizoctonia* biology. Reports of isolates of AG 2-2 producing sexual structures are rare (Olaya and Abawi 1994; Toda and Hyakumachi 2006), and mostly come from Japan (Kiyoshi et al. 2014). In addition, reports of the formation of basidiospores all involve 'type IV' isolates (Kiyoshi et al. 2014; Naito 1990; Toda & Hyakumachi 2006). We are unaware of reports that have observed or induced basidiospore production in 'type IIIB' isolates. Nevertheless, high

levels of genetic diversity within field populations have been suggested to indicate the possibility of populations with at least some level of sexual recombination (Ajayi-Oyetunde et al. 2019). Data from the current study, particularly the lack of widespread admixture and the deficit of heterozygosity at several loci, supports clonal reproduction as the primary mode of reproduction in AG 2-2. However, there are several indications in our data that sexual recombination may occur, at least occasionally, in natural populations. For example, Kiyoshi et al. (2014) showed that heterogeneous, heterokaryotic parents would produce homokaryotic progeny through basidiospore formation, resulting in the simplification of clonal diversity through generations. This "simplification" could explain why there is a cluster of homogeneous isolates nested within a clade of highly heterogeneous isolates. Therefore, we hypothesize that the members of cluster 2 within clade AG 2-2BR are clonal descendants of basidiospore derived progeny.

In contrast, the pattern of admixture observed in several isolates (Figure 2.3) could be interpreted to be the result of asexual reproduction through the formation of heterokaryons during anastomosis. The formation of heterokaryons has been reported in AG 2-2IV (Kiyoshi et al. 2014; Toda & Hyakumachi 2006) and the exchange of entire nuclei, as would be expected in anastomosis interactions, could result in a heterokaryotic progeny with approximately 50/50 association with two genetic groups. Thirty (83%) of the isolates shown on the structure plot have more than 95% of their genetic variation associated with a single cluster (Figure 2.3). The other six isolates have more than 90% of their genetic variation associated with two clusters, where the association is split approximately 50/50 between the two groups. The exception to this is isolate ACC3-LP (the only AG 2-2LP isolate in the current study) in which about 84% of its genetic diversity is shared with isolate C116S (from Japan) and 12% with cluster 2 that contains the other three isolates from Japan.

Thirteen loci were initially identified for use as part of a microsatellite panel to genotype field isolates. We reduced the panel size to eight loci in order to maximize utilization of a 96-well plate and reduce overall cost of genotyping. The genotype accumulation curve indicated that more than 90% of the genotypes could be distinguished with eight loci (Figure 2.1) Therefore, we chose the eight loci with the highest PIC values and developed conditions suitable for duplexing. The result was that twenty-four isolates can be genotyped in an individual run utilizing a single 96-well plate. It may be possible to add an additional dye color and include some of the extra loci in the set by triplexing the reactions, but we found this endeavor challenging due to fragment size overlap. Since eight loci seemed to provide sufficient genotype information, we did not pursue adding additional loci to our eight-loci panel. Alternatively, these additional loci could be analyzed separately and possibly used to provide additional discrimination for populations that have high numbers of unresolved individuals.

In the current study, we provide evidence that the traditional subgroups of AG 2-2 are not phylogenetically supported and should be abandoned. Instead, we propose three genetic subgroups, AG 2-2PR, AG 2-2BR (that contains a mix of 'type IIIB' and 'type IV' isolates) and tentatively retaining AG 2-2LP as defined by Hyakumachi et al. (1998). In addition, we have developed a set of highly polymorphic microsatellite markers that can provide high-throughput analysis of *R. solani* AG 2-2 populations. We expect these results and supporting molecular markers will lead to the formation and investigation of novel hypotheses regarding the population biology of *R. solani* AG 2-2, especially regarding the formation of heterokaryons and the prevalence of sexual or asexual reproduction in natural populations.

REFERENCES

- Adams, G.C. 1988. *Thanatephorus cucumeris (Rhizoctonia solani*), a species complex of wide host range. Adv Plant Pathol, 6: 535-552.
- Ajayi-Oyetunde, O.O. and Bradley, C.A. 2018. *Rhizoctonia solani*: taxonomy, population biology and management of Rhizoctonia seedling disease of soybean. Plant Pathol, 67:3-17.
- Ajayi-Oyetunde, O.O., Everhart, S.E., Brown, P.J., Tenuta, A.U., Dorrance, A.E. and Bradley, C.A. 2019. Genetic structure of *Rhizoctonia solani* AG-2-2IIIB from soybean in Illinois, Ohio, and Ontario. Phytopathology, 109:2132-2141.
- Anderson, J.A., Churchill, G.A., Autrique, J.E., Tanksley, S.D. and Sorrells, M.E. 1993. Optimizing parental selection for genetic linkage maps. Genome, 36:181-186.
- Aoyagi, T., Kageyama and Hyakumachi, M. 1998. Characterization and survival of *Rhizoctonia solani* AG 2-2LP associated with large patch disease of zoysia grass. Plant Dis, 82:857-863.
- Baisi, A., Martin, F. N., Cacciola, S. O., di San Lio, G. M., Grünwald, N. J., and Schena, L. 2016. Genetic analysis of *Phytophthora nicotianae* populations from different hosts using microsatellite markers. Phytopathology, 106:1006-1014.
- Bolton, M.D., Panella, L., Campbell, L. and Khan, M.F.R. 2010. Temperature, moisture and fungicide effects in managing Rhizoctonia root and crown rot of sugar beet. Phytopathology, 100:689-697.
- Brantner, J.R. and Windels, C.E. 2007. Distribution of *Rhizoctonia solani* AG 2-2 intraspecific groups in the Red River Valley and Southern Minnesota. Sugarbeet Res Ext Rep, 38:242-246.
- Brownstein, M.J., Carpten, J.D. and Smith, J.R. 1996. Modulation of non-templated nucleotide addition by *Taq* polymerase: primer modifications that facilitate genotyping. BioTechniques, 20:1004-1010.
- Burpee, L.L. and Martin, S.B. 1996. Biology of turfgrass disease incited by *Rhizoctonia* species. Pgs. 359-368 in: *Rhizoctonia* Species: Taxonomy, Molecular Biology, Ecology, Pathology and Disease Control. Sneh, B, Jabaji-Hare, S., Neate, S. and Dijst, G. (eds.) Kluwer Academic Publishers, Dordrecht, The Netherlands.
- Carling, D.E. 1996. Grouping in *Rhizoctonia solani* by hyphal anastomosis interactions. Pgs. 37-47 in: *Rhizoctonia* Species: Taxonomy, Molecular Biology, Ecology, Pathology and Disease Control. Sneh, B, Jabaji-Hare, S., Neate, S. and Dijst, G. (eds.) Kluwer Academic Publishers, Dordrecht, The Netherlands.
- Carling, D. E., Kuninaga, S. and Brainard, K. A. 2002. Hyphal anastomosis reactions, rDNA internal transcribed spacer sequences, and virulence level among subsets of *Rhizoctonia solani* anastomosis group-2 (AG-2) and AG-BI. Phytopathology, 92:43-50.

- Cappelli, C., Corazza, L., Luongo, L. and Stravato, V.M. 1999. Interactions between crucifers and *Rhizoctonia solani* AG 2-1, AG 2-2IIIB, AG 2-2IV, AG 4. Phytopathol Mediterr, 38:37-39.
- Ciampi, M.B., Meyer, M.C., Costa, M.J.N., Zala, M., McDonald, B.A., and Ceresini, P.C. 2008. Genetic structure of populations of *Rhizoctonia solani* anastomosis group-1 IA from soybean in Brazil. Phytopathology, 98:932-941.
- Cubeta, M.A. and Vilgalys, R. 1997. Population biology of the *Rhizoctonia solani* complex. Phytopathology, 87:480-484.
- Cubeta, M.A., Echandi, E., Abernethy, T. and Vilgalys, R. 1991. Characterization of anastomosis groups of binucleate *Rhizoctonia* species using restriction analysis of an amplified of an amplified ribosomal RNA gene. Phytopathology, 81:1395-1400.
- Dieringer, D. and Schlötterer, C. 2003. Microsatellite analyser (MSA): a platform independent analysis tool for large microsatellite data sets. Mol Ecol Notes, 3:167-169.
- Edwards, K.J., Barker, J.H.A., Daly, A., Jones, C. and Karp, A. 1996. Microsatellite libraries enriched for several microsatellite sequences in plants. BioTechniques, 20:758-760.
- Ellegren, H. 1991. DNA typing of museum birds. Nature, 354:113.
- Ellegren, H. 2004. Microsatellites: simple sequences with complex evolution. Nat Rev Genet, 5:435-445.
- Engelkes, C.A. and Windels, C.E. 1996. Susceptibility of sugar beet and beans to *Rhizoctonia solani* AG-2-2 IIIB and AG-2-2 IV. Plant Dis, 80:1413-1417.
- Ferrucho, R.L., Zala, M., Zhang, Z., Cubeta, M.A., Garcia-Dominguez, C. and Ceresini, P.C. 2009. Highly polymorphic *in-silico*-derived microsatellite loci in the potato-infecting fungal pathogen *Rhizoctonia solani* anastomosis group 3 from the Columbian Andes. Mol Ecol Resour, 9:1013-1016.
- Ferrucho, R.L., Ceresini, P.C. Ramirez-Escobar, U.M, McDonald, B.A., Cubeta M.A., and Garcia-Dominguez, C. 2013. The population genetic structure of *Rhizoctonia solani* AG-3PT from potato in the Columbian Andes. Phytopathology, 103:862-869.
- Godoy-Lutz, G., Kuninaga, S., Steadman, J.R. and Powers, K. 2008. Phylogenetic analysis of *Rhizoctonia solani* subgroups associated with web blight symptoms on common bean based on ITS-5.8S rDNA. J Gen Plant Pathol, 74:32-40.
- Gonzalez, D. Carling, D.E., Kuninaga, S., Vilgalys, R. and Cubeta, M.A. 2001. Ribosomal DNA systematics of *Ceratobasidium* and *Thanatephorus* with *Rhizoctonia* anamorphs. Mycologia, 93:1138-1150.
- Grover, A. and Sharma, P.C. 2016. Development and use of molecular markers: past and present. Crit Rev Biotechnol, 36:290-302.

- Gurevich, A., Saveliev, V., Vyahhi, N. and Tesler, G. 2013. QUAST: quality assessment tool for genomes assemblies. Bioinformatics, 29:1072-1075.
- Hanson, L.E. and Minier, D. 2016. *Rhizoctonia solani*: understanding the terminology. Bean Improv Coop Annu Rep, 58:x-xiii.
- Haratian, M., Safaie, N., Sharifnabi, B., Mahmudi, S. B. and Ariana, A. 2013. Genetic structure of population of *Rhizoctonia solani* AG-4 from five provinces in Iran. Plant Pathol, 62:649-656.
- Hecker, R.J. and Rupple, E.G. 1975. Inheritance of resistance to Rhizoctonia root rot in sugarbeet. Crop Sci, 15:487-490.
- Hodel, R.G.J., Segovia-Salcedo, M.C., Landis, J.B., Crowl, A.A., Sun, M., Liu, X., Gitzendanner, M.A., Douglas, N.A., Germain-Aubrey, C.C., Chen, S., Soltis, D.E., and Soltis, P.S. 2016. The report of my death was an exaggeration: A review for researchers using microsatellites in the 21st century. Appl Plant Sci, 4:1600025. doi:10.3732/apps.1600025
- Hyakumachi, M., Mushika, T., Ogiso, Y., Tdoa, T., Kageyama, K. and Tsuge, T. 1998. Characterization of a new cultural type (LP) of *Rhizoctonia solani* AG2-2 isolated from warm-season turfgrasses, and its genetic differentiation from other cultural types. Plant Pathol, 47:1-9.
- Ithurrart, M.E.F., Büttner, G. and Petersen, J. 2004. Rhizoctonia root rot in sugar beet (*Beta vulgaris* ssp. *altissima*) epidemiology aspects in relation to maize (*Zea mays*) as a host plant. J Plant Dis Protect, 111:302-312.
- Jefferies, A.J., Wilson, V. and Thein, S.L. 1985. Hypervariable 'minisatellite' regions in human DNA. Nature, 314:67-73.
- Jombart, T. 2008. adegenet: an R package for the multivariate analysis of genetic markers. Bioinformatics, 24:1403-1405.
- Jombart, T. and Ahmed, I. 2011. adegenet 1.3-1: new tools for the analysis of genome-wide SNP data. Bioinformatics, 27:3070-3071.
- Kamvar, Z.N., Tabima, J.F. and Grünwald, N.J. 2014. Poppr: an R package for genetic analysis of populations with clonal, partially clonal, and/or sexual reproduction. PeerJ, 2:e281. doi:10.7717/peerj.281
- Kamvar, Z.N., Tabima, J.F. and Grünwald, N.J. 2015. Novel R tools for analysis of genome-wide population genetic data with emphasis on clonality. Front Genet, 6:208 doi:10.3389/fgene.2015.00208

- Kirk, W.W., Wharton, P.S., Schafer, R.L., Tumbalam, O., Poindexter, S., Guza, C., Fogg, R., Schlatter, T., Stewart, J. Hubbell, L., and Ruppal, D. 2008. Optimizing fungicide timing for the control of Rhizoctonia crown and root rot of sugar beet using soil temperature and plant growth stages. Plant Dis, 92:1091-1098.
- Kiyoshi, T., Naito, S., Akino, S., Ochi, S. and Kondo, N. 2014. Progeny derived from *Thanatephorus cucumeris* (*Rhizoctonia solani*) AG-2-2 IV isolates on sugar beet foliage show more clonal diversity in somatic compatibility grouping than those from roots and petioles. J Gen Plant Pathol, 80:136-146.
- Kuninaga, S. and Yokosawa, R. 1985. DNA base sequence homology in *Rhizoctonia solani* Kühn VI. Genetic relatedness among seven anastomosis groups. Ann Phytopathol Soc Jap, 51:127-132.
- Leslie, J.F. 1996. Fungal vegetative compatibility promises and prospects. Phytoparasitica, 24:3-6.
- Liu, Z.L., Nickrent, D.L. and Sinclair, J.B. 1990. Genetic relationships among isolates of *Rhizoctonia solani* anastomosis group-2 based on isozyme analysis. Can J Plant Pathol, 12:376-382.
- Liu, Z.L. and Sinclair, J.B. 1993. Differentiation of intraspecific groups within anastomosis group 1 of *Rhizoctonia solani* using ribosomal DNA internal transcribed spacer and isozyme comparisons. Can J Plant Pathol, 15:272-280.
- MacNish, G.C. and Sweetingham, M.W. 1993. Evidence of stability of pectic zymogram groups within *Rhhizoctonia solani* AG-8. Mycol Res, 97:1056-1058.
- Marcais, G. and Kingsford, C. 2011. A fast, lock-free approach for efficient parallel counting of occurrences of k-mers. Bioinformatics, 27:764-770.
- Martin, F., Widels, C., Hanson, L. and Brantner, J. 2014. Analysis of population structure and pathogenicity of *Rhizoctonia solani* AG2-2 (ISGIIIB and IV) isolates from Michigan, Minnesota and North Dakota. Sugarbeet Res Rep. Beet Sugar Development Foundation, Denver, CO. Published on CD.
- McCabe, P.A., Gallacher, M.P. and Deacon, J.W. 1999. Evidence for segregation of somatic incompatibility during hyphal tip subculture of *Rhizoctonia solani* AG 4. Mycol Res, 103:1323-1331.
- Meirmans, P.G. and Van Tienderen, P.H. 2004. GENOTYPE and GENODIVE: two programs for the analysis of genetic diversity of asexual organisms. Mol Ecol Notes, 4:792-794.
- Minier, D.H. 2019. Diversity of the fungal pathogen *Rhizoctonia solani* AG2-2. (Master's thesis). Michigan State University, East Lansing, MI. ProQuest, Ann Arbor, MI.

- Minier, D.H. and Hanson, L.E. 2021. Effect of low temperature on the aggressiveness of *Rhizoctonia solani* AG 2-2 isolates on sugar beet (*Beta vulgaris*) seedlings. Plant Dis, 105:3111-3117.
- Naito, S. 1990. Ecological role of basidiospore of *Thanatephorus cucumeris* (Frank) Donk in the incidence of foliage blight of sugar beets in Japan. Japan Agr Res Q, 23:268-275.
- Naito, S. Yamaguchi, T., Sugimoto, T. and Homma, Y. 1993. A simple method for the long-time culture storage of *Rhizoctonia* spp. on barleys'[(*Hordeum vulgare*] grains. Ann Rep Soc Plant Protect N Japan, 44:20-23.
- Muzhinji, N., Woodhall, J. W., Truter, M., and Van der Waals, J. E. 2016. Population genetic structure of *Rhizoctonia solani* AG 3-PT from potatoes in South Africa. Fungal Biol, 120:701-710.
- Neher, O.T. and Gallian, J.J. 2011. *Rhizoctonia* on sugar beet: importance, identification and control in the Northwest. PNW 629. Pacific Northwest Extension Publication, University of Idaho, Moscow, ID.
- Ng, N.L. and Tan, S.G. 2015. Inter-simple sequence repeats (ISSR) markers: are we doing it right? ASM Sci J, 9:30-39.
- Novelli, V.M., Cristofani-Yaly, M., Bastianel, M. Palmieri, D.A. and Machado, M.A. 2013. Screening of genomic libraries Pgs. 17-24 in: *Microsatellites: Methods and Protocols*. Kantartzi, S.K. (ed.). Springer, New York, NY.
- Nurk S., Bankevich, A., Antipov, D., Gurevich, A., Korobeynikov, A., Lapidus, A., Prjibelsky, A., Pyshkin, A., Sirotkin, A., Sirotkin, Y., Stepanauskas, R., McLean, J., LAsken, R., Clingenpeel, S.R., Woyke, T., Tesler, G., Alekseyev, M.A. and Pevzner, P.A. 2013.
 Assembling genomes and mini-metagenomes from highly chimeric reads. Pgs. 158-170 in: Research in Computational Molecular Biology. RECOMB 2013: Lecture Notes in Computer Science, vol 7821. Deng M., Jiang R., Sun F., Zhang X. (eds.). Springer, Berlin, Germany. doi:10.1007/978-3-642-37195-0_13
- O'Brien, P.A. 1994. Molecular markers in Australian isolates of *Rhizoctonia solani*. Mycol Res, 98:665-671.
- Ogoshi, A. 1987. Ecology and pathology of anastomosis and intraspecific groups of *Rhizoctonia solani* Kühn. Annul Rev Phytopathol, 25:124-143.
- Ohkura, M., Abawi, G.S., Smart, C.D., & Hodge, K.T. 2009. Diversity and aggressiveness of *Rhizoctonia solani* and *Rhizoctonia*-like fungi on vegetables in New York. Plant Dis, 93:615-624.
- Olaya, G. and Abawi, G.S. 1994. Characteristics of *Rhizoctonia solani* and binucleate *Rhizoctonia* species causing foliar blight and root rot on table beets in New York State. Plant Dis, 78:800-804.

- Pannecoucque, J. and Hofte, M. 2009. Detection of rDNA ITS polymorphism in *Rhizoctonia solani* AG 2-1 isolates. Mycology, 101:26-33.
- Pannecoucque, J., Van Beneden, S. and Höfte, M. 2008. Characterization and pathogenicity of *Rhizoctonia* isolates associated with cauliflower in Belgium. Plant Pathol, 57:737-746.
- Parker, P.G., Snow, A.A., Schug, M.D., Booton, G.C. and Fuerst, P.A. 1998. What molecules can tell us about populations: choosing and using a molecular marker. Ecology, 79:361-382.
- Parmeter, J.R. jr., Sherwood, R.T. and Platt, W.D. 1969. Anastomosis grouping among isolates of *Thanatephorus cucumeris*. Phytopathology, 59:1270-1278.
- Pritchard, J.K., Stephens, M. and Donnelly, P. 2000. Inference of population structure using multilocus genotype data. Genetics, 155:945-959.
- Puhalla, J.E. 1985. Classification of strains of *Fusarium oxysporum* on the basis of vegetative compatibility. Can J Bot, 63:127-150.
- R Core Team. 2022. R: a language and environment for statistical computing. R Foundation for Statistical Computing, Vienna, Austria. https://www.R-project.org/
- Ronquist, F., Teslenko, M., van der Mark, P. Ayres, D.L., Darling, A., Höhna, S., Larget, B., Liu, L., Suchard, M.A. and Huelsenbeck, J.P. 2012. MRBAYES 3.2: efficient Bayesian phylogenetic inference and model selection across a large model space. Syst Biol, 61:539-542.
- Rousset, F. 2008. Genepop'007: a complete reimplementation of the Genepop software for Windows and Linux. Mol Ecol Resour, 8:103-106.
- Saitou, N. and Nei, M. 1987. The neighbor-joining method: a new method for reconstructing phylogenetic trees. Mol Biol Evol, 4:406-425.
- Salazar, O., Julian, M.C. and Rubio, V. 2000. Primers based on specific rDNA-ITS sequences for PCR detection of *Rhizoctonia solani*, *R. solani* AG2 subgroups and ecological types, and binucleate *Rhizoctonia*. Mycol Res, 104:281-285.
- dos Santos Pereira, D.A., Ceresini, P.C., Castroagudin, V.L., Ramos-Molina, L.M., Chavarro-Mesa, E., Negrisoli, M.M., Campos, S.N., Pegolo, M.E.S. and Takada, H.M. 2017. Population genetic structure of *Rhizoctonia oryzae-sativae* from rice in Latin America and its adaptive potential to emerge as a pathogen on *Urochloa* pastures. Phytopathology, 107:121-131.
- Schlötterer, C., Amos, B. and Tautz, D. 1991. Conservation of polymorphic simple sequence loci in cetacean species. Nature, 354:63-65.
- Selkoe, K.A. and Toonin, R.J. 2006. Microsatellites for ecologists: a practical guide to using and evaluating microsatellite markers. Ecol Lett, 9:615-629.

- Sharon, M., Kuninaga, S., Hyakumachi, M., Naito, S. and Sneh, B. 2008. Classification of *Rhizoctonia* spp. using rDNA-ITS sequence analysis supports the genetic basis of the classical anastomosis grouping. Mycoscience, 49:93-114.
- Sneh, B., Burpee, L. and Ogoshi, A. 1991. Identification of *Rhizoctonia* species. APS Press, St. Paul, MN.
- Stamatakis, A, 2014. RAxML version 8: a tool for phylogenetic analysis and post-analysis of large phylogenies. Bioinformatics, 30:1312-1313.
- Strausbaugh, C.A., Eujayl, I.A., Panella, L.W. and Hanson, L.E. 2011a. Virulence, distribution and diversity of *Rhizoctonia solani* from sugar beet in Idaho and Oregon. Can J Plant Pathol, 33:210-226.
- Strausbaugh, C.A., Rearick, E., Eujayl, I. and Foote, P. 2011b. Influence of *Rhizoctonia*-bacterial root rot complex on storability of sugar beet. J Sugar Beet Res, 48:155-180.
- Stojšin, V., Budakov, D., Jacobsen, B., Grimme, E., Bagi, F., and Jasnic, S. 2007. Identification of *Rhizoctonia solani* isolates from sugar beet roots by analyzing the ITS region of ribosomal DNA. *Zbornik Matice Srpske Za Prirodne Nauke*, 113:161-171.
- Sumner, D.R. and Bell, D.K. 1982. Root diseases induced in corn by *Rhizoctonia solani* and *Rhizoctonia zeae*. Phytopathology, 72:86-91.
- Sumner, D.R. and Minton, N.A. 1989. Crop losses in corn induced by *Rhizoctonia solani* AG-2-2 and nematodes. Phytopathology, 79:934-941.
- Tautz, D. 1989. Hypervariability of simple sequences as a general source for polymorphic DNA markers. Nucleic Acids Res, 17:6463-6471.
- Tamura, K., Stecher, G. and Kumar, S. 2012. MEGA11: molecular evolutionary genetics analysis version 11. Mol Biol Evol, 38:3022-3027.
- Toda, T. and Hyakumachi, M. 2006. Heterokaryon formation in *Thanatephorus cucumeris* anastomosis group 2-2 IV. Mycologia, 98:726-736.
- Vaghefi, N., Kikkert, J.R., Bolton, M.D., Hanson, L.E., Secor, G.A. and Pethybridge, S.J. 2017. *De novo* genome assembly of *Cercospora beticola* for microsatellite marker development and validation. Fungal Ecol, 26:125-134.
- Vilgalys, R. and Cubeta, M. A. 1994. Molecular systematics and population biology of *Rhizoctonia*. Annu Rev Phytopathol, 32:135-155.
- Vilgalys, R. and Gonzalez, D. 1990. Organization of ribosomal DNA in the basidiomycete *Thanatephorus praticola*. Curr Genet, 18:277-280.

- Vurture, G.W., Sedlazeck, F.J., Nattestad, M., Underwood, C.J., Fang, H., Gurtowski, J. and Schatz, M.C. 2017. GenomeScope: fast reference-free genome profiling from short reads. Bioinformatics, 33:2202-2204.
- Wang, J. and Chilvers, M.I. 2016. Development and characterization of microsatellite markers for *Fusarium virguliforme* and their utility within clade 2 of the *Fusarium solani* species complex. Fungal Ecol, 20:7-14.
- Waterhouse, R.M., Seppey, M., Simão, F.A., Manni, M., Ioannidis, P., Klioutchnikov, G., Kriventseva, E.V. and Zdobnov, E.M. 2017. BUSCO applications from quality assessments to gene predictions and phylogenomics. Mol Biol Evol, 35:543-548.
- Wibberg, D. Anderson, L. Rupp, O., Goesmann, A. Pühler, A., Varrelmann, M., Dixelius, C. and Schlüter, A. 2016. Draft genome sequence of the sugar beet pathogen *Rhizoctonia solani* AG2-2IIIB strain BBA69670. J Biotechnol, 222:11-12.
- Windels, C.E. and Brantner, J.R. 2005. Previous crop influences *Rhizoctonia* on sugarbeet. 2004a Sugarbeet Res Ext Rept, 35:227-231.
- Windels, C.E. and Brantner, J.R. 2006. Crop rotation effects on *Rhizoctonia solani* AG 2-2. 2005 Sugarbeet Res Ext Rept, 36:286-290.
- Windels, C.E., Jacobsen, B.J. and Harveson, R.M. 2009. Rhizoctonia root and crown rot. Pgs. 33-36 in: Compendium of Beet Diseases and Pests (2nd ed.). Harveson, R.M., Hanson, L.E. and Hein, G.L. (eds.) APS Press, St. Paul, MN.
- Winter, D.J. 2012. MMOD: an R library for the calculation of population differentiation statistics. Mol Ecol Res, 12:1158-1160.
- Whitney, H.S., & Parmeter, J.R. jr. 1963. Synthesis of heterokaryons in *Rhizoctonia solani* Kühn. Can J Plant Pathol, 41:879-886.
- You, F.M., Huo, N., Gu, Y.Q., Luo, M., Ma, Y., Hane, D., Lazo, G.R., Dvorak, J. and Anderson, O.D. 2008. BatchPrimer3: a high throughput web application for PCR sequencing primer design. BMC Bioinformatics, 9:253. doi:10.1186/1471-2105-9-253
- Zala, M., McDonald, B.A., Bernardes de Assis, J., Ciampi, M.B., Storari, M., Peyer, P., and Ceresini, P.C. 2008. Highly polymorphic microsatellite loci in the maize- and rice-infecting fungal pathogen *Rhizoctonia solani* anastomosis group 1-1A. Mol Ecol Resour, 8:686-689.
- Zane, L., Bargelloni, L. and Patarnello, T. 2002. Strategies for microsatellite isolation: a review. Mol Ecol, 11:1-16.
- Zheng, L., Shi, F. and Hsiang, T. 2013. Genetic structure of a population of *Rhizoctonia solani* AG2-2 IIIB from *Agrostis stolonifera* revealed by inter-simple sequence repeat (ISSR) markers. Can J Plant Pathol, 34: 476-481.

CHAPTER 3:

POPULATION STRUCTURE OF RHIZOCTONIA SOLANI AG 2-2 REVEALS CRYPTIC SOURCES OF GENETIC DIVERSITY

Introduction

Soil-borne fungal pathogens can be difficult to manage because of unique challenges such as the difficulty identifying infections in a timely manner due to the delay in above-ground symptom expression (Leclerc et al. 2014; Rush et al. 1992), the difficulty in delivering chemical controls effectively, and the longevity of many soil-borne fungal survival structures (Panth et al. 2020; Sussman 1968). The lack of effective chemical controls has prompted a renewed focus on physical and cultural controls for the management of soil-borne diseases, such as adjusting planting dates, managing soil wetness, deep plowing, and sanitation (Katan 2000). However, cultural practices often have negative effects on other agronomic conditions. For example, deep plowing can reduce inoculum load in some cases but can also increase soil erosion, mineral leaching and reduced total organic carbon levels (Karlen et al. 2013).

Some of the most effective strategies employed against soil-borne fungal diseases are host resistance and crop rotation (Katan 2000; Mihajlović et al. 2017). While these strategies can be effective, it is not always possible to develop an effective management program that utilizes these approaches. In particular, host resistance for many soil-borne diseases is simply not available. Additionally, choosing suitable crop rotation programs can be challenging, especially against pathogens that may have a wide host range and an aggressive, necrotrophic lifestyle (Okubara eet al. 2014). Populations with high levels of genetic diversity can exacerbate the situation and reduce the effectiveness of management strategies by overcoming host resistance and limiting crop rotation choices (Reeleder 2003). Thus, it is critical to understand not only the life history traits of plant pathogens, but also the extent and significance of the biological diversity of populations.

Rhizoctonia solani AG 2-2 is one of the most important soil-borne pathogens of sugar beet, causing Rhizoctonia root and crown rot (Buhre et al. 2009; Neher & Gallian 2011; Windels et al. 2009). It is a major problem in many growing regions around the world (Buhre et al. 2009; Strausbaugh et al. 2011a). Rhizoctonia solani is a species complex, where members are distinguished by their ability to anastomose with other members of the same anastomosis group (Carling 1996; Cubeta & Vilgalys 1997; Parmeter et al. 1969). At least 13 anastomosis groups (AG) have been described and the individual AG can be thought of as independently evolving lineages. Several AG contain well-defined cultural types, referred to as intraspecific groups (ISG), including R. solani AG 2-2 (Sharon et al. 2008; Sneh et al. 1991). Traditionally, AG 2-2 has been separated into three ISGs, originally separated by host range (2-2IIIB, 2-2IV, and AG 2-2LP), but more commonly AG 2-2IIIB and AG 2-2IV are separated by their ability to grow at 35°C. Recently, these subgroups have been shown to be phylogenetically unsupported (Carling et al. 2002; Martin et al. 2014; Strausbaugh et al. 2011a). Instead, based on the analysis presented in chapter 1 (current dissertation), we have proposed reorganizing AG 2-2 into three subgroups, AG 2-2LP, AG 2-2BR and AG 2-2PR, which do not rely on growth at 35°C for categorization.

Patch' that it causes on warm-season grasses (Hyakumachi et al. 1998). Subgroups AG 2-2BR and AG 2-2PR each contain a mix of 'type IIIB' and 'type IV' isolates and are proposed to be named based on the crop which the group is most severe (BR = <u>Beta</u> rot; PR = <u>Phaseolus</u> rot; Minier 2019; Minier & Hanson 2021). In addition, each of the subgroups AG 2-2BR and AG 2-2PR consist of two genetic clusters that do not form monophyletic groups. Clusters 1 & 2 are contained in subgroup AG 2-2BR and clusters 3 & 4 are contained in subgroup AG 2-2PR.

Each genetic cluster has unique characteristics that are explored in more detail in the current study.

In general, *Rhizoctonia solani* AG 2-2, is an aggressive necrotroph, and can result in losses of 30 to 60% in sugar beet fields (Neher & Gallian 2011; Windels et al. 2009) and reduced storability after harvest (Strausbaugh et al. 2011b). Complete crop losses for individual fields are possible when disease levels are greater than 50% due to poor harvestability and associated problems with processing and storage (Windels et al. 2009). Host resistance to Rhizoctonia root and crown rot is available in commercial varieties although resistance is incomplete, and the varieties have yield potential below that of the best approved varieties (Jacobsen et al. 2004). The most effective management strategies for limiting damage from Rhizoctonia root and crown rot involve those that minimize introduction of the pathogen or limit the buildup of inoculum.

Crop rotation is among the more important strategies for limiting inoculum build up in sugar beet production with a 3-year minimum between sugar beet crops being commonly recommended (Buhre et al. 2009; Windels et al. 2009). Rotation with non-host crops is crucial to reducing inoculum load prior to a subsequent sugar beet crop (Panth et al. 2020). However, many of the crops commonly grown in rotation with sugar beet are also susceptible to *R. solani*AG 2-2, including soybean (Fenille et al. 2002; Nelson et al. 1996), common bean (Muyolo et al. 1993; Peña et al. 2013), and corn (Ithurrart et al. 2004; Sumner & Milton 1989). Furthermore, reports describing the contribution of rotational crops to the reduction of disease have been inconsistent. For example, wheat is considered a non-host, yet Rush & Winter (1990) reported that wheat in rotation with sugar beet increased disease severity. This increase in disease pressure was likely due to colonization of the stubble (Neate 1987; Rush & Winter 1990).

Another example comes from Coons & Kotila (1935) who showed corn decreased disease

severity while Windels & Brantner (2005) found that corn increased disease severity on a following sugar beet crop. Ruppel (1985) determined that alfalfa was not a host to strains of *R. solani* isolated from sugar beets in contrast to previous findings by Maxson (1938).

Some of these discrepancies may be attributed to the variability of individual strains of *R. solani* AG 2-2. The genetics of *R. solani* AG 2-2, that underlies variability in virulence and host preference, is complicated and not yet fully understood. *R. solani* AG 2-2 is heterokaryotic and multi-nucleate with between 3 and 13 nuclei per cell (Ogoshi 1987; Sneh et al. 1991). The sexual stage for *R. solani* AG 2-2 has rarely been observed, but when present, has been identified as *Thanatephorus cucumeris* (Frank)Donk and reports have been limited to one subgroup, 'type IV' (AG 2-2IV) isolates (Kiyoshi et al. 2014; Qu et al. 2013; Toda & Hyakumachi 2006). While there is at least one report describing the infection of sugar beet by basidiospores (Naito & Sugimoto 1980), much of the work with basidiospores derived from AG 2-2 involved the formation of new somatic compatibility groups from the formation of heterokaryons (Kiyoshi et al. 2014; Qu et al. 2013; Toda & Hyakumachi 2006).

The reproductive strategy of *R. solani* AG 2-2 is primarily clonal, with a lack of asexual spores (Sneh et al. 1991) and a sexual stage that has not been observed in the field in most the growing regions around the world. Even so, high levels of diversity exist within *R. solani* AG 2-2 populations (Ajayi-Oyetunde et al. 2019; Strausbaugh et al. 2011a; Zheng et al. 2013). The source of this diversity is uncertain, but we hypothesize diversity is generated through parasexual exchange of nuclei during anastomosis and the presence of cryptic sexual recombination in some growing regions. Regardless of the source, high levels of diversity are expected to contribute to pathogen persistence and increase the challenges of disease management (Wang et al. 2017).

At least some individuals within *R. solani* AG 2-2 appear to have both heterothallic and homothallic mating systems and genetic exchange can occur between homothallic and heterothallic isolates (Toda & Hyakumachi 2006). Genetic exchange relies on the transfer of nuclei during anastomosis, which is regulated by vegetative compatibility and is a separate system from sexual compatibility (Leslie 1996). Collectively, these characteristics make the genetics of *R. solani* AG 2-2 challenging to assess.

The objective of the current study is to demonstrate the utility of these newly identified subgroups to generate novel hypotheses regarding the generation and distribution of genetic diversity in *R. solani* AG 2-2. We expect these hypotheses will lead to an enhanced understanding of *R. solani* AG 2-2 genetics and improved management strategies. To this end, we utilized a set of eight microsatellite markers that were described in chapter 2 (current dissertation) to examine the distribution patterns, reproductive strategy, and diversity of *R. solani* AG 2-2 populations at multiple scales including global, state and field levels. By exploring the populations at several levels, we provide a survey of diversity and organization in *R. solani* AG 2-2 populations that affect sugar beet. The relationship of genotype and subgroup to sugar beet, dry bean, and soybean as hosts was also investigated, to assist in crop rotation selections that may be altered due to the presence of certain subgroups within a particular field. In order to facilitate such choices, we have developed a set of subgroup-specific primers that may be used to identify field isolates to subgroup. In the long term, we expect this information will allow for more informed decisions regarding crop rotation choices.

Methods

Isolate collection

A total of 147 isolates of *Rhizoctonia solani* AG 2-2 were genotyped using a set of eight microsatellite markers as described in chapter 2 (current dissertation). The samples were drawn from three collections (Table 3.1): 86 isolates from the collection of Dr. Linda Hanson (USDA-ARS, East Lansing, MI), 17 isolates from the field crop pathology program of Dr. Martin Chilvers (MSU-PSM) and 44 isolates collected for the current study from the USDA Cercospora disease nursery at Saginaw Valley Research and Extension Center (SVREC).

Isolates from the collection of Dr. Linda Hanson were recovered from storage at -20°C by placing a single grain of infested barley on potato dextrose agar (PDA, Sigma-Aldrich, St. Louis, MO) and allowing culture to grow for 5-7 days at room temperature. Isolates from Dr. Chilvers field crop program were recovered in 2014 from symptomatic dry bean and soybean roots in Michigan. Each isolate was purified by hyphal tip transfer (Leslie & Summerell 2006) and stored on barley grains at -20°C until use. Cultures were recovered by placing a single infested grain on PDA and growing for 5-7 days at room temperature.

Isolates from the Cercospora nursery (located at the Saginaw Valley Research and Extension Center, Frankenmuth, MI) were collected in 2016 and 2017 from symptomatic, adult sugar beet roots. The nursery is separated into four quadrants, with each field approximately 4 hectares in size and separated by a grass strip approximately 10 meters wide. Sugar beets are grown in a particular quadrant every fourth year following a crop rotation schedule of sugar beet, corn, soybeans, and wheat with sugar beet following wheat. Collection followed nursery rotation with isolates from 2016 collected from the field in the northwest quadrant and from the field in the

northeast quadrant in 2017. Isolates were purified by hyphal tip transfer and stored on barley grains at -20°C.

Fungal tissue was grown in petri dishes on malt extract broth (MEB; Sigma-Aldrich) without shaking for 5 days. Hyphal mats were harvested using forceps, placed in 50 ml centrifuge tubes, and rinsed with sterile phosphate buffered saline (PBS; Cold Spring Harb Protoc 2006, doi:10.1101/pdb.rec8247). Fungal tissue was lyophilized (VirTis Genesis, SP Scientific, Warminster, PA) and ground in a modified paint shaker using 6 mm ceramic beads (Zircoa, Inc., Solon, OH). DNA was extracted from lyophilized tissue as reported in chapter 2 (current dissertation) using a modified protocol based on the OmniPrep for Fungi kit (G-Biosciences, St. Louis, MO).

Geographic Populations

Isolates were organized by geographic areas representative of the major sugar beet growing regions throughout the world (Table 3.1). Europe was considered a single growing region although we recognize that there are likely distinct regions within the European continent that should be considered separate geographical populations, much like exist in the US. However, the precise origin of some of the isolates included from Europe was uncertain and our access to European sugar beet practices was limited so we classified 'Europe' as a single geographical region for the purposes of the current study. The 'Midwest' region included isolates from Michigan, Ohio, and Wisconsin. Isolates from the 'West' region were collected from Idaho, Montana, and Colorado. Isolates from the 'Red River Valley' included those isolates collected from Minnesota and North Dakota and isolates from the 'South' were collected from Texas and Arizona (Table 3.1).

Table 3.1 Isolates of *Rhizoctonia solani* used in the current study.

Name	MLG ^a	ISG ^b	Clusterc	Collection	Original Collector	Crop ^d	Locale ^e	Region ^f	County g
Taltfalt	1	PR	3	Hanson	L Holmquist	sugar beet	Sweden	Europe	-
R14-12	2	PR	3	Hanson	CH Seed	spinach	-	-	-
Vander-2	3	PR	3	Hanson	L Holmquist	fodder beet	N Zealand	N Zealand	-
Cookson	4	PR	3	Hanson	L Holmquist	fodder beet	N Zealand	N Zealand	-
R15-100	5	PR	4	Chilvers	J Jacobs	sugar beet	Michigan	Midwest	Saginaw
Plattling	6	PR	3	Hanson	L Holmquist	sugar beet	Germany	Europe	-
Rickard	6	PR	3	Hanson	B Holtschulte	sugar beet	-	Europe	-
Cavalie	7	PR	3	Hanson	B Holtschulte	sugar beet	-	Europe	-
Rs331	8	PR	3	Hanson	C Windels	sugar beet	Minnesota	RedRiver	-
99-15	9	PR	4	Hanson	-	soybean	Ohio	Midwest	-
F24	9	PR	4	Hanson	C Strausbaugh	sugar beet	Idaho	West	-
39AR	10	PR	4	Hanson	C Truman	sugar beet	Ontario	Ontario	-
R14-10	10	PR	4	Hanson	C Truman	sugar beet	Ontario	Ontario	-
R14-9	10	PR	4	Hanson	C Truman	sugar beet	Ontario	Ontario	-
Roland	10	PR	4	Hanson	L Holmquist	sugar beet	Germany	Europe	-
R15-73	11	PR	4	Hanson	D Minier	sugar beet	Michigan	Midwest	Saginaw
R15-93	12	PR	4	Hanson	D Minier	sugar beet	Michigan	Midwest	Saginaw
H502	13	BR	2	Hanson	L Herr	-	Ohio	Midwest	-
R33	13	BR	2	Hanson	C Rush	sugar beet	Texas	South	-
RH188	13	BR	2	Hanson	A Ogoshi	sugar beet	Japan	Japan	-
RH193	13	BR	2	Hanson	A Ogoshi	sugar beet	Japan	Japan	-
7A1	14	BR	2	Hanson	B Bill	-	Minnesota	RedRiver	-
Rs106	15	BR	2	Hanson	C Windels	sugar beet	Minnesota	RedRiver	-
H549	16	BR	2	Hanson	L Herr	sugar beet	Ohio	Midwest	-
Bayern	17	BR	2	Hanson	L Holmquist	sugar beet	Germany	Europe	-
91003	18	BR	2	Hanson	L Holmquist	sugar beet	-	-	-
Rs481	18	BR	2	Hanson	C Windels	sugar beet	Minnesota	RedRiver	-
Rs542	18	BR	2	Hanson	C Windels	sugar beet	Minnesota	RedRiver	-
Gg670a	19	PR	3	Hanson	L Holmquist	sugar beet	Holland	Europe	-
Hubert	19	PR	3	Hanson	L Holmquist	sugar beet	Germany	Europe	-
Ifz	19	PR	3	Hanson	L Holmquist	sugar beet	Germany	Europe	-
R18-19	19	PR	3	Hanson	L Holmquist	sugar beet	Germany	Europe	-
Rs296	20	BR	2	Hanson	C Windels	sugar beet	Minnesota	RedRiver	-
H582	21	BR	2	Hanson	L Herr	-	Ohio	Midwest	-
Rs588	22	BR	2	Hanson	C Windels	sugar beet	Minnesota	RedRiver	-
2C13	23	BR	2	Hanson	B Bugbee	sugar beet	Montana	West	-
Rs496	24	BR	2	Hanson	C Windels	sugar beet	Minnesota	RedRiver	-
Rs200	25	BR	2	Hanson	C Windels	sugar beet	Minnesota	RedRiver	-
5C5	26	BR	2	Hanson	B Bugbee	sugar beet	Minnesota	RedRiver	-
R164S	27	BR	2	Hanson	A Ogoshi	sugar beet	Japan	Japan	-
R86	28	BR	1	Hanson	C Rush	wheat	Texas	South	-

a) multi-locus genotype

b) intraspecific group

c) genetic cluster determined by popper

d) crop type isolate was recovered from

e) geographic location isolate was collected

f) category used in the current study to group isolates by geographic region of isolation

g) county which isolates was collected for those isolates recovered from Michigan. If isolate was collected from the Cercospora Nursery, designation indicates isolate was from Saginaw County in either 2016 (SV16) or 2017 (SV17)

Table 3.1 (Con't)

Name	MLG ^a	ISG ^b	Cluster c	Collection	Original Collector	Crop d	Locale e	Region ^f	County g
Johnson	29	PR	3	Hanson	L Holmquist	fodder beet	N Zealand	N Zealand	-
11-272a	30	PR	3	Hanson	L Holmquist	sugar beet	Holland	Europe	_
Kratzer	31	PR	3	Hanson	L Holmquist	sugar beet	Germany	Europe	_
99-11	32	PR	3	Hanson	-	soybean	Ohio	Midwest	_
99-12	32	PR	3	Hanson	_	soybean	Ohio	Midwest	_
R17-6	32	PR	3	Cercospora	D Minier	sugar beet	Michigan	Midwest	SV17
R15-66	33	PR	4	Chilvers	J Jacobs	soybean	Michigan	Midwest	Allegan
R15-82	34	PR	4	Chilvers	J Jacobs	soybean	Michigan	Midwest	Clinton
R15-83	34	PR	4	Chilvers	J Jacobs	soybean	Michigan	Midwest	Clinton
R15-84	34	PR	4	Chilvers	J Jacobs	soybean	Michigan	Midwest	Clinton
Rs255	35	PR	3	Hanson	C Windels	sugar beet	Minnesota	RedRiver	_
F517	36	PR	3	Hanson	C Strausbaugh	sugar beet	Idaho	West	_
87-36-1	37	PR	3	Hanson	C Windels	dry bean	N Dakota	West	-
F30	37	PR	3	Hanson	C Strausbaugh	sugar beet	Idaho	West	-
F36	37	PR	3	Hanson	C Strausbaugh	sugar beet	Idaho	West	-
F551	37	PR	3	Hanson	C Strausbaugh	sugar beet	Idaho	West	-
R16-20	37	PR	3	Cercospora	D Minier	sugar beet	Michigan	Midwest	SV16
R16-7	37	PR	3	Cercospora	D Minier	sugar beet	Michigan	Midwest	SV16
R17-31	37	PR	3	Cercospora	D Minier	sugar beet	Michigan	Midwest	SV17
R15-30	38	PR	3	Chilvers	J Jacobs	dry bean	Michigan	Midwest	Saginaw
R15-1	39	PR	3	Chilvers	J Jacobs	dry bean	Michigan	Midwest	Saginaw
R15-5	39	PR	3	Chilvers	J Jacobs	dry bean	Michigan	Midwest	Ingham
R15-15	40	PR	3	Chilvers	J Jacobs	dry bean	Michigan	Midwest	Saginaw
R15-59	40	PR	3	Chilvers	J Jacobs	soybean	Michigan	Midwest	Gratiot
2048 SB	41	PR	3	Hanson	L. Hanson	sugar beet	Michigan	Midwest	Midland
2049 SB	41	PR	3	Hanson	L. Hanson	sugar beet	Michigan	Midwest	Bay
2C1	41	PR	3	Hanson	B Bugbee	sugar beet	Montana	West	-
87-36-2	41	PR	3	Hanson	C Windels	dry bean	N Dakota	West	-
87-36-3	41	PR	3	Hanson	C Windels	dry bean	N Dakota	West	-
R09-23	41	PR	3	Hanson	L. Hanson	sugar beet	Michigan	Midwest	Bay
R15-17	41	PR	3	Chilvers	J Jacobs	dry bean	Michigan	Midwest	Saginaw
R15-25	41	PR	3	Chilvers	J Jacobs	dry bean	Michigan	Midwest	Saginaw
R15-34	41	PR	3	Chilvers	J Jacobs	dry bean	Michigan	Midwest	Saginaw
R15-48	41	PR	3	Chilvers	J Jacobs	dry bean	Michigan	Midwest	Montcalm
R15-53	41	PR	3	Chilvers	J Jacobs	dry bean	Michigan	Midwest	Saginaw
R16-1	41	PR	3	Cercospora	D Minier	sugar beet	Michigan	Midwest	SV16
R16-11	41	PR	3	Cercospora	D Minier	sugar beet	Michigan	Midwest	SV16
R16-12	41	PR	3	Cercospora	D Minier	sugar beet	Michigan	Midwest	SV16
R16-13	41	PR	3	Cercospora	D Minier	sugar beet	Michigan	Midwest	SV16
R16-15	41	PR	3	Cercospora	D Minier	sugar beet	Michigan	Midwest	SV16
R16-16	41	PR	3	Cercospora	D Minier	sugar beet	Michigan	Midwest	SV16
R16-18	41	PR	3	Cercospora	D Minier	sugar beet	Michigan	Midwest	SV16
R16-2	41	PR	3	Cercospora	D Minier	sugar beet	Michigan	Midwest	SV16
R16-21	41	PR	3	Cercospora	D Minier	sugar beet	Michigan	Midwest	SV16
R16-3	41	PR	3	Cercospora	D Minier	sugar beet	Michigan	Midwest	SV16
R16-4	41	PR	3	Cercospora	D Minier	sugar beet	Michigan	Midwest	SV16
R16-5	41	PR	3	Cercospora	D Minier	sugar beet	Michigan	Midwest	SV16

Table 3.1 (Con't)

Name	MLG ^a	ISG ^b	Cluster c	Collection	Original Collector	Crop d	Locale ^e	Region f	County g
R16-6	41	PR	3	Cercospora	D Minier	sugar beet	Michigan	Midwest	SV16
R16-8	41	PR	3	Cercospora	D Minier	sugar beet	Michigan	Midwest	SV16
R17-10	41	PR	3	Cercospora	D Minier	sugar beet	Michigan	Midwest	SV17
R17-11	41	PR	3	Cercospora	D Minier	sugar beet	Michigan	Midwest	SV17
R17-12	41	PR	3	Cercospora	D Minier	sugar beet	Michigan	Midwest	SV17
R17-13	41	PR	3	Cercospora	D Minier	sugar beet	Michigan	Midwest	SV17
R17-14	41	PR	3	Cercospora	D Minier	sugar beet	Michigan	Midwest	SV17
R17-21	41	PR	3	Cercospora	D Minier	sugar beet	Michigan	Midwest	SV17
R17-22	41	PR	3	Cercospora	D Minier	sugar beet	Michigan	Midwest	SV17
R17-23	41	PR	3	Cercospora	D Minier	sugar beet	Michigan	Midwest	SV17
R17-27	41	PR	3	Cercospora	D Minier	sugar beet	Michigan	Midwest	SV17
R17-28	41	PR	3	Cercospora	D Minier	sugar beet	Michigan	Midwest	SV17
R17-5	41	PR	3	Cercospora	D Minier	sugar beet	Michigan	Midwest	SV17
R17-7	41	PR	3	Cercospora	D Minier	sugar beet	Michigan	Midwest	SV17
R17-8	41	PR	3	Cercospora	D Minier	sugar beet	Michigan	Midwest	SV17
R17-9	41	PR	3	Cercospora	D Minier	sugar beet	Michigan	Midwest	SV17
R17-J	41	PR	3	Hanson	D Minier	sugar beet	Michigan	Midwest	Saginaw
R18-11	41	PR	3	Hanson	D Minier	sugar beet	Michigan	Midwest	Saginaw
R18-5	41	PR	3	Hanson	J Jacobs	sugar beet	Michigan	Midwest	Saginaw
R18-9	41	PR	3	Hanson	D Minier	soybean	Michigan	Midwest	Saginaw
Rs1146	41	PR	3	Hanson	C Windels	sugar beet	Minnesota	RedRiver	Jaginaw
Rs393	41	PR	3	Hanson	C Windels	sugar beet	Minnesota	RedRiver	_
R15-21	42	PR	3	Chilvers	J Jacobs	dry bean	Michigan	Midwest	Saginaw
R15-21	42	PR	3	Chilvers	J Jacobs	dry bean	Michigan	Midwest	Ingham
R15-60	42	PR	3	Chilvers	J Jacobs	soybean	Michigan	Midwest	Gratiot
R15-61	42	PR	3	Chilvers	J Jacobs	soybean	Michigan	Midwest	Gratiot
R15-01	42	PR	3	Chilvers	J Jacobs	dry bean	Michigan	Midwest	Ingham
Rs1012	43	PR	3	Hanson	C Windels	sugar beet	Minnesota	RedRiver	ingnam
R15-67	44	PR	3	Chilvers	J Jacobs	soybean	Michigan	Midwest	Shiawassee
R15-07	44	PR	3	Chilvers	J Jacobs	soybean	Michigan	Midwest	Shiawassee
Slovakia	45	PR	4	Hanson	B Holtschulte	sugar beet	-	Europe	Sillawassee
R15-78	46	PR	4	Chilvers	J Jacobs	soybean	Michigan	Midwest	Allegan
24BR	47	PR	4	Hanson	C Truman	sugar beet	Ontario	Ontario	Anegan
R15-98	47	PR	4	Hanson	D Minier	sugar beet	Michigan	Midwest	Saginaw
R16-14	47	PR	4	Cercospora	D Minier	sugar beet	Michigan	Midwest	SV16
R10-14 R17-24	47	PR	4	Cercospora	D Minier	sugar beet	Michigan	Midwest	SV10
R17-24 R17-26	47	PR	4	Cercospora	D Minier	sugar beet	Michigan	Midwest	SV17
Rs850	48	PR	4	Hanson	C Windels	sugar beet	Minnesota	RedRiver	- -
R17-16	49	PR	4	Cercospora	D Minier	sugar beet	Michigan	Midwest	SV17
R17-16 R17-15	50	PR	4	Cercospora	D Minier D Minier	sugar beet sugar beet	Michigan	Midwest	SV17 SV17
R17-13 R17-18	50	PR	4	Cercospora	D Minier D Minier	sugar beet sugar beet	Michigan	Midwest	SV17
R17-18 R17-19	50	PR		Cercospora	D Minier D Minier	sugar beet sugar beet	Michigan	Midwest	SV17 SV17
R17-19 R17-20	50	PR PR	4 4	Cercospora	D Minier D Minier	sugar beet sugar beet	Michigan Michigan	Midwest	SV17 SV17
R17-20 R17-29	50	PR PR		Cercospora	D Minier D Minier	sugar beet sugar beet	Michigan Michigan	Midwest	SV17 SV17
R17-29 R17-30	50	PR PR	4 4	Cercospora	D Minier D Minier	sugar beet sugar beet	Michigan Michigan	Midwest	SV17 SV17
Rs300	51	BR	1	Hanson	C Windels	sugar beet sugar beet	Minnesota	RedRiver	S V 1 /
						•			-
C116S	52	PR	3	Hanson	A Ogoshi	mat rush	Japan	Japan	

Table 3.1 (Con't)

Name	MLG ^a	ISG ^b	Cluster	Collection	Original Collector	Crop d	Locale e	Region ^f	County g
R15-63	53	PR	3	Chilvers	J Jacobs	soybean	Michigan	Midwest	Ithaca
R18-32	54	PR	3	Hanson	A Stouffer- Hopkins	turf	Michigan	Midwest	
R15-80	55	BR	1	Chilvers	J Jacobs	soybean	Michigan	Midwest	- Midland
R15-80	56	PR	4	Chilvers	J Jacobs	soybean	Michigan	Midwest	Shiawassee
R15-74 R15-90	50 57	BR	4	Chilvers	J Jacobs J Jacobs	-	C	Midwest	Clinton
	57 58	BR BR				soybean	Michigan	Midwest	Clinton
R15-86			4	Chilvers	J Jacobs	soybean	Michigan		
R15-87	59	PR	4	Chilvers	J Jacobs	soybean	Michigan	Midwest	Clinton
R15-72	60	PR	4	Chilvers	J Jacobs	soybean	Michigan	Midwest	Shiawassee
R15-76	60	PR	4	Chilvers	J Jacobs	soybean	Michigan	Midwest	Ithaca
R15-88	60	PR	4	Chilvers	J Jacobs	soybean	Michigan	Midwest	Clinton
R15-92	60	PR	4	Chilvers	J Jacobs	soybean	Michigan	Midwest	Clinton
B Hill	61	BR	1	Hanson	L Holmquist	fodder beet	N Zealand	N Zealand	-
R14-14	62	BR	1	Hanson	CH Seed	swiss chard	-	-	-
Rs890	63	BR	1	Hanson	C Windels	sugar beet	Minnesota	RedRiver	-
R18-31	64	BR	1	Hanson	N Lukasco	carrot	Michigan	Midwest	Oceana
W-22	65	BR	1	Hanson	RT Sherwood	dry bean	Wisconsin	Midwest	-
Alburry	66	BR	1	Hanson	L Holmquist	fodder beet	N Zealand	N Zealand	-
R16-10	67	BR	1	Cercospora	D Minier	sugar beet	Michigan	Midwest	SV16
R16-9	67	BR	1	Cercospora	D Minier	sugar beet	Michigan	Midwest	SV16
Rs866	68	BR	1	Hanson	C Windels	sugar beet	Minnesota	RedRiver	-
DKL4	69	BR	1	Hanson	L Holmquist	sugar beet	Denmark	Europe	-
Italien	69	BR	1	Hanson	B Holtschulte	sugar beet	-	Europe	-
R09-25	70	BR	1	Hanson	L. Hanson	sugar beet	Michigan	Midwest	Gratiot
F16	71	BR	1	Hanson	C Strausbaugh	sugar beet	Idaho	West	-
F508	72	BR	1	Hanson	C Strausbaugh	sugar beet	Idaho	West	-
R15-81	72	BR	1	Chilvers	J Jacobs	soybean	Michigan	Midwest	Clinton
F521	73	BR	1	Hanson	C Strausbaugh	sugar beet	Idaho	West	-
R4	73	BR	1	Hanson	C Rush	sugar beet	Texas	South	-
R1	74	BR	1	Hanson	E Ruppel	sugar beet	Colorado	West	-
R15-95	74	BR	1	Hanson	D Minier	sugar beet	Michigan	Midwest	Saginaw
R-8	74	BR	1	Hanson	E Ruppel	sugar beet	Arizona	South	-
R9	74	BR	1	Hanson	E Ruppel	sugar beet	Colorado	West	-

Data Analysis

Basic population statistics were determined using 'poppr' v.2.1.8 (Kamvar et al. 2014; Kamvar et al. 2015) in R v.4.2.1 (R Core Team 2022). Cluster assignment was conducted using the R package 'adegenet' v.2.1.8 (Jombart 2008) with the number of axes retained in the principal components analysis step set to six. Allowing the number of clusters to be determined automatically resulted in two clusters that corresponded to AG 2-2BR and AG 2-2PR. However, given that important characteristics have been shown to distinguish sub-clusters within each of the main clades, the number of clusters was set to four to be consistent with those described in chapter 2 (current dissertation).

Discriminate analysis of principal comments (DAPC) was conducted in the R package 'adegenet' v.2.1.8 on the clone-corrected datasets for crop-type and Michigan counties. Cross validation based on 1000 reps was used to determine appropriate values for the number of axes ('n.da') and principal components ('n.pca') to be retained. The clone-corrected dataset for crop-type 'n.pca' was set to 15 and 'n.da' set to 3. The Michigan county dataset, 'n.pca' was set to 4 and 'n.da' set to 4.

Basic statistics such as number of alleles, allelic richness, and heterozygosity were determined with MSAnalyzer v.4.05 (Dieringer & Schlötterer 2003). Hardy-Weinberg exact tests, genotypic differentiation and pairwise F_{ST} values were determined using genepop v.4.5.1 (Rousset 2008). Index of association plots (Brown et al. 1980) were generated using the R package 'poppr' on clone-corrected datasets with 999 permutations.

Structure plots were generated using Structure v.2.3.4 (Pritchard et al. 2000) on clone-corrected datasets. All simulations were conducted with a burn-in period of 12,000 reps followed by 120,000 MCMC reps after the burn-in period. We used the admixture model of ancestry with

sampling locations used as prior information about group membership. Alpha was inferred and considered to be the same for each population.

Development of subgroup specific primers

Lineage specific primers were identified through selective exclusion by comparing whole genome sequences of representative isolates from the three subgroups, AG 2-2BRa, AG 2-2BRb, and AG 2-2PR. Whole genomes were sequenced using Illumina and were described in chapter 2 (current dissertation). The genome sequence of isolate 'R1' was used to represent subgroup AG 2-2BRa and was aligned to another isolate of AG 2-2BRa using minimap2 v.2.24 (Li 2018). Reads that mapped were retained and aligned to another isolate of AG 2-2BRa and mapped reads again were retained. This provided a set of reads that were shared between three isolates of AG 2-2BRa. These reads were then mapped to three isolates from subgroup AG 2-2BRb and reads that did not map were retained. The process was repeated for subgroup AG 2-2PR and the final set of unmapped reads was assembled using SPAdes v.3.11.0 (Nurk et al. 2013) with k-mer selection set to 'automatic' and error correction 'on'. The resulting assemblies contained contigs that were presumed to be common to AG 2-2BRa but absent from AG 2-2BRb and AG 2-2PR. Starting with the longest contig, primer pairs were generated using Primer3 v.2.3.7 (Untergasser et al. 2012) and the predicted PCR product compared to the other assemblies using a BLAST algorithm until three primer pairs were generated that were predicted to amplify only for subgroup AG 2-2BRa. The entire process of selective exclusion was repeated with isolate 'Rzc6' from subgroup AG 2-2BRb and isolate 'Rzc115' from subgroup AG 2-2PR.

A set of nine primers pairs, three pairs for each subgroup, were identified and oligos ordered from Integrated DNA Technologies (Coralville, IA). Initial testing was conducted on eight

isolates using the following PCR conditions: reactions were performed in 25µl volumes with 15ng of DNA template, 1 x Phusion II HF buffer (Thermo Fisher Scientific. Waltham, MA), 1.5 mM MgCl₂, 0.5 µM of each primer, 200 µM each dNTP, and 1 unit of Phusion II HF polymerase (Thermo Fisher Scientific). Final PCR conditions consisted of 1 cycle of 98°C for 1 min. followed by 30 cycles of 98°C for 10 s, 58°C for 10 s, 72°C for 15 s and a final extension cycle of 72°C for 5 min. Amplicons were run on a 0.75% agarose gel, stained using RedSafe Nucleic Acid Staining Solution (iNtRON Biotechnology, Gyeonggi-do, Korea) and visualized on a UVP ChemStudio 815 gel imager (Analytik Jena US, Upland, CA). The presence of a band from a specific primer set indicated association with that subgroup.

One primer pair for each genetic group amplified as predicted for all 8 initially screened isolates (Table 3.2) and were then tested on a total of 71 isolates, including one AG 2-2LP isolate, seven isolates that were not in AG 2-2, and 15 isolates of unknown subgroup. After preliminary identification of subgroup for these 15 unknowns using the lineage specific primers, they were all genotyped using the microsatellite markers and included in cluster analysis. Subgroup predicted by lineage-specific markers was compared to subgroups assigned by genotype analysis. A subset of 23 isolates was independently analyzed by Dr. Carmen Medina-Mora (Michigan State University) using this set of lineage specific primers as confirmation of the process and consistency of identification across laboratories.

Table 3.2 Subgroup specific primers for *Rhizoctonia solani* AG 2-2.

Primer	Sequence 5' -> 3'	Approx. product size	Ta ^a
BRa-4-3F	CTCTGAGAGAAATAAGCATC	490	57°C
BRa-491-3R	CTGTAACGTTGTAAGTGTTC		
BRb-1164-3F	CAAGTCATCTAATTGCTTTA	980	57°C
BRb-2145-3R	CCTCCTAGTGTACTTGATT		
PR-212-3F	GGGCAATCCTCCTCGTTCAA	660	57°C
PR-870-3R	TAACGTTCACTGAGGAGGGC		

a) annealing temperature

Cloning and sequencing of potential hybrid from the Cercospora nursery

Isolate 'R17-15' was identified from the Cercospora nursery collection as being a member of subgroup AG 2-2PRb and had variation that was shared with AG 2-2BRa and AG 2-2PRa (Table 3.3; Figure 3.1). Our hypothesis was that isolate 'R17-15' was representative of a hybrid that resulted from the exchange of nuclei of isolates of subgroup AG 2-2BRa and AG 2-2PRa. To test this hypothesis, we compared isolate 'R17-15' to the isolates 'R16-10' and 'R17-6', also from the Cercospora nursery, that were classified as AG 2-2BRa and AG 2-2PRa respectively. Four genes, calmodulin, 6-tubulin, rpb1, and rpb2, were amplified by PCR as described in chapter 2 (current dissertation). PCR products were cloned using Zero Blunt TOPO PCR cloning kit for sequencing (Thermo Fisher Scientific) following manufacturer's instructions. DNA was extracted from colonies containing the vector (pCR-4Blunt-TOPO; Invitrogen, Carlsbad, CA) and PCR product using a GeneJET plasmid miniprep kit (Thermo Fisher Scientific) following manufacturer's instructions. Vector products were sequenced by the Michigan State University Genomic Core (East Lansing, MI) using the primer set M13Forward(-20) (5'- GTAAAACGACGCCAG) and M13Reverse (5'- CAGGAAACAGCTATGAC). Results were analyzed using Geneious Prime 2021.2.2 (Biomatters Ltd., Auckland, New Zealand).

Table 3.3 Cluster association of 84 *Rhizoctonia solani* AG 2-2 isolates. Cluster designation matches those identified by cluster analysis in the R package 'poppr' v.2.1.8. Bolding indicates isolates that could not be confidently assigned to a single cluster with greater than 85% confidence or have more than 10% association with more than one cluster.

				l cluster						d cluster	
Isolate	cluster	1	2	3	4	Isolate	cluster	1	2	3	4
Italian	1	0.966	0.006	0.015	0.014	C116S	3	0.004	0.008	0.965	0.023
R18-31	1	0.981	0.004	0.005	0.010	R09-23	3	0.005	0.002	0.981	0.011
R09-25	1	0.962	0.003	0.007	0.028	R15-1	3	0.008	0.003	0.977	0.013
R15-81	1	0.980	0.003	0.004	0.013	R15-15	3	0.008	0.002	0.970	0.019
R15-95	1	0.984	0.004	0.005	0.008	R15-21	3	0.007	0.002	0.978	0.012
R16-10	1	0.980	0.005	0.004	0.011	R15-63	3	0.005	0.002	0.591	0.402
W-22	1	0.955	0.005	0.012	0.027	R16-20	3	0.004	0.003	0.980	0.013
R15-80	1	0.983	0.003	0.004	0.011	R17-6	3	0.006	0.003	0.799	0.192
Bhill	1	0.665	0.206	0.061	0.068	R18-32	3	0.006	0.003	0.591	0.400
Alburry	1	0.793	0.091	0.063	0.054	R15-30	3	0.008	0.002	0.974	0.015
Rs866	1	0.966	0.016	0.009	0.009	R15-67	3	0.006	0.003	0.599	0.392
Rs890	1	0.956	0.021	0.012	0.011	Cookson	3	0.063	0.015	0.911	0.011
Rs300	1	0.513	0.472	0.005	0.009	Johnson	3	0.016	0.006	0.967	0.012
R-8	1	0.980	0.015	0.003	0.002	Vandeer2	3	0.042	0.004	0.949	0.005
R86	1	0.810	0.179	0.006	0.005	Rs1012	3	0.006	0.036	0.947	0.011
R4	1	0.979	0.015	0.003	0.003	Rs1146	3	0.005	0.013	0.978	0.004
F508	1	0.984	0.005	0.005	0.005	Rs255	3	0.053	0.062	0.856	0.029
F521	1	0.984	0.007	0.006	0.003	Rs331	3	0.004	0.011	0.522	0.463
R1	1	0.984	0.007	0.006	0.003	2C1	3	0.008	0.004	0.983	0.005
F16	1	0.987	0.005	0.005	0.003	F30	3	0.007	0.004	0.983	0.005
Bayern	2	0.003	0.984	0.008	0.004	F517	3	0.056	0.030	0.858	0.056
R164S	2	0.006	0.985	0.006	0.003	24BR	4	0.010	0.199	0.013	0.778
RH193	2	0.003	0.989	0.006	0.002	39AR	4	0.007	0.192	0.009	0.793
H502	2	0.004	0.986	0.004	0.006	Roland	4	0.004	0.177	0.018	0.801
H582	2	0.006	0.982	0.004	0.008	Slovakia	4	0.005	0.211	0.033	0.751
H549	2	0.096	0.760	0.006	0.138	R15-100	4	0.060	0.002	0.032	0.906
Rs106	2	0.005	0.988	0.005	0.002	R15-66	4	0.011	0.142	0.009	0.838
Rs200	2	0.121	0.855	0.018	0.006	R15-73	4	0.095	0.005	0.039	0.860
Rs296	2	0.006	0.848	0.130	0.017	R15-74	4	0.142	0.005	0.141	0.712
Rs481	2	0.006	0.987	0.005	0.003	R15-86	4	0.132	0.003	0.090	0.776
Rs496	2	0.008	0.985	0.005	0.003	R15-90	4	0.132	0.003	0.163	0.703
Rs588	2	0.007	0.971	0.018	0.005	R15-93	4	0.126	0.008	0.024	0.842
7A1	2	0.005	0.987	0.005	0.003	R16-14	4	0.010	0.178	0.012	0.799
5C5	2	0.012	0.936	0.049	0.004	R17-15	4	0.031	0.004	0.008	0.956
R33	2	0.012	0.983	0.003	0.002	R17-16	4	0.017	0.004	0.010	0.969
2C13	2	0.035	0.946	0.014	0.005	99-15	4	0.006	0.194	0.008	0.791
Cavalie	3	0.003	0.004	0.960	0.034	R15-72	4	0.237	0.003	0.195	0.565
Taltfalt	3	0.002	0.003	0.989	0.005	R15-78	4	0.009	0.243	0.011	0.737
Plattling	3	0.003	0.007	0.982	0.008	R15-82	4	0.095	0.003	0.056	0.846
Kratzer	3	0.005	0.014	0.935	0.046	R15-87	4	0.318	0.003	0.195	0.483
Hubert	3	0.006	0.005	0.967	0.023	Rs850	4	0.036	0.037	0.016	0.910
11-272a	3	0.004	0.013	0.973	0.011	F24	4	0.011	0.204	0.011	0.774

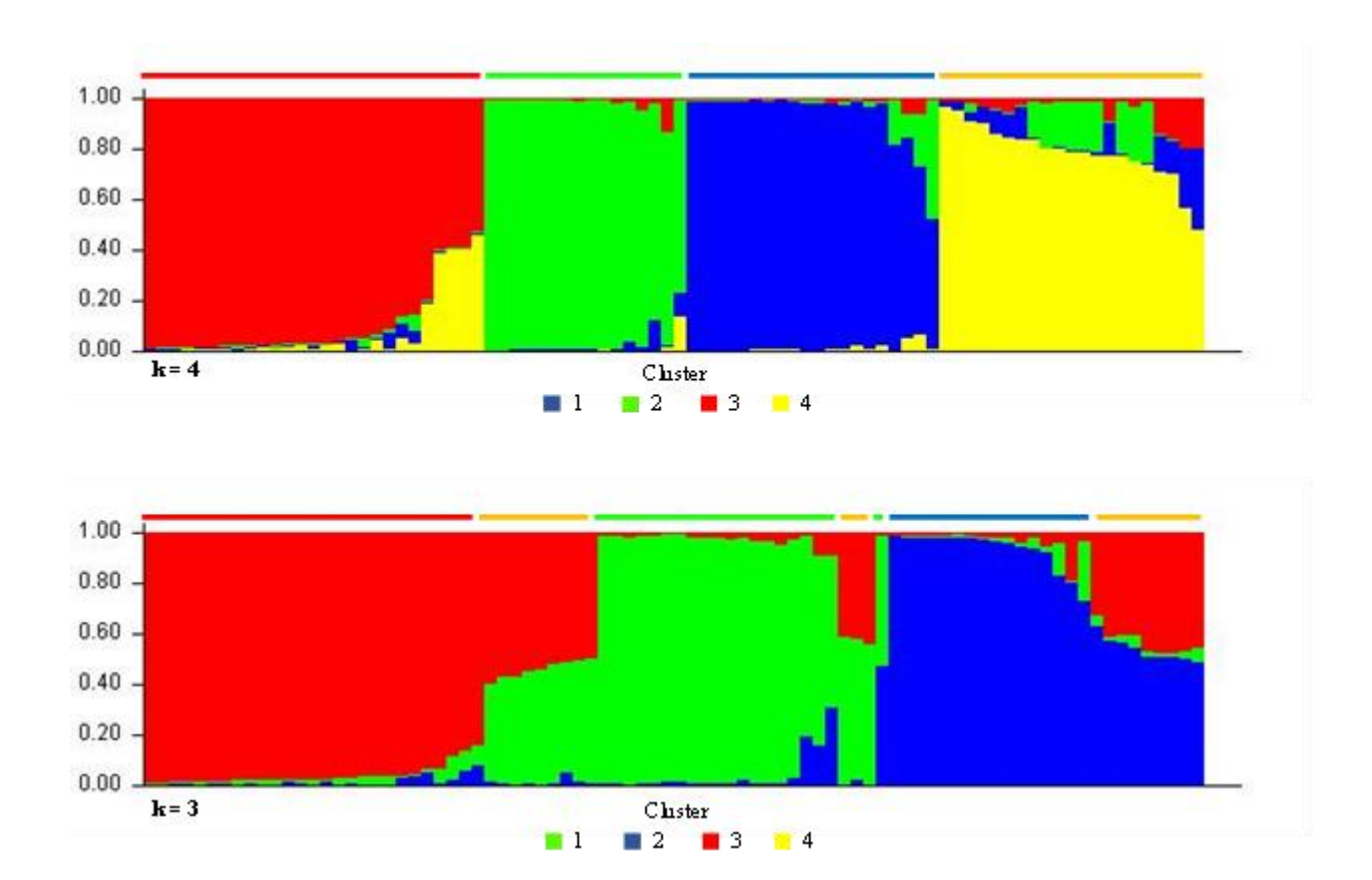


Figure 3.1 Structure plots for 84 *Rhizoctonia solani* AG 2-2 isolates from a clone corrected dataset. Colored bars above plots represent cluster association of individual isolates as determined using the R package 'poppr' v.2.1.8. For the upper plot, the number of populations was set to four (k=4) and for the lower plot number of populations was set to three (k=3). Arrow indicates isolate 'R17-15', that was used to test for potential hybridization in the Cercospora nursery.

Results and Discussion

Subgroup and cluster assignment

In the current study, we used the conventions for identification and naming for the *R. solani* AG 2-2 subgroups that were outlined in chapter 2 of the current dissertation. The 167 isolates genotyped in the current study grouped into 4 clusters that were consistent with the newly defined subgroups, AG 2-2BR and AG 2-2PR. Clusters 1 and 2 (AG 2-2BR) consisted of 24 and 19 isolates respectively and clusters 3 and 4 (AG 2-2PR) had 88 and 36 isolates respectively (Table 3.4). A total of 74 multi-locus genotypes (MLG) were identified among all isolates with cluster 3 (AG 2-2PRa) having 25 MLGs. Much of cluster 3 was made up of clones with a clonal fraction of 72% with 45 isolates represented by a single genotype (MLG50), 28 of which came from the Cercospora nursery collection (Table 3.1). Hardy-Weinberg tests indicated a significant deficit of heterozygotes in cluster 2 while cluster 4 had a significant excess of heterozygotes (Table 3.4).

Table 3.4 Summary statistics for 167 *Rhizoctonia solani* AG 2-2 isolates based on 13 microsatellite loci. Genetic clusters were identified by cluster analysis using the R package 'poppr' v.2.1.8. Heterozygosity and index of association statistics were calculated using a clone corrected dataset.

Genetic	N a	MLG ^b	Clonal fraction	eMLG °	Evenness	H_{exp}^{d}	$H_1 = H_{deficit}^{e}$	$H_1 = H_{\text{excess}}^{\text{f}}$	F_{IS}^{g}	Ia ^h	$ar{r}_{d}$ i
1	24	17	29%	14.4	0.86	0.469	0.724	0.238	- 15	1.046	0.158
2	19	14	26%	14.0	0.80	0.304	< 0.001	1.000	0.517	0.198	0.043
3	88	25	72%	8.7	0.35	0.468	0.064	0.928	0.041	3.198	0.487
4	36	18	50%	11.9	0.78	0.641	0.992	0.007	-	2.058	0.296
Total	167	74	56%	13.7	0.32	0.681	-	-	-	3.377	0.486

- a) number of samples
- b) multi-locus genotype
- c) effective number of MLGs at lowest common sample size
- d) expected heterozygosity Nei's gene diversity
- e) heterozygosity deficit (p value)
- f) heterozygote excess (p value)
- g) inbreeding coefficient
- h) index of association
- i) linkage disequilibrium index

The number of alleles per locus ranged from 5 to 18 with a total of 65 alleles over all loci. Allelic richness ranged from 1.63 to 1.83 with an average of 1.72 across all loci (Table 3.5). When analyzed as a single population, Hardy-Weinberg (HW) tests identified 7 loci with a significant deficit of heterozygotes and high positive F_{IS} values (0.133 to 0.449). Since a heterozygote deficit and positive F_{IS} values are typically interpreted as indicating an inbred population (Spielman et al. 1977; Wright 1965) and the biological expectation was that these populations were primarily clonal, we hypothesized a Wahlund effect. The analysis of samples at such a large scale, as was represented by the global population, may result in a deficit of heterozygotes due to unaccounted for population substructure (De Meeûs 2018; Waples 2015).

Table 3.5 Allelic statistics for the 8 microsatellite loci used for genotyping 167 *Rhizoctonia solani* AG 2-2 isolates. Heterozygosity and Hardy-Weinberg testing was performed on the clone corrected dataset.

					clone corrected population						
Locus	No. alleles	Allelic Richness	Min Allele	Max Allele	$H_{\text{exp}}^{}a}$	$H_{obs}{}^{b} \\$	$H_{\text{deficit}}^{}c}$	$H_{\text{excess}}{}^{\text{d}}$	F _{IS} e		
2547	5	1.63	214	230	0.634	0.419	< 0.001	1.000	0.341		
4660	8	1.69	132	159	0.692	0.459	< 0.001	0.999	0.337		
5583	5	1.78	183	198	0.778	0.527	< 0.001	1.000	0.324		
5487	5	1.64	126	141	0.636	0.351	< 0.001	1.000	0.449		
759	18	1.83	122	188	0.834	0.689	< 0.001	1.000	0.175		
6145	9	1.72	123	159	0.716	0.622	< 0.001	1.000	0.133		
8703	7	1.75	202	220	0.745	0.662	0.078	0.926	0.112		
6150	8	1.75	126	158	0.753	0.622	0.023	0.975	0.175		
value over all loci	65	1.72	-	-	0.724	0.544	< 0.001	1.000	0.249		

a) expected heterozygosity

b) observed heterozygosity

c) p-value for heterozygosity deficit

d) p-value for heterozygosity excess

e) inbreeding coefficient

When the global population was organized into subgroups based on cluster analysis and heterozygosity reanalyzed, results were more in line with biological expectations (Table 3.6). One locus (2547) showed evidence of heterozygote deficiency (p = 0.027) when calculated over all subgroups. F_{IS} values were negative for most loci (Table 3.6) except for 2547 (F_{IS} = 0.047), 5487 (F_{IS} = 0.069) and 5583 (F_{IS} = 0.157). Overall, the population was in Hardy-Weinberg equilibrium when population substructure was considered and had an F_{IS} value of -0.019. Consistent with a Wahlund effect, each subgroup had unique characteristics associated with heterozygosity indicating differences in life histories (Garnier-Géré & Chikhi 2013).

Table 3.6 Population statistics for the four subgroups of *Rhizoctonia* solani AG 2-2 based on clone corrected dataset of genotypes of 167 isolates.

	F _{IS} values for subgroups ^a										
Locus	AG2-2BRa	AG2-2BRb	AG2-2PRa	AG2-2PRb	over all subgroups	H _{excess} ^c	$H_{\text{deficit}}^{}d}$				
2547	0.652	-	0.007	-0.041	0.047	0.968	0.027				
4660	0.000	0.874	0.015	-0.691	-0.007	0.372	0.636				
5583	0.230	0.866	0.202	-0.351	0.157	0.789	0.191				
5487	-0.077	0.632	-0.029	-0.256	0.069	0.798	0.195				
759	-0.088	0.262	-0.038	-0.099	-0.036	0.826	0.162				
6145	-0.176	-0.110	0.142	-0.160	-0.060	0.843	0.133				
8703	-0.450	-	0.013	-0.286	-0.185	0.057	0.944				
6150	-0.045	-0.020	0.007	-0.337	-0.106	0.246	0.747				
value over all loci	-0.060	0.517	0.041	-0.272	-0.019	0.853	0.119				
H_{excess}	0.238	1.000	0.928	0.007	-	-	-				
$H_{ m deficit}$	0.724	< 0.001	0.064	0.992	-	-	-				

a) inbreeding coefficient by subgroup

b) Hardy-Weinberg tests for all populations

c) p-value for heterozygote excess

d) p-value for heterozygote deficit

Subgroup AG 2-2BRa (cluster 1) was in Hardy-Weinberg equilibrium (Table 3.6) with a slightly negative F_{IS} value (-0.060) which is consistent with clonal reproduction (Balloux et al. 2003; Weir & Cockerham 1984; Wright 1965). There was strong evidence of a heterozygote deficit in subgroup AG 2-2BRb (cluster 2) with a high F_{IS} value (0.517) which is characteristic of a strongly inbred population (Spielman et al. 1977; Wright 1965). We previously hypothesized that sexual reproduction in R. solani AG 2-2 results in genotypic simplification due to haploidization of basidiospores (chapter 2, current dissertation). Our results lend support to this hypothesis and the implications of sexual reproduction are discussed in more detail later in the current manuscript. Subgroup AG 2-2PRb showed strong evidence for an excess of heterozygotes (p = 0.007) and a highly negative F_{IS} value (-0.272). We interpret this data as being consistent with a highly clonal population (Balloux et al. 2003; Wright 1949). Overall, we view these observations as support for population structure as identified by cluster analysis and support for the subgroups AG 2-2BRa (cluster 1), AG 2-2BRb (cluster 2), AG 2-2PRa (cluster 3), and AG 2-2PRb (cluster 4).

STRUCTURE analysis of the clone-corrected regional dataset was able to assign 56 of 84 (67%) genotypes to a cluster with greater than 85% confidence (Table 3.3). Twenty-nine of 36 (81%) isolates in clusters 1 and 2 (AG 2-2BR) could be assigned to their respective group with greater than 85% confidence. For the other seven isolates, association was split between groups 1 and 2 except for one isolate ('Rs296') where group association was split with group 3 and one isolate ('H549') where group association was split with group 4 (Table 3.3).

Twenty-two out of 48 (46%) isolates in clusters 3 and 4 (AG 2-2PR) could be confidently assigned to a single group with greater than 85% confidence (Table 3.3). The five isolates from cluster 3 that could not be confidently assigned to a single group had group association split

between groups 3 and 4. The 16 isolates from cluster 4 that could not be confidently assigned to a single group had group association split between groups 3 and 4 (5 isolates), groups 2 and 4 (8 isolates), groups 1 and 4 (3 isolates), groups 1, 2 and 4 (1 isolate), and groups 1, 3 and 4 (3 isolates).

Each of the groups identified by STRUCTURE analysis corresponded to subgroups

AG 2-2BRa (cluster 1), AG 2-2BRb (cluster 2), AG 2-2PRa (cluster 3), and AG 2-2PRb (cluster

4). Observations of association patterns for cluster 4 support our hypothesis that AG 2-2PRb consists primarily of hybrids that contain nuclei from different genetic groups. This conclusion is even more evident when the STRUCTURE analysis is set for three populations (Figure 3.1).

Each group of isolates that were associated with a single cluster are separated by a group of isolates where cluster association was split. These admixed isolates all correspond to AG 2-2PRb (cluster 4) as determined by cluster analysis.

None of the isolates identified with AG 2-2PRa had more than 6.3% membership association with AG 2-2BRa or AG 2-2BRb, while members of AG 2-2PRb that had less than 85% membership had between 10% and 20% association with either cluster 1 or cluster 2 in roughly equal proportions. Collectively, these observations support the hypothesis that subgroup AG 2-2PRb is made up of what we have referred to as hybrids that result from recombination between AG 2-2PRa and either AG 2-2BRa or AG 2-2BRb. Nuclear exchange between AG 2-2BRa and AG 2-2BRb apparently does occur as indicated by several isolates that share group association between the groups. However, this exchange may often be masked due to the genetic similarity between AG 2-2BRa and AG 2-2BRb.

Distribution of global population

A total of 164 isolates were assigned to eight geographical regions with the number of isolates per region ranging from 4 to 99. The region that included the highest number of isolates was the Midwest region with 99 samples, 92 of which were from Michigan. Despite the high number of isolates recovered from Michigan, there were no isolates from AG 2-2BRb (cluster 2) recovered from the state. There were, however, three isolates from Ohio included in the Midwest region that were identified as AG 2-2BRb (Figure 3.2). In contrast, the Red River Valley region had a large proportion of isolates identified as AG 2-2BRb (50%) and accounts for about half of all AG 2-2BRb isolates recovered from all regions in the current study.

The reason for the prevalence of AG 2-2BRb isolates in the Red River Valley is uncertain, although our observations are consistent with previous reports from the region (Brantner & Windels 2007). The close relationship between the Japan population and Red River Valley (genotypic differentiation; p = 0.204; $F_{ST} = 0.012$) might suggest that the AG 2-2BRb population in the Red River Valley originated in Japan (or possibly *visa-versa*). However, there were no identical genotypes shared between Japan and the Red River Valley. Rather, genotypes identical with those from Japan were identified in the Midwest and South regions (Figure 3.2). This could be due to a more recent introduction of genotypes to the Midwest and South regions while isolates introduced to the Red River Valley have had time to undergo recombination and diversification.

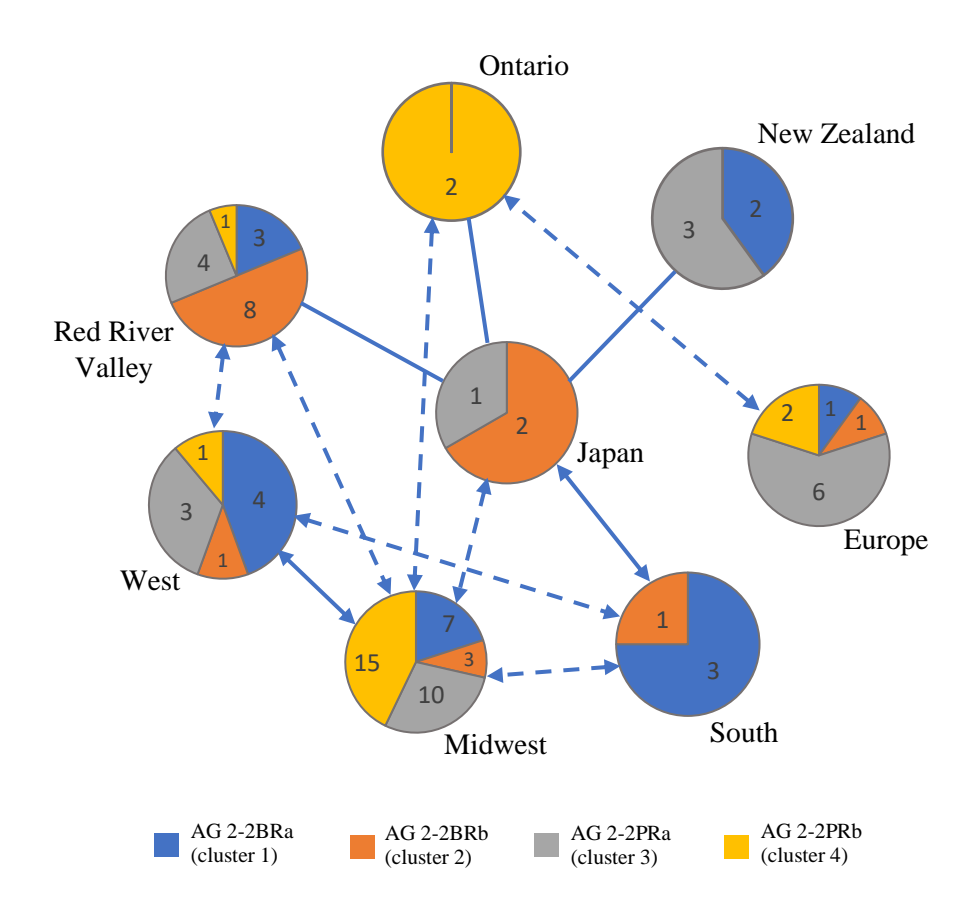


Figure 3.2 Distribution of *Rhizoctonia solani* AG 2-2 genotypes among 8 sugar beet growing regions. Pie charts indicate number of unique genotypes collected from each region with each slice representing the number of isolates in each subgroup. Solid lines connecting circles indicate a lack of genotypic differentiation (p > 0.05). Arrow heads indicate one or more multi-locus genotypes (MLG) are shared between regions. Dashed lines indicate populations are significantly differentiated but share one or more MLGs.

Genotypic differentiation tests (exact G test, Fisher's method; Raymond & Rousset 1995) showed significant differentiation between the New Zealand and all other populations except the Japan population (p = 0.268). Moreover, the Japan population was not significantly differentiated from the Ontario population (p = 0.223), the Red River Valley population (p = 0.204) or the South population (p = 0.162). All other population pairs were significantly differentiated (exact G test, p < 0.05) except the Midwest and West regions (p = 0.065).

Researchers in Europe have reported that isolates present in their growing regions were limited to 'type IIIB' (Buhre et al. 2009; Ithurrart et al. 2004). However, in the current study, we identified isolates recovered from Europe in each of the four genetic clusters, including one isolate ('Bayern') from subgroup AG 2-2BRb, which was the cluster that contains primarily 'type IV' isolates. The population from Europe, examined in the current study, was relatively distinct from other populations throughout the world. While there was evidence of significant genotypic differentiation between European isolates and all other regions, F_{ST} values between Europe and the Midwest and between Europe and the West region were fairly low (0.037 and 0.042 respectively; Table 3.7). In addition, a single genotype, MLG59, was shared between Europe and Ontario (Table 3.7). Overall, the Europe population appears to have remained relatively isolated from other growing regions throughout the world but is substantially more diverse than previously reported.

Despite *R. solani* AG 2-2 having a worldwide distribution, it was surprising that genotypes were shared across considerable geographical distances. In the current study, nine genotypes were shared between different regions including seven from the Midwest region and six from the West region (Table 3.8). These genotypes are shared between regions as distant as Japan and the Midwest or Europe and Ontario. Since *R. solani* does not produce asexual spores that can be

dispersed by wind or water, we expect transport primarily occurs by moving infested soil, equipment, or personal items. The significant genotypic similarity between geographical distant regions highlights the importance of sanitation in preventing the spread of *Rhizoctonia* propagules (Rodriguez-Salamanca 2015).

Table 3.7 Genotypic differentiation for regional populations of *Rhizoctonia solani* AG 2-2 based on 8 microsatellite loci. *p*-value is the result of exact G-tests performed in Genepop v.4.5.1. Non-significant results are bolded indicating a lack of genotypic differentiation between populations. F_{ST} values were also calculated using Genepop. Values below 0.100 are bolded indicating low levels of genetic differentiation between populations. Shared multi-locus genotypes (MLG) lists those genotypes shared between populations.

Popu	lation	n pairs	Chi ^{2 a}	df ^b	<i>p</i> -value	F_{ST}^{c}	shared MLG d
Ontario	&	Europe	37.00	16	0.002	0.139	59
Ontario	&	Japan	19.93	16	0.223	0.138	
Europe	&	Japan	48.69	16	< 0.001	0.195	
Ontario	&	Midwest	65.66	16	< 0.001	0.168	66
Europe	&	Midwest	Infinity	16	< 0.001	0.037	
Japan	&	Midwest	91.01	16	< 0.001	0.246	18
Ontario	&	N Zealand	46.45	16	< 0.001	0.228	
Europe	&	N Zealand	36.68	16	0.002	0.104	
Japan	&	N Zealand	19.02	16	0.268	0.108	
Midwest	&	N Zealand	Infinity	16	< 0.001	0.149	
Ontario	&	RedRiver	37.35	16	0.002	0.056	
Europe	&	RedRiver	58.90	16	< 0.001	0.109	
Japan	&	RedRiver	20.38	16	0.204	0.012	
Midwest	&	RedRiver	Infinity	16	< 0.001	0.138	50
N Zealand	&	RedRiver	50.47	16	< 0.001	0.119	
Ontario	&	South	44.32	16	< 0.001	0.282	
Europe	&	South	63.27	16	< 0.001	0.233	
Japan	&	South	21.45	16	0.162	0.095	18
Midwest	&	South	86.86	16	< 0.001	0.262	18,17
N Zealand	&	South	32.40	16	0.009	0.129	
RedRiver	&	South	37.62	16	0.002	0.085	
Ontario	&	West	62.56	16	< 0.001	0.131	
Europe	&	West	38.82	16	0.001	0.042	
Japan	&	West	53.98	16	< 0.001	0.174	
Midwest	&	West	25.29	16	0.065	0.017	58,46,50,15,17
N Zealand	&	West	44.87	16	< 0.001	0.083	
RedRiver	&	West	42.76	16	< 0.001	0.069	50
South	&	West	36.40	16	0.003	0.128	16,17

a) Chi square value

b) degrees of freedom

c) fixation index

d) multi-locus genotypes shared between regions

Table 3.8 Multi-locus genotypes (MLG)of *Rhizoctonia solani* AG 2-2 isolates shared between geographical regions. Shared genotypes are indicated by an 'x'.

			G	rowing re	gion		
MLG^{a}	Midwest	West	Ontario	South	Red River	Europe	Japan
15	X	Х					
16		X		X			
17	X	X		X			
18	X			X			X
46	X	X					
50	X	X			X		
58	X	X					
59			X			X	
66	X		X				

a) multi-locus genotype

Relationship of genotypes to crop type

A total of 158 samples from four host crops, including sugar beet (112), soybean (25), dry bean (16) and fodder beet (5), were examined for a relationship between genotype and host. There was a total of 66 unique genotypes across all samples with 45 from sugar beet, 17 from soybean, 7 from dry bean and 5 from fodder beet (Table 3.9). Isolates from sugar beet included representatives from all four genetic subgroups, AG 2-2BRa (14%), AG 2-2BRb (14%), AG 2-2PRa (52%) and AG 2-2PRb (20%). Soybean isolates were split between subgroups AG 2-2BRa (8%), AG 2-2PRa (36%), and AG 2-2PRb (56%). Isolates from dry bean were the most restricted in respect to subgroup with 15 (94%) from AG 2-2PRa and only 1 (6%) isolate from AG 2-2BRa (Figure 3.3). Isolates from additional crops were represented by a single isolate each and included carrot, swiss chard and wheat in subgroup AG 2-2BRa and isolates from spinach and turf in subgroup AG 2-2PRa. Further investigation of the subgroups that affect these additional crops and host susceptibility to them will be needed.

Table 3.9 Summary statistics for 158 *Rhizoctonia solani* AG 2-2 isolates by crop type.

			Clone		Clo	ne Correc	ted
Crop	N^{a}	MLG ^b	fraction	eMLG ^c	Hexp ^d	Ia e	rbarD ^f
sugar beet	112	45	59.8%	7.22	0.677	1.85	0.266
fodder beet	5	5	0.0%	5	0.628	1.923	0.289
soybean	25	17	32.0%	8.44	0.647	1.669	0.241
dry bean	16	7	56.3%	5.34	0.495	5.613	0.833
Total	158	66	58.2%	7.77	0.675	1.927	0.277

- a) number of samples
- b) multi-locus genotypes
- c) effective multi-locus genotypes
- d) expected heterozygosity
- e) index of association
- f) linkage disequilibrium index

The DAPC plot (Figure 3.4) shows that fodder beet had a distinct distribution compared to the other crops. However, this distinction is likely related to geography rather than host specificity since the only location where isolates were included from fodder beet was New Zealand. Both major subgroups AG 2-2BR and AG 2-2PR were recovered from fodder beet, despite the small number of samples. Dry bean was the only crop with any evidence for crop specificity as AG 2-2PRa made up 94% of the isolates recovered from the crop. On the other hand, the DAPC plot did not support dry bean isolates as a separate population (Figure 3.4). In other words, although the group that was recovered from dry beans was primarily AG 2-2PRa, the same group also affects sugar beet and soybeans. This is consistent with previous findings where group AG 2-2PRa was more aggressive on dry beans, as a whole, than the other subgroups (Minier 2019). It is possible that samples were selected because of obvious or severe symptoms and the selection process skewed the results to favor the AG 2-2PRa isolates, which cause more severe symptoms on dry beans. Conversely, planting dry beans may increase the prevalence of AG 2-2PRa isolates due to selection. Further investigation of the effects of including specific crops in rotation on AG 2-2 populations is warranted.

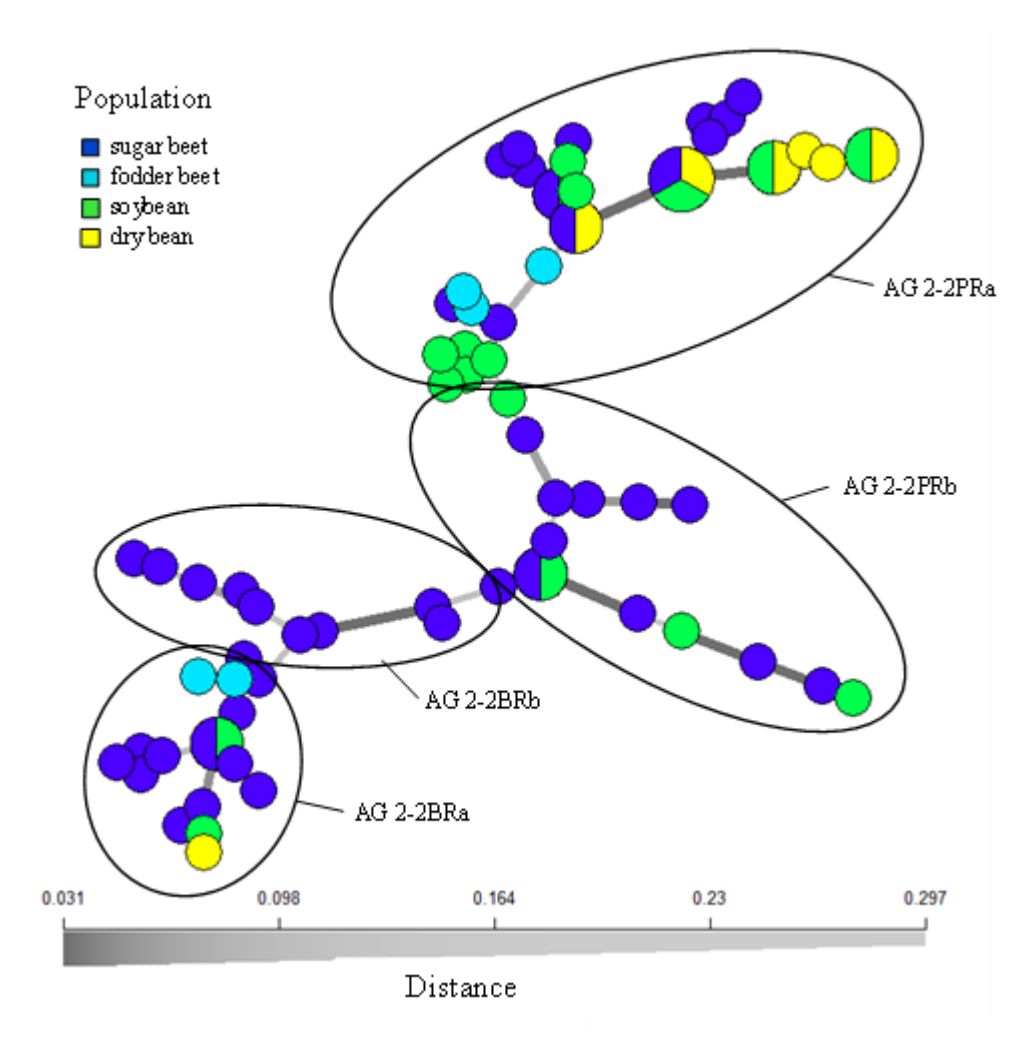


Figure 3.3 Minimum spanning network of 74 isolates of *Rhizoctonia solani* AG 2-2 recovered from four host crops. The data set was corrected for clones and is represented by 64 unique genotypes. The number of isolates per genotype is indicated by the size of the circles and host is indicated by color. Edges connecting genotypes indicated genetic distance with thicker, darker lines indicating closer relationships and thinner, lighter lines more distant relationships. Ellipses are drawn around isolates associated with the indicated subgroups.

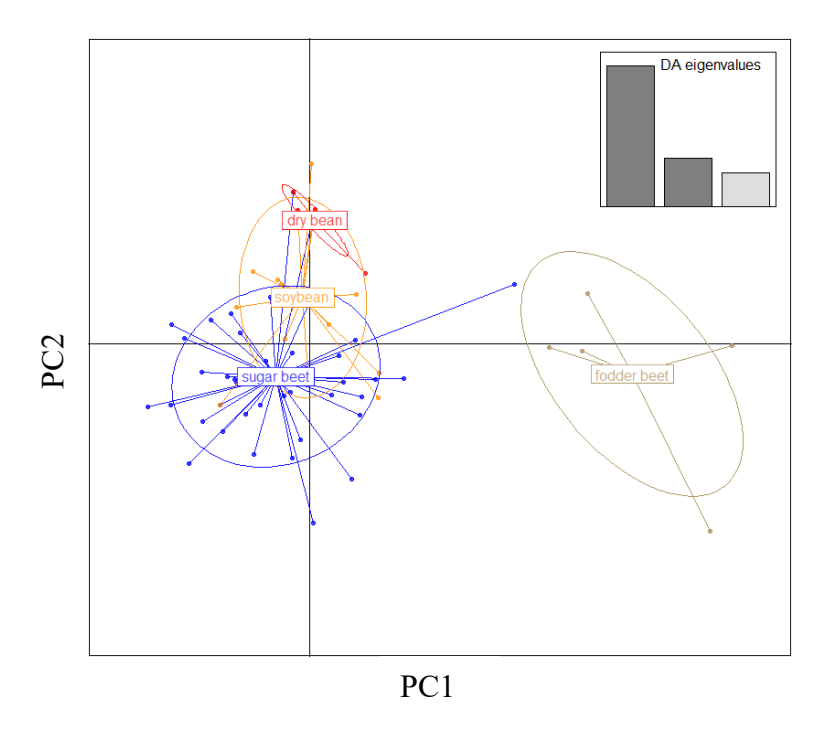


Figure 3.4 Discriminant analysis of principal components for 74 *Rhizoctonia solani* AG 2-2 isolates from four host crops. Fifteen principal components (PC) and three discriminant functions (DA) were retained during analysis to describe relationships between clusters. Scatter plot shows first two PCs of the analysis with eigenvalues of the discriminant functions indicated in the upper right corner.

Isolates recovered from soybean were more diverse than those from dry bean with representatives from all subgroups except AG 2-2BRb. Since the majority of soybean isolates came from Michigan and no AG 2-2BRb isolates were detected in Michigan, this could be a factor in why no isolates from AG 2-2BRb were recovered from soybean. Additional sampling from soybean in regions that have a substantial AG 2-2BRb population could help establish the susceptibility of soybean to AG 2-2BRb. We hypothesize that soybeans are susceptible to all subgroups of AG 2-2 (except AG 2-2LP), which would be consistent with previous reports from the Red River Valley region (Brantner & Windels 2007). Curiously, the only crop from which AG 2-2BRb isolates were recovered was sugar beet. Sampling various crops from a region with

high levels of AG 2-2BRb would be needed to ensure that AG 2-2 being restricted to sugar beet is not a result of sampling bias.

Rhizoctonia solani AG 2-2 is distributed worldwide but its occurrence in particular areas or even within specific agricultural fields is patchy (Anees et al. 2010; Truscott & Gilligan 2001) and it is likely that cultivated crops have exerted a strong influence on prevalence and distribution (Ogoshi 1987). Reports have indicated that crop rotations affect *R. solani* AG 2-2 populations, but these reports have focused on differences between 'type IIIB' and 'type IV' populations (Buhre et al. 2009; Engelkes & Windels 1996; Windels & Brantner 2006). Future work on the effects of crop rotation on populations of AG 2-2 should focus on the newly identified genetic groups as outlined in the current study.

Diversity of Michigan population

The population from Michigan consisted of 92 individuals from 10 counties. The collection included 56 isolates recovered from sugar beet, 22 from soybean, 12 from dry bean and 1 each from carrot and turf grass. The majority of isolates from Michigan were in subgroup AG 2-2PRa and AG 2-2PRb with 58 (63%) and 25 (27%) isolates respectively. AG 2-2BRa also had a small number of representatives with 9 (10%) but no AG 2-2BRb isolates were recovered from Michigan despite sampling from diverse collection areas. Isolates R09-23 and R09-25 were both identified as 'type IV' based on growth at 35°C (unpublished) but were identified as AG 2-2PRa and AG 2-2BRa respectively. The reason for the lack of AG 2-2BRb isolates in Michigan is uncertain, especially since AG 2-2BRb isolates were identified from the neighboring state of Ohio. We expect that the lack of AG 2-2BRb isolates collected from the state is a result of a) the nature of historical introductions and b) the effects of crop rotation choices. There were three

AG 2-2PRb genotypes present in Michigan that had substantial group association with AG 2-2BRb (R15-66 (14%); R15-78 (24%); R16-14 (18%); Table 3.3). Based on the hypothesis that AG 2-2PRb is a group of hybrid individuals, this observation suggests that AG 2-2BRb does have a historical presence in Michigan. Therefore, crop rotation may have played a larger role in current population structure than historical introduction.

Saginaw county contained the largest number of genotypes with 15 (52% of total Michigan genotypes) and shared one or more genotypes with five other counties, Bay, Midland, Montcalm, Ingham, and Gratiot (Figure 3.5). Midland and Gratiot counties also shared substantial genotypic connection to other counties with Midland County sharing genotypic diversity with all reported counties except Oceana County. Likewise, Gratiot County shared genotypic diversity with all other counties reported except Oceana and Allegan, the western-most counties tested.

Because we have little historical data regarding distribution patterns of *R. solani* AG 2-2 in Michigan, it is not practical to determine migration patterns. We do, however, have concerns over distribution patterns that may reflect the movement of genotypes between farms. For example, MLG50 is shared between Saginaw County and Montcalm County but not with Gratiot County which is spatially intermediate between Saginaw and Montcalm counties. Ingham county shares diversity with Saginaw, Bay, Midland, and Gratiot counties but not the adjacent counties Clinton and Shiawassee. These observations should not be construed as conclusive evidence of the movement of isolates between farms but should serve as a reminder of the importance of sanitation when moving equipment, vehicles, and personnel between farm locations.

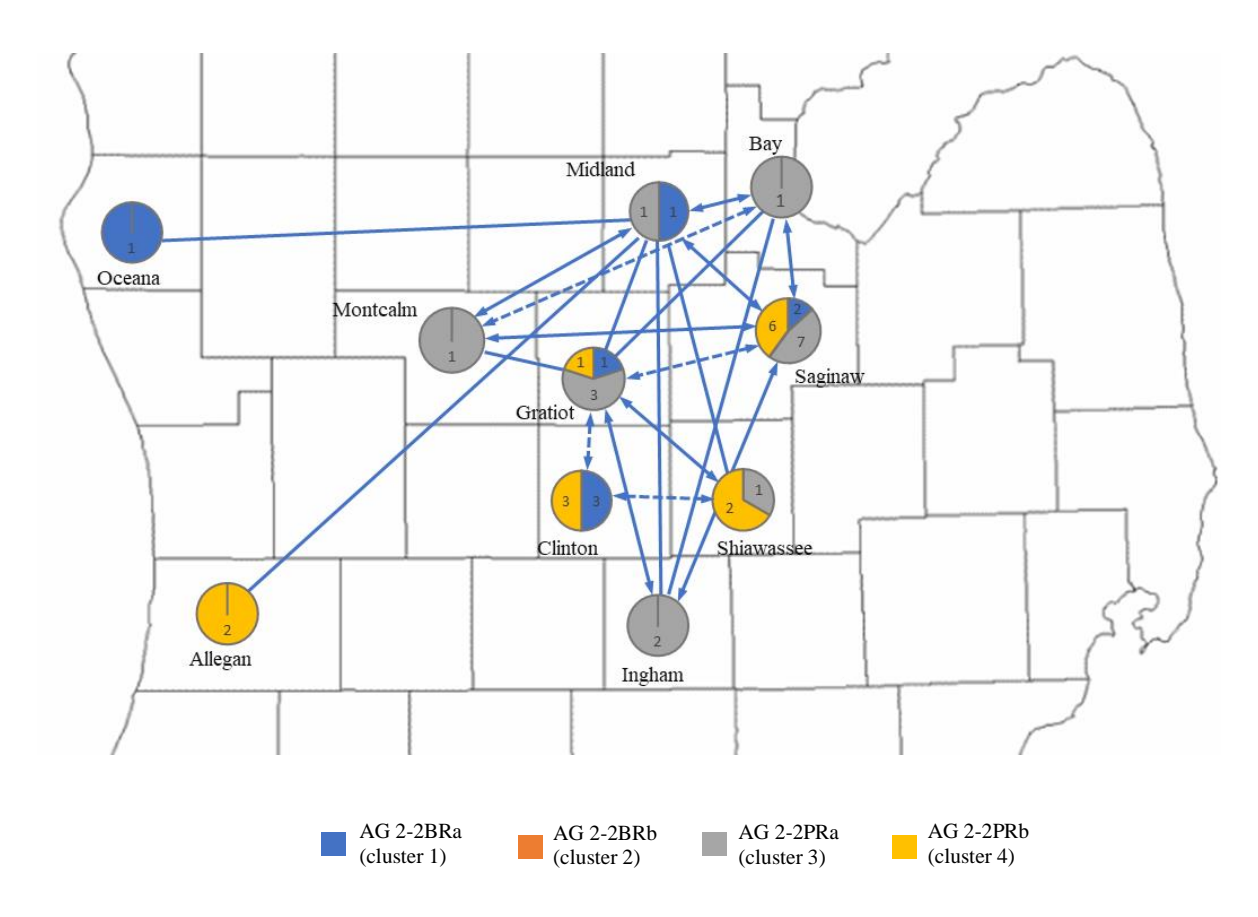


Figure 3.5 Distribution of *Rhizoctonia solani* AG 2-2 genotypes among 10 Michigan counties. Pie charts indicate number of unique genotypes collected from each county with each slice representing the number of isolates in each subgroup. Solid lines connecting circles indicate a lack of genotypic differentiation and a FST value less than 0.10. Arrow heads indicate one or more multi-locus genotypes (MLG) are shared between populations. Dashed lines indicate populations are significantly differentiated but share one or more MLGs.

Overall, the *R. solani* AG 2-2 population in Michigan is widespread and shows little evidence of population structure (Figure 3.6). Samples from the western counties of Oceana and Allegan were not genotypically differentiated from some counties on the eastern side of the state (Figure 3.5; Table 3.10). Multi-locus genotypes are shared between numerous counties and there was no apparent structure based on geographic origin or crop type. There was no evidence of sexual reproduction in the state ($\bar{r}_d = 0.361$, p = 0.001; Figure 3.7) which is hypothesized to be due in part to the lack of AG 2-2BRb isolates.

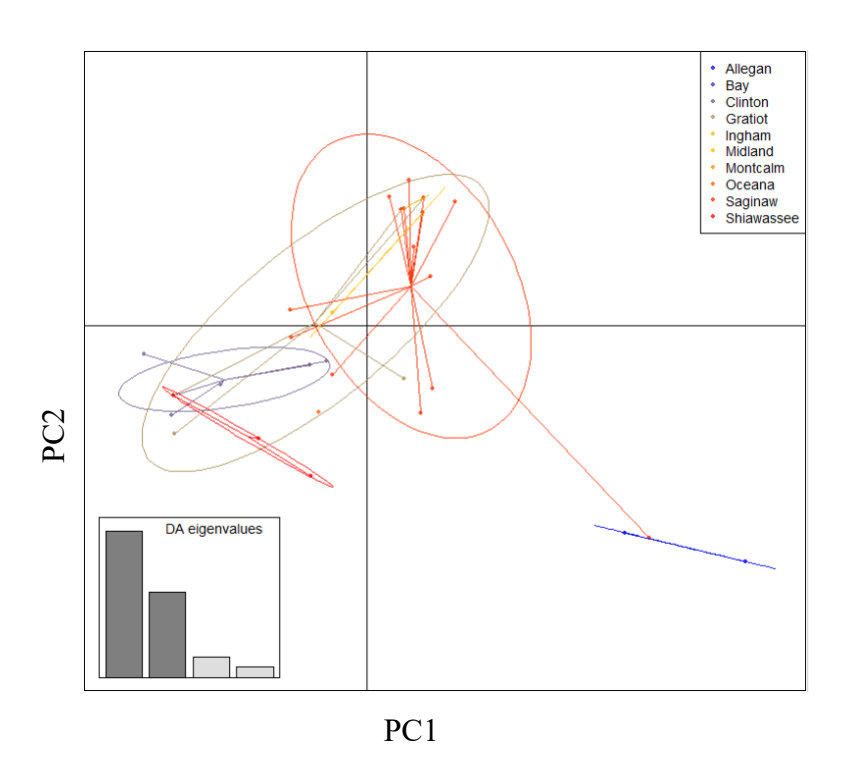


Figure 3.6 Discriminate analysis of principal components for 38 *Rhizoctonia solani* AG 2-2 isolates from 10 Michigan counties. Four principal components (PC) and four discriminant functions (DA) were retained during analysis to describe relationships between clusters. Scatter plot shows first two PCs of the analysis with eigenvalues of the discriminant functions indicated in the lower left corner.

Table 3.10 Genotypic differentiation for Michigan county populations of *Rhizoctonia solani* AG 2-2. *p*-value is the result of exact G-tests performed in Genepop v.4.5.1. Non-significant results are bolded indicating a lack of genotypic differentiation between populations. F_{ST} values were also calculated using Genepop. Values below 0.100 are bolded indicating low levels of genetic differentiation between populations. Shared multi-locus genotypes (MLG) lists those genotypes shared between populations.

` /		\mathcal{C}	J 1			1 1	
Population 1	Pair		Chi ² a	Df ^b	<i>p</i> -value	Fst c	Shared d MLG
Allegan	&	Bay	15.39	16	0.496	0.442	
Allegan	&	Clinton	49.48	16	0.000	0.248	
Bay	&	Clinton	45.29	16	0.000	0.281	
Allegan	&	Gratiot	34.69	16	0.004	0.223	
Bay	&	Gratiot	10.63	16	0.832	0.006	
Clinton	&	Gratiot	46.14	16	0.000	0.100	74
Allegan	&	Ingham	33.98	16	0.005	0.438	
Bay	&	Ingham	4.63	4	0.328	0.067	
Clinton	&	Ingham	60.09	16	0.000	0.287	
Gratiot	&	Ingham	8.25	16	0.941	0.008	51
Allegan	&	Midland	11.00	14	0.686	0.096	
Bay	&	Midland	0.00	16	1.000	0.000	50
Clinton	&	Midland	33.33	16	0.007	0.069	
Gratiot	&	Midland	5.80	16	0.990	-0.055	
Ingham	&	Midland	17.44	16	0.357	0.083	
Allegan	&	Montcalm	10.98	12	0.530	0.380	
Bay	&	Montcalm	NA	NA	NA	0.000	50
Clinton	&	Montcalm	25.22	16	0.066	0.225	
Gratiot	&	Montcalm	3.89	16	0.999	-0.144	
Ingham	&	Montcalm	2.78	4	0.596	0.480	
Midland	&	Montcalm	0.00	16	1.000	-0.456	50
Allegan	&	Oceana	10.99	12	0.530	0.365	
Bay	&	Oceana	17.58	16	0.349	0.614	
Clinton	&	Oceana	22.55	16	0.126	0.189	
Gratiot	&	Oceana	22.87	16	0.117	0.262	
Ingham	&	Oceana	22.19	16	0.137	0.587	
Midland	&	Oceana	0.00	8	1.000	-0.338	
Montcalm	&	Oceana	NA	NA	NA	0.621	
Allegan	&	Saginaw	61.75	16	0.000	0.369	
Bay	&	Saginaw	1.76	16	1.000	-0.044	50
Clinton	&	Saginaw	Infinity	16	0.000	0.196	

a) Chi square value

b) degrees of freedom

c) fixation index

d) multi-locus genotypes shared between regions

Table 3.10 (Con't)

Population 1	Pair		Chi ^{2 a}	Df ^b	<i>p</i> -value	Fst ^c	Shared d MLG
Gratiot	&	Saginaw	32.04	16	0.010	0.027	49,51
Ingham	&	Saginaw	16.23	16	0.437	0.016	48,51
Midland	&	Saginaw	25.58	16	0.060	0.052	50
Montcalm	&	Saginaw	0.00	16	1.000	-0.144	50
Oceana	&	Saginaw	42.05	16	0.000	0.365	
Allegan	&	Shiawassee	30.90	16	0.014	0.287	
Bay	&	Shiawassee	23.99	16	0.090	0.235	
Clinton	&	Shiawassee	37.77	16	0.002	0.120	74
Gratiot	&	Shiawassee	19.36	16	0.250	0.044	74
Ingham	&	Shiawassee	39.79	16	0.001	0.253	
Midland	&	Shiawassee	18.87	16	0.275	0.085	
Montcalm	&	Shiawassee	14.68	16	0.548	0.135	
Oceana	&	Shiawassee	22.51	16	0.127	0.359	
Saginaw	&	Shiawassee	61.44	16	0.000	0.143	

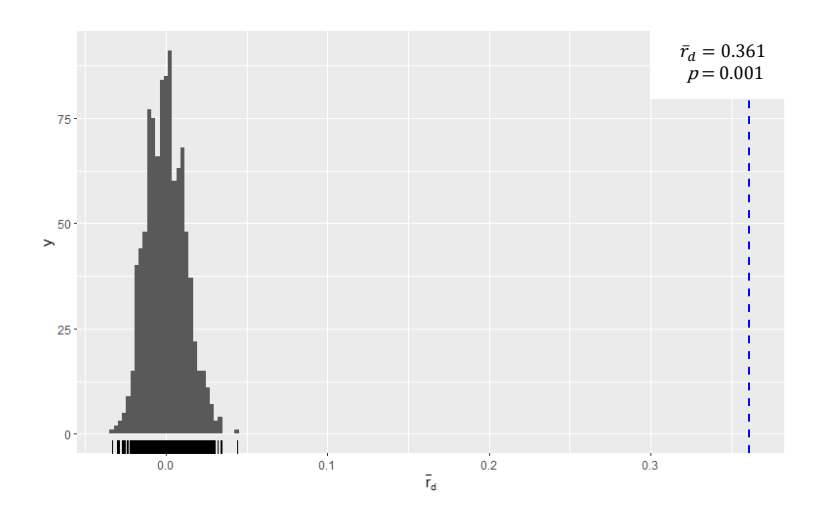


Figure 3.7 Index of association plot for 29 multi-locus genotypes from a Michigan population of *Rhizoctonia solani* AG 2-2. \bar{r}_d value is shown on x-axis with dotted line indicating value for the given dataset. Predicted distribution based on 999 permutations is shown as gray bars.

Cercospora nursery population

Populations collected from the Saginaw Valley Research and Extension Center (SVREC) came from adjacent fields following sugar beet in a fixed rotation cycle. Forty-two (95%) of the 44 isolates recovered were in subgroup AG 2-2PR and two (5%) were in subgroup AG 2-2BRa. These proportions are consistent with the overall Michigan population found in this study where AG 2-2BRa was about 9% of the population and AG 2-2PR about 91% of the population. No isolates from subgroup AG 2-2BRb were isolated from any Michigan location including the SVREC population. There were 10 (23%) isolates from subgroup AG 2-2PRb (cluster 4), which is slightly higher than the Michigan population at large in which there were about 16%.

There was a total of 7 multi-locus genotypes (MLG) identified in the SVREC population, 4 MLGs in the SV16 population and 6 MLGs in the SV17 population (Figure 3.8). A majority of the isolates recovered (64%) were in MLG50 (14 isolates from each subpopulation). Three MLGs were shared between populations (MLG49, MLG50, MLG66) and four were unique to the subpopulations, MLG10 in the SV16 population and MLG43, MLG68, and MLG69 in the SV17 population (Figure 3.8). The SV16 population contained one MLG from AG 2-2BRa (cluster 1), one MLG from AG 2-2PRb (cluster 4) and two MLGs from AG 2-2PGa. The SV17 population consisted of three MLGs from each AG 2-2PRa (cluster 3) and AG 2-2PRb (cluster 4).

There was a total of eight private alleles present in the population, four in each subpopulation (Figure 3.9). Density plot from discriminant analysis of principal components (DAPC) illustrates the relationship between subpopulations (Figure 3.10). While each population shared a large portion of the principal components, each population had independent peaks reflecting the unique MLGs in each subpopulation. Genotypic differentiation tests indicated no significant

difference between subpopulations ($X^2 = 6.626$, df = 16, p = 0.980) with negative a F_{ST} value ($F_{ST} = -0.044$).

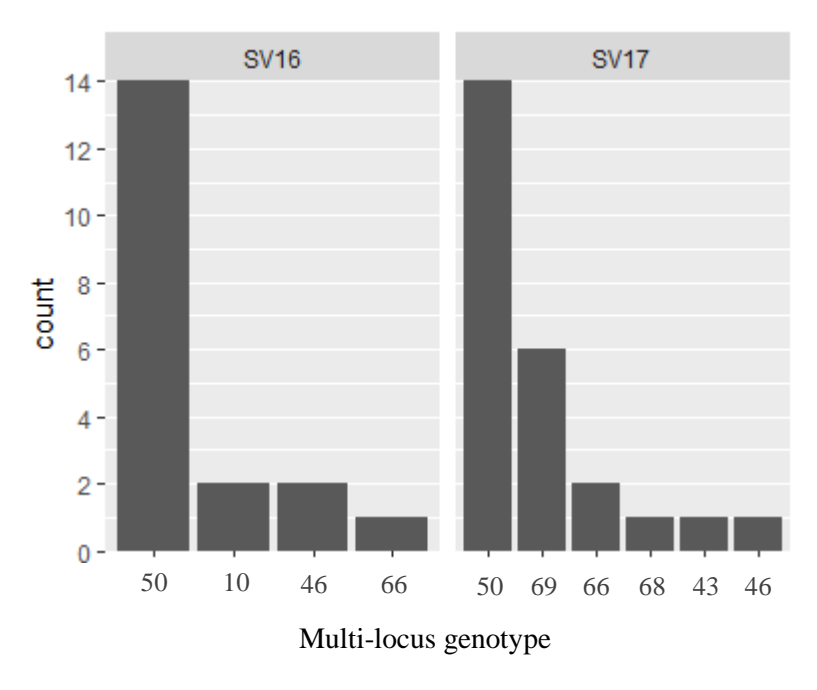


Figure 3.8 Histogram of multi-locus genotypes for 44 isolates of *Rhizoctonia solani* AG 2-2 from USDA Cercospora nursery in Michigan. Isolates were recovered from two adjacent fields in subsequent years, 2016 (SV16) and 2107 (SV17).

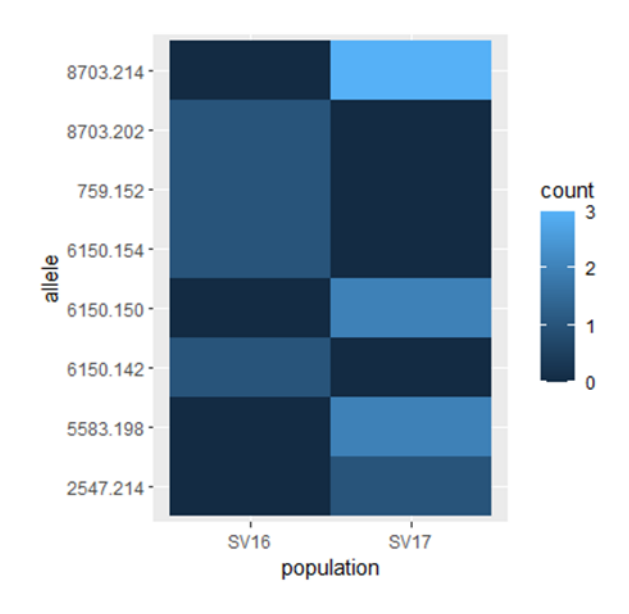


Figure 3.9 Private alleles in two populations of *Rhizoctonia solani* AG 2-2 from the USDA Cercospora nursery in Michigan. Populations were collected in 2016 (SV16) and 2017 (SV17).

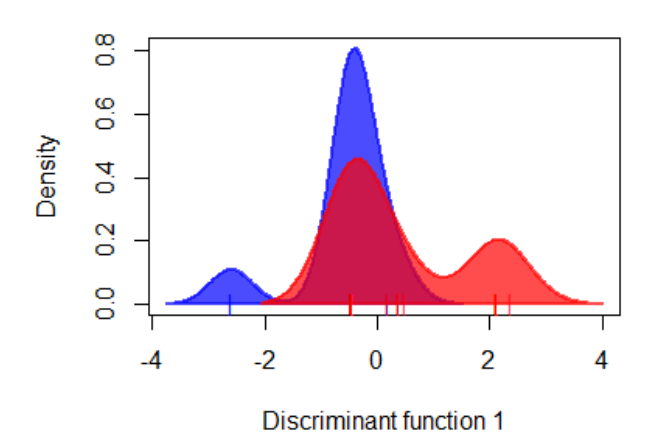


Figure 3.10 Density plot from discriminant analysis of principal components for two populations of *Rhizoctonia solani* AG 2-2 from the USDA Cercospora nursery in Michigan. Distribution colored blue represents the 2016 population and red represents the 2017 population.

There was no evidence of sexual recombination within the population. The index of association plot indicated a significant linkage between alleles ($\bar{r}_d = 0.721$, p = 0.001; Figure 3.11) which is characteristic of clonally reproducing populations (Balloux et al. 2003; Wright 1965). Global Hardy-Weinberg tests indicate evidence of a slight heterozygote excess in the SV17 population (p = 0.045). Individually, one locus (2547) showed evidence of heterozygote excess (p = 0.041) and one locus (5487) showed evidence of a deficiency of heterozygotes (p = 0.002). Estimates of F_{IS} were negative for all loci except 5487 ($F_{IS} = 0.714$) and 6145 ($F_{IS} = 0.091$). Estimate of F_{IS} across all loci was $F_{IS} = -0.072$. Collectively we interpret this evidence as supporting a population with primarily clonal reproduction (Balloux et al. 2003; Wright 1965).

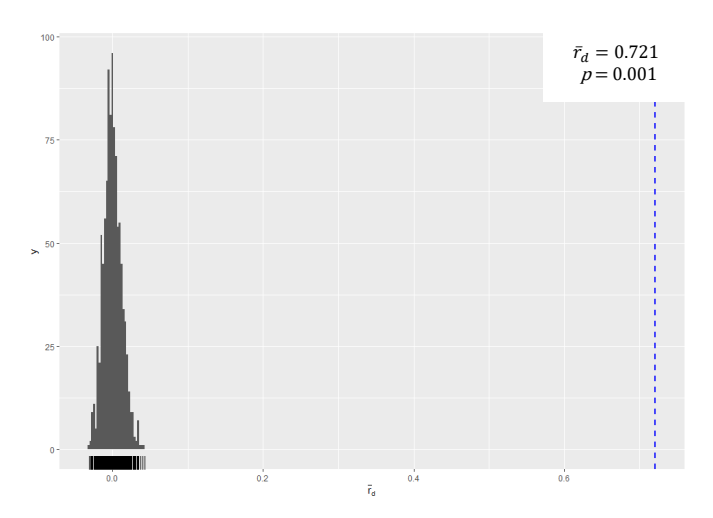


Figure 3.11 Index of association plot for 7 multi-locus genotypes for a population of *Rhizoctonia solani* AG 2-2 from the USDA Cercospora nursery in Michigan. \bar{r}_d value is shown on x-axis with dotted line indicating value for the given dataset. Predicted distribution based on 999 permutations is shown as gray bars.

Prior to 2010, the field that currently contains the Cercospora nursery was not subdivided and the rotation at that time included corn, dry bean, soybean, and wheat with sugar beets not having been grown there in the previous 20 years (personal communication, former grower). The field took its current configuration in 2010 with the field being divided into quadrants separated by a grass strip 10 meters wide and beginning the current rotation of sugar beet, corn, dry beans, and wheat. During that time, no inoculation of *Rhizoctonia* spp. has been performed on this section of the farm, thus we consider these to be natural populations.

Overall, the evidence supports SV16 and SV17 as a single population despite the limited separation for over 12 years. Of course, it is likely there has been movement of propagules from field to field during cultivation that would tend to homogenize the populations. Another factor that likely contributes to maintaining homogeneity between fields is that the rotation scheme was identical for each field and has remained fairly constant for almost 12 years. Despite these

factors that may homogenize the two field populations, there were marked differences between the populations. There were eight private alleles and four unique MLGs between the two populations. These observations are consistent with the patchy nature of RRCR (Anees et al. 2010; Truscott & Gilligan 2001) and may indicate that individual isolates have a relatively limited distribution.

Reproductive mode and presence of a cryptic sexual stage

Previously, we hypothesized that AG 2-2BRb (cluster 2) consists of isolates that had undergone sexual recombination (chapter 2, current dissertation). In the current study, we examined 19 AG 2-2BRb isolates from six growing regions. Clonal fraction of the group was 26.3% with 14 unique MLGs. Hardy-Weinberg tests indicated a deficit of heterozygotes with a F_{IS} value of 0.517, which is consistent with a highly inbred, sexually reproducing population (Brzyski et al. 2018; Wright 1965). The index of association plot (Brown et al. 1980) provided additional evidence with support for a lack of linkage between alleles, which is also consistent with a sexually reproducing population ($\bar{r}_d = 0.027$, p = 0.230; Figure 3.12). These observations provide support for our hypothesis that AG 2-2BRb (cluster 2) consists of isolates that have undergone sexual recombination despite the rarity of the teleomorph in nature.

Since the population from the Red River Valley had a high proportion of AG 2-2BRb genotypes (50%), we tested this population for evidence of sexual reproduction. When the entire population from the Red River Valley was considered, there was strong evidence of linkage between markers ($\bar{r}_d = 0.347$, p = 0.001) and therefore, no evidence of sexual reproduction (Brown et al. 1980; Wright 1949). However, when only members of AG 2-2BRb (cluster 2) from the region were considered, there was evidence of a sexually recombinant population

 $(\bar{r}_d = -0.026, p = 0.645)$. Therefore, we hypothesize a portion of the population in the Red River Valley may have a sexual mode of reproduction and thus we predict a mixed mode of reproduction in the Red River Valley population.

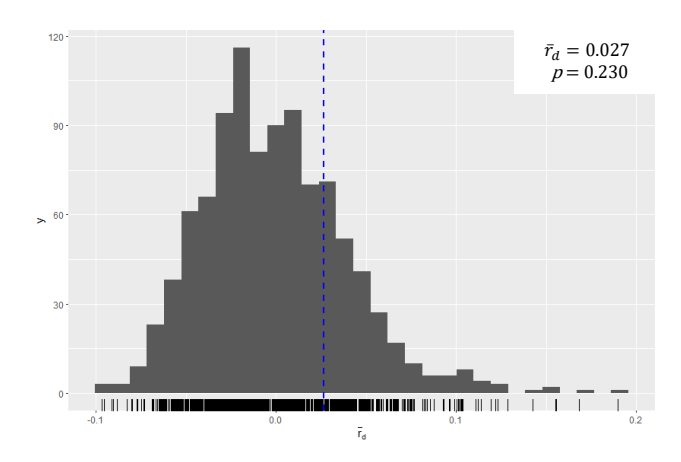


Figure 3.12 Index of association plot for 14 multi-locus genotypes of subgroup *Rhizoctonia solani* AG 2-2BRb. \bar{r}_d value is shown on x-axis with dotted line indicating value for the given dataset. Predicted distribution based on 999 permutations is shown as gray bars.

The conclusion of a mixed mode of reproduction is consistent with the observations of Ajayi-Oyetunde et al. (2019) who determined a population of AG 2-2 isolates from Ontario to have a mixed mode of reproduction. The Ontario population was made up entirely of 'type IIIB' isolates and to the best of our knowledge, the sexual stage has not been observed to occur in AG 2-2 'type IIIB' isolates. It is possible the isolates from the Ontario population were misidentified as 'type IIIB', especially if a genetic comparison was used to determine subgroup association rather than *in-vitro* growth trials. It is also possible that 'type IIIB' isolates can form a sexual stage but have not been observed doing so. Alternatively, our data suggests another explanation. All the isolates from Ontario in the current study were identified as AG 2-2PRb (cluster 4), and group association was split with about 80% association with AG 2-2PRb (cluster 4) and 20% with

AG 2-2BRb (cluster 2). In addition, there was a lack of genetic differentiation between the Ontario population and the Japan population, which had a high proportion of AG 2-2BRb isolates. Therefore, our hypothesis is that AG 2-2BRb (cluster 2) is present in Ontario, has undergone sexual recombination at some point, and has produced heterokaryons by asexual recombination with AG 2-2PRa. Examination of additional isolates from Ontario would be needed to test this hypothesis.

Rhizoctonia solani AG 2-2 populations having a cryptic mode of sexual reproduction in field populations could have implications in management by increasing genetic diversity (Heitman 2010), reducing deleterious mutations through purifying selection and increasing adaptability to environmental conditions (Brandt et al. 2017; MacPherson et al. 2021). For example, recombination has the potential to intensify the evolution of multiple-fungicide resistance (De Miccoli Angelini et al. 2015; Takahashi et al. 2021). In addition, basidiospores can be dispersed more readily than hyphal fragments and can even be carried by air and water currents (Naito 1996). Foliar blight of sugar beet has been associated with basidiospore dispersal (Naito & Sugimoto 1980; Naito 1990) and has been observed in several states within the United States including: Arizona, Colorado, Michigan, Minnesota, Ohio, and Wisconsin, but can be caused by AG other than AG 2-2 (Windels 2009).

Hymenia of *R. solani* AG 2-2 have been reported to occur on sugar beet leaf bases and at the soil surface (Naito 1996). However, it is uncertain what environmental conditions are necessary for the formation of a sexual stage in a field setting. Since the soil-over-culture method is preferred for inducing the sexual stage in the lab (Flentje 1956; Ogoshi 1972; Toda & Hyakumachi 2006), it may be that in most circumstances the hymenia are formed at the soil surface and are just too difficult to detect in most situations. Instead, identifying the sexual stage

in a field setting may require indirect evidence from population genetics such as we present in the current study. The potential for sexual reproduction in some regions highlights the need for experiments involving the nature of heterothallic and homothallic mating systems in AG 2-2 (Toda & Hyakumachi 2006), the fate of basidiospore derived isolates (Kiyoshi et al. 2014) and the consequences of heterokaryosis in the generation of diversity (Qu et al. 2013).

Hybridization and the generation of genetic diversity

Observations in previous studies indicated the possibility that some isolates were hybrids, with genetic composition originating from two or more parental sources from different subgroups (chapter 2, current dissertation). These isolates showed evidence of admixture and clustered together separately from the main genetic clusters that corresponded with the subgroups. In the current study, we observed 11 additional isolates with similar characteristics and investigated the phenomenon further. Isolates with evidence of admixture grouped together according to cluster analysis regardless of whether genetic diversity was shared between clade AG 2-2PR and AG 2-2BRa or between AG 2-2PR and AG 2-2BRb (Figure 3.1).

The isolate 'slovakia' was one of the samples that showed evidence of admixture and also had a whole genome sequence available. Based on structure analysis, we expected genes to be shared between AG 2-2PR and AG 2-2BRb (Table 3.3) by what we hypothesize to be the exchange of nuclei during anastomosis. To test this, we identified gene sequences for β-tubulin, Calmod, Rpb1, and Rpb2 from the genome assemblies of 'slovakia' and six additional isolates that were representative of subgroups AG 2-2BRa, AG 2-2BRb, and AG 2-2PRa. The resulting neighbor-joining trees for all four genes showed that the genome of 'slovakia' contained two alleles of each gene, with one allele most similar to sequences from isolates in clade AG 2-2BRb

and the other most similar to sequences from isolates in clade AG 2-2PRa (Figure 3.13). These observations provide support for our hypothesis that members of AG 2-2PRb are formed from hybrids between AG 2-2BR and AG 2-2PR.

To determine if the hypothesized hybridization occurs in natural populations, we examined a set of isolates from the SVREC population that had similar characteristics as the 'slovakia' sample. Isolate 'R17-15' (AG 2-2PRb) had group association split between AG 2-2PR and AG 2-2BRa and appeared to be a hybrid. Isolates 'R17-6' (AG 2-2PR) and 'R16-10' (AG 2-2BRa) were selected from the Cercospora nursery population and the β -tub, Calmod, Rpb1, and Rpb2 genes were cloned and sequenced for all three isolates. The results were mixed with two genes (Calmod and Rpb1) having alleles that were associated with both group AG 2-2BRa and AG 2-2PR (Table 3.11). Both alleles for the β -tub gene were similar to alleles from AG 2-2PR while both alleles for the Rpb2 gene were similar to alleles from AG 2-2BRa. While these results do not offer conclusive evidence of hybridization or asexual recombination, they are suggestive that such events do occur in natural populations.

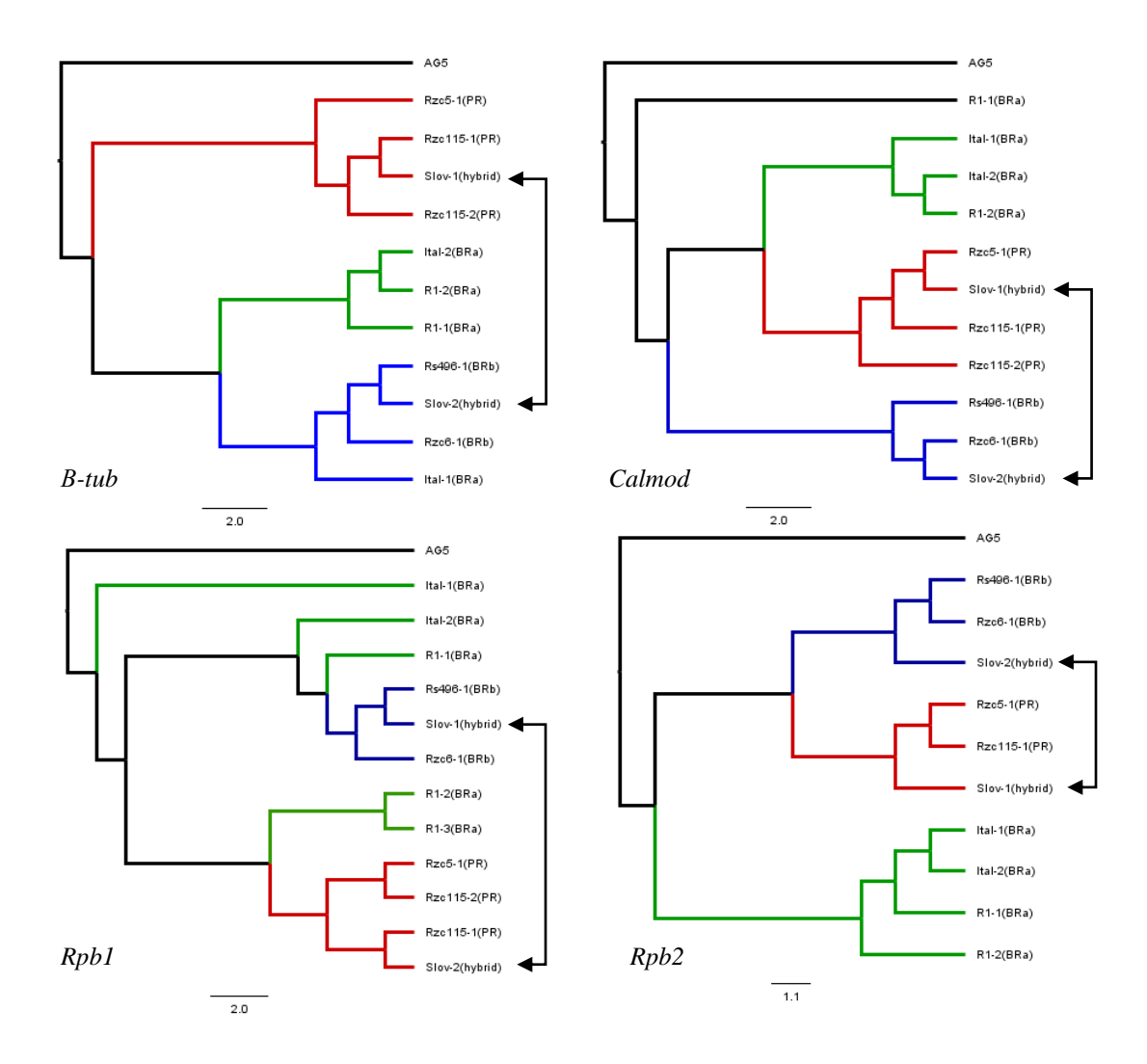


Figure 3.13 Gene trees of four gene sequences for seven *Rhizoctonia solani* AG 2-2 isolates. Trees were generated using the neighbor-joining method with an AG-5 isolate included as an outgroup. Alleles from the suspected hybrid 'slovakia' are indicated by arrows and show the relationship between those alleles and the subgroups, which are indicated by colored branches (green = AG 2-2BRa, blue = AG 2-2BRb, and red = AG 2-2PR).

Table 3.11 Association of alleles of four genes from potential hybrid 'R17-15' with alleles from isolates in subgroups AG 2-2BRa and AG 2-2PRa.

	Number of alleles associated with subgroups						
	BRa	BRb	PRa				
Btub	0	0	2				
Calmod	1	0	1				
Rpb1	2	0	1				
Rpb2	2	0	0				

Subgroup specific primers

Fifty-eight of sixty-three isolates (92%) were correctly identified to subgroup using the group specific primer set (Table 3.12). Four isolates failed to amplify for any primer except for the AG 2-2 specific primers (Carling et al. 2002). One isolate ('R9') amplified with both AG 2-2BRa and AG 2-2PR primer pairs producing ambiguous results. Phylogenetically, isolate 'R9' is clearly in subgroup AG 2-2BRa, so it is unclear why amplification occurred with the AG 2-2PR primers. However, there have been conflicting assignments of subgroup for isolate 'R9' (Carling et al. 2002; Engelkes & Windels 1996; Stojšin et al. 2007; Strausbaugh et al. 2011a), so there may be a unique genetic condition in this isolate that results in conflicting subgroup association. None of the non-AG 2-2 isolates amplified with the group specific primers.

Curiously, the AG 2-2LP isolate was expected to amplify with at least one primer set but did not (Table 3.12), providing further support that AG 2-2LP should be considered a separate subgroup from AG 2-2BR and AG 2-2PR as suggested in chapter 2 (current dissertation).

Table 3.12 Results of subgroup specific primer testing for 71 isolates of *Rhizoctonia solani*. The columns for the primer pairs shows the results of testing a specific isolate with the indicated primer pair, where a '+' indicates a positive PCR reaction and '-' indicates a negative PCR reaction. The predicted subgroup is indicated in the column 'ID". Cluster as determined by cluster analysis is indicated.

	P	rimer pai	rs				P	rimer pai	rs		
Isolate	BRa	BRb	PR	ID	Cluster	Isolate	BRa	BRb	PR	ID	Cluste
Italian	+	-	-	BRa	1	R17-31	-	-	+	PR	3
R09-25	+	-	-	BRa	1	Rs1012	-	-	+	PR	3
R1	+	-	-	BRa	1	Rs1146	-	-	+	PR	3
R15-80	-	-	-	-	1	Rs393	-	-	+	PR	3
R16-10	+	-	-	BRa	1	C116S	-	-	-	-	3
R16-9	+	-	-	BRa	1	24BR	-	-	+	PR	4
F16	+	-	-	BRa	1	R14-10	-	-	+	PR	4
R9	+	-	+	-	1	R15-72	-	-	+	PR	4
Rs300	-	-	-	-	1	R15-74	-	-	+	PR	4
Rs866	+	-	-	BRa	1	R15-76	-	-	+	PR	4
F508	+	-	-	BRa	1	R15-78	-	-	+	PR	4
F521	+	-	-	BRa	1	R15-82	-	-	+	PR	4
R86	+	-	-	BRa	1	R15-83	-	-	+	PR	4
Bayern	-	+	-	BRb	2	R15-84	-	-	+	PR	4
91.003	-	+	-	BRb	2	R15-87	-	-	+	PR	4
Rs481	-	+	-	BRb	2	R15-88	-	-	+	PR	4
Rs496	-	+	-	BRb	2	R15-92	-	-	+	PR	4
Rs588	-	+	-	BRb	2	R15-98	-	-	+	PR	4
2C13	-	+	-	BRb	2	R17-15	-	-	+	PR	4
H502	-	+	-	BRb	2	R17-19	-	-	+	PR	4
R164S	-	+	-	BRb	2	R17-24	-	-	+	PR	4
H549	-	-	-	-	2	R17-30	-	-	+	PR	4
H582	-	+	-	BRb	2	Roland	-	-	+	PR	4
RH188	-	+	-	BRb	2	F24	-	-	+	PR	4
Cavalie	-	-	+	PR	3	Rs850	-	-	+	PR	4
R15-30	-	-	+	PR	3	2C1	-	-	+	PR	4
R15-5	-	-	+	PR	3	R16-14	-	-	+	PR	4
R15-6	-	-	+	PR	3	R15-12	-	-	-	-	AG-4
R15-60	-	-	+	PR	3	R15-14	-	-	-	-	AG-5
R15-61	-	-	+	PR	3	R15-43	-	-	-	-	AG-E
R15-67	-	-	+	PR	3	R15-51	-	-	-	-	AG-5
R15-70	-	-	+	PR	3	ACC3-LP	-	-	-	-	AG2- 2LP
R16-12	-	-	+	PR	3	R-5	-	-	-	-	AG-4
R16-4	-	-	+	PR	3	R15-8	-	-	-	-	AG-5
R16-8	-	-	+	PR	3	ST6-1	-	-	-	-	AG-5
R17-10	_	_	+	PR	3						

We were unable to develop markers that could distinguish AG 2-2PRa and AG 2-2PRb, presumably because they contain much of the same genomic content. We expected that AG 2-2PRb would amplify with both PRa and BR primers since the evidence supports AG 2-2PRb being hybrids of AG 2-2PR and AG 2-2BR. However, the AG 2-2PRb (cluster 4) isolates we tested amplified only with AG 2-2PR primers and not with either AG 2-2BR primers. We do not currently have an explanation for why this was the case.

These primers provide a means for rapidly identifying these newly classified subgroups of AG 2-2 which could provide researchers and managers with valuable information about population composition. They may also provide the foundation for the development of qPCR probes that could allow high-throughput screening of isolates.

Conclusions

The heterokaryotic and multi-nucleate nature of *R. solani* AG 2-2 makes the genetics of the group especially complicated. This complexity and the inconsistent conclusions that have often followed have left some open questions regarding the population genetics of the group, particularly regarding the origin of diversity and evolutionary relationships. We expect that the research presented in the current study will guide future research that can lead to a better understanding of the biology of this important pathogen and improve our ability to control the diseases it incites.

One of the more important conclusions to come from the current study is that it appears cryptic sexual reproduction occurs in natural populations but is limited to a single subgroup, AG 2-2BRb. The potential for a sexual stage has implications for future management strategies, especially resistance breeding and fungicide sensitivity, by introducing recombination and

increasing diversity. The other source of diversity that the current study substantiated is the hybridization or parasexual exchange of nuclei between subgroups. While genetic exchange has been demonstrated previously (Kiyoshi et al. 2013; Toda & Hyakumachi 2006), our observations demonstrate that these putative hybrids form a genetic cluster that is distinct from the parental isolates. The effect of this hybridization on characteristics such as virulence still needs to be explored.

It is widely accepted that *Rhizoctonia solani* AG 2-2 has a worldwide distribution, but the current study provides additional information regarding the specifics of that distribution, most notably, the identification of all four genetic groups in Europe, the prevalence of the subgroup AG 2-2BRb in the Red River Valley, and the lack of the same group collected from Michigan. We encourage other researchers to expand on our work to develop a more complete representation of regional and local populations. More specifically, assessments of diversity should focus on relating regional diversity to those processes, such as sexual reproduction, that substantially contribute to the genetic diversity of populations and can potentially complicate management strategies.

To the best of our knowledge, this is the first report to provide evidence of the long-range dispersal of *R. solani* AG 2-2 genotypes. In several cases, genotypes were shared between regions separated by an ocean, or shared between regions without being detected in regions that are spatially intermediate. The later condition could be explained by insufficient sampling from these intermediate regions, but nevertheless, the dispersal across substantial distances in clear. This observation highlights the necessity for the sanitation of equipment, materials and personal gear when moving between growing areas. One area related to *R. solani* AG 2-2 dispersal that has not been adequately explored is the role of the horticultural trade on the movement of

propagules. Horticultural plants have an enormous potential to move microbes between regions, either as a host or through contaminated soil, and could possibly explain the sharing of genotypes between areas such as Japan and the United States.

There was little evidence of host preference related to subgroup in the current study. Although isolates recovered from dry bean were mostly restricted to AG 2-2PRa, previous studies have shown that dry beans are susceptible to all subgroups (Minier 2019). Significant differences in aggressiveness between groups has previously been demonstrated with subgroup AG 2-2PR being the most aggressive on dry bean (Minier 2019), which may result in selection for the more aggressive genotypes. Similar selection for more aggressive genotypes has also been demonstrated for corn (Windels & Brantner 2005, 2006). Thus, we expect that crop rotation choices can have a critical effect on *Rhizoctonia solani* AG 2-2 populations and could affect not only a following sugar beet crop, but the rotational crops as well. Crop rotation continues to be an important consideration in the management of RRCR and additional studies are needed to examine the effects of different crops on *R. solani* AG 2-2 populations. The markers outlined in the current study provide valuable tools for the evaluation of *R.* solani AG2-2 populations that can be used to improve management of Rhizoctonia root and crown rot of sugar beet.

REFERENCES

- Ajayi-Oyetunde, O. O., Everhart, S. E., Brown, P. J., Tenuta, A. U., Dorrance, A. E. and Bradley, C. A. 2019. Genetic structure of *Rhizoctonia solani* AG-2-2IIIB from soybean in Illinois, Ohio, and Ontario. Phytopathology, 109:2132-2141.
- Anees, M., Edel-Hermann, V. and Steinberg, C. 2010. Build up of patches caused by *Rhizoctonia solani*. Soil Biol Biochem, 42:1661-1672.
- Balloux, F., Lehmann, L. and de Meeûs, T. 2003. The population genetics of clonal and partially clonal diploids. Genetics, 164:1635-1644.
- Brandt, A., Schaefer, I., Glanz, J., Schwander, T., Maraun, M., Scheu, S. and Bast, J. 2017. Effective purifying selection in ancient asexual oribatid mites. Nat Commun, 8:873. doi:10.1038/s41467-017-01002-8
- Brantner, J. R. and Windels, C. E. 2007. Distribution of *Rhizoctonia solani* AG 2-2 intraspecific groups in the Red River Valley and Southern Minnesota. Sugarbeet Res Ext Rep, 38:242-246.
- Brown, A.H.D., Feldman, M.W. and Nevo, E. 1980. Multilocus structure of natural populations of *Hordeum spontaneum*. Genetics, 96:523-536.
- Brzyski, J.R., Stieha, C.R. and McLetchie, D.N. 2018. The impact of asexual and sexual reproduction in spatial genetic structure within and between populations of the dioecious plant *Marchantia inflexa* (*Marchantiaceae*). Ann Bot-London, 122:993-1003.
- Buhre, C.K., Kluth, C., Bürchy, K., Märländer, B., and Varrelmann, M. 2009. Integrated control of root and crown rot in sugar beet: Combined effects of cultivar, crop rotation, and soil tillage. Plant Dis, 93:155-161.
- Carling, D.E. 1996. Grouping in *Rhizoctonia solani* by hyphal anastomosis interactions. Pg. 37-47 in *Rhizoctonia* Species: Taxonomy, Molecular Biology, Ecology, Pathology and Disease Control. Sneh, B, Jabaji-Hare, S., Neate, S. and Dijst, G. (eds.) Kluwer Academic Publishers, Dordrecht, The Netherlands.
- Carling, D. E., Kuninaga, S. and Brainard, K. A. 2002. Hyphal anastomosis reactions, rDNAinternal transcribed spacer sequences, and virulence level among subsets of *Rhizoctonia solani* anastomosis group-2 (AG-2) and AG-BI. Phytopathology 92:43-50.
- Coons, G.H. and Kotila, J.E. 1935. Influence of preceding crops on damping off of sugar beets. Phytopathology, 25:13. (Abstr.)
- Cubeta, M. A. and Vilgalys, R. 1997. Population biology of the *Rhizoctonia solani* complex. Phytopathology 87:480-484.
- De Meeûs, T. 2018. Revisiting F_{IS}, F_{ST}, Wahlund effects, and null alleles. J Hered, 109:446-456.

- De Miccolis Angelini, R.M., Pollastro, S. and Faretra, F. 2015. Genetics of fungicide resistance. Pgs. 13-34 in Fungicide Resistance in Plant Pathogens. Ishii, H. and Hollomon, D. (eds.) Springer, Tokyo, Japan.
- Dieringer, D. and Schlötterer, C. 2003. Microsatellite analyser (MSA): a platform independent analysis tool for large microsatellite data sets. Mol Ecol Notes, 3:167-169.
- Engelkes, C. A. and Windels, C. E. 1996. Susceptibility of sugar beet and beans to *Rhizoctonia solani* AG-2-2 IIIB and AG-2-2 IV. Plant Dis, 80:1413-1417.
- Fenille, R.C., de Souza, N.L. and Kuramae, E.E. 2002. Characterization of *Rhizoctonia solani* associated with soybean in Brazil. Eur J Plant Pathol, 108:783-792.
- Flentje, N.T. 1956. Studies on *Pellicularia filamentosa* (Pat.) Rogers: I. Formation of the sexual stage. T Brit Mycol Soc, 39:343-356.
- Garnier-Géré, P. and Chikhi, L. 2013. Population subdivision, Hardy-Weinberg equilibrium and the Wahlund effect. eLS. doi: 10.1002/9780470015902.a0005446.pub3
- Gibson, A.K. 2022. Genetic diversity and disease: the past, present, and future of an old idea. Evolution, 76:20-36.
- Heitman, J. 2010. Evolution of eukaryotic microbial pathogens via covert sexual reproduction. Cell Host Microbe, 8:86-99.
- Hyakumachi, M., Mushika, T., Ogiso, Y., Tdoa, T., Kageyama, K. and Tsuge, T. 1998. Characterization of a new cultural type (LP) of *Rhizoctonia solani* AG2-2 isolated from warm-season turfgrasses, and its genetic differentiation from other cultural types. Plant Pathol, 47:1-9.
- Ithurrart, M.E.F., Büttner, G. and Petersen, J. 2004. Rhizoctonia root rot in sugar beet (*Beta vulgaris* ssp. *altissima*) epidemiology aspects in relation to maize (*Zea mays*) as a host plant. J Plant Dis Protect, 111:302-312.
- Jacobsen, B., Kephart, K., Zidack, M., Johnson, M. and Ansley, J. 2004. Effect of fungicide and fungicide application timing on reducing yield loss to Rhizoctonia crown and root rot. Sugarbeet Res Ext Rep, 35:224-226.
- Jombart, T. 2008. adegenet: a R package for the multivariate analysis of genetic markers. Bioinformatics, 24:1403-1405.
- Kamvar, Z.N., Tabima, J.F. and Grünwald, N.J. 2014. Poppr: an R package for genetic analysis of populations with clonal, partially clonal, and/or sexual reproduction. PeerJ, 2:e281. doi:10.7717/peerj.281.
- Kamvar, Z.N., Tabima, J.F. and Grünwald, N.J. 2015. Novel R tools for analysis of genome-wide population genetic data with emphasis on clonality. Front Genet, 6:208. doi:10.3389/fgene.2015.00208

- Karlen, D.L., Cambardella, C.A., Kovar, J.L. and Colvin, T.S. 2013. Soil quality responses to long-term tillage and crop rotation practices. Soil Till Res, 133:54-64.
- Katan, J. 2000. Physical and cultural methods for the management of soil-borne pathogens. Crop Prot, 19:725-731.
- Kiyoshi, T., Naito, S., Akino, S., Ochi, S. and Kondo, N. 2014. Progeny derived from *Thanatephorus cucumeris* (*Rhizoctonia solani*) AG-2-2 IV isolates on sugar beet foliage show more clonal diversity in somatic compatibility grouping than those from roots and petioles. J Gen Plant Pathol, 80:136-146.
- Leclerc, M. Doré, T., Gilligan, C.A., Lucas, P. and Filipe, J.A.N. 2014. Estimating the delay between host infection and disease (incubation period) and assessing its significance to the epidemiology of plant diseases. PloS One 9:e86568. doi:10.1371/journal.pone.0086568
- Leslie, J.F. 1996. Fungal vegetative compatibility promises and prospects. Phytoparasitica, 24:3-6.
- Leslie, J.F. and Summerell, B.A. 2006. The *Fusarium* Laboratory Manual. Blackwell Publishing, Ames, IA.
- Li, H. 2018. Minimap2: pairwise alignment for nucleotide sequences. Bioinformatics, 34:3094-3100.
- MacPherson, B., Scott, R. and Gras, R. 2021. Sex and recombination purge the genome of deleterious alleles: an individual based modeling approach. Ecol Complex, 45:100910. doi:10.1016/j.ecocom.2021.100910
- Martin, F., Windels, C., Hanson, L. and Brantner, J. 2014. Analysis of population structure and pathogenicity of *Rhizoctonia solani* AG2-2 (ISGIIIB and IV) isolates from Michigan, Minnesota and North Dakota. Sugarbeet Res Rep. Beet Sugar Development Foundation, Denver, CO. Published on CD.
- Maxson, A.C. 1938. Root-rots of the sugar beet. P Am Soc Sugar Beet Technol, 1938:60-64.
- Mihajlović, M., Rekanović, E., Hrustić, J., Grahovac, M. and Tanović, B. 2017. Methods for management of soilborne plant pathogens. *Pesticidi i fitomedicina*, 32:9-24.
- Minier, D.H. 2019. Diversity of the fungal pathogen *Rhizoctonia solani* AG2-2. (Master's thesis). Michigan State University, East Lansing, MI. ProQuest, Ann Arbor, MI
- Minier, D.H. and Hanson, L.E. 2021. Effect of temperature on the aggressiveness of *Rhizoctonia solani* AG 2-2 isolates on sugar beet (*Beta vulgaris*) seedlings. Plant Dis, 105:3111-3117.
- Muyolo, N.G., Lipps, P.E. and Schmitthenner, A.F. 1993. Anastomosis grouping and variation in virulence among isolates of *Rhizoctonia solani* associated with dry bean and soybean in Ohio and Zaire. Phytopathology, 83:438-444.

- Naito, S. 1996. Basidiospore dispersal and survival. Pgs. 197-205 in *Rhizoctonia* Species: Taxonomy, Molecular Biology, Ecology, Pathology and Disease Control. Sneh, B, Jabaji-Hare, S., Neate, S. and Dijst, G. (eds.) Kluwer Academic Publishers, Dordrecht, The Netherlands.
- Naito, S. 1990. Ecological role of basidiospores of *Thanatephorus cucumeris* (Frank) Donk and development of foliage blight of sugar beet. (In Japanese with English abstract) Jpn Agr Res Quart, 23:268-275.
- Naito, S. and Sugimoto, T. 1980. Relationship between basidiospore dispersal of *Thanatephorus cucumeris* (Frank) Donk. (In Japanese with English abstract) Ann Phytopath Soc Japan, 46:216-223.
- Neate, S.M. 1987. Plant debris in soil as a source of inoculum of *Rhizoctonia* in wheat. T Brit Mycol Soc, 88:157-162.
- Neher, O. T. and Gallian, J. J. 2011. *Rhizoctonia* on sugar beet: importance, identification and control in the Northwest. PNW 629. Pacific Northwest Extension Publication, University of Idaho, Moscow, ID.
- Nelson, B., Helms, T., Christianson, T. and Kural, I. 1996. Characterization and pathogenicity of *Rhizoctonia* from soybean. Plant Dis, 80:74-80.
- Nurk S., Bankevich, A., Antipov, D., Gurevich, A., Korobeynikov, A., Lapidus, A., Prjibelsky, A., Pyshkin, A., Sirotkin, A., Sirotkin, Y., Stepanauskas, R., McLean, J., LAsken, R., Clingenpeel, S.R., Woyke, T., Tesler, G., Alekseyev, M.A. and Pevzner, P.A. 2013.
 Assembling genomes and mini-metagenomes from highly chimeric reads. Pgs. 158-170 in: Research in Computational Molecular Biology. Deng M., Jiang R., Sun F. and Zhang X. (eds.) RECOMB 2013: Lecture Notes in Computer Science, vol 7821. Springer, Berlin, Germany. doi:10.1007/978-3-642-37195-0_13
- Ogoshi, A. 1972. On the perfect stage of anastomosis group 2 of *Rhizoctonia solani* Kühn. Ann Phytopathol Soc Jap, 13:285-293.
- Ogoshi, A. 1987. Ecology and pathology of anastomosis and intraspecific groups of *Rhizoctonia solani* Kühn. Annul. Rev. Phytopathol. 25:124-143.
- Okubara, P.A., Dickman, M.B. and Blechl, A.E. 2014. Molecular and genetic aspects of controlling the soilborne necrotrophic pathogens *Rhizoctonia* and *Pythium*. Plant Sci, 228:61-70.
- Parmeter, J.R. jr., Sherwood, R.T. and Platt, W.D. 1969. Anastomosis grouping among isolates of *Thanatephorus cucumeris*. Phytopathology, 59:1270-1278.
- Peña, P.A., Steadman, J.R., Eskridge, K.M. and Urrea, C.A. 2013. Identification of sources of resistance to damping-off and early root/hypocotyl damage from *Rhizoctonia solani* in common bean (*Phaseolus vulgaris* L.). Crop Prot, 54:92-99.

- Qu, P., Saldajeno, M.G.B. and Hyakumachi, M. 2013. Mechanism of the generation of new somatic compatibility groups with *Thanetephorus cucumeris* (*Rhizoctonia solani*). Microbes Environ, 28:325-335.
- R Core Team 2022. R: a language and environment for statistical computing. R Foundation for Statistical Computing, Vienna, Austria. https://www.R-project.org/
- Raymond, M. and Rousset, F. 1995. An exact test for population differentiation. Evolution, 49:1280-1283.
- Reeleder, R.D. 2003. Fungal plant pathogens and soil biodiversity. Can J Soil Sci, 83:331-336.
- Rousset, F. 2008. Genepop'007: a complete reimplementation of the Genepop software for Windows and Linux. Mol Ecol Resour, 8:103-106.
- Ruppel, E.G. 1985. Susceptibility of rotation crops to a root rot isolate of *Rhizoctonia solani* from sugar beet and survival of the pathogen in crop residues. Plant Dis, 69:871-873.
- Ruppel, E.G., Schneider, C.L., Hecker, R.J. and Hogaboam, G.J. 1979. Creating epiphytotics of Rhizoctonia root rot and evaluating for resistance to *Rhizoctonia solani* in sugarbeet field plots. Plant Dis Rep, 63:518-522.
- Rush, C.M. and Winter, S.R. 1990. Influence of previous crops on Rhizoctonia root and crown rot of sugar beet. Plant Dis, 74:421-425.
- Rush, C.M., Mihail, J.D. and Singleton, L.L. 1992. Introduction. Pgs. 3-6 in: Methods for Research on Soilborne Phytopathogenic Fungi. Singleton, L.L., Mihail, J.D. and Rush, C.M. (eds.). APS Press, St. Paul, MN.
- Sharon, M., Kuninaga, S., Hyakumachi, M., Naito, S. and Sneh, B. 2008. Classification of *Rhizoctonia* spp. using rDNA-ITS sequence analysis supports the genetic basis of the classical anastomosis grouping. Mycoscience 49:93-114.
- Sneh, B., Burpee, L. and Ogoshi, A. 1991. Identification of *Rhizoctonia* species. APS Press, St. Paul, MN.
- Spielman, R.S., Neel, J.V. and Li, F.H.F. 1977. Inbreeding estimation from population data: models, procedures and implications. Genetics, 85:355-371.
- Strausbaugh, C. A., Eujayl, I. A., Panella, L. W. and Hanson, L. E. 2011a. Virulence, distribution and diversity of *Rhizoctonia solani* from sugar beet in Idaho and Oregon. Can J Plant Pathol, 33:210-226.
- Strausbaugh, C.A., Rearick, E., Eujayl, I. and Foote, P. 2011b. Influence of *Rhizoctonia*-bacterial root rot complex on storability of sugar beet. J Sugar Beet Res, 48:155-180.
- Sumner, D.R. and Minton, N.A. 1989. Crop losses in corn induced by *Rhizoctonia solani* AG-2-2 and nematodes. Phytopathology, 79:934-941.

- Sussman, A.S. 1968. Longevity and survivability of fungi. Pgs. 447-486 in: The Fungi: An Advanced Treatise. Volume III: The Fungal Population. Ainsworth, G.C. and Sussman, A.S. (eds.) Academic Press, New York, NY.
- Takahashi, H., Oiki, S., Kusuya, Y., Urayama, S. and Hagiwara, D. 2021. Intimate genetic relationships and fungicide resistance in multiple strains of *Aspergillus fumigatus* isolated from a plant bulb. Environ Microbiol, 23:5621-5638.
- Toda, T. and Hyakumachi, M. 2006. Heterokaryon formation in *Thanatephorus cucumeris* anastomosis group 2-2 IV. Mycologia, 98:726-736.
- Truscott, J.E. and Gilligan, C.A. 2001. The effect of cultivation on the size, shape, and persistence of disease patches in fields. P Natl Acad Sci, 98:7128-7133.
- Untergasser, A., Cutcutache, I., Koressaar, T., Ye, J., Faircloth, B.C., Remm, M. and Rozen, S.G. 2012. Primer3 new capabilities and interfaces. Nucleic Acids Res, 40:e115. doi:10.1093/nar/gks596
- Waples, R.S. 2015. Testing for Hardy-Weinberg proportions: have we lost the plot? J Hered, 106:1-19.
- Weir, B.S. and Cockerham, C.C. 1984. Estimating F-statistics for the analysis of population structure. Evolution, 38:1358-1370.
- Windels, C.E. 2009. Rhizoctonia foliar blight. Pgs. 14-15 in: Compendium of Beet Diseases and Pests (2nd ed.). Harveson, R.M., Hanson, L.E. and Hein, G.L. (eds.) APS Press, St. Paul, MN.
- Windels, C.E. and Brantner, J.R. 2005. Previous crop influences *Rhizoctonia* on sugarbeet. 2004a Sugarbeet Res Ext Rept, 35:227-231.
- Windels, C.E. and Brantner, J.R. 2006. Crop rotation effects on *Rhizoctonia solani* AG 2-2. 2005 Sugarbeet Res Ext Rept, 36:286-290.
- Windels, C.E., Jacobsen, B.J. and Harveson, R.M. 2009. Rhizoctonia root and crown rot. Pgs:33-36 in: Compendium of Beet Diseases and Pests (2nd ed.). Harveson, R.M., Hanson, L.E. and Hein, G.L. (eds.) APS Press, St. Paul, MN.
- Wright, S. 1949. The genetic structure of populations. Ann of Eugenic, 15:323-354.
- Wright, S. 1965. The interpretation of population structure by F-statistics with special regard to systems of mating. Evolution, 19:395-420.
- Zheng, L., Shi, F. and Hsiang, T. 2013. Genetic structure of a population of *Rhizoctonia solani* AG2-2 IIIB from *Agrostis stolonifera* revealed by inter-simple sequence repeat (ISSR) markers. Can J Plant Pathol, 34:476-481.

	CHAPTER 4:
HISTOPATHOLOGY OF RHIZOCT	ONIA ROOT AND CROWN ROT OF SUGAR BEET

Introduction

Rhizoctonia root and crown rot (RRCR) is a major disease of sugar beets in growing regions throughout the world. RRCR affects approximately 25% of cultivated sugar beet area in the United States and 10% of the sugar beet area in Europe (Harveson 2008). Yield losses can exceed 50% in severe cases and epidemics are often more intense when crop rotations are shortened to under three years (Bühre et al. 2009). In addition, the presence of diseased beets in storage piles reduces storability and processing quality (Strausbaugh & Gillen 2008).

The causal agent of RRCR is the fungal pathogen, *Rhizoctonia solani* AG 2-2 (Kühn). *R. solani* is a species complex consisting of several independent lineages known as anastomosis groups (AG), that are separated by the ability of the hyphae to fuse or anastomose (Parmeter et al. 1969; Sneh et al. 1991). Currently, at least 13 AGs have been identified and this classification system represents our best understanding of relationships within the *R. solani* complex (Gonzalez et al. 2016. Several AG have been further subdivided into intraspecific groups (ISG) based on factors such as DNA hybridization, sclerotia size, zymography patterns, and/or temperature tolerance (Sneh et al. 1991). *Rhizoctonia solani* AG 2-2 has traditionally been separated into three subgroups, AG 2-2IIIB, AG 2-2IV, and AG 2-2LP, although the legitimacy of these subgroups is questionable (current study; Martin et al. 2014; Strausbaugh et al. 2011).

Above ground symptoms of RRCR include sudden, permanent collapse of the leaves with the petiole often becoming blackened where it attaches to the crown (Windels et al. 2009). Root rot symptoms begin as dark, circular to oval lesions that often develop in a ladder-like pattern.

Lesions coalesce as the disease progresses and may eventually envelop the entire root (Harveson 2008). Symptomatic tissue is often limited to external layers and does not generally spread into the internal tissues until the more advanced stages of the disease. It is not uncommon for the

entire surface of the beet to become covered with rot prior to the disease spreading into the interior of the root (Windels et al. 2009). In the most advanced stages of the disease, the entire root becomes rotten and unharvestable. Heavy presence of a brown or whitish mycelium can often be observed covering tissue exposed by cracking and cavity rot (Harveson 2008).

The sugar beet (*Beta vulgaris* L.) is an herbaceous dicotyledonous root crop, grown for its ability to accumulate sucrose in the root tissues (Cooke & Scott 1993). The mature root consists of three morphological regions, the crown, the neck, and the root (Artschwager 1926). The crown is the rounded upper section of the "root" body that bears leaves in a large tuft and is stem tissue. The neck develops from the hypocotyl and comprises the broadest portion of the beet. The bulk of the beet tissue is the true root, which tapers to a slender taproot. The root is more or less flattened on two sides with a prominent groove that forms a shallow spiral containing the lateral rootlets. Rather than an epidermis that covers many herbaceous roots, the sugar beet root is covered by a thin corky layer called the periderm (Artschwager 1926).

The anatomy of the sugar beet is rather unique among non-woody herbaceous plants (Artschwager 1926; Elliot & Weston 1993). A horizontal section through the mature root shows concentric growth rings that are comprised of bands of vascular tissue separated by storage parenchyma (Figure 4.1). These vascular rings are composed of bundles of vascular tissue that are widest at the area of the cambium and taper towards the phloem. Between the vascular bundles lies a narrow band of parenchyma that consists of elongated cells.

The annular rings develop from secondary cambium that initiates from the pericycle (Artschwager 1926). When the cambial initials divide, the inner daughter cells become secondary xylem and phloem while the outer cells become the initials of a new supernumerary cambium. Since these supernumerary cambia are initiated in rapid succession, practically all

rings are formed within 4 to 6 weeks after germination, when the root is just a couple millimeters in diameter (Artschwager 1926; Trebbi & McGrath 2009).

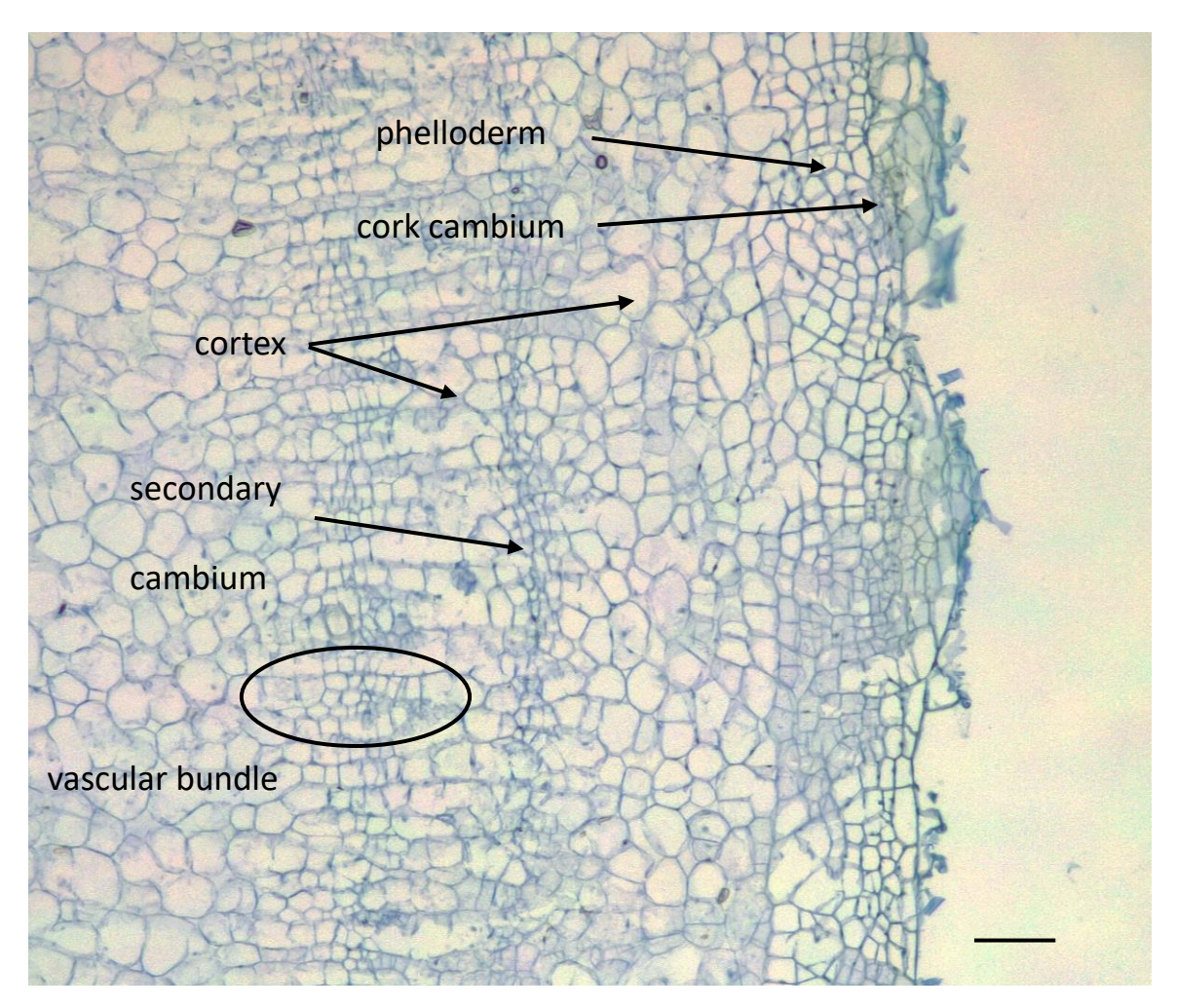


Figure 4.1 Partial cross section of 8-week-old sugar beet root showing outer vascular rings and periderm. Section was stained with toluidine blue O and imaged on an Olympus BX60 microscope. Scale bar = $100 \mu m$.

Expansion of the root proceeds by division of the parenchyma cells that separate the vascular rings. Since the pericycle originates inside of the endodermis (Beeckman & De Smet 2014), expansion of the secondary tissues forces the endodermis outward and, along with the primary cortex and the epidermis, is eventually sloughed off (Artschwager 1926). As the primary tissues are being sloughed off, the pericycle differentiates into a band of meristematic cells called the phellogen or cork cambium. The cells of the phellogen differentiate to form cork cells toward the outside and phelloderm toward the inside of the phellogen layer. The phellogen forms a thin layer five to eight cells wide that are somewhat flattened and suberized.

The presence of an endodermis in sugar beet seedlings has been implicated in resistance to Rhizoctonia damping-off (Nagendran 2006; Nagendran et al. 2009). However, in mature sugar beet roots, the endodermis has been sloughed off and is therefore unavailable to play a role in adult plant resistance. Liu et al. (2019) confirmed earlier reports (Gaskill 1968; Ruppel et al. 1979) that a good level of resistance to *Rhizoctonia* AG 2-2 was not expressed in most commercial varieties until the six- to eight-leaf stage (approx. 4 to 5 weeks after emergence) which is consistent with reports that younger plants are more susceptible than older plants (Engelkes & Windels 1994; Ruppel & Hecker 1988). There are a small number of exceptions which express seedling resistance (Nagendran et al. 2009, McGrath et al. 2015) but the mechanism is largely unknown (Galewski et al. 2022). This shift to higher levels of resistance corresponds to a developmental phase change from the seedling stage to the adult stage that occurs between 4 and 6 weeks after emergence (Trebbi & McGrath 2009). During this transition, gene expression changes drastically and is generally associated with increased sucrose accumulation and the completion of vascular ring formation (Artschwager 1926; Trebbi & McGrath 2009).

Ruppel (1973) compared the reactions of sugar beet varieties that were either susceptible or resistant to *Rhizoctonia solani* AG 2-2- and noted that *R. solani* hyphae did not penetrate beyond the periderm and outer secondary cortex in the resistant roots. These observations suggest a physiological barrier that developed in resistant roots, but Ruppel (1973) did not observe wound periderm or suberization related to fungal penetration. Hyphal spread proceeded tangentially more rapidly than radially, and necrosis proceeded the hyphae in all roots examined.

In a generalized model of the infection process for *R. solani*, the process begins when hyphae grow towards the plant and over the root surface (Keijer 1996). At this stage, hyphae are rounded and not attached to the surface. Prior to penetration into the plant tissue, the hyphae become flattened and adhere to the surface. The hyphae begin directed growth, following the anticlinal walls of the surface cells. Side branches form in a pattern that has been described as T-shaped branches (Keijer 1996) that aggregate and form infection cushions. Several studies have connected a reduction in the size and number of infection cushions to a reduction in disease severity (Kousik et al. 1994; Yang et al. 1992).

Fungal hyphae detect the plant surface and establish infection using various strategies that fall into two general categories, surface sensing and chemical exudates (Badri & Vivanco 2009; Kou & Naqvi 2016). Hyphae that orient along the anticlinal walls may exhibit characteristics of surface sensing, but surface characteristics alone may not be sufficient to initiate infection. For example, some rust fungi are unable to recognize stomata from non-host plants (Wynn & Staples 1981). Marshall and Rush (1980) noted that infection structures did not form on replicas of rice sheath surfaces and the hyphae did not follow the junctions of the anticlinal walls like occurred on rice sheaths themselves. Other physicochemical signals from the surface have been associated

with infection structure formation such as surface hardness, hydrophobicity, plant waxes, and cutin (Kou & Naqvi 2016).

The typical route of penetration of root tissue is by the formation of infection pegs (Keijer 1996). But on leaves or other above ground tissues, hyphae of *R. solani* have been reported as entering through stomata (Bashyal et al. 2018; Manian & Manibhushanrao 1982; Zheng & Wang 2011) and forming appressoria for direct penetration (Bashyal et al. 2018; Naito & Sugimoto 1978; Zheng & Wang 2011). Less is known regarding the infection process of roots or underground structures. Ruppel (1973) reported that penetration of sugar beet root by *R. solani* AG 2-2 occurred by infection cushions or directly by individual hyphae on sugar beet roots. In potato, *R. solani* AG 3 formed infection cushions, appressoria, and penetrated directly through lenticels and epidermal cracks on tubers (Zhang et al. 2016). While sugar beets roots do not have lenticles, the root surface is similar to potato tuber skin in that it consists of a periderm and an outer corky layer. Potato skin has been demonstrated to respond to infection by wound healing suberization (Lulai 2007). Thus, there is the potential that sugar beet periderm also responds to wounding or fungal invasion by suberization and that this could serve as a defense response, but this needs further study.

Penetration of sugar beet tissue has been reported to occur inter- and intracellularly with hyphae closer to the site of penetration proceeding intracellularly and in the advanced portion of the lesions proceeding intercellularly (Ruppel 1973). Necrosis consistently precedes the hyphae but reports of necrosis occurring under *R. solani* infection cushions are inconsistent. In cotton, Weinhold and Motta (1973) reported the removal of pectic substances beneath infection cushions prior to hyphal penetration. However, it is more commonly reported that infection pegs form beneath the cushion and mechanical force is used to penetrate epidermal cells (Armentrout &

Downer 1987; Hofman & Jongebloed 1988; Yang et al. 1992). Appressoria also have been identified in *R. solani* on potato (Zhang et al. 2016), rice (Marshall & Rush 1980), soybean (Zheng & Wang 2011), and sugar beet leaves (Naito & Sugimoto 1978). Of these reports of appressoria formation in *R. solani*, only the sugar beet leaves were infected with AG 2-2 while the other crops were infected with other AG. Reports of infection structures on sugar beet root, or any roots for that matter, are limited.

The infection process for necrotrophic pathogens often involves the utilization of cell wall degrading enzymes (Bellincampi et al. 2014; King et al. 2011; Kubicek et al. 2014). Several enzymes have been implicated in cell well degradation including cellulases, polygalacturonases, pectin and pectate lyases, and pectin methylesterases (Bellincampi et al. 2014; Kubicek et al. 2014). Necrotrophic pathogens utilize a number of cell wall degrading enzymes (CWDE) to depolymerize the cell wall (Bellincampi et al. 2014; D'Ovidio et al. 2004; Kubieck et al. 2014). The diversity of cell wall degrading enzymes present in a pathogen has been associated with host range and virulence (Alghisi & Favaron 1995; Cook et al. 1999; King et al. 2011). *Rhizoctonia solani* isolates appear to have a diverse array of cell wall degrading enzymes (Anderson et al. 2016; Rafiei et al. 2023; Scala et al. 1980; Wibberg et al. 2016) and several CWDEs have been characterized from *R. solani* isolates including pectic lyase (Bugbee 1990), polygalacturonase (Scala et al. 1980; Xue et al. 2018) and laccase (Wahleithner et al. 1996).

There is considerable variability in the infection process among *R. solani* AG, crop types, and plant tissue. It is important to keep in mind that *R. solani* cannot be thought of as a homogenous group and behavior that is true in one system may not be true in a different system. Anastomosis groups can be thought of as independent species and this concept was just gaining traction when much of the work regarding the infection process was being done. In addition, a

comprehensive histopathological study of RRCR has not been done since Ruppel (1973). Since that time, many advances have been made in microscopy methodology and staining techniques. In addition, new RRCR resistant sugar beet varieties have been released since then, including SR98/2 examined in the current study (McGrath et al. 2015). SR98/2 is a smooth-rooted sugar beet germplasm derived from the EL51 breeding line (PI 598074) with good resistance to Rhizoctonia damping-off and RRCR (Nagendran et al. 2009). The SR98/2 germplasm is one of the few releases with good resistance to damping-off and adult plant RRCR, while retaining acceptable agronomic properties (Nagendran et al. 2009, McGrath et al. 2015). These characteristics make it an excellent choice for examination of physiological characteristics associated with RRCR resistance.

Materials and Methods

Sample preparation

Seed for sugar beet varieties 'C869' (RRCR susceptible; Lewellen 2004) and 'SR98/2' (RRCR resistant; McGrath et al. 2015) were surface sanitized in 0.6% sodium hypochlorite plus 0.1% tween 20 for 15 minutes, rinsed twice in sterile water and soaked overnight in 0.3% hydrogen peroxide to reduce germination variability (McGrath et al. 2000). Sanitized seed was treated with a 2% solution of metalaxyl (Allegiance-FL; Bayer Crop Science, Research Triangle Park, NC) to manage Pythium damping-off and planted in soilless potting mix (Suremix Pearlite; Michigan Grower Products, Galesburg, MI). Plants were cultivated in a growth chamber (Conviron PGW 36, Controlled Environments Inc., Pembina, ND) set to 23°C and a 14-hr photoperiod.

Plants were grown to the 8 to 10 leaf growth stage, after the seedling to adult transition, and inoculated with a single grain of barley infested with isolate 'R1', an AG 2-2BRa isolate (type 'IIIB') known to be highly aggressive (Nagendran et al. 2009). Two roots of each variety were harvested at 3, 4, 5, 7, 9 and 12 days after inoculation and gently washed with tap water. Root tissue with visible symptoms was sampled by cutting into 3 to 5 mm cuboid shaped pieces and fixed in 10% neutral buffered formalin solution (Sigma Aldrich, St. Louis, MO) with shaking for 4 days. Tissue samples were rinsed with 70% ethanol and stored in 70% ethanol until embedding. Fixed samples were embedded in paraffin wax at the Investigative HistoPathology Laboratory (Michigan State University, East Lansing, MI). Sections were cut 12 to 15 μm thick on a Reichert-Jung 820 Histocut microtome (Reichert Technologies, Buffalo, NY). transferred to glass slides, and dried at 57°C overnight.

Prepared sections were dewaxed through a xylene/ethanol rehydration series (Nagy et al. 2007) with two changes of Neo-Clear (Sigma Aldridge), one change of histological grade xylenes (Sigma Aldridge), two changes each of 100% and 95% ethanol, and one change each of 70% and 50% ethanol and finally, distilled water. Each step was conducted for 8 minutes with samples being air dried after washing with xylenes to minimize contamination of subsequent ethanol washes. Dewaxed slides were dried at 35°C overnight.

Brightfield microscopy

General tissue staining was performed by covering sample with 0.05% (w/v) toluidine blue O (Sigma Aldrich) in phosphate buffered saline (PBS, pH 7.6; Cold Spring Harbor Protocols; 2007) for 1 to 2 minutes and rinsing twice with distilled water (O'Brien et al. 1964). Samples were dried at 35°C for 1 to 2 hours and mounted using Eukitt quick-hardening mounting medium

(Sigma Aldrich). Images were collected on an Olympus BX60 microscope (Evident Corporation, Tokyo, Japan) fitted with a Spot Insight 12MP CMOS camera (SPOT Imaging, Sterling Heights, MI).

Epi-illumination microscopy

Epi-illumination was conducted using a Keyence VHX-6000 digital microscope (Keyence Corporation of America, Itasca, IL). To improve visualization of the tissues within the root groove, cross sections of fresh root tissue were cut free hand, stained with 0.05% w/v Ruthenium red (Sigma Aldrich) for 2 minutes, rinsed three times in distilled water and imaged with the Keyence VHX-6000 digital microscope.

To visualize surface hyphae and the formation of infection cushions, fresh, non-inoculated root sections were harvested, washed under running tap water and surface disinfested with a 0.6% sodium hypochlorite plus 0.1% tween 20 solution for 2 minutes and then rinsed in sterile distilled water. Sections were cut freehand with a razor blade into pieces that were about 1 cm square and 5 mm thick. Four of these pieces were placed on a 2% (w/v) water agar plate so the periderm surface was facing up. A 4 mm plug from an actively growing culture of isolate 'R1' was placed approximately 1 cm from the sections and the hyphae were allowed to grow onto the root pieces. Infested pieces were removed from the agar plate 2 days after hyphae contacted the root surface and stained with lactophenol cotton blue solution (Sigma Aldrich). Sections were visualized on a Keyence VHX-6000 digital microscope on the same day as collection and staining. A total of 12 sections were observed for each sugar beet variety.

Confocal and epifluorescence microscopy

Staining with berberine hemisulfate (Sigma-Aldrich) was performed according to Brundrett et al. (1988) to visualize suberin and lignin deposits. Thin sections, 12 to 15 μm thick, on glass slides were covered with 0.1% (w/v) berberine hemisulfate in distilled water for 30 min and then rinsed twice in distilled water. Samples were counter stained with 0.5% (w/v) aniline blue WS (Sigma-Aldrich), rinsed twice in distilled water and mounted in a drop of 0.1% FeCl₃ (Sigma Aldrich) in 50% glycerin. A cover slip was applied and immediately sealed with clear nail polish. Images were collected with an Olympus BX60 fluorescent microscope (Evident Corporation) fitted with a SPOT Insight 12MP CMOS camera (SPOT Imaging) using a DAPI excitation filter (band pass 352-402 nm). At least six sections at five and seven days after inoculation were observed for each sugar beet variety.

Autofluorescence was examined by imaging at least six unstained sections 12 to 15 µm thick using epifluorescence with a double (FITC/TxRed) excitation filter (band pass 460-490, 532-554 nm). These unstained sections were also examined with a Nikon A1Rsi LSCM using 408 nm, 489 nm and 561 nm diode lasers with 430-480 nm, 500-550 nm, and 570-620 nm band pass filters respectively.

For the safranin O/calcofluor white staining, six samples of each sugar beet variety were stained with a 0.1% aqueous solution of safranin O (Sigma Aldrich) for 3-5 minutes and then destained by rinsing in an ethanol series of 25, 50, 70, and 95% ethanol for 10 minutes each until dye no longer leached from samples. The samples were returned to distilled water by passing them back through the ethanol series of 70, 50, and 25% ethanol for 10 minutes each and then into distilled water (Kitin et al. 2020). One drop of 10% potassium hydroxide was placed on each sample and two drops of Calcofluor white stain (0.1% calcofluor white M2R plus 0.05% Evans

blue; Sigma Aldrich) were added. After incubating for 5 minutes at room temperature, samples were rinsed twice in distilled water, dried at 35°C for 1 to 2 hours, and a cover slip mounted using Eukitt quick-hardening mounting medium (Sigma Aldrich). Stained samples were imaged using epifluorescence on the Olympus BX60 fluorescence microscope with a SPOT Insight 12MP CMOS camera using a triple (DAPI/FITC/TxRed) excitation filter (band pass 352-402, 460-490, 532-554 nm).

Fungal hyphae within the root tissues were visualized using the fluorescence techniques described by Carotenuto and Genre (2020). First, root sections were treated with 10% bleach for 5 minutes to remove cellular and nuclear membranes. The treated samples were flooded with a 10 mg/ml solution of wheat germ agglutinin conjugated to Alexa Fluor 488 (WGA) and incubated for 1 hour at room temperature. After washing three times in PBS, two drops of propidium iodide (100 ng/ml; Sigma-Aldrich) were added to the slide to cover the sample for 1-2 minutes. Samples were rinsed three times with PBS and mounted with Fluoro-Gel mounting medium (Electron Microscopy Sciences, Hatfield, PA). Stained samples were imaged on a Nikon A1Rsi laser scanning confocal microscope (LSCM; Nikon Instruments Inc., Melville, NY) with either a PlanApo 20x VC (NA 0.75) or a PlanApo λ 10x (NA 0.45) objective. Alexa Fluor 488 fluorophore was imaged using a 489 nm diode laser with a 500-550 nm band pass emission filter. Propidium iodide was imaged using a 561 nm diode laser and a 570-620 nm band pass emission filter. Images were z-stacked using 5 slices with a 1 µm step size, and an area scan was conducted with a 10% overlap. At least six sections of each sugar beet variety at each of the six time points that tissue was harvested was observed using this technique and representative samples were selected for imaging on the confocal microscope.

Sections displaying changes in autofluorescence were examined for alterations in pectin esterification using the rat monoclonal antibodies LM19 and LM20 (Verhertbruggen et al. 2008). Sequential sections were hydrated in PBS (pH 7.6) for 15 minutes and then treated with a 10% bleach solution for 5 minutes to remove cellular and nuclear membranes. Samples were rinsed twice in PBS and treated with 5% bovine serum albumin (Sigma Aldrich) to reduce non-specific binding of primary antibodies (Miller & Shakes 1995). Samples were rinsed twice in PBS and incubated with a 1:10 dilution of either LM19 or LM20 antibodies for 30 minutes. Samples were washed in PBS three times and incubated with a 1:100 dilution of anti-rat IgG linked to Alexa Fluor 488 (Thermo Fisher) for 20 minutes. Samples were rinsed three times in PBS and mounted with Fluoro-Gel mounting medium (Electron Microscopy Sciences). Imaging was performed on a Nikon A1Rsi LSCM (Nikon Instruments Inc.) using a 489 nm diode laser with a 500-550 nm band pass emission filter and an Apo 60x Oil λS (NA=1.40) objective. At least 10 sections for each treatment were observed using the Olympus BX60 fluorescent microscope and three representative samples were selected for imaging on the confocal microscope.

A complete list of stains and physiological targets that were used in the current study are shown in Table 1.

Table 4.1 Reagents used in the current study to label cell wall components of sugar beet and *Rhizoctonia solani* AG 2-2.

Reagent	Target	Excitation laser	Emission filter	Notes
Safranin O	lignin	488	570-560	
Toluidine blue O	general cell walls stain	-	-	polychromatic stain - normal tissue stains blue/purple; lignified tissue stains green/blue
Lactophenol cotton blue	chitin	-	-	general stain for fungi
Wheat-germ agglutinin – Alexa fluor 488	chitin	488	500	binds to N-acetyl-D-glucosamine
Calcofluor white	cellulose, chitin	380	475	binds to 1-3,β- and 1-4,β- polysaccharides in cellulose and chitin
Propidium Iodide	cell wall pectin	535	615	preference for unesterified pectin
Berberine hemisulfate	lignin, suberin	430	580	
Aniline blue WS	callose	405	500	binds to 1-3,β-glucans
LM19 rat IgM monoclonal antibody	unesterified pectin	-	-	binds to α-1,4 galacturonic acid residues of unesterified pectin
LM20 rat IgM monoclonal antibody	methyl esterified pectin	-	-	binds to α-1,4 galacturonic acid residues of esterified pectin
Alexa Fluor 488 goat anti- rat IgG (H+L)	LM19, LM20 primary antibody	488	500	secondary antibody binds to rat IgM primary antibody

Results

Infection cushion formation

The external cork cells of the root tissue were irregularly shaped and roughly arranged in rows (Figure 4.2). However, the hyphae on the root surface generally did not follow the anticlinal walls (Figure 4.2) as has been reported for other systems with a true epidermis (Armentrout & Downer 1987; Pannecoucque & Höfte 2009; Yang et al. 1992). Instead, runner hyphae crossed the tissue at oblique angles, branching at regular intervals. The frequency of branching increased in the side branches, creating shorter and shorter spurs developing into dense aggregates of hyphae. Some of these branch spurs did orient with the anti-clinal walls, but that behavior was inconsistent, and most did not. T-shaped branching was not observed, only increasingly shorter branch spurs (Figure 4.2). Three days after inoculation, hyphae were denser on the surface of the susceptible variety (Figure 4.2A) than on the resistant variety (Figure 4.2B).

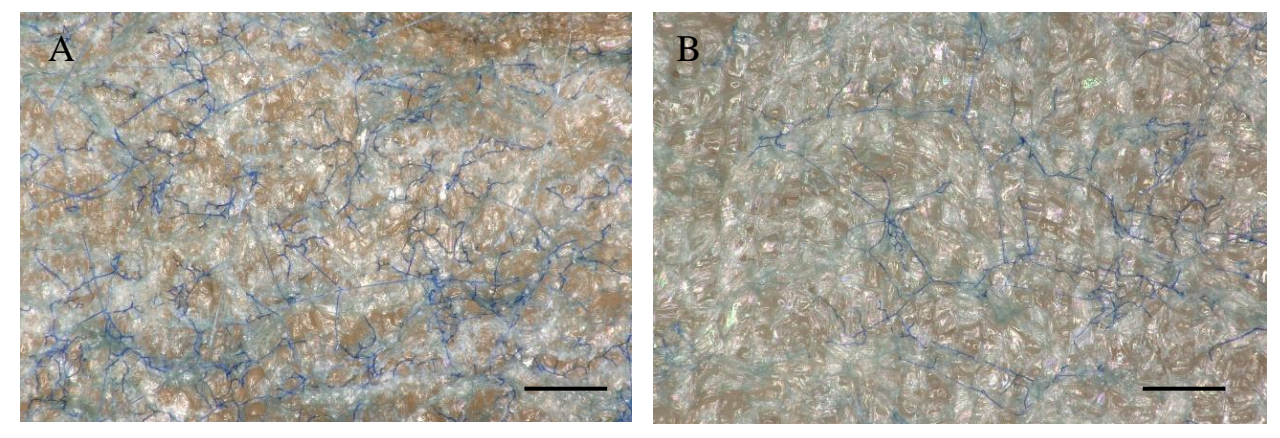


Figure 4.2 Hyphae of *Rhizoctonia solani* AG 2-2 on the surface of an 8-week-old sugar beet root two days after inoculation. A) susceptible variety C869. B) resistant variety SR98/2. Hyphae were stained using lactophenol blue and imaged with a Keyence VHX-6000 digital microscope (200x). Scale bar = $250 \mu m$.

The aggregates of hyphae, formed from branch spurs, developed into small infection cushions within 3 days after inoculation (Figure 4.3). Cells that made up the infection cushions were thick walled, had a high affinity for trypan blue and were extensively interconnected. There were no obvious surface features associated with infection cushion development except that occasionally hyphae were observed accumulating around wounds and natural cracks in the cork layer (Figure 4.4). Infection cushions appeared to form where two or more hyphae overlapped, but this attribute was difficult to qualify. But, since the hyphae originated from the same source, it is unclear why this interaction would be necessary for infection cushion formation.

Regardless, the formation of infection cushions was apparently not needed for penetration of the outer cork cells. Hyphae was observed penetrating the outer cell wall three days after inoculation, without forming an infection cushion (Figure 4.5). The outer layer of the periderm was penetrated directly in several cases and hyphae could be observed growing within and among the cork cells. It was unclear how hyphae penetrated into the outer cortex, whether intraor intercellularly, but the outer cortex was colonized rapidly once hyphae entered the tissue.

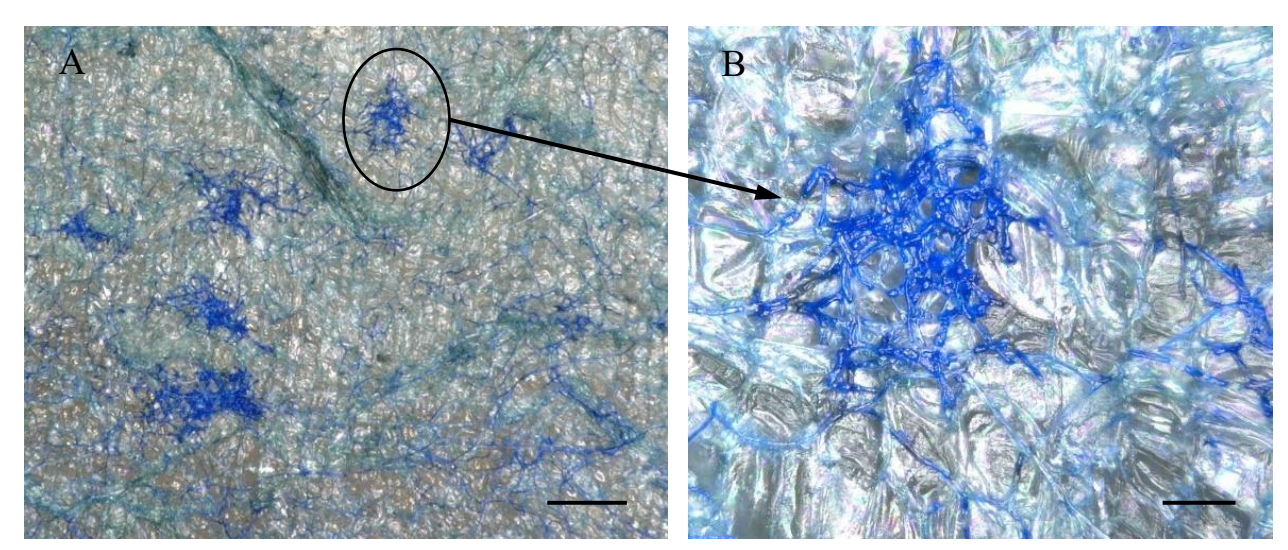


Figure 4.3 Infection cushions of *Rhizoctonia solani* AG 2-2 forming on the surface of susceptible sugar beet variety C869 two days after inoculation. A) Hyphae were stained with lactophenol blue and imaged with a Keyence VHX-6000 digital microscope at 100x (scale bar = $250 \mu m$). B) Infection cushion circled in image A is shown at 500x (scale bar = $50 \mu m$).

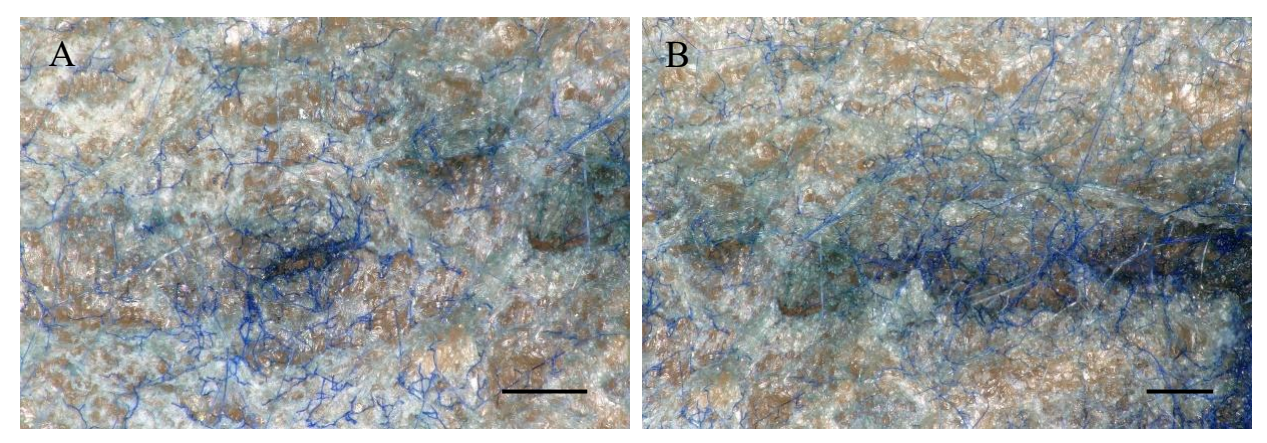


Figure 4.4 Hyphae of *Rhizoctonia solani* AG 2-2 aggregating around natural openings in the cork layer of sugar beet variety C869 two days after inoculation. A) Hyphae were stained using lactophenol blue and imaged with a Keyence VHX-6000 digital microscope at 150x and B) at 200x. Scale bars = $250 \mu m$.

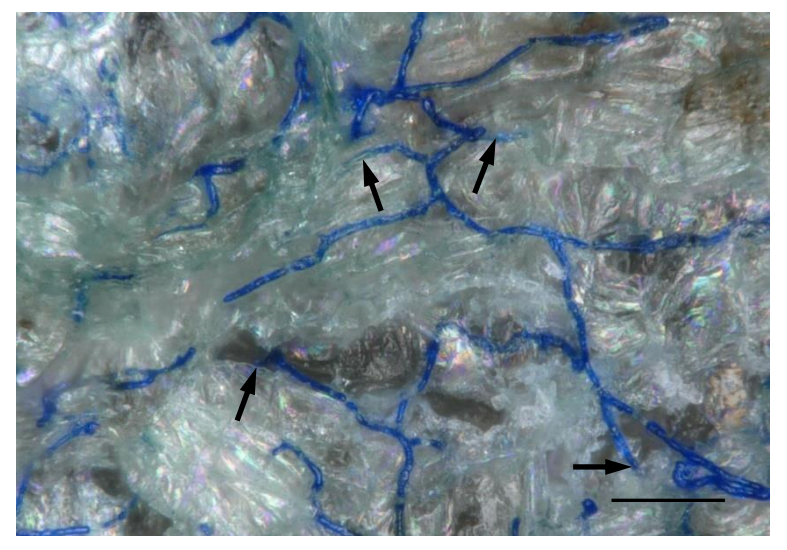


Figure 4.5 Hyphae of *Rhizoctonia solani* AG 2-2 on the surface of root tissue sugar beet variety C869 two days after inoculation. Arrows indicate hyphae that are directly penetrating the outer cork layer. Hyphae were stained with lactophenol blue and imaged with a Keyence VHX-6000 digital microscope at 1000x. Scale bar = $50 \mu m$.

Hyphae that entered through the smooth root surface were observed within the outer layers of cork cells by three days after inoculation (Figure 4.6). Colonization occurred rapidly within the outermost cortex, proceeding inter- and intracellularly between the periderm and the outer cambium. Hyphae breached the outermost cambium by invading the parenchyma cells between vascular bundles or in other areas where breaks occur in the outer cambium. The regions of interfascicular parenchyma increased in size in the vascular rings closer to the center of the root and there was evidently less restriction to fungal invasion.

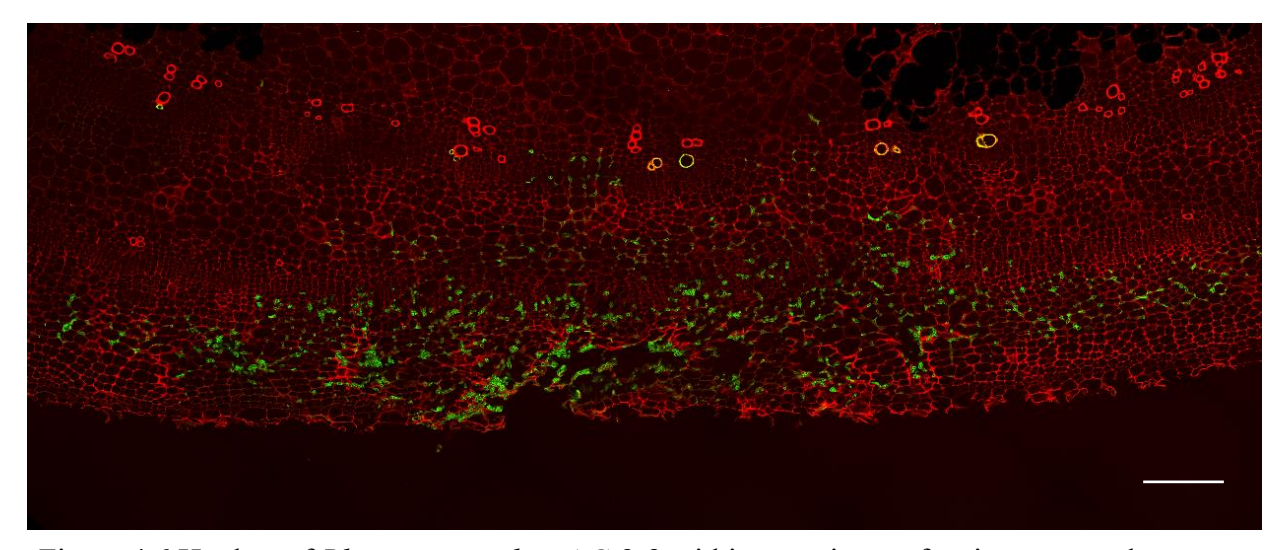


Figure 4.6 Hyphae of *Rhizoctonia solani* AG 2-2 within root tissue of resistant sugar beet variety SR98/2 three days after inoculation. Fungal hyphae were labeled using wheat germ agglutin conjugated with Alexa Fluor 488 and are colored green. Plant tissue was stained with propidium iodide and is colored red. Image was collected on a Nikon A1Rsi laser scanning microscope. Scale bar = $250 \mu m$.

Invasion through tissue associated with lateral roots

The tissues associated with the root groove and lateral roots form complicated folds and grooves that appear to provide access to fungal hyphae (Figure 4.7). Fungal hyphae were observed growing within these folds and penetrating tissue directly without forming an infection cushion. Cork cells were present on the outer surfaces of the root groove tissues, but tissue connections between lateral roots and the main root tissue were irregular and provided multiple routes for fungal hyphae to invade. Hyphae were observed in and around lateral roots and appeared to follow lateral root tissue into the main root and from there, spread rapidly (Figure 4.8).



Figure 4.7 Longitudinal section through the root groove region of a sugar beet root (variety C869) stained with ruthenium red. Arrow indicates a gap between folds of tissue. Scale bar = $500 \mu m$.

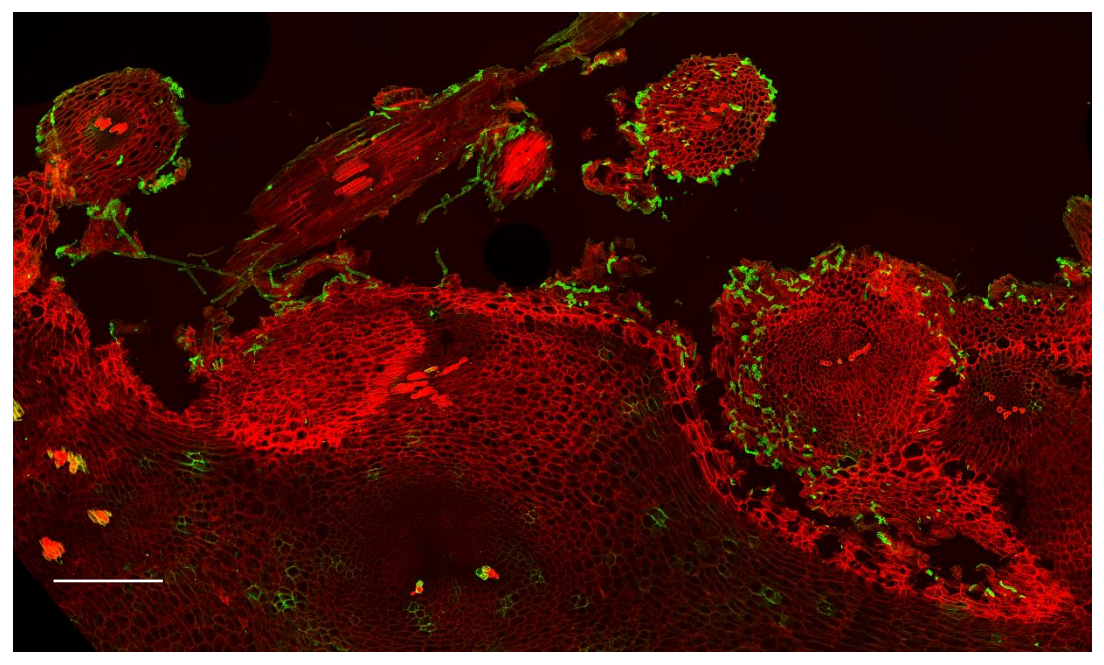


Figure 4.8 Hyphae of *Rhizoctonia solani* AG 2-2 within the root groove of a sugar beet root (variety C869) growing among lateral roots three days after inoculation. Fungal hyphae were labeled using wheat germ agglutin conjugated with Alexa Fluor 488 and are colored green. Plant tissue was stained with propidium iodide and is colored red. Image was collected on a Nikon A1Rsi laser scanning microscope. Scale bar = $250 \mu m$.

Alteration of cell wall components

Substantial maceration was observed in the cortex tissues shortly after colonization by fungal hyphae (Figure 4.6 & 4.9A). Prior to maceration, the tissue underwent several changes. Within three days after inoculation, a zone of discoloration developed in the area surrounding the invading hyphae that extended up to 500 µm beyond any visible hyphae. Under visible light, these regions were darkened and appeared brown to black and were comparable to the dark lesions that are characteristic of RRCR. This discolored region exhibited strong fluorescence when excited using the FITC/TxRed excitation filter (460-490, 532-554 nm), which occurred with (Figure 4.10) or without propidium iodide staining (Figure 4.11 & 4.12). When unstained sections were stimulated with the 561 nm (red) laser or 489 nm (green), fluorescence was

increased in the lesion compared to healthy tissue (Figure 4.12A & 4.12B). However, there was a reduction or lack of fluorescence in the lesion when stimulated with the 408 nm (blue) laser (Figure 4.12C). A composite RBG image clearly shows the area of cell wall changes associated with a lesion (Figure 4.12D). Both resistant and susceptible varieties exhibited similar levels and patterns of fluorescence, although lesions were generally larger in the susceptible variety. These fluorescent zones were so conspicuous they served as excellent predictors for the presence of fungal hyphae and in no case was fungal hyphae observed within the root tissue without an area of fluorescence enclosing it.

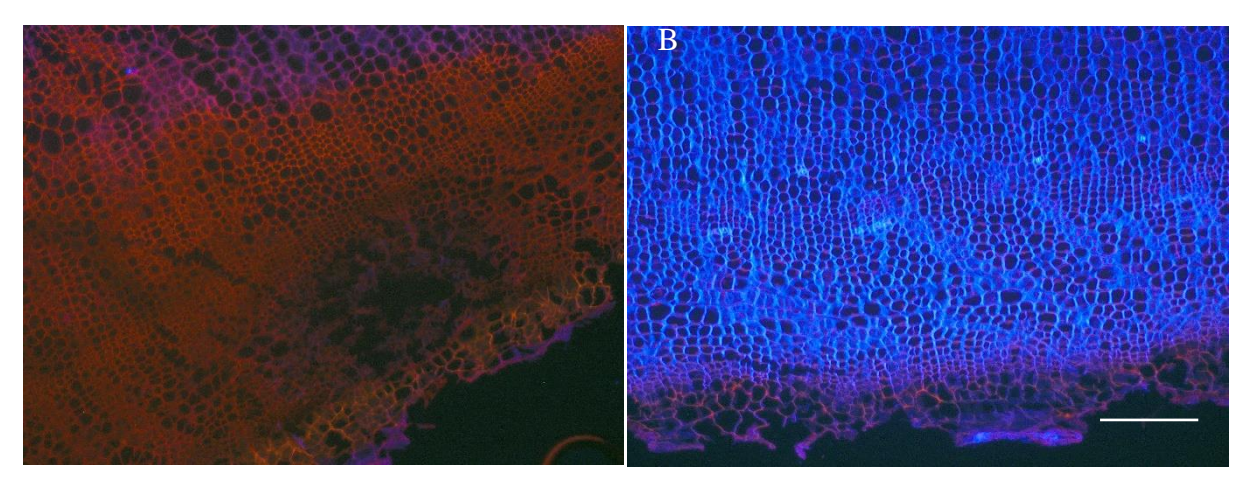


Figure 4.9 Sugar beet tissue stained with calcofluor white and safranin O seven days after inoculation. A) tissue infected with *Rhizoctonia solani* AG 2-2. B) uninfected tissue. Images were taken on an Olympus BX60 fluorescence microscope using a DAPI/FITC/TxRed excitation filter (band pass 352-402, 460-490, 532-554 nm). Scale bar = 250 μ m.

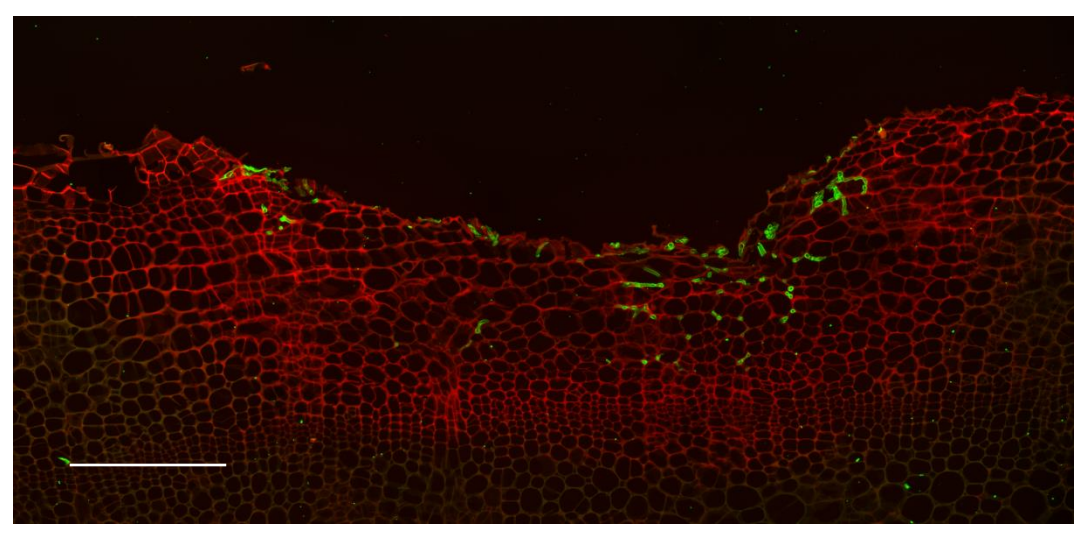


Figure 4.10 Fluorescence associated with lesion caused by *Rhizoctonia solani* AG 2-2 in sugar beet root (variety C869) three days after inoculation. Fungal hyphae were labeled using wheat germ agglutin conjugated with Alexa Fluor 488 and are colored green. Plant tissue was stained with propidium iodide and is colored red. Image was collected on a Nikon A1Rsi laser scanning microscope. Scale bar = 250 μ m.

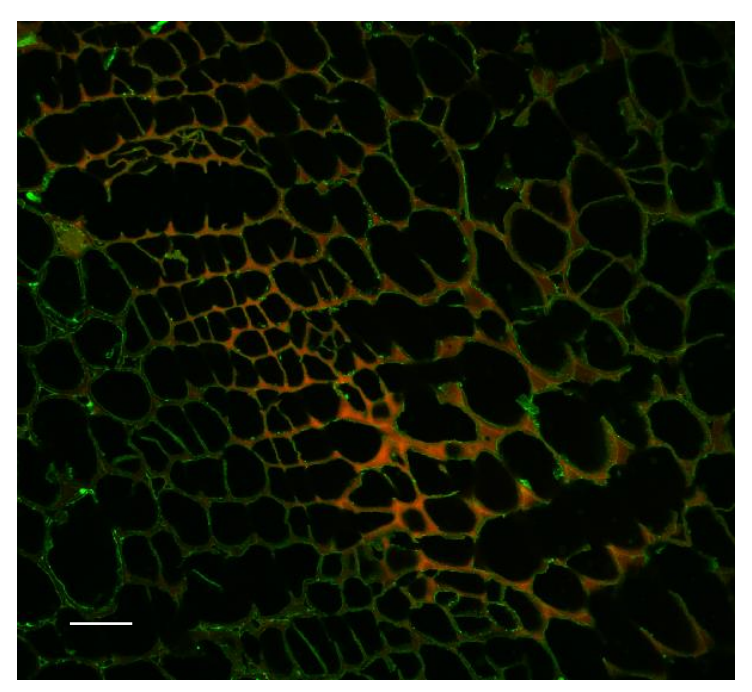


Figure 4.11 Sugar beet root tissue infected with *Rhizoctonia solani* AG 2-2 showing thickened cell walls. Tissue was immunolabeled with the monoclonal antibody LM19. Goat anti-rat IgG secondary antibody conjugated with Alexa Fluor 488 dye was used as a fluorescent label. Image was collected on a Nikon A1Rsi laser scanning microscope. Scale bar = $25 \mu m$.

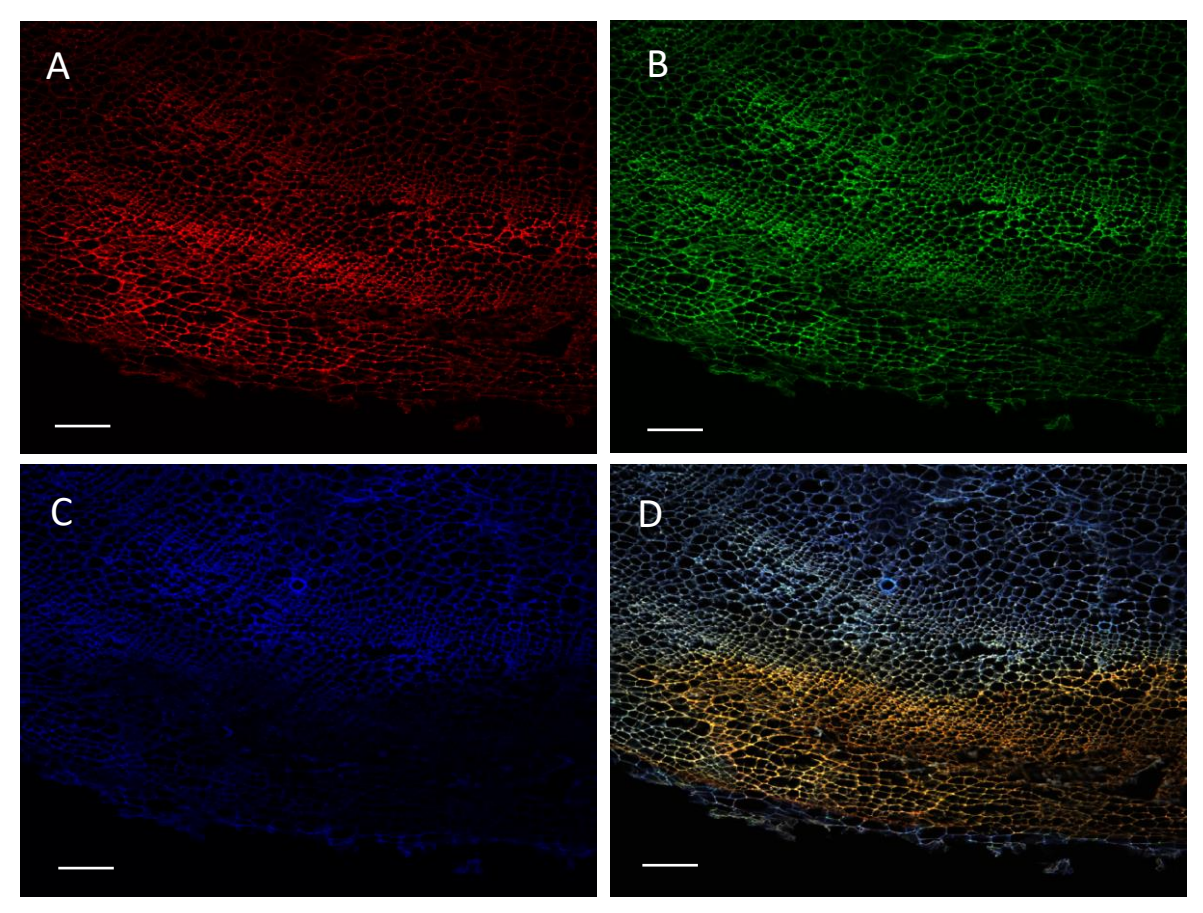


Figure 4.12 Fluorescence associated with lesion caused by *Rhizoctonia solani* AG 2-2 in sugar beet root (variety C869) three days after inoculation. Tissue was unstained and the same sample was examined using A) 561 nm (red) laser, B) 488 nm (green) laser, C) 408 nm (blue) laser and D) a RBG composite. Image was collected on a Nikon A1Rsi laser scanning microscope. Scale bar = $100 \mu m$.

Cellulose was plentiful in healthy tissue as indicated by a strong fluorescent signal from calcofluor white staining (Figure 4.9B). As the tissue became colonized, the fluorescent signal from calcofluor white was obscured by red/orange fluorescence of the safranin O stain (Figure 4.9A). The region of increased fluorescence associated with safranin O corresponded with alterations in fluorescence associated with the development of lesions (Figure 4.10). In addition, the cell walls in the area of the lesion became thickened and exhibited conspicuous autofluorescence as previously described (Figure 4.11 & 4.12).

Samples that had been stained with berberine hemisulfate showed increased fluorescence at the margins of the lesions (Figure 4.13). Increased fluorescence associated with berberine hemisulfate coincided with the region of increased fluorescence associated with lesion development. Fluorescence associated with berberine hemisulfate was strongest at the margin of the lesion, but not as intense as the highly suberized cork cells or xylem. It is notable that increased fluorescence related to berberine hemisulfate staining was more apparent in the resistant variety than in the susceptible variety.

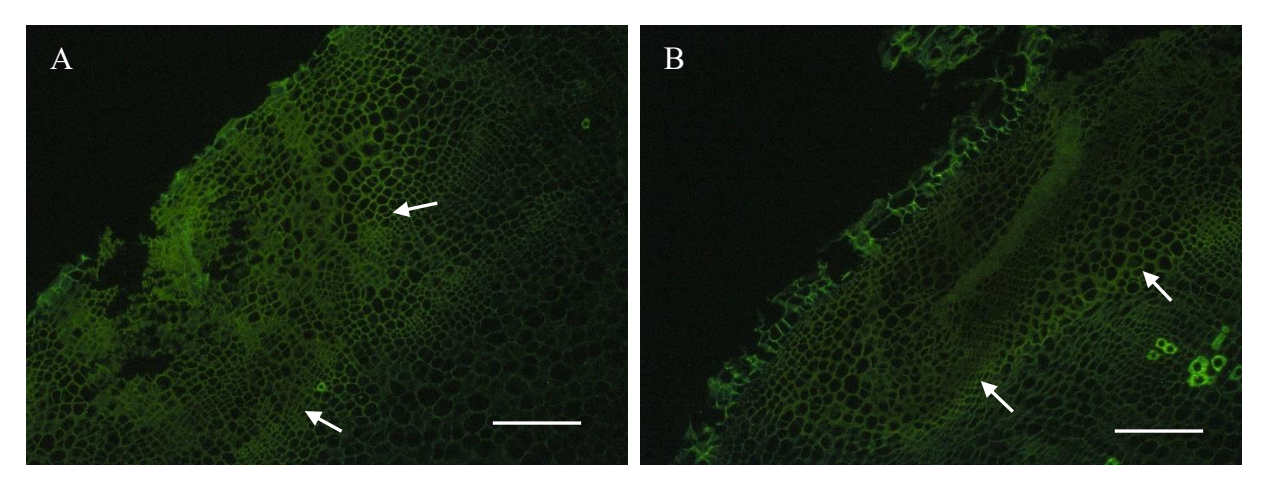


Figure 4.13 Sugar beet tissue infected with *Rhizoctonia solani* AG 2-2 and stained with berberine hemisulfate. Image was collected on an Olympus BX60 microscope using a DAPI excitation filter (band pass 352-402 nm). Arrows indicate regions of increased fluorescence that correspond to the margin of a distinct lesion. Scale bar = $200 \mu m$.

There were minimal differences in distribution of pectic epitopes stained by immunolabeling by antibodies LM19 and LM20 (Figures 4.14 & 4.15). Both pectic epitopes were present in similar quantities in healthy tissues, although the LM20 labeled epitope may have been present in slightly greater quantities than the LM19 labeled epitope. In infected tissue, the LM19 labeled epitope was eliminated more rapidly in the susceptible variety 'C869' than was the LM20 labeled epitope, which remained present in the intracellular spaces (Figure 4.14). In the resistant variety SR98/2, the LM19 labeled epitope was clumped into aggregates around the inside of the cell walls (Figure 4.15B). The LM20 labeled epitope exhibited clumping as well, but to a lesser extent than the LM19 labeled epitope. Overall, the prevalence of both epitopes was reduced in the cell walls of infected tissue compared to healthy tissue. The resistant variety retained more labeled material than did the susceptible variety especially for the epitope bound by LM19 (Figure 4.15), although it appeared to have been extricated from the cell wall.

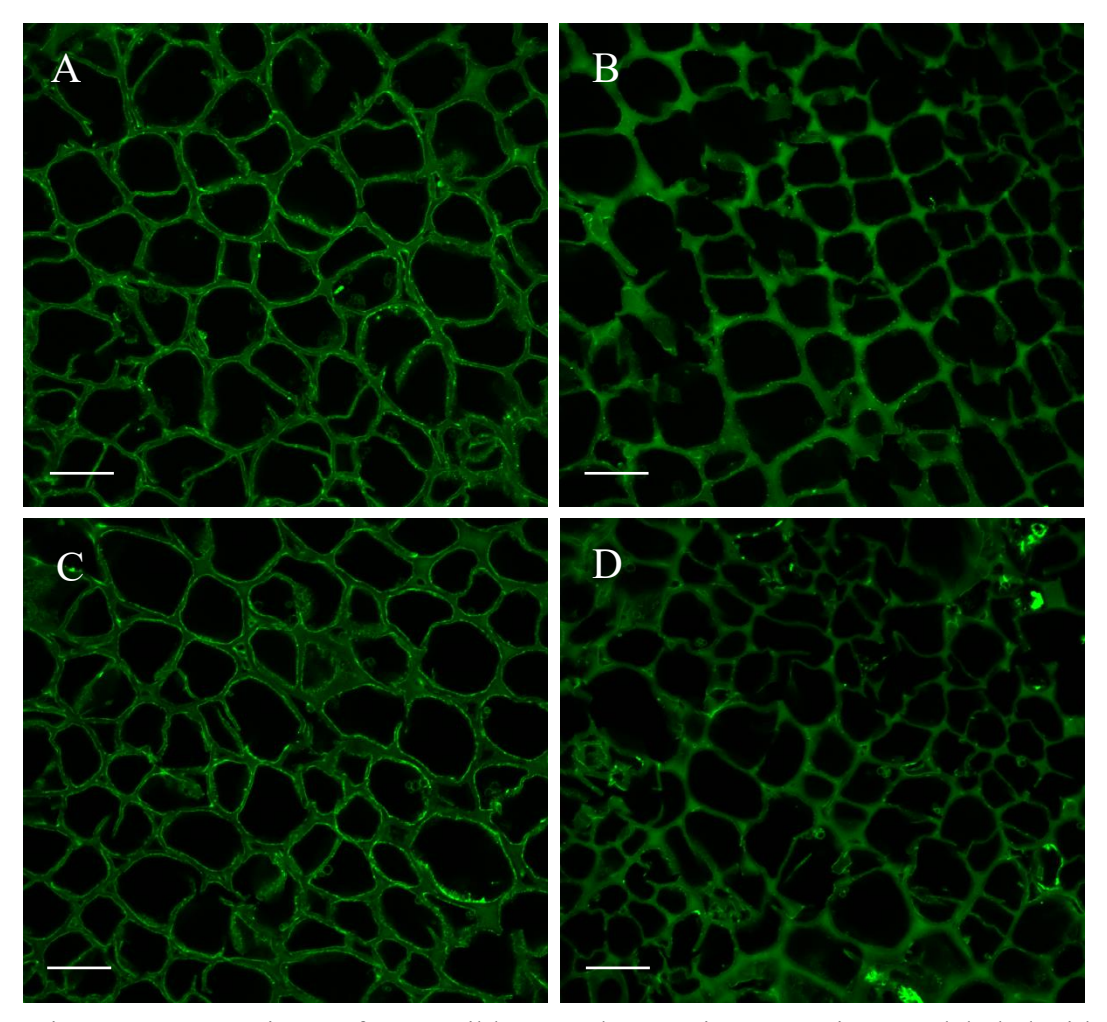


Figure 4.14 Root tissue of susceptible sugar beet variety C869 immunolabeled with the rat IgM monoclonal antibodies LM19 and LM20 four days after inoculation. Goat anti-rat IgG secondary antibody conjugated with Alexa Fluor 488 dye was used as a fluorescent label. A) LM19 healthy B) LM19 infected C) LM20 healthy D) LM20 infected. Images were collected on a Nikon A1Rsi laser scanning microscope. Scale bar = 25 μm .

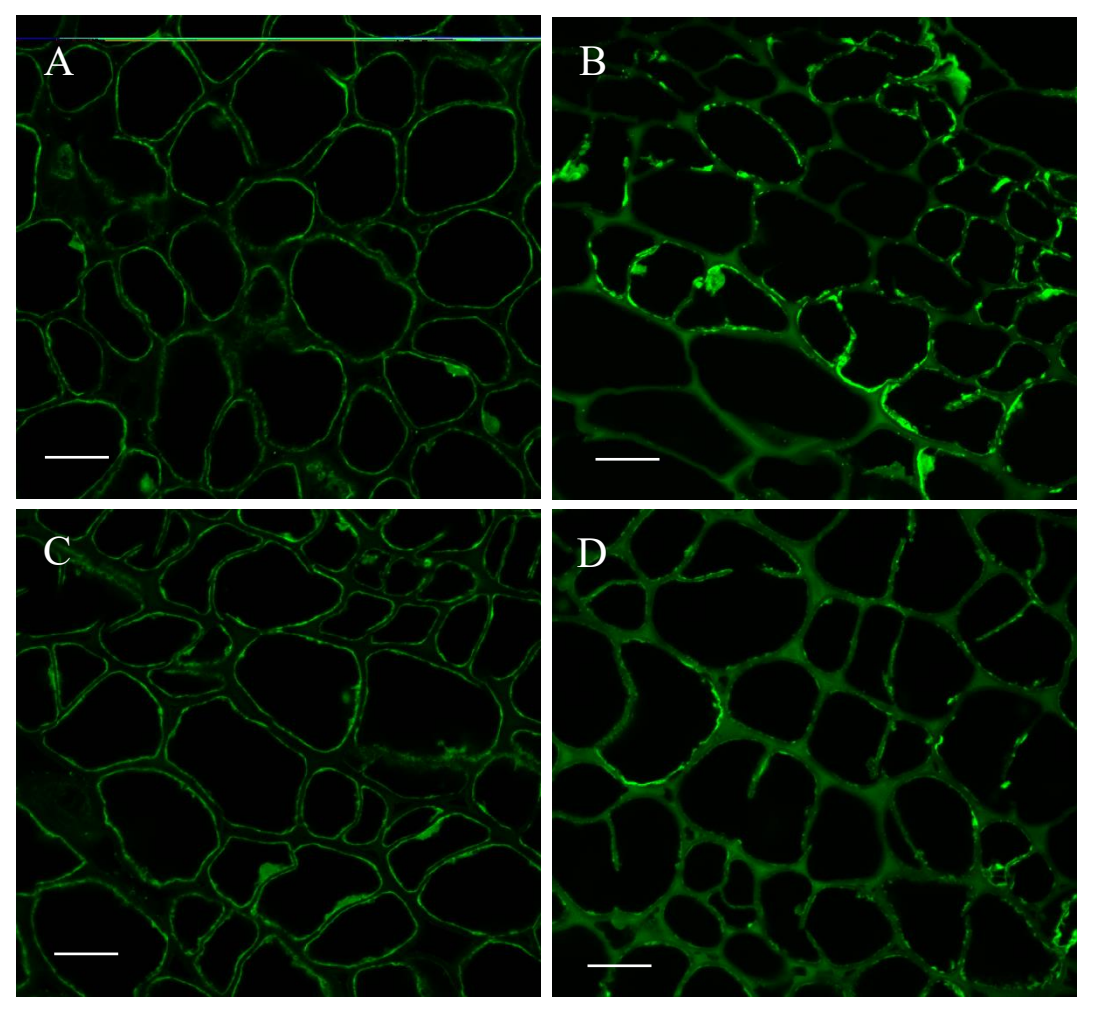


Figure 4.15 Root tissue of resistant sugar beet variety SR98/2 immunolabeled with the rat IgM monoclonal antibodies LM19 and LM20 three days after inoculation. Goat anti-rat IgG secondary antibody conjugated with Alexa Fluor 488 dye was used as a fluorescent label. A) LM19 healthy B) LM19 infected C) LM20 healthy D) LM20 infected. Images were collected on a Nikon A1Rsi laser scanning microscope. Scale bar = 25 μm .

Discussion

Colonization and infection cushion formation

Hyphae were denser on the susceptible sugar beet variety than on the resistant variety which has been hypothesized to result in a higher number of infection sites and more severe disease symptoms (Bassi et al. 1979; Pannecoucque & Höfte 2009; Zhang et al. 2016) and something similar may occur on sugar beet. Much of the increase in the density of the surface hyphae was due to an apparent increase in branching proliferation. Denser hyphae have been associated with increased lesion size in tomato where lesion size was proportional to the size of the infection cushion (Hofman & Jongebloed 1988).

The observation of hyphae spreading over the root surface without following the anticlinal walls, which is in contrast to many reports of the infection process for *R. solani* (Armentrout & Downer 1987; Yang et al. 1992). However, the observation is consistent with Ruppel's (1973) original report and results from potato as reported by Zhang et al. (2016). The similarity of potato skin to the surface of beet root in that both consist of a periderm and a cork outer layer may provide an explanation for the absence of directed growth. Cork cells may lack the uniform cell characteristics, such as a linear orientation, that is common with epidermal cells (Albersheim et al. 2011).

As well as surface topology, root exudates have been shown to have a potential role in hyphae recruitment, determination of invasion sites, and infection cushion formation for some *R. solani* AG (Badri & Vivanco 2009; Kou & Naqvi 2016; Lombardi et al. 2018; Marshall & Rush 1980). Increased production of exudates could result in higher levels of hyphal colonization and a greater number of potential infection sites which has been shown to be positively correlated to disease severity for mungbean (Bashyal et al. 2018) and tomato fruit (Bassi et al. 1979) infected

with *R. solani*. Observations in the current study of denser hyphae on the susceptible compared to the resistant variety are consistent with this correlation and may indicate higher levels of specific types of exudates produced by the susceptible variety. The site of infection cushion formation coinciding with hyphal overlap may be an indication of locations with increased levels of exudate leakage and warrants further testing. Rather than requiring hyphal interaction, it could be hypothesized that different hyphae are simply attracted to the same location. The potential role of exudates in the recruitment of *R. solani* AG 2-2 hyphae and the formation of infection cushions needs further study.

Shortening branch lengths leading to the formation of infection cushions has previously been reported (Armentrout & Downer 1987; Hofman & Jongebloed 1988; Yang et al. 1992). However, in the current study, the shortening hyphae did not form t-shaped branches as has been reported for other systems. This lack of t-shaped branching may be related to the lack of parallel anticlinal walls in the sugar beet surface cells that would serve to orient the branches. T-shaped branches do not form in potato, which has a periderm and cork cells similar to those in sugar beet (Demirci & Döken 1998; Zhang et al. 2016). Whether *R. solani* AG 2-2 forms t-shaped branches on hosts with an epidermis, such as dry beans, is uncertain and is worthy of investigation.

Penetration of the periderm

Tissue colonization was observed within three days of inoculation (Figure 4.10) and hyphae were observed penetrating the periderm within 2 days after hyphae came into contact with the root surface (Figure 4.5). Ruppel (1973) observed hyphae within the cork cells within two days but did not report evidence of hyphae in the outer cortex and accompanying necrosis until four days after inoculation. However, penetration of the periderm was reported in potato in as little as

8 hours after inoculation with *R. solani* AG 3, although most of the infection occurred through epidermal cracks and lenticles (Zhang et al. 2016). The periderm apparently poses little to no barrier to penetration by *R. solani* since penetration and colonization of the periderm occurs rapidly in both potato (AG 3) and sugar beet (AG 2-2). However, similar to the colonization of cork cells by *Aspergillus nidulans* reported by Martins et al. (2014), the cork layer remained largely intact indicating superficial degradation of the cork cells and/or mechanical force.

Penetration and invasion of the cortex

Hyphae appear to be able to penetrate the outer cells directly without requiring the formation of infection cushions, infection pegs or appressoria. This observation is in contrast with many studies of the infection process in *R. solani* that reported the involvement of specialized infection structures in penetration. Yang et al. (1992) reported direct penetration of canola hypocotyls by means of the anticlinal walls of the epidermal cells. Since in much of the early stages of infection and in younger portions of the lesions the hyphae proceeded intracellularly, hypothesizing that invasion occurs through the anticlinal walls would be reasonable. However, there were no conclusive observations in the current study that supported this hypothesis. It is possible that the invading hyphae penetrate the cork cells at any favorable point, but transition to intracellular after penetrating the periderm. This hypothesis would be challenging to prove as it would likely take many, many sections to capture an individual hypha making such a transition. The proverbial "needle in the haystack."

Another hypothesis would be that *R. solani* AG 2-2 has several strategies for entering the host tissue and can react to a variety of situations, essentially employing a barrage strategy in order to overpower cell wall barriers. The potential ability of the fungus to attack from multiple

routes is suggestive of substantial diversity in pathogenicity and virulence factors present in the genome of *R. solani* AG 2-2 (King et al. 2011; Wibberg et al. 2106). In the current study, evidence was observed for the degradation of pectin, methylated pectin, lignin, and cellulose reflecting a diverse arsenal of cell wall degrading enzymes produced by *R. solani* AG 2-2 isolates, as has been reported previously (Bugbee 1990; Scala et al. 1980; Wahleithner et al. 1996; Wibberg et al. 2016).

While tissues within the root groove typically have an outer cork layer, the periderm is less distinct and the transition to parenchyma tissue is more rapid, with breaks in the cork layer occurring due to the emergence of lateral roots. In addition, the tissues within the folds of the root groove generally lack a layer of secondary cambium. In the smooth root section, the outermost secondary cambium appears to act as a temporary barrier, encouraging hyphae to spread laterally. This does not appear to be the case in tissues within the root groove, where hyphae appear less restricted in their spread (Figure 4.8). The result being that invasion can spread to deeper internal tissues and could damage the ability of the lateral roots to take up water and nutrients effectively. While damage to feeder roots often leads to wilting, this symptom is not typically associated with RRCR rot of sugar beet. Instead, leaves suddenly and permanently collapse resulting in a rosette of dead leaves and petioles (Harveson 2008). Although phytotoxins have been reported from R. solani infecting sugar beet (Aoki et al. 1963; Hyakumachi et al. 1980), this sudden collapsing of leaves may be associated with the ease of hyphal spread within tissues of the root groove. Although hyphae were observed within feeder roots in the current study (Figure 4.8), the type of feeder root decay associated with some wilt pathogens is not typically observed in sugar beet infected with R. solani AG 2-2 (L. Hanson, personal communication). More study on the health of feeder roots and the effect of invasion within the

root groove is needed to assess the relationship of these observations to the symptom of sudden leaf collapse.

Response of cell wall

The presence of autofluorescence complicated the analysis. Initially, the phenomenon was detected during staining with propidium iodide which exhibited increased fluorescence within the lesion. This observation was hypothesized to indicate an abundance in demethylated pectin as propidium iodide has been reported to have a higher affinity for demethylated pectin than methylated pectin (Rounds et al. 2011). It was therefore hypothesized that *R. solani* utilized a pectin de-methylesterase to increase susceptibility of cell wall pectin to polygalacturonases (Baher & Braybrook 2011; Karr & Albersheim 1970). However, immunofluorescence did not support changes in methylation state as the reason for increased propidium iodide binding. Prior to cell wall fragmentation and elimination of pectin, the cell wall appeared to thicken as autofluorescence in the red spectra increased (Figure 4.11). This increase in autofluorescence and apparent cell wall thickening within the lesion is likely to be associated with as yet unknown physical changes in cell wall structure.

Safranin O in combination with calcofluor white can distinguish between cellulosic and lignified tissue (Bond et al. 2008; Kitin et al. 2020; Sant'Anna et al. 2013). Ruppel (1973) reported that cell walls within a lesion were thickened and had greater affinity for safranin, possibly indicating a concentration or localization of suberin within infected tissues. Safranin O is an azo dye commonly used to stain lignified tissues such as xylem (Bond et al. 2008) and observations in the current study of increased safranin O staining in infected tissues could indicate lignification (Figure 4.9), the potential of which was not explored in Ruppel (1973). The

increase in fluorescence associated with berberine hemisulfate that was less intense than the highly suberized cork cells could also support lignification rather than suberization as the source of increased safranin O staining.

Healthy sugar beet cell walls contain relatively low levels of lignin (Dinand et al. 1999; McGrath & Townsend 2015) but contain unique phenolic cross-links between ferulic acid and pectic arabinosyl and galactosyl residues that influence such properties as intercellular adhesion, texture and lignification (Guillon & Thibault 1989; Marry et al. 2006; Waldron et al. 1999). Deposition of lignin as a defense response reinforces the cellulose microfibrils and makes the cell wall more resistant to cell wall degrading enzymes (Bellincampi et al. 2014; Bhuiyan et al. 2009). Increased lignification has been associated with disease resistance in cotton (Smit & Dubery 1996; Xu et al. 2011), *Camelina sativa* (Enyck et al. 2012), wheat (Dushnicky et al. 1998; Menden et al. 2007) and has been recognized as part of a generalized response to biotic stresses (Bhuiyan et al. 2009; Nicholson & Hammerschmidt 1992; Xie et al. 2018).

It is uncertain whether *R. solani* AG 2-2 is pathogenic on woody plants. Other *R. solani* AG, including AG 4 and others where the anastomosis group was not determined, have been reported from pine and other tree species (Mehrotra 1990; Starkey & Enebak 2012). Laccase genes have been characterized from an isolate in a closely related group, *R. solani* AG 6 (Wahleithner et al. 1996). An analysis of the *R. solani* AG 2-2 genome revealed high numbers of secreted proteins including 1097 putative carbohydrate active enzymes (CAZymes) that may function as cell wall degrading enzymes (Wibberg et al. 2016). Fifteen instances of genes that had been putatively identified as 'laccase' were identified in the AG 2-2 draft genome published by Wibberg et al. (2016), indicating the potential for lignin degradation. Quantification of lignin content and

confirmation of the presence of laccase, or other lignin degrading enzymes, in infected tissue is needed to test this hypothesis.

Pectin modifications

Elimination of binding sites for LM19 and LM20 antibodies from the cell wall indicated degradation of both methylated and demethylated pectin epitopes (Figure 4.14 & 4.15). While this occurred in both the resistant and susceptible varieties, it appeared to occur more rapidly in the susceptible variety than the resistant, although quantification was not attempted. In the susceptible variety (CR869), much of the unesterified pectin was eliminated from the cell walls of infected tissue, while in the resistant variety (SR98/2), the unesterified pectin appeared to aggregate and form clumps along the inner surface of the cell wall (Figure 4.15). This observation may indicate the accumulation of pectin fragments liberated from the cell wall by enzymatic action (Cervone et al. 1989; Pontiggia et al. 2015; Ridley et al. 2001). The presence of pectic fragments, or oligogalacturonides (OG), has been associated with defense responses such as cell wall reinforcement and could be considered a damage-associated defense response (Bellincampi et al. 2014). Cell wall reinforcements could include deposition of callose (Flors et al. 2008) and lignin (Eynck et al. 2012; Xu et al. 2011), and catalyzation of cross-linkages between cell wall components (Deepak et al. 2010; Passardi et al. 2004). Further work is needed to assess the nature of the pectin accumulation and the potential responses initiated in the current system.

The incomplete degradation of pectin fragments and the potential accumulation of OGs may be attributed to interactions between polygalacturonase and polygalacturonase-inhibiting proteins (Cook et al. 1991; Davidsson et al. 2017; De Lorenzo et al. 1994). Polygalacturonase enzymes

can exhibit differential degradation patterns based on substrate recognition (Cook et al. 1999).

Secretion of a variety of polygalacturonase isoforms by an invading fungal pathogen can reduce oligogalacturonide fragments to sizes that do not elicit a defense response (Benedetti et al. 2014; Scala et al. 1980). Inhibition of one or more polygalacturonase isoforms could limit the pathogen's capacity to avoid triggering plant defenses by increasing the accumulation of OGs of the size that can trigger defense responses.

Several polygalacturonase inhibitor proteins (PGIP) have been identified that confer resistance to fungal pathogens in sugar beets (Li & Smigocki 2016) and other crops (Chen et al. 2019; Kalunke et al. 2015; Liu et al. 2016). Inhibitor proteins can be induced as a response to wounding (Li & Smigocki 2016) and are important players in plant innate immunity (Di Matteo et al. 2006; Federici et al. 2006). The potential accumulation of OGs in the resistant variety could be a factor in triggering a defense response resulting in responses such as lignin deposition. Investigation of expressed PGIP genes could provide insight into defense mechanisms in sugar beet and provide targets for breeding programs, similar to work done with dry bean (Desiderio et al. 1997; D'Ovidio et al. 2004).

The degradation of highly esterified pectin, indicated by a reduction in binding of the LM20 antibody, implicates the presence of pectin lyase which is the only known enzyme that can degrade highly methylated pectin (Yadav et al. 2009). Pectin lyase (PNL; EC 4.2.2.10) has been isolated from *R. solani* AG 2-2 and was shown to have higher activity on sugar beet tissue than polygalacturonase in both culture and infected tissue (Bugbee 1990). Further support for the involvement of pectin lyase comes from the *Rhizoctonia*-resistant sugar beet cultivar FC712 (Panella 2001). Bugbee 1993 showed reduced pectin lyase activity in variety FC712 compared to

susceptible varieties and attributed the reduction in activity to a proteinaceous pectin lyase inhibitor from the host, although this enzyme was not isolated.

Conclusions

Rhizoctonia solani AG 2-2 utilizes multiple routes to penetrate and invade sugar beet root tissue, including infection cushions, direct penetration of the periderm, colonization of natural openings and wounds, and through vulnerable tissues in the root groove (current study; Ruppel 1973). This diversity in infection routes is expected to allow the fungus to be adaptable in its approach to infection and colonization. Although the behavior of *R. solani* AG 2-2 on sugar beet during the early stages of infection differs from reports on several other crops (Bashyal et al. 2018; Bassi et al. 1979; Hofman & Jongebloed 1988; Marshal & Rush 1980; Pannecoucque & Höfte 2009), the process is similar to that of AG 3 on potato tubers (Zhang et al. 2016) and possibly reflects the presence of a periderm rather than an epidermis.

Structural components of the root tissues can help explain some of the characteristic symptoms of Rhizoctonia root and crown rot. The outer cambium appears to act as a temporary barrier for hyphal colonization influencing the hyphae to spread laterally, producing shallow lesions in a characteristic ladder-like pattern. Necrosis precedes the hyphae in all lesions, indicating the likely presence of secreted CWDEs and a corresponding defense response in the root tissue that attempts to reinforce cell walls against degradation.

Wibberg et al. (2016) identified almost 1100 putative carbohydrate-active genes within the genome of *R. solani* AG 2-2. Our observations support diverse enzymatic functions involved in the colonization of sugar beet roots. We observed evidence for the degradation of cellulose, pectin, methylated pectin, and lignin and degradation of these cell wall components may involve

the enzymes cellulase (El-Samawaty et al. 2008), polygalacturonase (Scala et al. 1980), pectin lyase (Bugbee 1990), and laccase (Wahleithner et al. 1996), all of which have been identified or characterized from *R. solani* isolates. Further research investigating the relationship and evolutionary history of cell wall degrading enzymes in *R. solani* AG 2-2 could provide new insights into pathogenesis and virulence on sugar beet. These processes also have implications in other hosts and research is needed to determine which enzymes are employed in common between the different hosts of *R. solani* AG 2-2 and whether any enzymes are unique to a given host.

The accumulation of pectin fragments could indicate the presence of proteinaceous inhibitors such as polygalacturonase-inhibiting proteins (PGIP). Several enzyme-inhibiting proteins have been characterized from sugar beet including a pectin lyase inhibitor (Bugbee 1993) and several polygalacturonase-inhibiting proteins (Li & Smigocki 2016). While the current study does not explicitly implicate CWDE inhibitors in resistance, it is likely they play a substantial role in resistant varieties as demonstrated by the accumulation of pectin fragments in the resistant variety. Potential PGIPs have been examined in several systems and have shown promise at limiting disease development (Federici et al. 2006; Li & Smigocki 2018; Tundo et al. 2016). Since PGIPs appear to have differential specificity (Desiderio et al. 1997; Sella et al. 2004), it is likely that a combination of PGIPs would be required to be effective against Rhizoctonia root and crown rot in a broad range of situations (Federici et al. 2001).

REFERENCES

- Albersheim, P., Darvill, A., Roberts, K., Sederoff, R., and Staehelin, A. 2011. Plant Cell Walls: from Chemistry to Biology. Garland Science, Taylor & Fransis Group, LLC. New York, NY.
- Alghisi, P and Favaron, F. 1995. Pectin degrading enzymes and plant-parasite interactions. Eur J Plant Pathol, 101:365-375.
- Anderson, J.P., Hane, J.K., Stoll, T., Pain, N., Hastie, M.L., Kaur, P., Hoogland, C., Gorman, J.J. and Singh, K.B. 2016. Proteomic analysis of *Rhizoctonia solani* identifies infection-specific, redox associated proteins and insight into adaptation to different plant hosts. Mol Cell Prot, 15:1188-1203.
- Aoki, H., Sassa, T. and Tamura, T. 1963. Phytotoxic metabolites of *Rhizoctonia solani*. Nature, 200:575-575.
- Artschwager, E. 1926. Anatomy of the vegetative organs of the sugar beet. J Agric Res, 33:143-176
- Armentrout, V.N. and Downer, A.J. 1987. Infection cushion development by *Rhizoctonia solani* on cotton. Phytopathology, 77:619-623.
- Badri, D.V. and Vivanco, J.M. 2009. Regulation and function of root exudates. Plant Cell Environ, 32:666-681.
- Bashyal, B.M., Kharayat, B.S., Kumar, J., Dubey, S.C. and Aggarwal, R. 2018. Histopathological studies of *Rhizoctonia solani* infection process in different cultivars of mungbean [*Vigna radiata* (L.) Wilczek]. Natl Acad Sci Lett, 41:269-273.
- Bassi, A. Jr., Moore, E.L. and Batson, W.E. Jr. 1979. Histopathology of resistant and susceptible tomato fruit infected with *Rhizoctonia solani*. Phytopathology, 69:556-559.
- Beeckman, T. and De Smet, I. 2014. Pericycle. Curr Biol, 24:R378-R379. doi:10.1016/j.cub.2014.03.031
- Bellincampi, D., Cervone, F. and Lionetti, V. 2014. Plant cell wall dynamics and wall-related susceptibility in plant-pathogen interactions. Front Plant Sci, 5:228. doi:10.3389/fpls.2014.0028
- Benedetti, M., Pontiggia, D., Raggi, S., Cheng, Z., Scaloni, F., Ferrari, S., Ausubel, F.M., Cervone, F. and De Lorenzo, G. 2014. Plant immunity triggered by engineered in vivo release of oligogalacturonides, damage-associate molecular patterns. P Natl Acad Sci USA, 112:5533-5538.
- Bhuiyan, N.H., Selvaraj, G., Wei, Y. and King, J. 2009. Role of lignification in plant defense. Plant Signal Behay, 4:158-159.

- Brundrett, M.C., Enstone, D.E. and Peterson, C.A. 1988. A berberine-aniline blue fluorescent staining procedure for suberin, lignin, and callose in plant tissue. Protoplasma, 146:133-142.
- Bond, L., Donaldson, L., Hill, S. and Hitchcock, K. 2008. Safranin fluorescent staining of wood cell walls. Biotech Histochem, 83:161-171.
- Bugbee, W.M. 1990. Purification and characteristics of pectin lyase from *Rhizoctonia solani*. Physiol Mol Plant P, 36:15-25.
- Bugbee, W.M. 1993. A pectin lyase inhibitor protein from cell walls of sugar beet. Phytopathology, 83:63-68.
- Bürhe, C. Kluth, C., Bürcky, K., Märländer, B. and Varrelmann, M. 2009. Integrated control of root and crown rot in sugar beet: combined effects of cultivar, crop rotation, and soil tillage. Plant Dis, 93:155-161.
- Carotenuto, G. and Genre, A. 2020. Fluorescent staining of arbuscular mycorrhizal structures using wheat germ agglutinin (WGA) and propidium iodide. Pgs. 53-59 in: Arbuscular Mycorrhizal Fungi: Methods and Protocols. Ferrol, N. and Lanfranco, L. (eds.) Humana Press, New York, NY.
- Cervone, F., Hahn, M.G., De Lorenzo, G., Darvill, A. and Albersheim, P. 1989. Host-pathogen interactions XXXIII. A plant protein converts a fungal pathogenesis factor into an elicitor of plant defense responses. Plant Physiol, 90:542-548.
- Chen, X., Chen, Y., Zhang, L., He, Z., Huang, B., Chen, C., Zhang, Q. and Zuo, S. 2019. Amino acid substitutions in a polygalacturonase inhibiting protein (OsPGIP2) increases sheath blight resistance in rice. Rice, 12:56. doi:10.1186/s12284-019-0318-6
- Cold Springs Harbor Protocols. 2007. 10X PBS. doi:10.1101/pdb.rec10768
- Cook, B.J., Clay, R.P., Bergmann, C.W., Albersheim, P. and Darvill, A.G. 1999. Fungal polygalacturonases exhibit different substrate degradation patterns and differ in their susceptibilities to polygalacturonase-inhibiting proteins. Mol Plant Microbe In, 12:703-711.
- Cooke, D.A. and Scott, R.K. (eds.) 1993. The Sugar Beet Crop: Science into Practice. Chapman & Hall, London, UK.
- Daher, F.B. and Braybrook, S.A. 2015. How to let go: pectin and plant cell adhesion. Front Plant Sci, 6:523. doi:10.3389/fpls.2015.00523
- Davidsson, P., Broberg, M., Kariola, T., Sipari, N., Pirhonen, M., Palva, E.T. 2017. Short oligogalacturonides induce pathogen resistance-associated gene expression in *Arabidopsis thaliana*. BMC Plant Biol, 17:19. doi:10.1186/s12870-016-0959-1
- De Lorenzo, G., Ceervone, F., Bellincampi, D., Caprari, C., Clark, A.J., Desiderio, A., Devoto, A., Forrest, R., Leckie, F., Nuss, L. and Salvi, G. 1994. Polygalacturonase, PGIP and oligogalacturonides in cell-cell communication. Biochem Soc T, 22:394-397.

- Deepak, S., Shailasree, S., Kini, R.K., Muck, A., Mithöfer, A., and Shetty, S.H. 2010. Hydroxyproline-rich glycoproteins and plant defense. J. Phytopathol, 158:585–593.
- Demirci, E. and Döken, M.T. 1998. Host penetration and infection by the anastomosis groups of *Rhizoctonia solani* Kühn isolated from potatoes. Turk J Agric For, 22:609-613.
- Desiderio, A., Aracri, B., Leckie, F., Mattei, B., Salvi, G., Tigelaar, H., Van Roekel, J.S.C., Baulcombe, D.C., Melchers, L.S., De Lorenzo, G. and Cervone, F. 1997. Polygalacturonase-inhibiting proteins (PGIPs) with different specificities are expressed in *Phaseolus vulgaris*. Mol Plant Microbe In, 10: 852-860.
- Di Matteo, A., Bonivento, D., Tsernoglou, D., Federici, L. and Cervone, F. 2006. Polygalacturonase-inhibiting protein (PGIP) in plant defense: a structural view. Phytochemistry, 67:528-533.
- Dinand, E., Chanzy, H. and Vignon, M.R. 1999. Suspension of cellulose microfibrils from sugar beet pulp. Food Hydrocolloid, 13:275-283.
- D'Ovidio, R., Mattei, B., Roberti, S. and Bellincampi, D. 2004. Polygalacturonases, polygalacturonase-inhibiting proteins and pectic oligomers in plant-pathogen interactions. Biochim Biophys Acta Proteins Proteom, 1696:237-244.
- Dushnicky, L.G., Ballance, G.M., Sumner, M.J. and MacGregor, A.W. 1998. The role of lignification as a resistance mechanism in wheat to a toxin-producing isolate of *Pyrenophora tritici-repentis*. Can J Plant Pathol, 20:35-47.
- Elliot, M.C. and Weston, G.D. 1993. Biology and physiology of the sugar beet plant. Pgs. 37-66 in: The Sugar Beet Crop: Science into Practice. Cooke, D.A. and Scott, R.K. (eds.) Chapman & Hall, London, UK.
- El-Samawaty, A., Asran-Amal, A., Omar, M. and Abd-Elsalam, K.A. 2008. Anastomosis groups, pathogenicity, and cellulase production of *Rhizoctonia solani* from cotton. Pest Technol, 2:117-124.
- Engelkes, C.A. and Windels, C.E. 1994. Relationship of plant age, cultivar, and isolate of *Rhizoctonia solani* AG-2-2 to sugar beet root and crown rot. Plant Dis, 78:685-689.
- Eynck, C., Seguin-Swartz, G., Clarke, W.E. and Parkin, I.A.P. 2012. Monolignol biosynthesis is associated with resistance to *Sclerotinia sclerotiorum* in *Camelina sativa*. Mol Plant Pathol, 13:887-899.
- Federici, L., Caprari, C., Mattei, B., Savino, C., Di Matteo, A., De Lorenzo, G., Cervone, F. and Tsernoglou, D. 2001. Structural requirements of endopolygalacturonase for the interaction with PGIP (polygalacturonase-inhibiting protein). P Natl Acad Sci, 98:13425-13430.
- Federici, L., Di Matteo, A., Fernandez-Recio, J., Tsernoglou, D. and Cervone, F. 2006. Polygalacturonase inhibitor proteins: players in plant innate immunity? Trends Plant Sci, 11:65-70.

- Flors, V., Ton, J., van Doorn, R., Jakab, G., Garcia-Agustin, P. and Mauch-Mani, B. 2008. Interplay between JA, SA and ABA signaling during basal and induced resistance against *Pseudomonas syringae* and *Alternaria brassicicola*. Plant J, 54:81-92.
- Gaskill, J.O. 1968. Breeding for Rhizoctonia resistance in sugar beet. J Am Soc Sugarbeet Technol, 15:107-119.
- Guillon, F. and Thibault, J.-F. 1989. Methylation analysis and mild acid hydrolysis of the 'hairy' fragments of sugar beet pectins. Carbohyd Res, 190:85-96.
- Harveson, R.M. 2008. Rhizoctonia root and crown rot of sugar beet. University of Nebraska-Lincoln Extension, G1841. https://extensionpublications.unl.edu/assets/pdf/g1841.pdf
- Hietala, A.M. and Sen, R. 1996. *Rhizoctonia* associated with forest trees. Pgs. 351-358 in: *Rhizoctonia* species: Taxonomy, Molecular Biology, Ecology, Pathology, and Disease Control. Eds. Sneh, B., Jabaji-Hare, S., Neate, S. and Dijst, G. Kluwer Academic Publishers, Dordrecht, The Netherlands.
- Hofman, T.W. and Jongebloed, P.H.J. 1988. Infection process of *Rhizoctonia solani* on *Solanum tuberosum* and effects of granular nematicides. Neth J Plant Pathol, 94:243-252.
- Hyakumachi, M., Kobayashi, K. and Ui, T. 1980. Production of fumaric acid by *Rhizoctonia solani*. Ann Phytopathol Soc Japan, 46:121-125.
- Kalunke, R.M., Tundo, S., Benedetti, M., Ceervone, F., De Lorenzo, G. and D'Ovidio, R. 2015. An update on polygalacturonase-inhibiting protein (PGIP), a leucine-rich repeat protein that protects crop plants against pathogens. Front Plant Sci, 6:146. doi:10.3389/fpls.2015.00146
- Karr, A.L. Jr. and Albersheim, P. 1970. Polysaccharide-degrading enzymes are unable to attack plant cell walls without prior action by a "wall-modifying enzyme". Plant Physiol, 46:69-80.
- Keijer, J. 1996. Initial steps of the infection process in *Rhizoctonia solani*. Pgs. 149-162 in: *Rhizoctonia* species: Taxonomy, Molecular Biology, Ecology, Pathology, and Disease Control. Eds. Sneh, B., Jabaji-Hare, S., Neate, S. and Dijst, G. Kluwer Academic Publishers, Dordrecht, The Netherlands.
- King, B.C., Waxman, K.D., Nenni, N.V., Walker, L.P., Bergstrom, G.C. and Gibson, D.M. 2011. Arsenal of plant cell wall degrading enzymes reflects host preference among plant pathogenic fungi. Biotechnol Biofuels, 4:4 doi:10.1186/1754-6834-4-4
- Kitin, P., Nakaba, S., Hunt, C.G., Lim, S. and Funada, R. 2020. Direct fluorescence imaging of lignocellulosic and suberized cell walls in roots and stems. AoB Plants, 12:plaa032 doi:10.1093/aobpla/plaa032
- Kou, Y. and Naqvi, N.I. 2016. Surface sensing and signaling networks in plant pathogenic fungi. Semin Cell Dev Biol, 57:84-92.

- Kousik, C.S., Snow, J.P. and Berggren, G.T. 1994. Factors affecting infection cushions development by *Rhizoctonia solani* A -IA and IB on soybean leaves. Plant Pathol, 43:237-244.
- Kubicek, C.P., Starr, T.L. and Glass, N.L. 2014. Plant cell wall-degrading enzymes and their secretion in plant-pathogenic fungi. Annu Rev Phytopathol, 52:427-451.
- Lewellen, R.T. 2004. Registration of rhizomania resistant, monogerm populations C869 and C869CMS sugarbeet. Crop Sci, 44:357-358.
- Li, H and Smigocki, A.C. 2016. Wound induced *Beta vulgaris* polygalacturonase-inhibiting protein genes encode a longer leucine-rich repeat domain and inhibit fungal polygalacturonases. Physiol Mol Plant P, 96:8-18.
- Li, H. and Smigocki, A.C. 2018. Sugar beet polygalacturonase-inhibiting proteins with 11 LRRs confer *Rhizoctonia*, *Fusarium* and *Botrytis* resistance in *Nicotiana* plants. Physiol Mol Plant P, 102:200-208.
- Liu, N., Ma, X., Zhou, S., Wang, P., Sun, Y., Li, X. and Hou, Y. 2016. Molecular and functional characterization of a polygalacturonase-inhibiting protein from *Cynanchum komarovii* that confers resistance in Arabidopsis. PLoS One, 11:e0146959.
- Liu, Y., Qi, A. and Khan, M.F.R. 2019. Age-dependent resistance to *Rhizoctonia solani* in sugar beet. Plant Dis, 103:2322-2329.
- Lombardi, N., Vitale, S., Turrà, D., Reverberi, M., Fanelli, C., Vinale, F., Marra, R., Ruocco, M., Pascale, A., d'Errico, G., Woo, S.L. and Lorito, M. 2018. Root exudates of stressed plants stimulate and attract *Trichoderma* soil fungi. Mol Plant Microbe In, 31:982-994.
- Lulai, E.C. 2007. The canon of potato science: 43. Skin-set and wound-healing/suberization. Potato Res, 50:387-390.
- Manian, S. and Manibhushanrao, K. 1982. Histopathological studies in rice sheath blight disease incited by *Rhizoctonia solani*. J Plant Dis Protect, 89:523-531.
- Marry, M., Roberts, K., Jopson, S.J., Huxham, I.M., Jarvis, M.C., Corsar, J., Robertson, E. and McCann, M.C. 2006. Cell-cell adhesion in fresh sugar-beet root parenchyma requires both pectin esters and calcium cross-links. Physiol Plantarum, 126:243-256.
- Marshall, D.S. and Rush, M.C. 1980. Infection cushion formation on rice sheaths by *Rhizoctonia solani*. Phytopathology, 70:947-950.
- Martin, F., Windels, C., Hanson, L. and Brantner, J. 2014. Analysis of population structure and pathogenicity of *Rhizoctonia solani* AG2-2 (ISG IIIB and IV) isolates from Michigan, Minnesota and North Dakota. Sugarbeet Res Rep. Beet Sugar Development Foundation, Denver, CO.

- Martins, I., Garcia, H., Varela, A., Núñez, O., Planchon, S., Galceran, M.T., Renaut, J., Ebelo, L.P.N. and Pereira, C.S. 2014. Investigating *Aspergillus nidulans* secretome during colonization of cork cell walls. J Proteomics, 98:175-188.
- McGrath, J.M., Derrico, C.A., Morales, M., Copeland, L.O. and Christenson, D.R. 2000. Germination of sugar beet (*Beta vulgaris* L.) seed submerged in hydrogen peroxide and water as a means to discriminate cultivar and seedlot vigor. Seed Sci Technol, 28:607-620.
- McGrath, J.M., Hanson, L.E. and Panella, L. 2015. Registration of SR98 sugarbeet germplasm with resistances to Rhizoctonia seedling and crown and root rot diseases. J Plant Regist, 9:227-231.
- McGrath, J.M. and Townsend, B.J. 2015. Sugar beet, energy beet, and industrial beet. Pgs. 81-100 in: Industrial Crops Breeding for BioEnergy and Bioproducts. Cruz, V.V. and Dierig, D.A. (eds.). Springer, New York, NY.
- Mehrotra, M.D. 1990. *Rhizoctonia solani*, a potentially dangerous pathogen of khasi pine and hardwoods in forest nurseries in India. Eur J Forest Pathol, 20:329-338.
- Menden, B., Kohlhoff, M. and Moerschbacher, B.M. 2007. Wheat cells accumulate a syringylrich lignin during the hypersensitive resistance response. Phytochemistry, 68:513-520.
- Miller, D.M. and Shakes, D.C. 1995. Immunofluorescence microscopy. Pgs. 365-394 in: Methods in Cell Biology, Vol. 48. Eds. Epstein, H.F. and Shakes, D.C. Academic Press, Cambridge, MA.
- Nagendran, S. 2006. Rhizoctonia disease in sugar beet: disease screening and cytohistopathology of sugar beet *Rhizoctonia solani* interaction. Dissertation. Michigan State University.
- Nagendran, S., Hammerschmidt, R. and McGrath, J.M. 2009. Identification of sugar beet germplasm EL51 as a source of resistance to post-emergence Rhizoctonia damping-off. Eur J Plant Pathol, 123:461-471.
- Nagy, A., Gertsenstein, M., Vintersten, K. and Behringer, R. 2007. Dewaxing and rehydrating sections prior to *in situ* hybridization. Cold Springs Harb Protoc, 4818. doi:10.1101/pdb.prot4818
- Naito, S. and Sugimoto, T. 1978. Basidiospore infection and lesion development on sugar beet leaves by *Thanatephorus cucumeris*(Frank)Donk. Ann Phytopath Soc Japan, 44:426-431. (in Japanese with English abstract)
- Nicholson, R.L. and Hammerschmidt, R. 1992. Phenolic compounds and their role in disease resistance. Annu Rev Phytopathol, 30:369-389.
- O'Brien, T.P., Feder, N. and McCully, M.E. 1964. Polychromatic staining of plant cell walls by toluidine blue O. Protoplasma, 59:368-373.

- Passardi, F., Penel, C., and Dunand, C. 2004. Performing the paradoxical: how plant peroxidases modify the cell wall. Trends Plant Sci, 9:534–540.
- Panella, L. 2001. Registration of FC712 (4X) tetraploid, multigerm sugarbeet germplasm. Crop Sci, 41:1374-1374.
- Pannecoucque, J. and Höfte, M. 2009. Interactions between cauliflower and *Rhizoctonia* anastomosis groups with different levels of aggressiveness. BMC Plant Biol, 9:95. doi:10.1186/1471-2229-9-95
- Parmeter, J.R. jr., Sherwood, R.T. and Platt, W.D. 1969. Anastomosis grouping among isolates of *Thanatephorus cucumeris*. Phytopathology, 59:1270-1278.
- Pontiggia, D., Ciarcianelli, J., Salvi, G., Cervone, F., De Lorenzo, G. and Mattei, B. 2015. Sensitive detection and measurement of oligogalacturonides in *Arabidopsis*. Front Plant Sci, 6:258. doi:10.3389/fpls.2015.00258
- Rafiei, V., Vélëz, H., Dixelius, C. and Tzelepis, G. 2023. Advances in molecular interactions on the *Rhizoctonia solani*-sugar beet pathosystem. Fungal Biol Rev, 44:100297. doi:10.1016/j.fbr.2022.11.005
- Ridley, B.L., O'Neill, M.A. and Mohnen, D. 2001. Pectins: structure, biosynthesis, and oligogalacturonide-related signaling. Phytochemistry, 57:929-967.
- Rounds, C.M., Lubeck, E., Hepler, P.K. and Winship, L.J. 2011. Propidium iodide competes with Ca²⁺ to label pectin in pollen tubes and *Arabidopsis* root hairs. Plant Physiol, 157:175-187.
- Rupple, E.G. 1973. Histopathology of resistant and susceptible sugar beet roots inoculated with *Rhizoctonia solani*. Phytopathology, 63:123-126.
- Ruppel, E.G. and Hecker, R.J. 1988. Variable selection pressure for different levels of resistance to Rhizoctonia root rot in sugarbeet. J Sugar Beet Res, 25:63-69.
- Ruppel, E.G., Schneider, C.L., Hecker, R.J. and Hogaboam, G.J. 1979. Creating epiphytoics of Rhizoctonia root rot and evaluating for resistance to *Rhizoctonia solani* in sugarbeet field plots. Plant Dis Rep, 63:518-522.
- Sant'Anna, C., Costa, L.T., Abud, Y., Biancatto, L., Costa Miguens, F. and De Souza, W. 2013. Sugarcane cell wall structure and lignin distribution investigated by confocal and electron microscopy. Microsc Res Techniq, 76:829-834.
- Scala, A., Camardella, L., Scala, F. and Cervone, F. 1980. Multiple forms of polygalacturonase in two strains of *Rhizoctonia solani*. J Gen Microbiol, 116:207-211.

- Sella, L., Castiglioni, C., Roberti, S., D'Ovidio, R. and Favaron, F. 2004. An endopolygalacturonase (PG) of *Fusarium moniliforme* escaping inhibition by plant polygalacturonase-inhibiting proteins (PGIPs) provides new insights into the PG-PGIP interaction. FEMS Microbiol Lett, 240:117-124.
- Smit, F. and Dubery, I.A. 1996. Cell wall reinforcement in cotton hypocotyls in response to a *Verticillium dahlia* elicitor. Phytochemistry, 44:811-815.
- Sneh, B., Burpee, L. and Ogoshi, A. 1991. Identification of *Rhizoctonia* Species. APS Press, St. Paul, MN.
- Sprockett, D.D., Piontkivska, H. and Blackwood, C.B. 2011. Evolutionary analysis of glycosyl hydrolase family 28 (GH28) suggests lineage-specific expansions in necrotrophic fungal pathogens. Gene, 479:29-36.
- Starkey, T. and Enebak, S.A. 2012. 15. Rhizoctonia blight of southern pines. Pgs. 63-65 in: Forest Nursery Pests, Agricultural Handbook No. 680. US Department of Agriculture Forest Service.
- Strausbaugh, C.A. and Gillen, A.M. 2008. Bacteria and yeast associated with sugar beet root rot at harvest in the Intermountain West. Plant Dis, 92:357-363.
- Strausbaugh, C.A., Eujayl, I.A., Panella, L.W. and Hanson, L.E. 2011. Virulence, distribution and diversity of *Rhizoctonia solani* from sugar beet in Idaho and Oregon. Can J Plant Pathol, 33:210-226.
- Trebbi, D. and McGrath, J.M. 2009. Functional differentiation of the sugar beet root system as indicator of developmental phase change. Physiol Plantarum, 135:84-97.
- Tundo, S., Janni, M., Moscetti, I., Mandalà, G., Savatin, D., Blechl, A., Favaron, F. and D'Ovidio, R. 2016. PvPGIP2 accumulation in specific floral tissues, but not in the endosperm, limits *Fusarium graminearum* infection in wheat. Mol Plant Microbe In, 29:815-821.
- Verhertbruggen, Y., Marcus, S.E., Haeger, A., Ordaz-Ortiz, J.J. and Knox, J.P. 2008. An extended set of monoclonal antibodies to pectin homogalacturonan. Carbohyd Res, 344:1858-1862.
- Wahleithner, J.A., Xu, F., Brown, K.M., Brown, S.H., Golightly, E.J., Halkier, T., Kauppinen, S., Pederson, A. and Schneider, P. 1996. The identification and characterization of four laccases from the plant pathogenic fungus *Rhizoctonia solani*. Curr Genet, 29:395-403.
- Waldron, K.W., Ng, A., Parker, M.L. and Parr, A.J. 1999. Ferulic acid dehydrodimers in the cell walls of *Beta vulgaris* and their possible role in texture. J Sci Food Agr, 74:221-228.
- Weinhold, A.R. and Motta, J. 1973. Initial host responses in cotton to infection by *Rhizoctonia solani*. Phytopathology, 63:157-162.

- Wibberg, D., Anderson, L., Tzelepis, G., Rupp, O., Blom, J., Jelonek, L., Pühler, A., Fogelqvist, J., Varrelmann, M., Schlüter, A. and Dixelius, C. 2016. Genome analysis of the sugar beet pathogen *Rhizoctonia solani* AG2-2IIIB revealed high numbers in secreted proteins and cell wall degrading enzymes. BMC Genomics, 17:245. doi:10.1186/s12864-016-2561-1
- Windels, C.E., Jacobsen, B.J. and Harveson, R.M. 2009. Rhizoctonia root and crown rot. Pgs. 33-36 in: Compendium of Beet Diseases and Pests (2nd ed.) Harveson, R.M., Hanson, L.E. and Hein, G.L. (eds.). APS Press, St. Paul, MN
- Wynn, W. and Staples, R. 1981. Tropisms of fungi in host recognition. Pgs. 45-69 in: Plant Disease Control: Resistance and Susceptibility. Staples, R.C. and Toenniessen, G.H. (eds.) Wiley, New York, NY.
- Xie, M., Zhang, J., Tschaplinski, T.J., Tuskan, G.A., Chen, J. and Muchero, W. 2018. Regulation of lignin biosynthesis and its role in growth-defense tradeoffs. Front Plant Sci, 9:1427. doi:10.3389/fpls.2018.01427
- Xu, L., Zhu, L., Tu, L., Liu, L., Yuan, D., Jin, L., Long, L and Zhang, X. 2011. Lignin metabolism has a central role in the resistance of cotton to the wilt fungus *Verticillium dahliae* by RNA-Seq-dependent transcriptional analysis and histochemistry. J Exp Bot, 62:5607-5621.
- Xue, C.Y., Zhou, R.J., Li, Y.J., Xiao, D. and Fu, J.F. 2018. Cell-wall-degrading enzymes produced in vitro and in vivo by *Rhizoctonia solani*, the causative fungus of peanut sheath blight. PeerJ, 6:e5580. doi:10.7717/peerj.5580
- Yadav, S., Yadav, P.K., Yadav, D. and Yadav, K.D.S. 2009. Pectin lyase: a review. Process Biochem, 44:1-10.
- Yang, J., Verma, P.R. and Tewari, J.P. 1992. Histopathology of resistant mustard and susceptible canola hypocotyls infected by *Rhizoctonia solani*. Mycol Res, 96:171-179.
- Zhang, X.Y., Huo, H.L., Xi, X.M., Liu, L.L., Yu, Z. and Hao, J.J. 2016. Histological observation of potato in response to *Rhizoctonia solani* infection. Eur J Plant Pathol, 145:289-303.
- Zheng, A. and Wang, Y. 2011. The research of infection process and biological characteristics of *Rhizoctonia solani* AG-1 IB on soybean. J Yeast Fungal Res, 2:93-98.

CHAPTER 5:

CONCLUSIONS

Rhizoctonia root and crown rot is a persistent problem in sugar beet growing regions around the world. The disease has proved challenging to manage because of a lack of satisfactory resistance in commercial varieties and rotational crops that are susceptible to the same strains of the pathogen. Discrepancies in *Rhizoctonia solani* anastomosis group (AG) 2-2 subgroups have led to inconsistencies and unanswered questions regarding the population biology of AG 2-2. For example, some studies have provided evidence of possible sexual reproduction in natural populations (Ajayi-Oyentunde et al. 2019; Kiyoshi et al. 2014; Toda & Hyakumachi 2006), but little is known about conditions and limitations for the formation of the sexual stage and recombination in natural populations.

To address some of the open questions regarding the population biology of *R. solani* AG 2-2, including global and regional distributions, and reproductive strategy, a major goal of this dissertation project was to develop a set of microsatellite markers to examine the population genetics of *R. solani* AG 2-2. This set of microsatellite markers, in combination with data from a multigene phylogeny, was used to redefine subgroups so they reflect a more natural classification. Results indicated two subgroups within AG 2-2 that were composed of a mix of isolates that were previously classified as AG 2-2IIIB and AG 2-2IV. These newly defined groups were termed AG 2-2BR (*Beta* rot) and AG 2-2PR (*Phaseolus* rot) based on which crop members of the group were most aggressive according to Minier (2019). Both subgroups contain two distinct genetic clusters, each with unique characteristics.

The major conclusions of this dissertation research are two-fold. First, this research identified several mechanisms that contribute to genetic diversity within AG 2-2. While both the sexual stage (*Thanatephorus cucumeris*) and the asexual exchange of nuclei have previously been demonstrated in *R. solani* AG 2-2 (Kiyoshi et al. 2014; Toda & Hyakumachi

2006), the contribution of these processes to the diversity of field populations and their consequences is not well understood. Evidence for sexual reproduction was found to be limited to a single genetic subgroup while the other groups appear to reproduce primarily clonally. However, AG 2-2 isolates can exchange nuclei as well as other genetic material asexually through anastomosis reactions (Kiyoshi et al. 2014; Toda & Hyakumachi 2006). This transfer of genetic material in a horizontal manner confuses relationships within the group. It is likely that the characterization of isolates will require sequencing of multiple genes rather than relying on single genetic regions, such as ITS, for identification. The lineage-specific markers developed in the current study should simplify assignment of isolates to specific subgroups. Identification of pathogenicity or virulence factors could provide additional information that might help identify risks associated with a given isolate.

Genetic exchange between isolates has previously been demonstrated in AG 2-2IV (Kiyoshi et al. 2014; Toda & Hyakumachi 2006) but to the best of my knowledge, has not been convincingly demonstrated in AG 2-2IIIB or between AG 2-2IIIB and AG 2-2IV isolates. The results of this dissertation project have provided evidence that genetic exchange does occur between the different subgroups of AG 2-2, creating hybrids that potentially have unique genetic composition. Further work that provides direct observations regarding genetic exchange, especially of nuclei, between AG 2-2 subgroups is needed as well as determination of the consequences of genetic exchange on features such as virulence or host preference.

Sexual reproduction in AG 2-2 has been controversial. While the sexual stage (*Thanatephorus cucumeris*) has been reported in several other anastomosis groups, it has rarely been reported in AG 2-2, particularly from the field. Furthermore, reports of hymenium formation in AG 2-2 have mostly been from Japan *in vitro* from AG 2-2IV

isolates (Kiyoshi et al. 2014; Toda & Hyakumachi 2006). The results of this dissertation research provide evidence for the presence of sexual reproduction in natural populations. Evidence of sexual reproduction was limited to the subgroup AG 2-2BRb, which was the predominant group recovered from the Red River Valley in the current study. The results of the current study indicate that sexual reproduction may be occurring in the Red River Valley region and further scrutiny should be given to field populations in the region to determine conditions that contribute to the formation of the sexual stage. While the sexual stage has been reported on beet from other regions (Windels 2009), the hymenial stage on beets has sometimes been associated with other anastomosis groups (Ohkura et al. 2009; Windels et al. 1997), including in the Red River Valley (Windels et al. 1997).

The analysis of AG 2-2 populations revealed several interesting aspects about population structure. Isolates recovered from Europe were more diverse than previously reported (Buddemeyer et al. 2004) with representatives from all four genetic groups recovered in the current study. No isolates from subgroup AG 2-2BRb were recovered from Michigan in this study, while AG 2-2BRb was the predominant group in samples from the Red River Valley region. Some regions had limited representation in the current work and further examination is needed to determine the nature of the population structure within those regions. Also, additional work is needed to examine population structure and diversity within individual fields and from varied cropping systems.

The current study provided evidence of long-distance dispersal with genotypes being shared between regions that were separated by large distances, even across oceans. For example, isolates from Japan shared substantial genotype diversity with many of the other regions around the world. In contrast, the Europe population was relatively isolated,

genetically, from other regions. While basidiospores can be dispersed aerially (Naito 1996) and the sexual stage has been reported in Japan, it seems unlikely that basidiospores would disperse on air currents to regions such as the Red River Valley but not to Europe. In addition, there was evidence of long-distance dispersal even within Michigan, despite the lack of evidence for sexual reproduction in the state. It is likely that at least some of the dispersal occurs through the movement of contaminated soil or equipment and more research is needed to determine how this movement occurs and how to better prevent it. This work also highlights the importance of sanitation in disease management.

The exchange of nuclei or other genetic material between isolates of different subgroups apparently plays a substantial role in the generation of diversity within *R. solani* AG 2-2. How this process is regulated presumably involves somatic compatibility factors, but more research is needed to determine these factors and how "hybridization" generates diversity. The evolution of field populations, whether through sexual recombination or "hybridization", could have important implications to disease management in areas such as fungicide resistance, host preference, and virulence.

The second major conclusion to come from the project concerns the involvement of multiple cell wall degrading enzymes in disease development. It appeared that lignin deposition occurred within the infected tissue in both the resistant and susceptible sugar beet varieties. The observation that these lignin deposits were degraded as tissue maceration progressed supports previous indications that ligninolytic enzymes, such as laccase, are produced by *R. solani* (Wahleithner et al. 1996). Genes involved in both the lignin defense response by the plant and lignin degradation by the fungus need to be identified and characterized.

The accumulation of suspected oligogalacturonides in infected sugar beet tissue was observed and was most pronounced in the resistant variety. Short oligogalacturonides have been shown to be triggers of plant immunity (Davidson et al. 2017) and could provide a mechanism for some of the defense response in resistant sugar beet. This accumulation of pectin fragments could also indicate one or more polygalacturonase-inhibitor proteins produced by the plant that prevent the polygalacturonases produced by the fungus from completely degrading pectin. Polygalacturonase-inhibitor proteins have been identified in sugar beet (Li & Smigocki 2018), dry bean (D'Ovidio et al. 2004), and soybean (Favaron et al. 1993). Further research on these inhibitors and their performance in sugar beet could provide more direct approaches to disease resistance in sugar beet.

Expectations were that there would be evidence of pectin methylesterase activity since highly methylated pectin is resistant to degradation by most enzymes (Yadav et al. 2009). However, there was no clear evidence of systematic demethylation in either the resistant or susceptible sugar beet varieties. Since pectin lyase is the only enzyme known to degrade methylated pectin, it is likely that the enzyme is involved in tissue degradation. Pectin lyase has previously been isolated from *R. solani* AG 2-2 (Bugbee 1990) and warrants further investigation. In addition, a pectin lyase inhibitor has also been isolated from sugar beet by Bugbee (1993). Further work examining pectin lyase inhibitors and their activity in sugar beet could identify additional resources for developing varieties with more complete resistance.

Consistent with previous studies (Ruppel 1972), histopathological observations showed less colonization on the surface of resistant varieties than on susceptible varieties. However, in contrast to reports of infection cushion formation on other crops and in other anastomosis

groups of *R. solani*, directed growth following anticlinal walls was not observed in the current study. In addition, in the current study the hyphae were not observed forming t-shaped branches prior to infection cushion formation. These observations may implicate exudates or other chemical signals rather than surface cues as the primary factor that stimulates infection cushion formation on adult sugar beet. This hypothesis is supported by the observation of increased colonization around wounds or natural defects in the periderm that expose the underlying cortex. The premise that leads to this conclusion being that the periderm helps to limit the loss of water and other chemicals present in the cortex tissue (Campilho et al. 2020) and so, damage to the periderm would result in increased attraction and colonization of fungal hyphae.

The histopathological observations outlined in this dissertation provide a description of some physiological features that help explain characteristic symptomology of Rhizoctonia root and crown rot of sugar beet. In particular, the outer cambial ring provides at least a temporary barrier against fungal penetration, directing hyphal growth laterally. This results in the characteristic symptom of shallow lesions that tend to form in a ladder-like pattern. As reported in previous studies (Ruppel 1972), necrosis consistently preceded the hyphae in both susceptible and resistant sugar beet varieties. This region of darkening tissue appears to be largely the result of a plant defense response rather than damage to the cell wall. The precise biochemical situation in this region and details of the plant-pathogen interaction still need to be elucidated. A transcriptome analysis of the affected region could help clarify the process responsible for the discolored region.

Based on observations discussed in this dissertation project and the current understanding of cell wall degradation defense, some enzymes that are most likely to have an impact on

disease resistance and deserve to be a focus of future research are polygalacturonase-inhibiting proteins and pectin lyase-inhibiting proteins. Both enzyme types have been isolated from sugar beet but their role in disease resistance is unknown.

Even if inhibitor enzymes were present in a variety, they could be ineffective against fungal wall-degrading enzymes that escape recognition due to mutations or sequence variations. Polygalacturonase-inhibiting proteins exhibit substrate specificity (Desiderio et al. 1997; Federici et al. 2001), meaning that if multiple forms of an enzyme are secreted by the fungus, some of them may escape recognition by the inhibitor proteins leaving the cell wall vulnerable to degradation. Transforming novel inhibitor proteins with appropriate specificities into sugar beet varieties or editing existing genes using technology such as CRISPR/Cas9 could provide additional specificity that may be needed to increase disease resistance.

This dissertation project represents a significant advance in our understanding of *Rhizoctonia solani* AG 2-2 population genetics. Not only does this work reclassify the subgroups to reflect more natural relationships, but it also provides new insight into the life history strategy of this important fungal pathogen. In particular, this study considers sources of genetic variation and how that variation might explain population structure. As a part of the life history strategy, the fungus utilizes several cell wall degrading enzymes, and this study proposes potential targets for breeding efforts to improve Rhizoctonia root and crown rot resistant sugar beet varieties.

REFERENCES

- Ajayi-Oyetunde, O.O., Everhart, S.E., Brown, P.J., Tenuta, A.U., Dorrance, A.E. and Bradley, C.A. 2019. Genetic structure of *Rhizoctonia solani* AG-2-2IIIB from soybean in Illinois, Ohio, and Ontario. Phytopathology, 109:2132-2141.
- Buddemeyer, J, Pfähler, B., Petersen, J. and Märländer 2004. Genetic variation in susceptibility of maize to *Rhizoctonia solani* (AG 2-2IIIB) symptoms and damage under field conditions in Germany. J Plant Dis Protect, 111:521-533.
- Bugbee, W.M. 1990. Purification and characteristics of pectin lyase from *Rhizoctonia solani*. Physiol Mol Plant P, 36:15-25.
- Bugbee, W.M. 1993. A pectin lyase inhibitor from cell walls of sugar beet. Phytopathology, 83:63-68.
- Campilho, A., Nieminen, K. and Ragni, L. 2020. The development of the periderm: the final frontier between a plant and its environment. Curr Opin Plant Biol, 53:10-14.
- D'Ovidio, R., Raiola, A., Capodicasa, C., Devoto, A., Pontiggia, D., Roberti, S., Galletti, R., Conti, E., O'Sullivan, D. and De Lorenzo, G. 2004. Characterization of the complex locus of bean encoding polygalacturonase-inhibiting proteins reveals subfunctionalization for defense against fungi and insects.
- Davidson, P. Broberg, M., Kariola, T., Sipari, N., Pirhonen, M. and Palva, E.T. 2017. Short oligogalacturonides induce pathogen resistance-associated gene expression in *Arabidopsis thaliana*. BMC Plant Biol, 17:19. doi: 10.1186/s12870-016-0959-1
- Desiderio, A., Aracri, B., Leckie, F., Mattei, B., Salvi, G., Tigelaar, H., Van Roekel, J.S.C., Baulcombe, D.C., Melcheers, L.S., Ed Lorenzo, G. and Cervone, F. 1997. Polygalacturonase-inhibiting proteins (PGIPs) with different specificities are expressed in *Phaseolus vulgaris*. Mol Plant Microbe In, 10:852-860.
- Favaron, F., D'Ovidio, R., Porceddu, E. and Alghisi, P. 1993. Purification and molecular characterization of a ssoybean polygalacturonase-inhibiting protein. Planta, 195:80-87.
- Federici, L., Caprari, C., Mattei, B., Savino, C., Di Matteo, A., De Lorenzo, G., Cervone, F. and Tsernoglou, D. 2001. Structural requirements of endopolygalacturonase for the interaction with PGIP (polygalacturonase-inhibiting protein). P Natl A Sci, 98:13425-13430.
- Kiyoshi, T., Naito, S., Akino, S., Ochi, S. and Kondo, N. 2014. Progeny derived from *Thanatephorus cucumeris* (*Rhizoctonia solani*) AG-2-2 IV isolates on sugar beet foliage show more clonal diversity in somatic compatibility grouping than those from roots and petioles. J Gen Plant Pathol, 80:136-146.

- Li, H and Smigocki, A.C. 2018. Sugar beet polygalacturonase-inhibiting proteins with 11 LRRs confer *Rhizoctonia, Fusarium*, and *Botrytis* resistance in *Nicotiana* plants. Physiol Mol Plant P, 102:200-208.
- Minier, D.H. 2019. Diversity of the fungal pathogen *Rhizoctonia solani* AG 2-2. (Master's thesis). Michigan State University, East Lansing, MI. ProQuest, Ann Arbor, MI.
- Naito, S. 1996. Basidiospore dispersal and survival. Pgs. 197-205 in: *Rhizoctonia* species: taxonomy, molecular biology, ecology, pathology and disease control. Edited by Sneh, B, Jabaji-Hare, S., Neate, S. and Dijst, G. Kluwer Academic Publishers, Dordrecht, The Netherlands.
- Ohkura, M, Abawi, G.S., Smart, C.D. and Hodge, K.T. 2009. Diversity and aggressiveness of *Rhizoctonia solani* and *Rhizoctonia*-like fungi on vegetables in New York. Plant Dis, 93:615-624.
- Rupple, E.G. 1973. Histopathology of resistant and susceptible sugar beet roots inoculated with *Rhizoctonia solani*. Phytopathology, 63:123-126.
- Toda, T and Hyakumachi, M. 2006. Heterokaryon formation in *Thanatephorus cucumeris* anastomosis group 2-2 IV. Mycologia, 98:726-736.
- Wahleithner, J.A., Xu, F., Brown, K.M., Brown, S.H., Golightly, E.J., Halkier, T., Kauppinen, S., Pederson, A. and Schneider, P. 1996. The identification and characterization of four laccases from the plant pathogenic fungus *Rhizoctonia solani*. Curr Genet, 29:395-403.
- Windels, C.E. 2009. Rhizoctonia foliar blight. Pgs. 14-15 in: Compendium of Beet Diseases and Pests (2nd ed.). Harveson, R.M., Hanson, L.E. and Hein G.L. (eds.). APS Press, St. Paul, MN.
- Windels, C.E., Kuznia, R.A. and Call, J. 1997. Characterization and pathogenicity of *Thanatephorus cucumeris* from sugar beet in Minnesota. Plant Dis, 81:245-249.